NOTICE

The quality of this microform is heavily dependent upon the quality of the original thesis submitted for microfilming. Every effort has been made to ensure the highest quality of reproduction possible.

If pages are missing, contact the university which granted the degree.

Some pages may have indistinct print especially if the original pages were typed with a poor typewriter ribbon or if the university sent us an inferior photocopy.

Previously copyrighted materials (journal articles, published tests, etc.) are not filmed.

Reproduction in full or in part of this microform is governed by the Canadian Copyright Act, R.S.C. 1970, c. C-30.

AVIS

La qualité de cette microforme dépend grandement de la qualité de la thèse soumise au microfilmage. Nous avons tout fait pour assurer une qualité supérieure de reproduction.

S'il manque des pages, veuillez communiquer avec l'université qui a conféré le grade.

La qualité d'impression de certaines pages peut laisser à désirer, surtout si les pages originales ont été dactylographiées à l'aide d'un ruban usé ou si l'université nous a fait parvenir une photocopie de qualité inférieure.

Les documents qui font déjà l'objet d'un droit d'auteur (articles de revue, tests publiés, etc.) ne sont pas microfilmés.

La reproduction, même partielle, de cette microforme est soumise à la Loi canadienne sur le droit d'auteur, SRC 1970, c. C-30.

Canada

AN EXPANSION PROCEDURE FOR RADIATION SOLUTIONS OF THE KORTEWEG DE VRIES EQUATION

by

Leslie John Mulder

B.Sc., Simon Fraser University, 1982

THESIS SUBMITTED IN PARTIAL FULFILLMENT OF

THE REQUIREMENTS FOR THE DEGREE OF

MASTER OF SCIENCE

in the Department

of

Physics

SIMON FRASER UNIVERSITY

August 1987

ISBN 0-315-42640-3

APPROVAL

Name: Leslie J. Mulder

Degree: Master of Science

Title of thesis: AN EXPANSION PROCEDURE FOR RADIATION SOLUTIONS OF THE KORTEWEG DE VRIES EQUATION

Examining Committee:

Chairman: Dr. J.F. Cochran

Dr, R.H. Enns
Senior Supervisor

Dr. K.S. Viswanathan

Dr. S.S. Rangnekar

Dr. G.N. Bojadziev
External Examiner
Professor
Department of Mathematics
Simon Fraser University

Date Approved: July 10th, 1987

PARTIAL COPYRIGHT LICENSE

I hereby grant to Simon Fraser University the right to lend my thesis, project or extended essay (the title of which is shown below) to users of the Simon Fraser University Library, and to make partial or single copies only for such users or in response to a request from the library of any other university, or other educational institution, on its own behalf or for one of its users. I further agree that permission for multiple copying of this work for scholarly purposes may be granted by me or the Dean of Graduate Studies. It is understood that copying or publication of this work for financial gain shall not be allowed without my written permission.

Title of Thesis/Project/Extended Essay

An Expansion Procedure for Radiation Solutions of the Korteweg de Vries Equation

Author:

(signature)

Leslie John MULDER

(name)

Aug 13/87

(date)

ABSTRACT

The KdV equation, first derived in 1895 by the team of Korteweg and de Vries, has demonstrated wider applicability than its original purpose of describing shallow water waves. The KdV equation is of interest not only from the standpoint of physical description but also from the point of view of Mathematical-Physics. With the discovery in 1967 by the team of Gardner,Greene, Kruskal, and Miura of a connection between the time-independent Schroedinger operator and the KdV equation came the birth of the Inverse Scattering Method. It is through this method that solutions to nonlinear initial value problems can be found by executing a sequence of linear operations. For the KdV equation two distinct types of solutions exist, one being the now famous soliton solutions, the other being the more complicated radiation solutions. Many researchers have looked at and discussed the soliton solutions, however, relatively few have explored the radiation solutions. The form of the radiation solutions has been explored for the asymptotic time regime and for short times. This thesis attempts to look at the radiation solutions for all times by use of an expansion in terms of harmonic Oscillator functions. In terms of these Oscillator functions a complete solution has been found by first expanding the spectral transform in terms of the Oscillator functions and then by using this expression to evaluate the solution of the Marchenko equation term by term through a Neumann series expansion. A calculation has been carried out for specific

initial data, up to second order in the Neumann series. The results of this calculation are discussed.

ACKNOWLEDGEMENTS

I gratefully acknowledge the time and patience that Dr. Richard Enns has expended on my behalf.

DEDICATION

To my Mother, Father, and Laura

TABLE OF CONTENTS

LIST OF FIGURES

CHAPTER I

THE KORTEWEG DE VRIES EQUATION

The Korteweg de Vries (KdV) equation was initially derived by the two Dutch scientists D.J. Korteweg and G. de Vries[1] (1895) to model the propagation of long surface waves in a rectangular canal. A very special form of these waves, now known as solitons, was first observed and recorded by J.S. Russell[2] in 1834. Subsequent to its initial derivation the KdV equation has been found to arise in other applications such as magnetohydrodynamic waves in a cold plasma (Gardner and Morikawa[3]), longitudinal vibrations of an anharmonic discrete-mass string (Zabusky[4], Kruskal[5]), ion-acoustic waves in a cold plasma (Washimi and Taniuti[6]), pressure waves in liquid-gas bubble mixtures (Wijngarten[7]), rotating flow down a tube (Leibovich[8]), and longitudinal dispersive waves in elastic rods (Nariboli[9]). This wide range of physical problems is in itself sufficient reason to justify interest in the KdV equation, but through the discovery, in 1967, of the Inverse Scattering Method (ISM) by the team of Gardner, Greene, Kruskal, and Miura[10] (GGKM) the equation generates interest, from the stand point of Mathematical-Physics, as a basis for understanding the Inverse Scattering Method.

Physically the KdV equation is a description of uni-directional long wavelength waves (where long is with respect to some characteristic length scale of the system) in a

slightly dispersive medium.

For historical reasons the following derivation of the KdV equation will be based on a hydrodynamical approach. To that end consider a level canal of rectangular cross-section and rigid walls containing a non-viscous, incompressible fluid of depth h at the surface of the earth. Since we are interested in the propagation of the waves along the canal we will ignore any variations across the width of the canal, and thus require only two spatial variables (x,z) to describe the fluid's motion. The coordinate system is choosen so that the bottom of the canal corresponds to the line z=-h and the still surface of the fluid corresponds to the line z=0 (i.e. the x axis).

The disturbed upper surface will be characterized by the functions

$$S'(x,z,t) = 0 \qquad 1a$$

or by

$$S(x,t) - z = 0 \qquad 1b$$

which are equivalent.

In order to model the motion of the fluid (non-viscous, incompressible, homogenous) we appeal to Euler's equation for fluid motion, which can be found in any standard hydrodynamics

text,

$$\frac{\partial \bar{v}}{\partial t} + \frac{1}{2}\nabla|\bar{v}|^2 - \bar{v} \times (\nabla \times \bar{v}) = -\frac{\nabla P}{\rho} + \bar{f} \qquad 2$$

where $\bar{v}$ is the fluid's velocity, P the internal pressure, ρ the density, and $\bar{f}$ the applied force per unit mass. At the outset it was assumed that the fluid was incompressible and now we will make the additional assumption that its motion is irrotational, i.e. $\nabla \times \bar{v}=0$. The second of these conditions implies that the velocity can be written in terms of a velocity potential

$$\bar{v} = \nabla\phi \qquad 3$$

and the former implies that

$$\frac{d\rho}{dt} = 0$$

which when combined with the continuity equation tells us that $\nabla\cdot\bar{v} = 0$, so that the velocity potential obeys Laplace's equation

$$\nabla^2\phi = 0. \qquad 4$$

Since the fluid is in a conservative (gravitational) force field, the applied force can be written as a gradient of a scalar function

$$\bar{f} = -\nabla u. \qquad 5$$

Under these assumptions equation 2 becomes

$$\nabla(\phi_t + \frac{1}{2}|\nabla\phi|^2 + \frac{P}{\rho} + u) = 0. \qquad 6$$

With the appropriate gauge transformation on ϕ this equation can be integrated to give

$$\phi_t + \frac{1}{2}|\nabla\phi|^2 + \frac{P}{\rho} + u = 0. \qquad 7$$

At the earth's surface the explicit form for the 'potential energy' is taken to be

$$u = gz - \frac{p_o}{\rho} \qquad 8$$

where the first term reflects the uniform gravitational field of the earth and the second a well choosen constant that takes into account the air pressure at the air-fluid interface. It should be noted that we are assuming that the fluctuations in the air-pressure at the air-fluid interface are negligible. On substitution of equation 8 into equation 7 we get the appropriate equation for non-viscous incompressible irrotational fluid flow near or at the surface of the earth

$$\phi_t + \frac{1}{2}|\nabla\phi|^2 + \frac{P-P_o}{\rho} + gz = 0, \qquad 9$$

with the caveat that $\nabla^2\phi = 0$.

The complete specification of the problem requires boundary conditions. At the lower boundary the rigid surface of the canal's floor requires that $\vec{v}\cdot\vec{n} = 0$, where $\vec{n}$ is the unit normal to the floor, which implies that

$$\phi_z = 0 \qquad \text{at } z=-h. \qquad 10$$

At the upper surface it is necessarily true that

$$\frac{dS'}{dt} = \bar{v}\cdot\nabla S' + \frac{\partial S'}{\partial t} = 0$$

since $S' = 0$. This then implies that

$$\phi_x S_x - \phi_z + \frac{\partial S}{\partial t} = 0 \qquad 11$$

and from equation 9 we get

$$-\phi_t + \frac{1}{2}|\nabla\phi|^2 + gS = 0. \qquad 12$$

Thus the specification of the full problem is given by the four equations

$$\nabla^2\phi = 0 \qquad \text{inside fluid} \qquad 13a$$

$$\phi_z = 0 \qquad z=-h \qquad 13b$$

$$\phi_t + \frac{1}{2}|\nabla\phi|^2 + gS = 0 \qquad \text{upper surface} \qquad 13c$$

$$\phi_x S_x + S_t = \phi_z. \qquad \text{upper surface} \qquad 13d$$

At this point it becomes worthwhile to convert all of the quantities that occur in the above equations into dimensionless form. For the z-coordinate a natural length is the depth of the fluid h, for the x-coordinate it is the wavelength λ, and for time it is the ratio of the wavelength and the linearized wave speed $c=\sqrt{gh}$, giving rise to the scale transformations,

$$\xi = \frac{x}{\lambda}; \qquad \zeta = \frac{z}{h}; \qquad \tau = \frac{c}{\lambda}t.$$

Since the problem is to be examined in terms of a smallness parameter ϵ it is appropriate to write

$$S = h\epsilon\sigma$$

$$\phi = \lambda c \epsilon \psi$$

where σ and ψ represent the normalized surface height and velocity potential respectively. On substituting these scaled

variables and functions into equations 13(a-d) we get

$$\psi_{\zeta\zeta} + \mu^2\psi_{\xi\xi} = 0 \qquad 14a$$

$$\psi_{\zeta} = 0 \qquad \text{at } \zeta=-1 \qquad 14b$$

$$\psi_{\tau} + \frac{\epsilon}{2}\left(\psi_{\xi}^2 + \frac{1}{\mu^2}\psi_{\zeta}^2\right) + \sigma = 0 \qquad 14c$$

$$\epsilon\psi_{\xi}\sigma_{\xi} + \sigma_{\tau} = \frac{1}{\mu^2}\psi_{\zeta} \qquad 14d$$

where $\mu = \frac{h}{\lambda}$.

In order to solve these equations in terms of a travelling wave, a solution to Laplace's equation (14a) of the form

$$\psi = Z(\zeta)e^{ik\xi - i\omega\tau} \qquad 15$$

is assumed. This will satisfy Laplace's equation and the boundary condition (14b) at $\zeta=-1$ if

$$Z(\zeta) = \text{const}\cdot\cosh(k\mu(\zeta+1)). \qquad 16$$

Thus we can assume a general solution of ψ as

$$\psi = \frac{1}{2\pi} \int_{-\infty}^{\infty} \bar{f}(k,\tau) \cosh(k\mu(\zeta+1)e^{ik\xi}dk \qquad 17$$

where $\bar{f}(k,\tau)$ is some as of yet unknown function.

The physical problem is stated such that the depth of the fluid is small in comparison with the wavelength, hence $k\mu$, where k is the wave number, is even smaller. This condition along with the assumption that $\bar{f}(k,\tau)$ goes to zero sufficiently rapidly for $|k| \longrightarrow \infty$, allows us to expand the hyperbolic cosine, in a power series in $k\mu(\zeta+1)$, under the integral sign, to obtain a reasonable approximation for ψ. Thus

$$\psi(\xi,\zeta,\tau) \simeq \frac{1}{2\pi} \int_{-\infty}^{\infty} \bar{f}(k,\tau)\left(1 + \frac{k^2\mu^2(\zeta+1)^2}{2!} + O(\mu^4)\right)e^{ik\xi}\, dk$$

$$\simeq \left(1 - \frac{\mu^2(\zeta+1)^2D^2}{2}\right) f(\xi,\tau) \qquad 18$$

with $D = \frac{\partial}{\partial\xi}$ and $f(\xi,\tau) = \frac{1}{2\pi} \int_{-\infty}^{\infty} \bar{f}(k,\tau)e^{ik\xi}dk.$

Similarly

$$\psi_\zeta \simeq -\mu^2(\zeta+1)\left(1 - \frac{\mu^2(\zeta+1)^2D^2}{6}\right) f_{\xi\xi}$$

$$\psi_\xi \simeq \left(1 - \frac{\mu^2(\zeta+1)^2D^2}{2}\right) f_\xi$$

$$\psi_\tau \simeq \left(1 - \frac{\mu^2(\zeta+1)^2D^2}{2}\right) f_\tau .$$

By substituting these forms for ψ and its derivatives into the equations for the upper surface (14c,d) with $\zeta = \epsilon\sigma$ we get

$$f_\tau + \sigma - \frac{\mu^2(\epsilon\sigma+1)^2}{2} f_{\xi\xi\tau} + \frac{\epsilon}{2} f_\xi{}^2$$

$$= O(\epsilon^2) + O(\epsilon\mu^2).$$

and

$$\epsilon f_\xi \sigma_\xi + \sigma_\tau - \frac{\epsilon\mu^2(\epsilon\sigma+1)^2}{2} \sigma_\xi f_{\xi\xi\xi} + O(\epsilon^2) + O(\epsilon\mu^2)$$

$$= -(\epsilon\sigma+1) f_{\xi\xi} + \frac{\mu^2(\epsilon\sigma+1)^3}{6} f_{\xi\xi\xi\xi}.$$

At this stage we make the critical approximations that will lead to the KdV equation. We want to retain information about both the wavelength λ and the amplitude S, in relation to the depth h. In order to accomplish this in a minimal way we must

keep terms of order ϵ and terms of order μ^2 (there are no lower). As for the cross terms we note that since $S<h<\lambda$ then $\epsilon\mu=(Sh/\lambda^2)$ is smaller than μ^2 and can thus be neglected along with all higher order cross-terms. This now defines what we mean by the term 'reasonable approximation'. By application of these restrictions to the above equations we get

$$f_\tau + \sigma + \frac{\epsilon}{2} f_\xi{}^2 = \frac{\mu^2}{2} f_{\xi\xi\tau} \qquad 19a$$

and

$$\sigma_\tau + f_{\xi\xi} + \epsilon(\sigma f_\xi)_\xi = \frac{\mu^2}{6} f_{\xi\xi\xi\xi}. \qquad 19b$$

To cast these equation into a more symmetric form differentiate equation 19a with respect to ξ and let $f_\xi=\chi$, to get

$$\chi_\tau + \sigma_\xi + \epsilon\chi\chi_\xi = \delta\chi_{\xi\xi\tau} \qquad 20a$$

and

$$\sigma_\tau + \chi_\xi + \epsilon(\sigma\chi)_\xi = \frac{\delta}{3}\chi_{\xi\xi\xi} \qquad 20b$$

where $\delta = \frac{\mu^2}{2}$.

From here on we need to appeal to perturbation methods by expressing both σ and χ in terms of perturbation expansions in both ϵ and δ, the smallness parameter and the system parameter. In order to carry out this expansion a technique described by S. Leibovich and A.R. Seebass[11] as a method of multi-scaling as it applies to systems of equations was used. To start, the system described by equation 20 is written as a vector relationship.

$$\underline{u}_\tau + (\underline{\underline{C}}_0 + \epsilon \underline{\underline{C}}_1)\underline{u}_\xi = \delta \underline{D}(\underline{u}) \qquad 21$$

where $$\underline{u} = \begin{vmatrix} \sigma \\ \chi \end{vmatrix}, \qquad \underline{D}(\underline{u}) = \begin{vmatrix} \frac{1}{3}\chi_{\xi\xi\xi} \\ \chi_{\xi\xi\tau} \end{vmatrix},$$

$$\underline{\underline{C}}_0 = \begin{vmatrix} 0 & 1 \\ 1 & 0 \end{vmatrix} \qquad \text{and} \qquad \underline{\underline{C}}_1 = \begin{vmatrix} \chi & \sigma \\ 0 & \chi \end{vmatrix}.$$

Now we assume that

$$\underline{u} = \underline{u}_0 + \epsilon \underline{u}_1 + \delta \underline{u}_2 + O(\epsilon^2, \epsilon\delta, \delta^2). \qquad 22$$

Since the spatial parts of equation 21 correspond to the three different and distinct length scales $1, \epsilon, \delta$ we anticipate three time scales $\tau_0 = \tau$, $\tau_1 = \epsilon\tau$, $\tau_2 = \delta\tau$ which implies that

$$\frac{\partial}{\partial \tau} = \frac{\partial}{\partial \tau_0} + \epsilon \frac{\partial}{\partial \tau_1} + \delta \frac{\partial}{\partial \tau_2} . \qquad 23$$

By substituting equation 22 into equation 21 and by using equation 23 and equating coefficients we get, to order ϵ, δ

$$\underline{u}_{0\tau_0} + \underline{\underline{C}}_0 \underline{u}_{0\xi} = 0 \qquad 24a$$

$$\underline{u}_{0\tau_1} + \underline{u}_{1\tau_0} + \underline{\underline{C}}_1 \underline{u}_{0\xi} + \underline{\underline{C}}_0 \underline{u}_{1\xi} = 0 \qquad 24b$$

$$\underline{u}_{0\tau_2} + \underline{u}_{2\tau_0} + \underline{\underline{C}}_0 \underline{u}_{2\xi} = \underline{D}(\underline{u}_0). \qquad 24c$$

The first of these equations is easy to solve by diagonalizing the matrix $\underline{\underline{C}}_0$ by the transformation

$$\underline{\underline{C}}_0 \longrightarrow \underline{\underline{C}}_0' = \underline{\underline{R}} \underline{\underline{C}}_0 \underline{\underline{R}}^{-1}.$$

This decouples the equations and gives

$$\underline{v}_{0\tau_0} + \underline{\underline{C}}_0' \underline{v}_{0\xi} = 0 \qquad 25$$

where $\underline{v}_0 = \underline{\underline{R}}\underline{u}_0$.

Since $\underline{\underline{C}}_0'$ is diagonal, by definition, we get two solutions to equation 25 of the form

$$\underline{v}_{01} = \begin{vmatrix} v(\xi-\omega_1\tau_0) \\ 0 \end{vmatrix}, \qquad \underline{v}_{02} = \begin{vmatrix} 0 \\ v(\xi-\omega_2\tau_0) \end{vmatrix} \qquad 26$$

where ω_1 and ω_2 are the eigenvalues of $\underline{\underline{C}}_0$, which in the case of the KdV equation are 1 and -1.

If we now turn our attention to the next orders (equations 24b,c) we see that

$$\underline{u}_{1\tau_0} + \underline{\underline{C}}_0\underline{u}_{1\xi} = -\underline{\underline{C}}_1\underline{u}_{0\xi} - \underline{u}_{0\tau_1} \qquad 27a$$

$$\underline{u}_{2\tau_0} + \underline{\underline{C}}_0\underline{u}_{2\xi} = \underline{D}(\underline{u}_0) - \underline{u}_{0\tau_2}. \qquad 27b$$

Again the left-hand side of these equations can be diagonalized by $\underline{\underline{R}}$, in which case we get

$$\underline{v}_{1\tau_0} + \underline{\underline{C}}_0'\underline{v}_{1\xi} = -\underline{\underline{R}}\underline{\underline{C}}_1\underline{\underline{R}}^{-1}\underline{v}_{0\xi} - \underline{v}_{0\tau_1} \qquad 28a$$

$$\underline{v}_{2\tau_0} + \underline{\underline{C}}_0'\underline{v}_{2\xi} = \underline{\underline{R}}\underline{\underline{D}} - \underline{v}_{0\tau_2}. \qquad 28b$$

Transforming to a moving reference frame through

$$\xi \longrightarrow x = \xi - \omega\tau$$

then $$\underline{v}_{1\tau_0} \longrightarrow \underline{v}_{1\tau_0} - \omega\underline{v}_{1x} + O(\epsilon),$$

and equations 28a,b become

$$\underline{v}_{1\tau_0} + (\underline{\underline{C}}_0' - \omega I)\underline{v}_{1x} = - \underline{\underline{R}}\underline{\underline{C}}_1\underline{\underline{R}}^{-1}\underline{v}_{0x} - \underline{v}_{0\tau_1} \qquad 29a$$

$$\underline{v}_{2\tau_0} + (\underline{\underline{C}}_0' - \omega I)\underline{v}_{2x} = \underline{\underline{R}}\underline{\underline{D}} - \underline{v}_{0\tau_2}. \qquad 29b$$

If we now multiply by one of the two basis vectors $\hat{e}_1$ or $\hat{e}_2$, which correspond to the two eigenvalues of $\underline{\underline{C}}_0$, and choose ω to be one of the two eigenvalues then the second terms of the left-hand sides of equations 29a and 29b vanish to give

$$\hat{e}\cdot\underline{v}_{1\tau_0} = -\hat{e}\cdot(\underline{\underline{RC}}_1\underline{\underline{R}}^{-1}\underline{v}_{0X} - \underline{v}_{0\tau_1}) \qquad 30a$$

$$\hat{e}\cdot\underline{v}_{2\tau_0} = \hat{e}\cdot(\underline{\underline{RD}} - \underline{v}_{0\tau_2}). \qquad 30b$$

Both of these equations are directly integrable in τ_0, but doing so would lead to a term linear in τ_0 which is undesirable since the ensuing series representation would be divergent for long times. This difficulty can be circumvented by exploiting the arbitrary nature of the solutions $\underline{v}_0$ to require the right-hand sides of equations 30a and 30b to be zero. This requirement leads to the two conditions

$$\hat{e}\cdot(\underline{\underline{RC}}_1\underline{\underline{R}}^{-1}\underline{v}_{0X} + \underline{v}_{0\tau_1}) = 0 \qquad 31a$$

$$\hat{e}\cdot(\underline{\underline{RD}} - \underline{v}_{0\tau_2}) = 0. \qquad 31b$$

It should be noted that inherent in this process is that the choice of eigenvalue determines the wave velocity that the resulting equations will reflect.

With the two conditions expressed in equation 31 and the solutions of equation 25 we can "reconstitute" $v_{0\tau}$ by using equation 23, i.e.

$$v_{0_T} = v_{0_{T_0}} + \epsilon v_{0_{T_1}} + \delta v_{0_{T_2}},$$ 32

which will be valid for all times of $O(1/\epsilon, 1/\delta)$ and less.

Returning to the calculation at hand we note that

$$\underline{\underline{C}}_0 = \begin{vmatrix} 0 & 1 \\ 1 & 0 \end{vmatrix}$$

implies that $\omega_1=1, \omega_2=-1$, and $\underline{\underline{R}} = \frac{1}{\sqrt{2}} \begin{vmatrix} 1 & 1 \\ 1 & -1 \end{vmatrix}$, $\underline{\underline{R}}^{-1} = \frac{1}{\sqrt{2}} \begin{vmatrix} 1 & 1 \\ 1 & -1 \end{vmatrix}$.

Choosing to look at the $\omega=1$ solution then

$$\underline{v}_0 = \begin{vmatrix} v(\xi-\tau) \\ 0 \end{vmatrix} = \begin{vmatrix} v(x) \\ 0 \end{vmatrix}.$$

Now by using the imposed conditions expressed in equation 31 we get

$$v_{\tau_1} = -\frac{(1,0)}{2} \begin{vmatrix} 1 & 1 \\ 1 & -1 \end{vmatrix} \begin{vmatrix} v & v \\ 0 & v \end{vmatrix} \begin{vmatrix} 1 & 1 \\ 1 & -1 \end{vmatrix} \begin{vmatrix} v_x \\ 0 \end{vmatrix}$$

$$= -\frac{3}{2} v v_x$$

and

$$v_{\tau_2} = \frac{(1,0)}{2} \begin{vmatrix} 1 & 1 \\ -1 & -1 \end{vmatrix} \begin{vmatrix} \frac{1}{3}v_{xxx} \\ -v_{xxx} \end{vmatrix}$$

$$= -\frac{1}{3}v_{xxx}.$$

Reconstituting these results by using equation 32 yields

$$v_\tau + \frac{3\epsilon}{2}vv_x + \frac{\delta}{3}v_{xxx} = 0, \qquad 33$$

which is a form of the KdV equation for right running waves. Equation 33 can be cast into the standard form by scaling the spatial coordinate x by $\sqrt[3]{(3/\delta)}$ and the function v by $(4/\epsilon)\sqrt[3]{(\delta/3)}$ to get

$$u_t + 6uu_x + u_{xxx} = 0. \qquad 34$$

In deriving equation 34 we explicitly considered the hydrodynamical situation. A slightly less convoluted derivation of this equation, due to V.E. Zakharov[12], can be obtained by considering a nonlinear medium with a sound-like dispersion relation of the form

$$\omega^2 = s^2k^2(1+\epsilon k). \qquad 35$$

For small ϵk^2 we get

$$\omega \simeq \pm sk(1+ \frac{\epsilon}{2}k^2 + O(\epsilon^2))$$

where the different signs correspond to the different directions of propagation. With this dispersion law any quantity u that describes the medium has an evolution equation of the form

$$u_t = -su_x + \frac{s\epsilon}{2}u_{xxx} + O(\epsilon^2). \qquad 36$$

If we now suppose that s depends weakly on the amplitude u then s can be writen in terms of a perturbation expansion in terms of u, i.e.

$$s = s_0 + s_1u + O(u^2).$$

Substituting this expression for s into equation 36 yields

$$u_t = -s_0 u_x - s_1 u u_x + \frac{\epsilon s_0}{2} u_{xxx} + O(u^3) + O(\epsilon u^2).$$

Keeping only those terms up to order ϵu and u^2 gives

$$u_t + s_0 u_x + s_1 u u_x - \frac{\epsilon s_0}{2} u_{xxx} = 0. \qquad 37$$

Transforming this result to a frame of reference moving with velocity s_0 reduces equation 37 to

$$u_t + s_1 u u_x - \frac{\epsilon s_0}{2} u_{xxx} = 0. \qquad 38$$

Finally with the appropriate change of scale on x and u we get the KdV equation in standard form

$$u_t + 6 u u_x + u_{xxx} = 0.$$

Thus in general the KdV equation can be obtained for a medium with a sound-like dispersion law of the form given in equation 35, and a propagation speed that depends on the amplitude of the disturbance in a linear fashion.

CHAPTER II

THE INVERSE SCATTERING METHOD

Through a set of surprising results the team of Gardner, Green, Kruskal, and Miura (GGKM) found a connection between the KdV equation and the Schroedinger operator

$$L = \frac{\partial^2}{\partial x^2} + u(x,t) \qquad 1$$

where $u(x,t)$ is the solution to the KdV equation. The connection that they found can be best expressed in terms of a question: given a linear operator L, as in the form of equation 1, what restrictions are there on the function u such that the spectrum of L remains invariant with respect to continuous changes in t?

It was through this question that P.D. Lax[13] addressed the findings of GGKM. As Lax pointed out, if the spectrum of L is invariant with respect to changes in t then all of the L operators belonging to the same one parameter family can be mapped into a single operator L_0 by a unitary transformation U. Consequently the operator

$$U^{\dagger}(t)L(t)U(t) = L_0, \qquad 2$$

where † denotes the adjoint, is invariant with respect to t.

It is known, by a theorem due to M.H. Stone[14], that a unitary operator can be written in terms of an antiself-adjoint ($B^\dagger=-B$) generator, and that the differential equation relating the generator B to U is given by

$$U_t = BU. \qquad 3$$

If we now differentiate equation 2 with respect to t we get

$$U_t^\dagger LU + U^\dagger L_t U + U^\dagger L U_t = 0$$

where if we use equation 3 and note that $U_t^\dagger=-U^\dagger B$ we see that

$$L_t = [B,L], \qquad 4$$

which is the key result that connects the operators L and B, and implicitly defines the differential form of the function u(x,t) such that L is isospectral.

We can cast more light on the meaning of equation 4 by considering a consequence of equation 3. To do this we introduce the idea that the eigenfunctions $\phi(t)$ of $L(t)$ evolve according to

$$\phi(t) = U(t)\phi(0). \qquad 5$$

This can be easily seen by considering equation 2 and noting that $L(0)\phi(0)=\lambda\phi(0)$ to get that

$$U^{\dagger}(t)L(t)U(t)\phi(0) = \lambda\phi(0)$$

or

$$L(t)\phi(t) = \lambda\phi(t).$$

Differentiating equation 5 yields

$$\phi_t = U_t\phi(0)$$

but by equation 3 this becomes

$$\phi_t = B\phi. \qquad 6$$

Now we can, in fact, see that equation 4 is the compatibility condition on $u(x,t)$ that ensures that the eigenfunctions of L are also solutions to equation 6 for all time.

From the point of view of non-linear differential equations this approach may seem to be backwards in that it requires that we find two as of yet unknown operators, L and B, satisfying $L_t = [B,L]$, to characterize an single differential equation. Having to find two things from one highlights one of the drawbacks of this approach to solving partial differential equations. However, for the KdV equation, and for that matter many other physically interesting equations, the so-called Lax pairs L and B have been found.

If L happens to be the Schroedinger operator

$$L = \frac{\partial^2}{\partial x^2} + u(x,t) = D^2 + u \qquad 7$$

with $L\phi = \lambda\phi$, and if

$$B = -2(2\lambda + u)D + u_x \qquad 8$$

where $D = \frac{\partial}{\partial x}$ and $u = u(x,t)$,

then, $$[B,L] = -6uu_x - u_{xxx}$$

and $$L_t = u_t.$$

Thus the compatiblity condition, equation 4, yields the KdV equation

$$u_t + 6uu_x + u_{xxx} = 0 \qquad 9$$

in standard form. This result is in essence the suprising discovery made by GGKM. It tells us that the spectrum of the Schroedinger operator will remain invariant with respect to t, for this choice of generator, if the "potential" u(x,t) evolves according to the KdV equation. One could of course choose different generators and then find different compatibility conditions thus leading to different partial differential equations.

The connection between the KdV equation and the Schroedinger operator derived in equations 7 through 9 does not in itself define an inverse scattering framework, but it does give us a way by which we can characterize a non-linear equation in terms

of two linear operators. The inverse scattering method for solving linear or non-linear partial differential equations uses the decomposition into Lax pairs in a special sequence of three linear steps. These step are:

1. Solve the eigenvalue problem $L\phi=\lambda\phi$ at $t=0$,
2. Let the asymptotic form of ϕ evolve according to $\phi_t=B\phi$,
3. Invert $L\phi=\lambda\phi$ at some later $t>0$ to obtain $u(x,t)$.

The first of these steps is well understood, since it is a standard eigenvalue problem from undergraduate mathematics. In the case of the Schroedinger operator it is simply the scattering of wave packets off of a potential barrier or well, which is again standard problem. The second step, the evolution of the eigenfunctions, is also well understood and becomes simple under the assumption that the function $u(x,t)$ is on compact support, i.e. that $u(x,t)=0$ for all $|x|$ greater than some $x_c>0$. The third and final step, the inversion of the L operator to restore $u(x,t)$ is however a problem about which, in general, little is known. For the Schroedinger operator this problem was solved through the work of Gel'fand[15], Levitan[15], Marchenko[16], and Faddev[17], during the fifties.

Since we are dealing specifically with the KdV equation, the discussion from here on will pertain solely to that equation and the construction of the inverse scattering framework for it.

The direct problem:

In anticipation of some of the concepts needed for the inversion problem certain seemingly unnecessary results will be derived here. For the sake of brevity many of the fine points have been neglected. For a much fuller treatment the texts by Calogero[18], Lamb[19],or Dodd et al[20] are recommended.

To continue with the problem, we seek solutions to the the eigenvalue problem

$$(D^2 + u(x,0))\phi = -k^2\phi, \qquad 10$$

which, as was mentioned earlier, corresponds to the standard scattering problem encountered in undergraduate physics. By assuming a solution of the form

$$\phi(x) = \alpha(x)e^{ikx} + \beta(x)e^{-ikx} \qquad 11$$

and by using the technique of variation of parameters, wherein we set

$$\alpha_x e^{ikx} + \beta_x e^{-ikx} = 0,$$

we find that

$$\alpha_x = -\frac{u\phi}{2ik}e^{-ikx}, \qquad 12a$$

$$\beta_x = \frac{u\phi}{2ik}e^{ikx}. \qquad 12b$$

For scattering problems on the infinite interval it is customary to express all the solutions of the Schroedinger equation in terms of Jost functions, or fundamental solutions. These functions have the asymptotic forms

$$\phi_1 \longrightarrow e^{-ikx} \qquad x \longrightarrow -\infty \qquad 13a$$

$$\phi_2 \longrightarrow e^{ikx} \qquad x \longrightarrow -\infty \qquad 13b$$

$$\psi_1 \longrightarrow e^{-ikx} \qquad x \longrightarrow \infty \qquad 13c$$

$$\psi_2 \longrightarrow e^{ikx} \qquad x \longrightarrow \infty. \qquad 13d$$

By using these asymptotic conditions and the results of the variation of parameters calculation, equations 12a,b we get

$$\phi_1 = e^{-ikx}\left(1 + \frac{1}{2ik}\int_{-\infty}^{x} u\phi_1 e^{iky}dy\right) - \frac{e^{ikx}}{2ik}\int_{-\infty}^{x} u\phi_1 e^{-iky}dy$$

which can be simplified to

$$\phi_1 = e^{-ikx} - \frac{1}{k}\int_{-\infty}^{x} u\phi_1 \sin(k(x-y))dy. \qquad 14a$$

By similar calculations we get

$$\phi_2 = e^{ikx} - \frac{1}{k}\int_{-\infty}^{x} u\phi_2 \sin(k(x-y))dy \qquad 14b$$

$$\psi_1 = e^{-ikx} + \frac{1}{k}\int_{x}^{\infty} u\psi_1 \sin(k(x-y))dy \qquad 14c$$

$$\psi_2 = e^{ikx} + \frac{1}{k}\int_{x}^{\infty} u\psi_2 \sin(k(x-y))dy, \qquad 14d$$

which then form the complete set of Jost functions for the Schroedinger eigenvalue problem for real k.

These solutions can be analytically continued in complex k space. If we look at the first and second terms of the Neumann series expansion for the four integral equations 14(a-d) we find for ϕ_1, at least, that

$$\phi_1 \simeq e^{-ikx}\left(1 - \frac{1}{2ik}\int_{-\infty}^{x} u\left(e^{2ik(x-y)} - 1\right) dy\right), \qquad 15$$

the other three having similar expressions. Equation 15 will be convergent if $Im(k)>0$ since $e^{2ik(x-y)} \longrightarrow 0$ if $k\longrightarrow\infty$ $Im(k)>0$. Similarly ψ_2 is convergent if $Im(k)>0$ and ϕ_2, ψ_1 are convergent if $Im(k)<0$. Thus ϕ_1 and ψ_2 have analytical continuations in the upper half plane, and ϕ_2 and ψ_1 in the lower half plane of k space. This result is important for both the direct and the inverse problems.

Since the Schroedinger eigenvalue problem is a second order differential equation only two of the Jost functions are needed to form a basis for its solution space. Thus any two of the solutions are expressible as linear combinations of the other two solutions. From equation 12 we note that the asymptotic behaviour of ϕ_1 as $x\longrightarrow\infty$ is of the form

$$\phi_1 \longrightarrow a(k)e^{-ikx} + b(k)e^{ikx} \qquad x\longrightarrow\infty.$$

If we also note that for real k

$$\phi_2(k) = \phi_1(-k) = \phi_1^*(k)$$

we get that

$$\phi_2 \longrightarrow a^*(k)e^{ikx} + b^*(k)e^{ikx} \qquad x\longrightarrow\infty.$$

Using the asymptotic ($x\longrightarrow\infty$) forms for ψ_1 and ψ_2 yields

$$\phi_1 = a(k)\psi_1 + b(k)\psi_2 \qquad 16a$$

$$\phi_2 = a^*(k)\psi_2 + b^*(k)\psi_1 \qquad 16b$$

which hold on all R.

If we now look at the Wronskian for ϕ_1 and ψ_2, which can both be analytically continued in the upper half plane for k, we get that

$$W(\phi_1,\psi_2) = 2ika$$

where we have used the asymptotic forms for ϕ_1 and ψ_2 since

$$\frac{d}{dx}W(\phi_1,\psi_2) = 0.$$

This tells us that a(k) is analytically continuable in the upper half plane, since both ϕ_1 and ψ_2 can be represented there.

With this result it is now possible to discuss the bound state solutions for the Schroedinger equation. On physical grounds we know that the bound state eigenvalues lie on the imaginary axis, with $k=i\kappa_n$ (κ_n real), that they are discrete and finite in number. From the asymptotic ($x\longrightarrow-\infty$) form for ϕ_1 we find that ϕ_1 is bounded if $\kappa_n>0$ and from the other asymptotic ($x\longrightarrow+\infty$) form that $a(i\kappa_n) = 0$. Similar analysis can be carried out for the other solutions, but that is unnecessary since we only need the bound states for ϕ_1. What is of interest is the fact that the discrete spectrum for ϕ_1 lies on the upper half of the imaginary axis and that a(k)=0 at these points. It should be mentioned that the zeros of a(k) are simple since the eigenfunctions of the one dimensional Schroedinger equation are non-degenerate, and that at the points of the discrete spectrum equation 16a reduces to

$$\phi_1 = b(i\kappa_n)\psi_2. \qquad 17$$

This set of results should be sufficient to construct the inverse framework, and is more than necessary for the direct problem. For the direct problem all that we really require are the functional forms of a(k) and b(k).

The Evolution Problem:

In order to pose this problem correctly we must introduce a more general form for the solution of the Schroedinger scattering problem. Here we let ϕ have the asymptotic behaviour

$$\phi \longrightarrow \alpha(t,k)e^{-ikx} \qquad x\longrightarrow -\infty \qquad 18a$$

$$\phi \longrightarrow \beta(t,k)e^{-ikx} + \gamma(t,k)e^{ikx} \qquad x\longrightarrow \infty. \qquad 18b$$

This slight change in the form of the solutions was introduced in order to illustrate a point; we can at any time t regain the original forms of ϕ by dividing through by α.

Noting that u(x,t) is on compact support we get from equation 8 that the asymptotic form of the evolution operator B is given by

$$B \longrightarrow 4k^2D \qquad x\longrightarrow \pm\infty.$$

Then by equation 6 the eigenfunctions evolve according to

$$\phi_t = 4k^2\phi_x.$$

By substitution of the asymptotic form for ϕ, equations 18(a,b) into the asymptotic evolution equation we get

$$\dot{\alpha} = -4ik^3\alpha \qquad 19a$$

$$\dot{\beta} = -4ik^3\beta \qquad 19b$$

$$\dot{\gamma} = 4ik^3\gamma, \qquad 19c$$

where the dot (˙) indicates differentiation with respect to time. Integrating these results leads to

$$\alpha(t) = \alpha(0)e^{-4ik^3t} \qquad 20a$$

$$\beta(t) = \beta(0)e^{-4ik^3t} \qquad 20b$$

$$\gamma(t) = \gamma(0)e^{4ik^3t}. \qquad 20c$$

If we now introduce the regular nomenclature of the scattering problem, with the reflection coefficient given by

$$r = \frac{\gamma}{\beta} = \frac{b}{a},$$

and the transmission coefficient by

$$t = \frac{\alpha}{\beta} = \frac{1}{a},$$

we find that by substitution of the time dependent forms given in equation 20(a-c) that the reflection and transmission coefficients evolve according to

$$r(t) = r(0)e^{8ik^3t} \qquad 21a$$

$$t(t) = t(0). \qquad 21b$$

The latter of these two equations shows that the spectrum of L remains invariant, since it implies that a(λ) is invariant.

By applying the same analysis for the discrete spectrum we get the asymptotic forms

$$\phi \longrightarrow \alpha_n(t)e^{\kappa_n x} \qquad x \longrightarrow -\infty$$

$$\phi \longrightarrow \gamma_n(t)e^{-\kappa_n x} \qquad x \longrightarrow \infty$$

and from

$$\phi_t = -4\kappa_n^2\phi_x$$

that

$$\dot{\alpha}_n = -4\kappa_n^3\alpha_n \qquad 22a$$

$$\dot{\gamma}_n = 4\kappa_n^3\gamma_n. \qquad 22b$$

On integeration these yield

$$\alpha_n(t) = \alpha_n(0)e^{-4\kappa_n^3 t}$$

$$\gamma_n(t) = \gamma_n(0)e^{4\kappa_n^3 t}.$$

Since b(k,t), from equation 17, is defined by $b=\gamma/\alpha$, we get that

$$b(i\kappa_n,t) = b(i\kappa_n,0)e^{8\kappa_n^3 t}. \qquad 23$$

The results given in equations 21 and 23 fully define the evolution problem for the eigenfunctions of L in terms of the evolution of the reflection and transmission coefficients.

The Inverse Problem:

Here we reconstruct the potential u(x,t) from the scattering data after it has evolved according to the KdV equation to some time t.

For the present we consider the solution ψ_2 and write it in the form

$$\psi_2 = e^{ikx} + \int_{-\infty}^{\infty} K(x,y)e^{iky}dy \qquad 24$$

where K(x,y) is some as of yet unknown function. From the asymptotic ($k\longrightarrow\infty$, $Im(k) > 0$) expansion of the actual solution for ψ_2, given in equation 14d,

$$\psi_2 \simeq e^{ikx} + \frac{e^{ikx}}{2ik} \int_x^\infty u\, dy + O\left(\frac{1}{k^2}\right) \qquad 25$$

we see that the function K(x,y) decays exponentially in this asymptotic limit. Thus by considering a contour in the upper half plane we find, from equation 24 that

$$K(x,y) = 0 \text{ if } y<x$$

and thus equation 25 can be rewritten as

$$\psi_2 = e^{ikx} + \int_x^\infty K(x,y)e^{iky}dy. \qquad 26$$

Moreover if we look at the asymptotic ($k \longrightarrow \infty$ $Im(k)>0$) expansion for equation 25 we get that

$$\psi_2 \simeq e^{ikx} - \frac{K(x,x)}{ik}e^{ikx} + O(1/k^2) \qquad 27$$

which was obtained by integrating by parts. Comparing, term by

term equations 23 and 26 reveals that

$$\int_x^\infty u(y)dy = -2K(x,x)$$

or that

$$u(x) = 2\frac{d}{dx}K(x,x) \qquad 28$$

which defines the relationship between the, as of yet, unknown function $K(x,x)$ and the scattering potential $u(x)$. Recalling equation 16a and noting that

$$\psi_1 = e^{-ikx} + \int_x^\infty K(x,y)e^{-iky}dy$$

yields

$$\phi_1 = a(k)(e^{-ikx} + \int_x^\infty K(x,y)e^{-iky}dy) +$$

$$b(k)(e^{ikx} + \int_x^\infty K(x,y)e^{iky}dy)$$

or that

$$\frac{\phi_1}{a(k)} - e^{-ikx} = \int_x^\infty K(x,y)e^{-iky}dy +$$

$$+ r(k)(e^{ikx} + \int_x^\infty K(x,y)e^{iky}dy).$$

By multiplying this equation by $e^{ikz}/2\pi$ and integrating over k we get

$$\frac{1}{2\pi}\int_{-\infty}^{\infty} \left(\frac{\phi_1}{a(k)} - e^{-ikx}\right)e^{ikz}dk =$$

$$K(x,z) + F(x+z) + \int_x^\infty F(y+z)K(x,y)dy \qquad 29$$

with $$F(\xi) = \frac{1}{2\pi}\int_{-\infty}^{\infty} r(k)e^{ik\xi}dk.$$

Since ϕ_1 is an analytic function of k in the upper half plane, and observing the restriction that z>x, and noting that a(k) has only simple poles in the upper half plane we get that the integral on the left hand side of 29 is just the sum of the residues of $\frac{\phi_1}{a(k)}$, thus

$$\frac{1}{2\pi}\int_{-\infty}^{\infty} \left(\frac{\phi_1}{a(k)} - e^{-ikx}\right)e^{ikz}\,dk = \sum \frac{i\phi_1(x,i\kappa_n)}{a'(i\kappa_n)}\,e^{-\kappa_n z}$$

where n is the number of zeros of a(k).

By the relation, equation 17, between ϕ_1 and ψ_2 at the points of the discrete spectrum we get that equation 29 can be rewritten in terms of ψ_2 by

$$\sum \frac{i\phi_1(x,i\kappa_n)}{a'(i\kappa_n)} e^{-\kappa_n z} = \sum \frac{ib(i\kappa_n)}{a'(i\kappa_n)} \psi_2(x,i\kappa_n) e^{-\kappa_n z} . \qquad 30$$

Setting the numbers $ib(i\kappa_n)/a'(i\kappa_n) = -M_n$, the left hand side of equation 30 becomes

$$- \sum M_n \psi_2(x,i\kappa_n) e^{-\kappa_n z} . \qquad 31$$

Since equation 24 can be written in terms of the eigenvalues we get that

$$\psi_2(i\kappa_n) = e^{-\kappa_n x} + \int_x^\infty K(x,y) e^{-\kappa_n y} dy, \qquad 32$$

and 30, finally, becomes

$$- \sum M_n e^{-\kappa_n x} - \sum M_n \int_x^\infty K(x,y) e^{-\kappa_n y} dy.$$

By redefining $F(\xi)$ by

$$F(\xi) \longrightarrow \tilde{F}(\xi) = F(\xi) + \sum M_n e^{-\kappa_n \xi}$$

we get that equation 28 becomes

$$0 = K(x,z) + \tilde{F}(x+z) + \int_x^\infty \tilde{F}(y+z) K(x,y) dy. \qquad 33$$

This is the Marchenko equation; a linear integral equation by which we can invert the Schroedinger operator to find the potential $u(x,t)$. It should be noted that all we need to know are the reflection coefficient $r(k)$, and the values of $a'(k)$ and $b(k)$ at the points in the discrete spectrum of $u(x,0)$, in order to construct $K(x,y)$ and by equation 28 $u(x)$.

This result can now be easily extended to take into account the time evolution of the scattering data ($r(k), a, b$) by recalling the results of the evolution problem and correspondingly redefining $\tilde{F}(\xi)$ to be

$$\tilde{F}(\xi,t) = \frac{1}{2\pi}\int_{-\infty}^{\infty} r(k,0)e^{ikx-8ik^3t}dk + \sum M_n\, e^{-\kappa_n\xi-8\kappa_n^3t}. \qquad 34$$

Since t enters as a parameter this result can now be used as the kernel for the Marchenko equation, from which the potential u(x,t) can be constructed from the initial data u(x,0) after it has evolved a time t.

The final results of the preceding sections define the inverse scattering formalism for the KdV equation, in general terms.

CHAPTER III

THE RADIATION SOLUTION

In chapter 2 we showed that the initial value problem for the KdV equation could, in principle, be solved by executing the sequence of linear steps that make up the Inverse Scattering method. The third and final step of this method involves solving the Marchenko equation, a linear Volterra type integral equation. The kernel of this equation, given by

$$F(\zeta) = \frac{1}{2\pi}\int_{-\infty}^{\infty} r(k)e^{ik\zeta}dk + \sum_{n=0}^{m} M_n^2 e^{-\kappa_n \zeta}, \qquad 1$$

was derived in chapter 2. As is easily seen this kernel is comprised of two distinct parts, the first (integral) part comes from the continuous spectrum of the Schroedinger operator, and the second (sum) from the discrete spectrum. These distinct forms physically manifest themselves in different ways. The continuous spectrum leads to radiation solutions, i.e. solutions that reflect the dispersive nature of the KdV equation by spreading spatially as time evolves. The discrete spectrum leads to the now famous soliton solutions, i.e. solutions that retain their profile as time evolves, even under collisions with similar objects, indicating that the dispersion inherent to the KdV equation is exactly cancelled by the non-linearity of the equation. In the case for arbitrary initial data the general

solution will be some non-linear mixture of these two types of solutions, however as time evolves it is the soliton solutions that survive asymptotically while the radiation solutions disperse. It is the dispersion of the radiation solution that indicates the appropriate direction for time.

It can be shown (see Appendix 1) that it is possible to construct initial data such that no solitons will appear. Physically this corresponds to an initial situation in which the fluid surface was depressed, as opposed to elevated. This asymmetry in the nature of the solutions to the KdV equation is evident if it is noted that the equation is not invariant under reflection about the fluid surface (u—>-u).

If the initial data is properly constructed to exclude soliton solutions the kernel for the Marchenko equation would become simply

$$F(\zeta) = \frac{1}{2\pi}\int_{-\infty}^{\infty} r(k)e^{ik\zeta}dk, \qquad 2a$$

or if we include the full time dependence of the reflection coefficient

$$F(\zeta,t) = \frac{1}{2\pi}\int_{-\infty}^{\infty} r(k)e^{ik\zeta+8ik^3t}dk. \qquad 2b$$

By chosing the initial data for the KdV equation appropriately

we have decoupled the two possible types of solutions that manifest themselves for arbitrary data. This allows us to concentrate on the radiation solutions without having to worry about the interaction of the two types of solutions. It should be reiterated that if no solitons exist initially then no solitons will ever appear. This is a consequence of the fact that the spectrum of the initial data is invariant as time evolves, and thus if no imaginary eigenvalues exist initially then none will magically appear at some later time.

As was mentioned earlier, relatively few people have looked at the radiation solutions of any of the non-linear evolution equations, much less for the KdV equation, owing to its complexity. However by using the method of stationary phase the team of M.J. Ablowitz and H. Segur[21] were able to extract the temporal asymptotic behaviour of the radiation solutions. By considering specific initial value problems for which the Schroedinger scattering problem was explicitly solvable and expanding the reflection coefficient in terms of an area-like expansion parameter the team of R.H.Enns and S.S. Rangnekar[22] obtained the short time behaviour. In earlier papers, using the dimensionless area as the natural parameter they were able to obtain the complete temporal evolution of the radiation solutions for the 3-wave problem, the sine-Gordon and the sinh-Gordon equatons, the modified KdV equation, and the non-linear Schroedinger equations. The first is characterized by the Zakharov - Manakov eigenvalue problem, the remainder by the

Zakharov - Shabat eigenvalue problem. It was anticipated that the same procedure would give the complete temporal evolution of the radiation solution of the KdV equation. Because of the different inverse scattering structure, this did not turn out to be the case, their series representation breaking down at some finite time. Thus, the complete time evolution of the radiation solution of the KdV equation has to the best of our knowledge not been carried out in the literature. The work of this thesis represents an alternative approach to solving the problem.

Fundamental to both of the previously mentioned approaches to solving the KdV equation is the idea that the Marchenko equation can be expanded in terms of a Neumann expansion, a succesive approximation scheme in which the solution is an iteration of the kernel,

$$K_0(x,y) = -F(x+y) \tag{3a}$$

$$K_1(x,y) = -F(x+y) + \int_x^\infty F(x+z)F(z+y)dz \tag{3b}$$

$$K_2(x,y) = -F(x+y) + \int_x^\infty F(x+z)F(z+y)dz$$

$$- \int_x^\infty \int_x^\infty F(x+w)F(w+z)F(z+y)dzdw \tag{3c}$$

etc.

The convergence of this sequence to the function K(x,y) has been shown by H.Segur[23]. Use of the representation will be made in what is to follow, however this is not the point that presents a stumbling block in trying to find analytical solutions.

One of the major difficulties encountered in the search for analytical solutions is the occurrence of the cubic term in the time evolution of the reflection data. As a consequence of this term, even for those reflection coefficients that are exactly solvable, the exact analytical form of the kernel of the Marchenko equation is elusive in that the final integration is difficult if not impossible to do analytically. This problem can be circumvented by noting that the kernel F(x,t) is a well defined function of two variables and can be expanded biorthogonally in terms of orthogonal functions in x and orthogonal functions in t, i.e.

$$F(x,t) = \sum f_{mn}\psi_m(x)\phi_n(t) \qquad 4$$

where $$\int_{-\infty}^{\infty} \psi_m(x)\psi_n(x)\,dx = \delta_{mn} \qquad 5a$$

and $$\int_{-\infty}^{\infty} \phi_m(x)\phi_n(x)\,dx = \delta_{mn}. \qquad 5b$$

With this type of representation the spatial and temporal dependence of $F(\xi,t)$ would be moved from under the integral defining F and into functions whose analytical structure is more readily accessible. However this expression leaves the calculation of the expansion coefficients f_{mn} to be done. By the orthogonality of the sets of functions ψ_m and ϕ_m the f_{mn}'s can be calculated by

$$f_{mn} = \int\int_{-\infty}^{\infty} F(\xi,t)\psi_m(\xi)\phi_n(t)d\xi dt,$$

or if we use the explicit form for F,

$$f_{mn} = \frac{1}{2\pi}\int\int\int_{-\infty}^{\infty} r(k)e^{ik\xi+8ik^3t}\psi_m(\xi)\phi_n(t)d\xi dtdk, \qquad 6$$

where we have rearranged the order of the integration.

Given this type of expansion for the kernel $F(x,t)$ we can now go about the task of solving the Marchenko equation,

$$K(x,y;t) + F(x+y;t) + \int_x^{\infty} K(x,z;t)F(z+y;t)dz = 0. \qquad 7$$

Defining

$$K(x,y;t) = k_{mn\alpha}\psi_m(x)\ \psi_m(y)\phi_m(t) \qquad 8a$$

and

$$F(x+y;t) = f_{m\alpha}\phi_m(x+y)\ \psi_\alpha(t)\ , \qquad 8b$$

$$= f_{mn\alpha}\phi_m(x)\ \phi_n(y)\ \psi_\alpha(t)\ , \qquad 8c$$

and

$$\int_x^\infty K(x,z;t)F(z+y;t)dz = g_{mn\alpha}\phi_m(x)\ \phi_n(y)\ \psi_\alpha(t)\ . \qquad 8d$$

where summation over repeated indices is assumed, and Roman subscripts indicate an expansion spatially and Greek subscripts a temporal expansion. On substitution of these representations into the Marchenko equation we get

$$(k_{mn\alpha} + f_{mn\alpha} + g_{mn\alpha})\phi_m(x)\ \phi_n(y)\ \psi_\alpha(t) = 0. \qquad 9$$

Since all of the functions $\phi_m(x)$, $\phi_n(y)$, and $\psi_\alpha(t)$ are linearly independent then all of the coefficients of equation 9 must be zero, i.e.

$$(k_{mn\alpha} + f_{mn\alpha} + g_{mn\alpha}) = 0. \qquad 10$$

However the $g_{mn\alpha}$'s are still dependent on the $k_{mn\alpha}$'s. This dependence can be determined by returning to the definition of the g's and noting that the right hand side of

$$g_{mn\alpha}\phi_m(x)\ \phi_n(y)\ \psi_\alpha(t) = \int_x^\infty K(x,z;t)F(z+y;t)\ dz$$

can be written as

$$\int_x^\infty k_{ij\beta}\phi_i(x)\ \phi_j(z)\ \psi_\beta(t)\ f_{kn\delta}\phi_k(z)\ \phi_n(y)\ \psi_\delta(t)\ dz \qquad 11a$$

$$= k_{ij\beta}f_{kn\delta}\phi_i(x)\ \phi_n(y)\ \psi_\beta(t)\ \psi_\delta(t) \int_x^\infty \phi_j(z)\ \phi_k(z)\ dz. \qquad 11b$$

Formally we can define

$$\int_x^\infty \phi_j(z)\ \phi_k(z)\ dz = I_{jkp}\phi_p(x)\ , \qquad 12a$$

and $$\phi_i(x)\ \phi_j(x) = P_{ijk}\phi_k(x)\ , \qquad 12b$$

and $$\psi_\alpha(t)\ \psi_\beta(t) = P_{\alpha\beta\gamma}\psi_\gamma(t)\ . \qquad 12c$$

With these expressions equation 11b becomes

$$- g_{mn\alpha}\phi_m(x)\ \phi_n(y)\ \psi_\alpha(t) = k_{ij\beta}f_{kn\gamma}I_{jkp}\ P_{ipm}\tilde{P}_{\alpha\beta\gamma}\phi_m(x)\ \phi_n(y)\ \psi_\alpha(t)$$

and thus

$$g_{mn\alpha} = k_{ij\beta}f_{kn\gamma}\ I_{jkp}P_{ipm}\tilde{P}_{\beta\gamma\alpha}. \qquad 13$$

If this expression is substituted into equation 10 for g we note that the Marchenko equation becomes

$$k_{mn\alpha} + f_{mn\alpha} + k_{ij\beta}f_{kn\gamma}I_{jkp}\ P_{ipm}\tilde{P}_{\beta\gamma\alpha} = 0,$$

or that $$k_{ij\beta}(\delta_{im}\delta_{jn}\beta_{\alpha\beta} + f_{kn\gamma}\ I_{jpq}P_{ipm}\ \tilde{P}_{\beta\gamma\alpha}) = - f_{mn\alpha}. \qquad 14$$

This can be written in a more compact form by letting

$$A_{ij\beta mn\alpha} = \delta_{im}\delta_{jn}\delta_{\alpha\beta} + f_{kn\gamma}\ I_{jkp}P_{ipm}\ \tilde{P}_{\beta\gamma\alpha}. \qquad 15$$

In this case equation 14 becomes

$$k_{ij\beta}A_{ij\beta mn\alpha} = - f_{mn\alpha}. \qquad 16$$

If we define the composite indices

$$I = ij\beta \qquad\qquad J = mn\alpha$$

then equation 16 yields the simple matrix equation

$$k_I A_{IJ} = -f_J. \qquad 17$$

This can, in principle, be solved to get the expansion coefficients of the function K(x,y,t) by assuming that the right inverse of [A] exists, and is defined by $[A^{-1}]$ with components $A^{-1}{}_{IJ}$, in which case we get that

$$k_I = -f_J \, A^{-1}{}_{JI}. \qquad 18$$

This equation defines the problem of solving the Marchenko equation. To find the solution we have to find the right inverse of the matrix [A]. This is, however, no simple task in that the matrix is infinite dimensional, and at best we can find the inverse of a truncated version of [A] and hope that the error associated with the truncation is small.

In order to find a scheme for inverting the operator A, it was noted that it is possible to set up an iterated approximation scheme for the Marchenko equation in integral form. To develop similar approach for the present representation of the Marchenko equation, equation 17, we return to equation 14 and rewrite it in the form

$$k_{mn\alpha} = -f_{mn\alpha} - k_{ij\beta} f_{kn\gamma} I_{jkp} P_{ipm} P_{\beta\gamma\alpha}. \qquad 19$$

In exactly the same way that the Neumann series was generated for the Marchenko equation, a successive approximation scheme can be implemented for equation 19, by iterating, i.e.

$$k^{0}_{mn\alpha} = -f_{mn\alpha} \qquad 20a$$

$$k^{1}_{mn\alpha} = -f_{mn\alpha} + f_{ij\beta} f_{kn\gamma} I_{jkp} P_{ipm} P_{\beta\delta\alpha} \qquad 20b$$

$$k^2_{mn\alpha} = -f_{mn\alpha} + f_{ij\beta}f_{kn\gamma}\, I_{jkp}P_{ipm}\tilde{P}_{\beta\gamma\alpha}$$

$$- f_{rs\delta}f_{tj\epsilon}I_{stu}\, P_{rui}\tilde{P}_{\delta\epsilon\beta}\, f_{kn\gamma}I_{jkp}P_{ipm}\, \tilde{P}_{\gamma\delta\alpha} \qquad 20c$$

.

.

.

etc.

Introducing the compact notation $I = I_{ijk}$ $P = P_{ijk}$ $\tilde{P} = \tilde{P}_{\alpha\beta\gamma}$ $f = f_{ij\alpha}$ and $k = k_{ij\alpha}$ the n^{th} approximation becomes

$$k^n = -f + ffI\tilde{P} - fffII\tilde{P}P\tilde{P} + ...$$

$$= -f \sum_{m=0}^{n} (-1)^m \, (fI\tilde{P})^m .$$

In the limit that $n \longrightarrow \infty$ we get

$$k^{\infty} = -f \sum_{m=0}^{\infty} (-1)^m \, (fIP\tilde{P})^m. \qquad 21$$

This is just the series representation for $(1+fIP\tilde{P})^{-1}$ and in fact $(1 + fIP\tilde{P})$ is just the matrix A that was previously defined. From this we see that in the limit that $n \longrightarrow \infty$ the sucessive approximation scheme converges to the actual value of k since

$$k^{\infty} = -f(1+fIP\tilde{P})^{-1} = -fA^{-1} = k,$$

and as such can be used to explore the radiation solutions for the KdV equation by looking at the behaviour of the successive terms.

In order to obtain the explicit form of the solution to the specific initial value at hand we must recall the result

$$u(x,t) = 2 \frac{d}{dx} K(x,x,t)$$

from chapter 2, where u(x,t) is the solution to the KdV equation and K(x,x,t) the corresponding solution to the Marchenko equation. The function K(x,y,t) is to be evaluated at y=x and then differentiated. In terms of the expanded representation of K(x,y,t) these operations take on the form

$$\frac{d}{dx}K(x,x,t) = k_{mn\alpha}\psi_{\alpha}(t) \quad \frac{d}{dx}(\phi_m(x)\ \phi_n(x)\ ). \qquad 22$$

This can be taken further by noting that there exist differential relations between the functions that comprise the set $\{\phi_m\}$, of the form

$$g_2(x)\ \frac{d}{dx}\phi_m(x) = g_1(x)\phi_m(x) + g_0(x)\phi_{m-1}(x)\ , \qquad 23$$

where we have assumed that the basis functions are solutions to second order ordinary differential equations. The functions g_0, g_1, and g_2 are in general functions of both the independent variable x and the order of the function being differentiated. With this interrelationship between the basis functions the derivatives on the left hand side of equation 22 can be explicitly evaluated to yield

$$u(x,t) = 2\left(\frac{g_1(x)}{g_2(x)} k_{mn\alpha} + \frac{g_0(x)}{g_2(x)} (k_{mn+1\alpha} + k_{m+1n\alpha}) \right) \cdot$$

$$\cdot \phi_m(x)\ \phi_n(x)\ \psi_\alpha(t) \ . \qquad 24$$

This gives an explicit representation for the radiation solution to the KdV equation.

So far we have derived these results for expansions in terms of arbitrary orthogonal functions ϕ_n and ψ_n . In order to carry out any explicit calculations these functions have to be defined. As a guiding criteria for making the appropriate choice we note that the kernel of the Marchenko equation $F(x,t)$ must be defined on the entire real line R, spatially, and on the interval $(0,\infty)$ temporally. Thus the set $\{\phi_n\}$ must be orthogonal on R and the set $\{\psi_n\}$ must be orthogonal on $(0,\infty)$.

Another guide for the selection of the appropriate basis functions was the idea that the integeral defined in equation 6 be explicitly doable. This requirement involved a search of various tables of integrals, primarily the one compiled by Gradstyen and Ryzhik[25]. Two possible candidates that came to light were the normalized oscillator functions, which are defined by

$$\Theta_m(x) = e^{-x^2/2}\ H_m(x)\ /\ \sqrt{2^m m!\sqrt{\pi}}, \qquad 25$$

where the functions $H_m(x)$ are the Hermite polynomials, and the Laguerre functions

$$L_m(x) = e^{-x/2}L_m(x) \qquad 26$$

where the functions $L_m(x)$ are the Laguerre polynomials. The oscillator functions are orthogonal on R and the Laguerre functions are orthogonal on the interval $\{0,\infty\}$. Other well explored sets of orthogonal functions that satisfy the imposed conditions may exist but this study made no attempt to search for them once the oscillator and Laguerre functions had been found to work.

Since the Laguerre polynomials are unity at the origin for all orders it was thought that the convergence of an expansion over these functions in the neighbourhood of the origin would be slow, and consequently they were rejected in preference for the oscillator functions.

For the purposes of this thesis we settled on the oscillator functions as the basis functions for both the spatial and temporal expansions and we formally identify the functions $\phi_n(x)$ and $\psi_n(t)$ with $\theta_n(x)$ and $\theta_n(t)$ respectively. The fact that the oscillator functions were used to expand temporally did not present a problem with respect to the domain of definition since the temporal part of the kernel $F(x,t)$ is well defined for $t<0$.

In satisfying the requirement that both the spatial and temporal integrals of equation 6 be doable we note that

$$\int_{-\infty}^{\infty} e^{iyx}\theta_m(x)\,dx = i^m\theta_m(y)\ , \qquad 27$$

from G-R sec. 7.374. From this we can evaluate the expansion coefficients of F(x,t) explicitly through

$$f_{m\alpha} = \frac{i^{m+\alpha}}{\sqrt{2\pi}} \int_{-\infty}^{\infty} r(k)\theta_m(k)\ \theta_\alpha(k^3)\,dk. \qquad 28$$

Similarly the components of the matrices $f_{mn\alpha}$, I_{ijk}, and P_{ijk} now take on the definite form,

$$f_{mn\alpha} = \frac{i^{m+n+\alpha}}{\sqrt{2\pi}} \int_{-\infty}^{\infty} r(k)\theta_m(k)\ \theta_n(k)\ \theta_\alpha(k^3)\ .dk \qquad 29a$$

and
$$I_{ijk} = \int_{-\infty}^{\infty}\int_{x}^{\infty} \theta_i(y)\ \theta_j(y)\,dy\ \theta_k(x)\,dx, \qquad 29b$$

and
$$P_{ijk} = \int_{-\infty}^{\infty} \theta_i(x)\ \theta_j(x)\ \theta_k(x)\,dx, \qquad 29c$$

and the components of I and P can be calculated explicitly (see Appendix 5).

With the basis functions chosen and the matrices I and P evaluated we can now proceed to, either calculate a truncated version of the matrix A and then invert it or we can evaluate the successive terms in the iteration scheme, to find reasonable approximations to the expansion coefficients of K(x,y,t). With the expansion coefficients calculated we can use the explicit form of equation 23, as it pertains to the Oscillator functions, i.e.

$$\frac{d}{dx}\theta_m(x) = -x\theta_m(x) + 2m\theta_{m-1}(x) \quad , \tag{30}$$

with $g_2(x)=1$, $g_1(x)=-x$, and $g_0=2m$, to get the radiation solution for the KdV equation

$$u(x,t) = 2(-xk_{mn\alpha} + 2m(k_{mn+1\alpha} + k_{m+1n\alpha})) \bullet$$

$$\bullet\ \theta_m(x)\ \theta_n(x)\ \theta_\alpha(t) \quad . \tag{31}$$

In the following chapters it is the latter approach that is pursued for various initial pulses. The inversion procedure is not explored due to lack of facility to carry out the calculation to high enough order for reasonable convergence.

CHAPTER IV

SQUARE WELL INITIAL VALUE PROBLEM

In the preceding three chapters the framework for obtaining the radiation solutions for the KdV equation was explored. Here those methods are applied to a concrete example.

As data for the initial value (U(x,0)) problem a finite square well of unit depth and arbitrary width w was chosen because of the ease with which the Schroedinger scattering problem can be solved and the reflection coefficient r(k) obtained. Without resorting to the integral representations of the solutions for the Schroedinger equation, see equations 2.14, the reflection coefficient can be obtained by the technique of matching solutions at the boundaries defined by x=0 and x=w. Assuming an incident wave from the right (x=∞) of wave number k and amplitude A, we get solutions for the three regions x<0, 0<x<w, w<x, of the form

$$\Phi_1 = Ae^{-ikx} + Be^{ikx} \qquad w<x \qquad 1a$$

$$\Phi_2 = Ce^{-i\sqrt{k^2-1}x} + De^{i\sqrt{k^2-1}x} \qquad 0<x<w \qquad 1b$$

$$\Phi_3 = e^{-ikx} \qquad x<0, \qquad 1c$$

where we have assumed, so as to be consistent with the ISM derivation in chapter 2, that the transmitted wave has unit amplitude. From the constraint that the solution Φ on R be continuous and continuously differentiable, we get that

$$\Phi_1 = \Phi_2 \quad \text{and} \quad \Phi_1' = \Phi_2' \quad \text{at } x=w, \tag{2a}$$

$$\text{and} \quad \Phi_2 = \Phi_3 \quad \text{and} \quad \Phi_2' = \Phi_3' \quad \text{at } x=0. \tag{2b}$$

From these four conditions we can solve for the unknowns A,B,C,and D, but since it is the reflection coefficient, defined here by the ratio of B/A, that is required in the application of the ISM, we need find A and B only. So as not to bore the reader, the results of this standard calculation are quoted as being:

$$r(k) = \frac{-i\sin(\sqrt{k^2-1}w)\, e^{-2ikw}}{2k\sqrt{k^2-1}\cos(\sqrt{k^2-1}w) - i(2k^2-1)\sin(\sqrt{k^2-1}w)}, \tag{3a}$$

$$\text{or} \quad = R(k)e^{i\phi(k)-2ikw} = \frac{\sin(\sqrt{k^2-1}w)e^{i\phi(k)-2ikw}}{(4k^2(k^2-1)+\sin^2(\sqrt{k^2-1}w))^{1/2}}, \tag{3b}$$

with $$\phi(k) = \tan^{-1}\left(\frac{2k^2-1}{2k\sqrt{k^2-1}}\tan(\sqrt{k^2-1}w)\right) - \frac{\pi}{2},$$

being the phase, and R(k) the modulus, of the reflection coefficient.

As is evident from equations 3a and 3b, the structure of the reflection coefficient, even for this simple potential, is not trivial. Since the functional form of the reflection coefficient is not transparent a set of plots are shown in figure 4.1, where we have plotted R(k) and $\phi(k)$ as function of k for w =0.1, 1.0, and 10.0, with $\phi(k)$ being reflected onto the interval $(-\pi/2, 3\pi/2)$.

Figure 4.1 ; The moduli R(k) and the phase $\phi(k)$ of the reflection coefficients for a) w=0.1, b)w=1.0, and c)w=10.0.

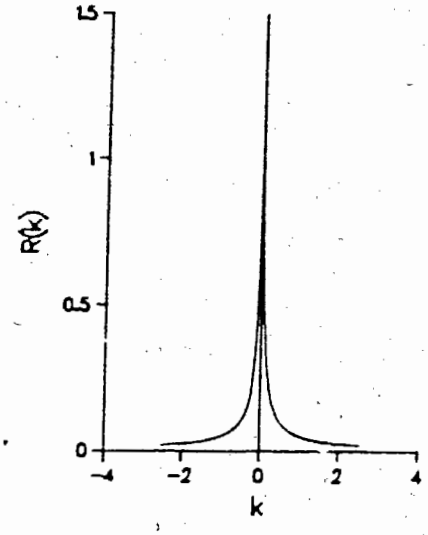

(a

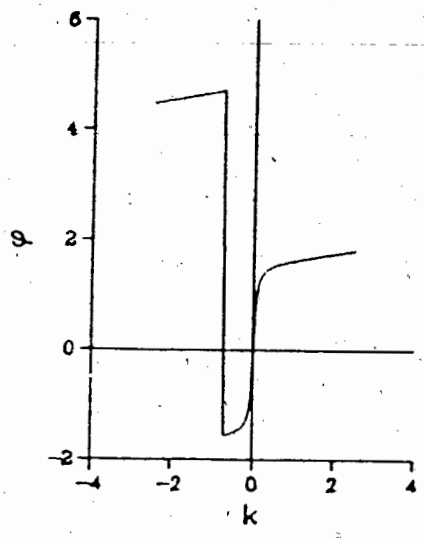

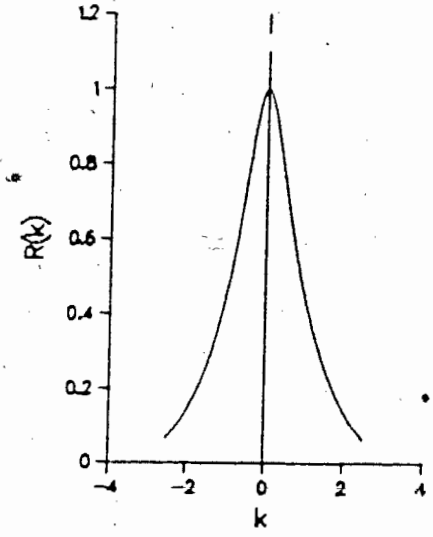

(b

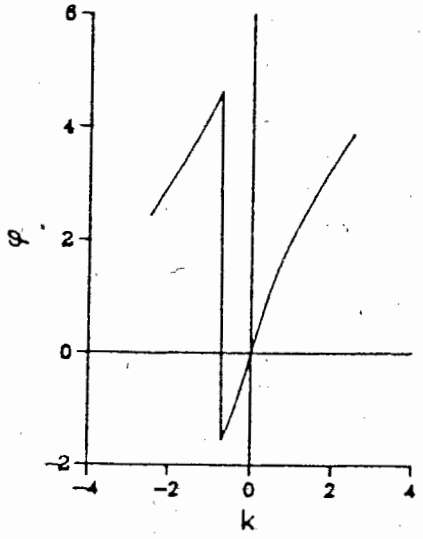

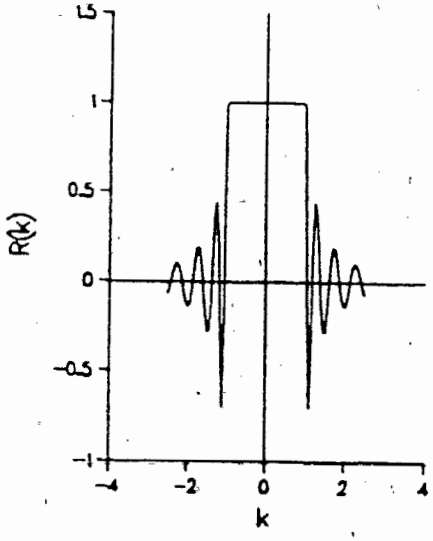

(c

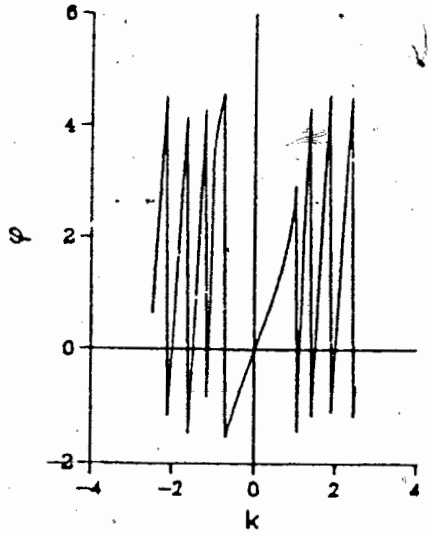

As can be seen from the preceding figures the function r(k) is bounded and at least continuous and continuously differentiable. Thus, by Parseval's theorem the Fourier transform of r(k) exists. It should be noted that the reflection coefficient is not the Fourier transform of a square well. Thus the initial value problem for the evolution of the kernel of the Marchenko equation is not the same as that of the initial value of the KdV problem. It is also interesting to note the changes in the modulus of the reflection coefficient from a spike for small initial pulse width to a square box for large initial width. The compactness of the reflection coefficient about k=0 suggests that the bulk of the information about the behaviour of the scattering problem comes from the long wavelength contributions, and that this region plays an important role.

To evaluate the kernel of the Marchenko equation

$$F(x,t) = \frac{1}{2\pi} \int_{-\infty}^{\infty} r(k) e^{ikx+8ik^3t} dk \qquad 4$$

through the expansion technique, we recall from chapter 3 that

$$F(x,t) = f_{m\alpha} \theta_m(x) \theta_\alpha(t) , \qquad 5$$

with $$f_{m\alpha} = \int_{-\infty}^{\infty} \int_{-\infty}^{\infty} F(x,t) \theta_m(x) \theta_\alpha(t) \, dx dt$$

or $$f_{m\alpha} = \frac{i^{m+\alpha}}{\sqrt{2\pi}} \int_{-\infty}^{\infty} r(k)\theta_m(k)\ \theta_\alpha(8k^3)\ dk,$$

after the spatial and the temporal integrals are executed.

As a preliminary test case an initial pulse width of unity (w=1) was chosen, and the corresponding f_m's were calculated using the algorithms developed in Appendix 3 for the Oscillator functions and a simple extended Simpson's rule used to calculate the remaining integral over the wave number k. A short table of these are listed in Appendix 7.

As a check on the accuracy of the algorithms used to calculate the $f_{m\alpha}$'s we used the fact that the function F(x,t) is real. Thus the imaginary part of the $f_{m\alpha}$'s must tend to zero as the accuracy of the numerical integration increased. By adjusting the range of the integration and the step size for the extended Simpson's rule it was possible to impose the realistic requirement of having the imaginary part 10^{-7} smaller than the real part. This requirement gives a rough estimate of the relative error in the integration as being the order of 10^{-7}. Since expansion coefficients are being calculated it was also necessary to know the order to which the expansion must be taken to have reasonable convergence. To get a feel for this, the $f_{m\alpha}$'s were calculated to high order, roughly 200, and then inverted through equation 5 , summed up to varying orders of m with α held fixed at 200, to return varying approximations of

F(x,0). These approximations were then compared with the results of a direct numerical calculation of F(x,0) to establish convergence criteria. Figure 4.2 shows the various results of this comparison. The first four plots depict the approximations to F(x,0) as m is increased, with α held fixed at 200, and the last the direct numerical result. Figure 4.3 shows the comparison of the 200 term approximation to F(x,0) with the numerical result on a much larger scale than in Figure 4.2.

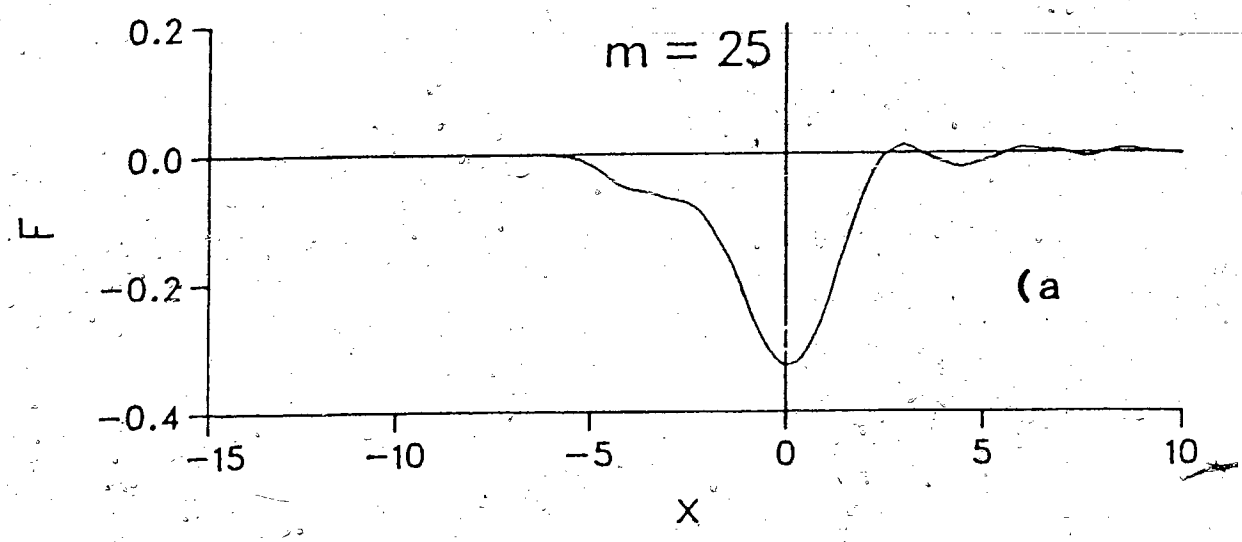
m = 25
0.2
0.0
−0.2
−0.4
F
−15
−10
−5
0
5
10
X
(a

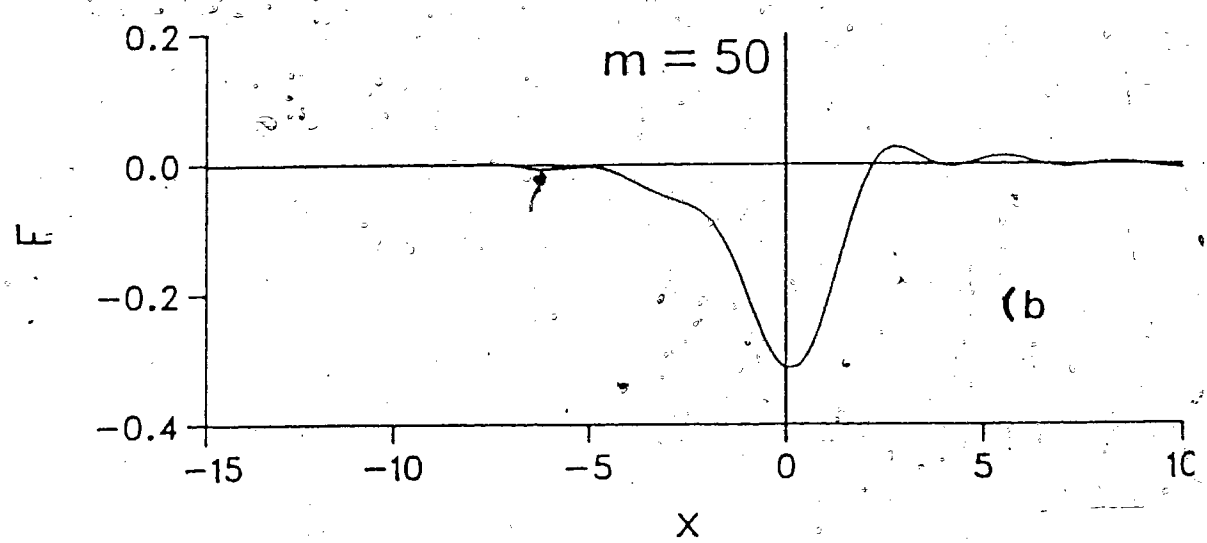
m = 50
0.2
0.0
−0.2
−0.4
F
−15
−10
−5
0
5
X
(b

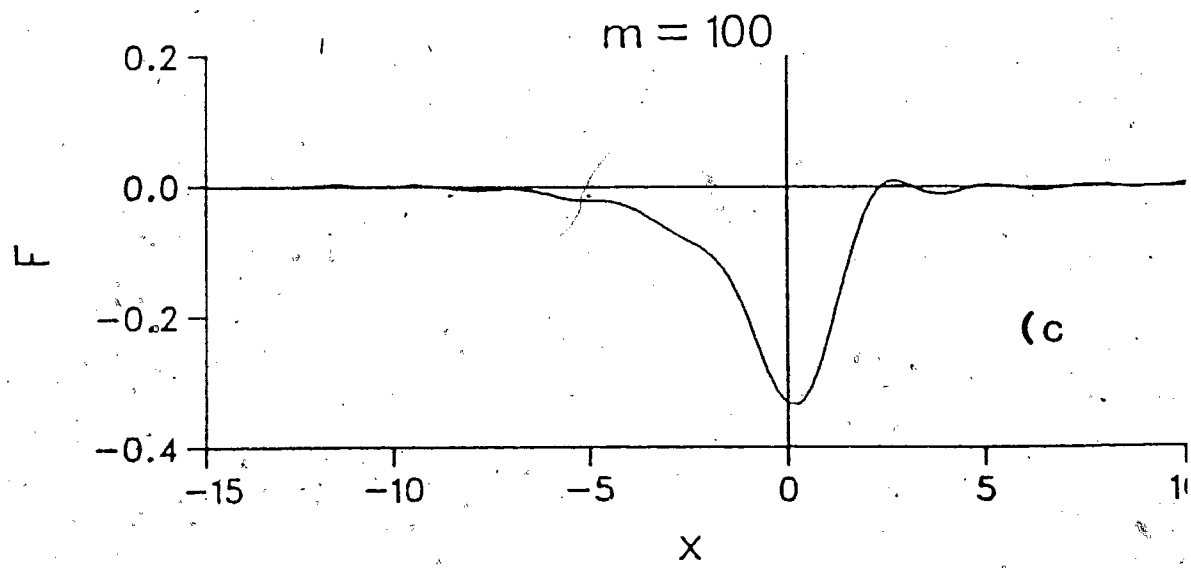
m = 100
0.2
0.0
−0.2
−0.4
F
−15
−10
−5
0
5
X
(c

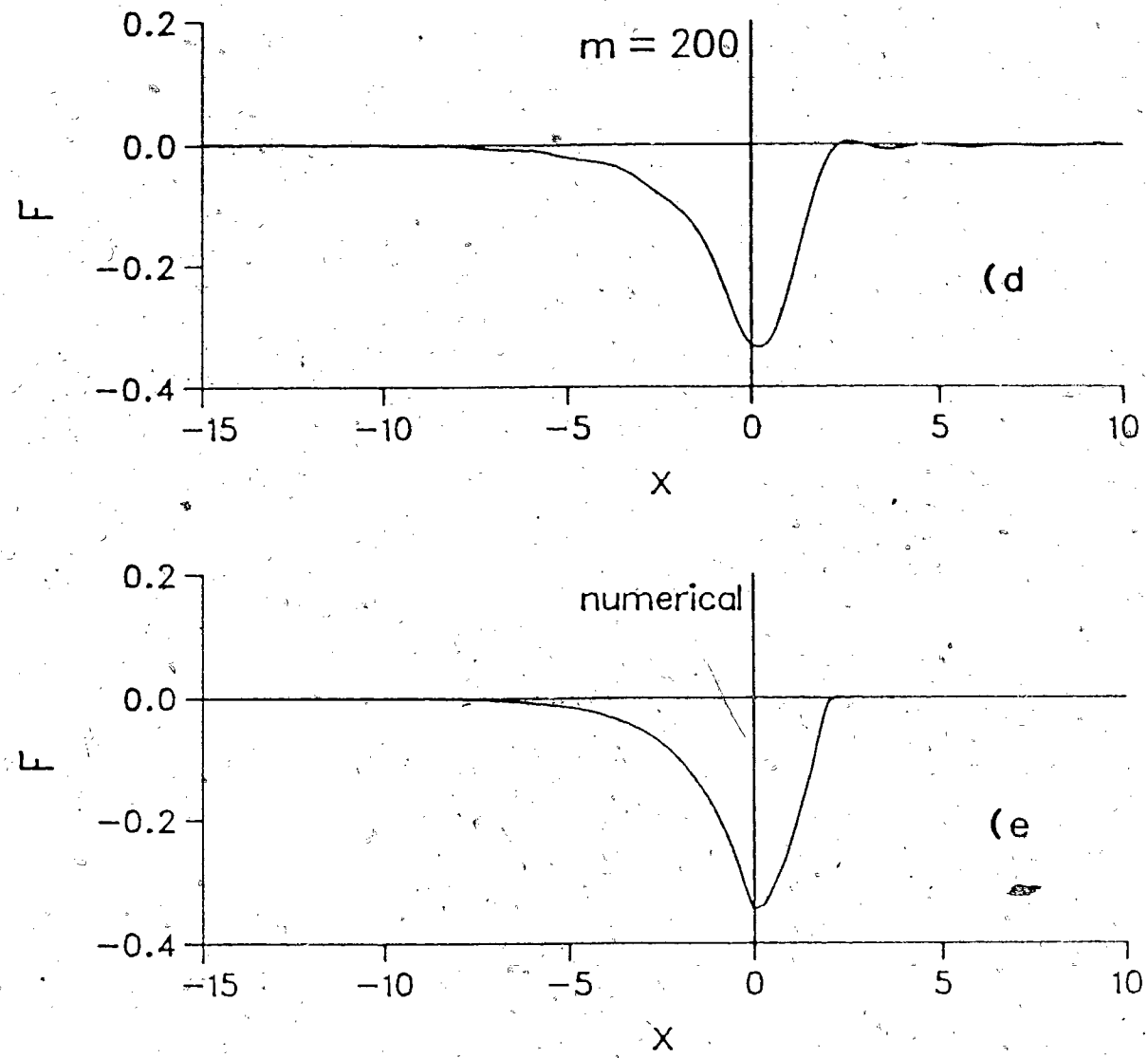

Figure 4.2 ; F(x,0) profiles summed to varying orders of m with α=200, for a) m=25, b) m=50, c) m=100, d) m=200, and e) F(x,0) calculated by numerical integration (exact).

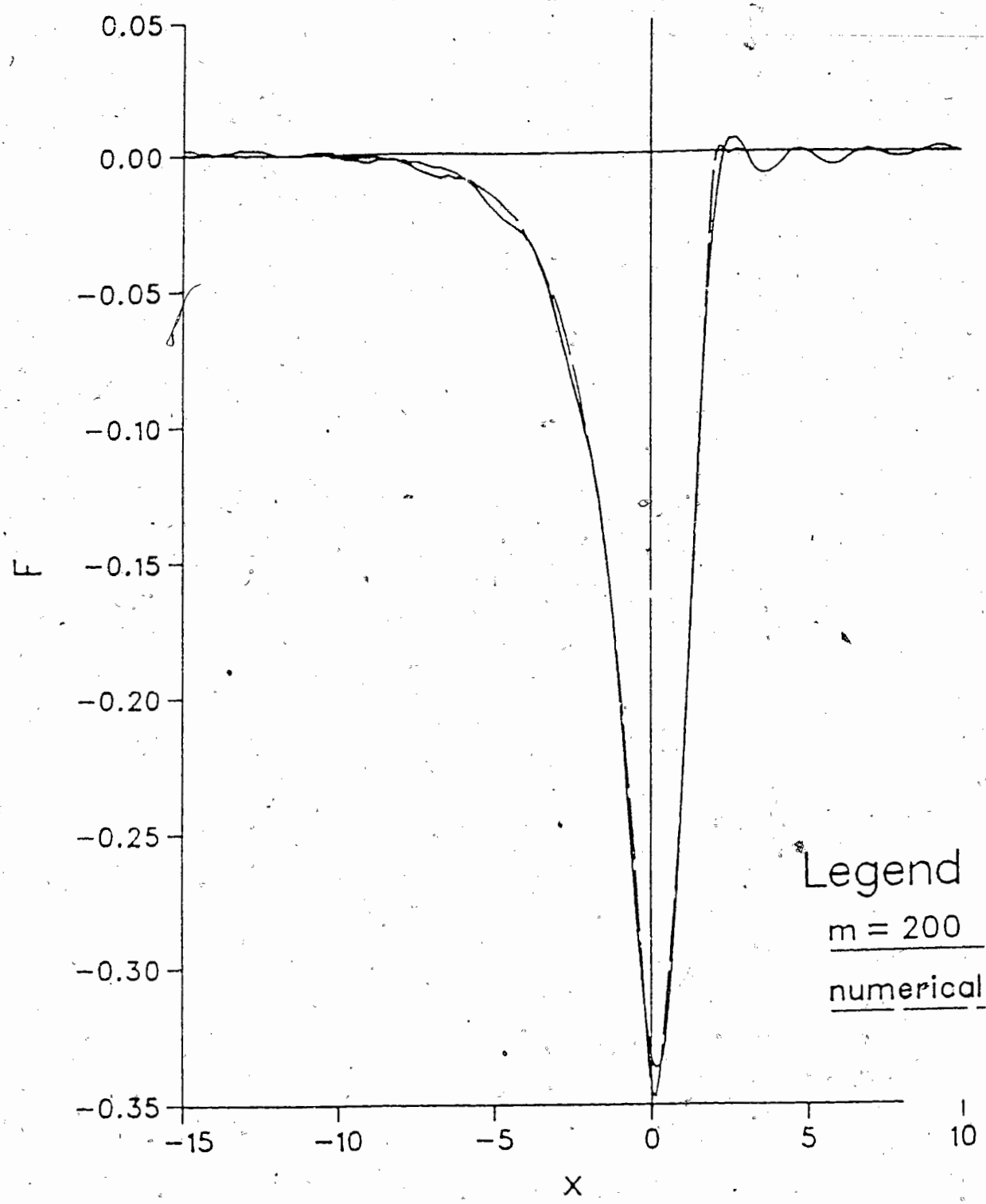

Figure 4.3 ; Expanded version of F(x,0) profile for $m=\alpha=200$ and F(x,0) calculated numerically.

From the comparison of the approximations of $F(x,0)$ with the actual result it is patently obvious that a large number of terms in the expansion of $F(x,t)$ are required in order to replicate $F(x,t)$ to any substantial degree. In retrospect this slow convergence is not entirely suprising in that the effective range for which the Oscillator functions are non-zero is given by $|x| < \sqrt{n}$, approximately, with n being the order. This can be seen by assuming that the dominant behaviour of the Oscillator functions, for 'large' x, is given by

$$x^n e^{-x^2/2}$$

where n is the order. Under this approximation, simple differentiation shows that the maximum value occurs at $|x| = \sqrt{n}$, giving us a crude approximation for the radius of convergence of the truncated series representation. This picture is not entirely correct in that the higher order terms of the expansion also contain the high frequency response of the reflection coefficient, and that truncation of the expansion eliminates these contributions. However, on the basis of the compactness of the reflection coefficients the contributions of the high frequency will be assumed negligible. Moreover the gross features of the $F(x,0)$ profile are evident for small order expansions as seen from the first few plots in figure 4.2.

With the parameters and the constraints of the expansion procedure set by the above criteria, we can proceed with the calculation of $K(x,x;t)$ via the Neumann series expansion of chapter 3. However, it should be noted that the reflection coefficient contains a term of the form e^{-2ikw} and that the kernel of the Marchenko equation has a similar spatial term of e^{2ikx}, this would suggest that it is natural to expand about the leading edge of the wave i.e. about $x=w$ as opposed to $x=0$. Taking this shift into account the explicit form of the expansion coefficients is

$$f_{m\alpha} = \frac{i^{m+\alpha}}{\sqrt{2\pi}} \int_{-\infty}^{\infty} \frac{\sin(\sqrt{k^2-1}w)e^{i\phi(k)}}{(4k^2(k^2-1)+\sin^2(\sqrt{k^2-1}w))^{1/2}} \Theta_m(k)\ \Theta_\alpha(8k^3)\ dk, \quad 6$$

as per chapter 3. This result can now be integrated numerically, up to some order in m and α and an approximation to $K_1(x,x;t)$, the first term in the Neumann series of $K(x,x;t)$, can be constructed via

$$K_1(x,x;t) = -F(2x;t) = -f_{m\alpha}\Theta_m(2x-2w)\ \Theta_\alpha(t)\ . \quad 7$$

This was done for the three initial pulse widths w=0.1, 1.0, and 10.0, with the sums on m and α being taken up to 200. The results are shown in figures 4.4-4.6. Included in each figure,

so as to provide a visual check on the accuracy of the Oscillator expansion method, are the corresponding results for $K_1(x,x;t)$ obtained by direct numerical integration of equation 3. The results of both calculations, Oscillator expansion and direct numerical, are shown as sections of the full two dimensional surfaces defined by $K_1(x,x;t)$, over the ranges $-25.0<x<10.0$ and $0<t<20.0$. The (10.0,0.0) corner being the closest. The plots were generated on the Calcomp plotter at S.F.U. using a commercially developed graphics package called DISSPLA, which was developed and marketed by ISSCO, Integrated Systems Software Corporation of California.

Figure 4.4 ; First term of Neumann series expansion, $-K_1(x,x;t)$, for w=0.1, a) Oscillator expansion, b) Numerical.

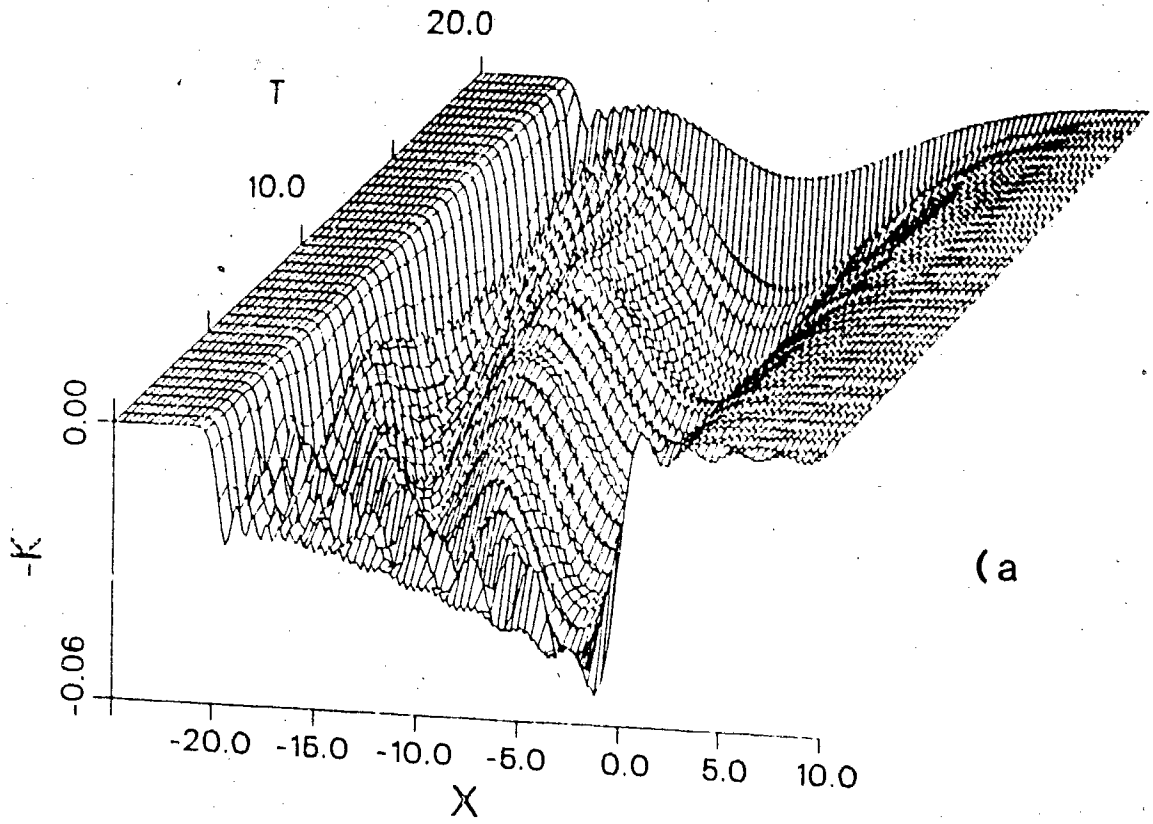
20.0
T
10.0
0.00
-K
-0.06
-20.0 -15.0 -10.0 -5.0 0.0 5.0 10.0
X

(a

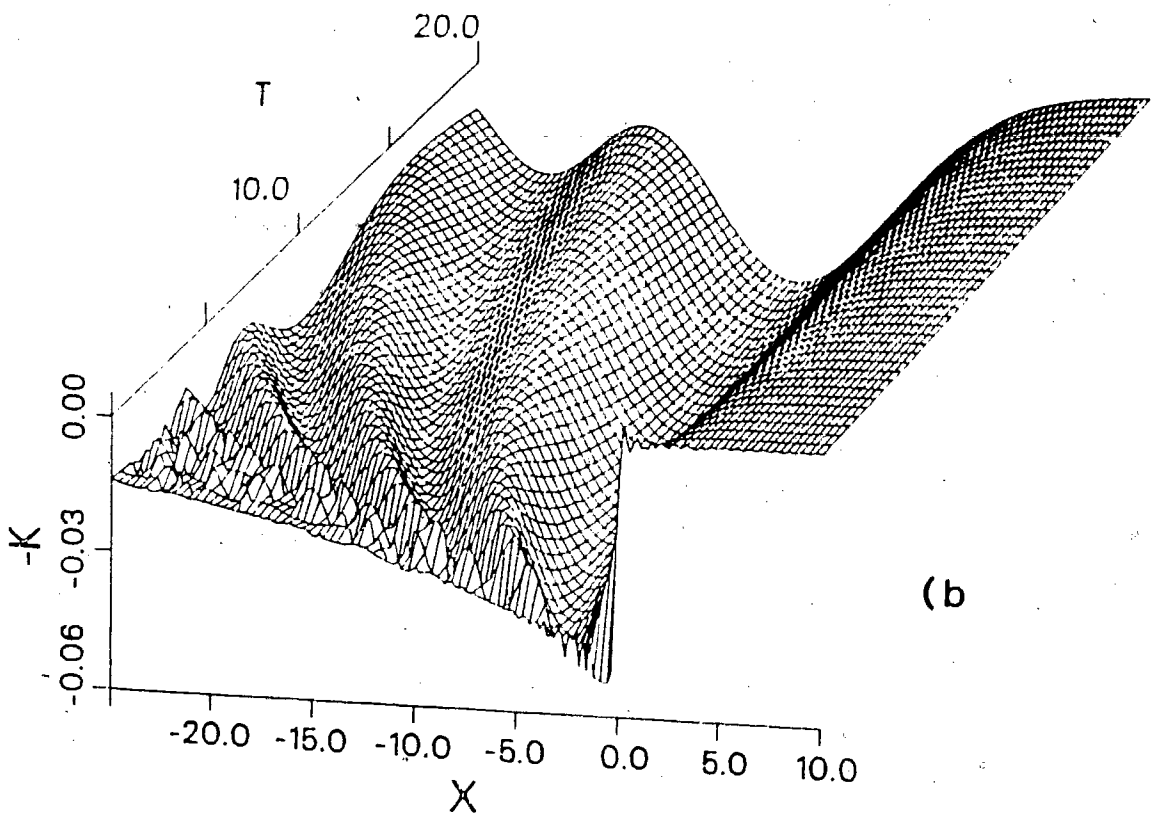
20.0
T
10.0
0.00
-K
-0.03
-0.06
-20.0 -15.0 -10.0 -5.0 0.0 5.0 10.0
X

(b

Figure 4.5 ; First term of Neumann series expansion, $-K_1(x,x;t)$, for w=1.0, a) Oscillator expansion, b) Numerical.

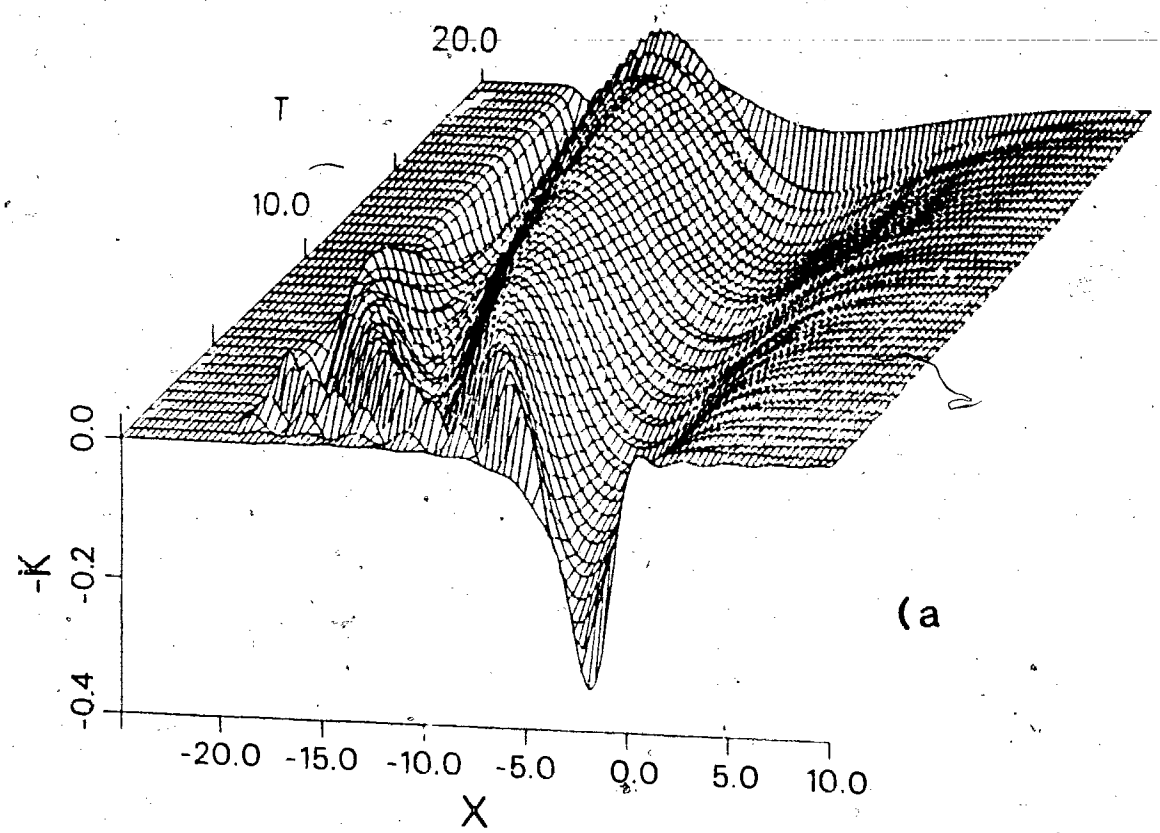
20.0
T
10.0
0.0
-K
-0.2
-0.4
-20.0 -15.0 -10.0 -5.0 0.0 5.0 10.0
X
(a

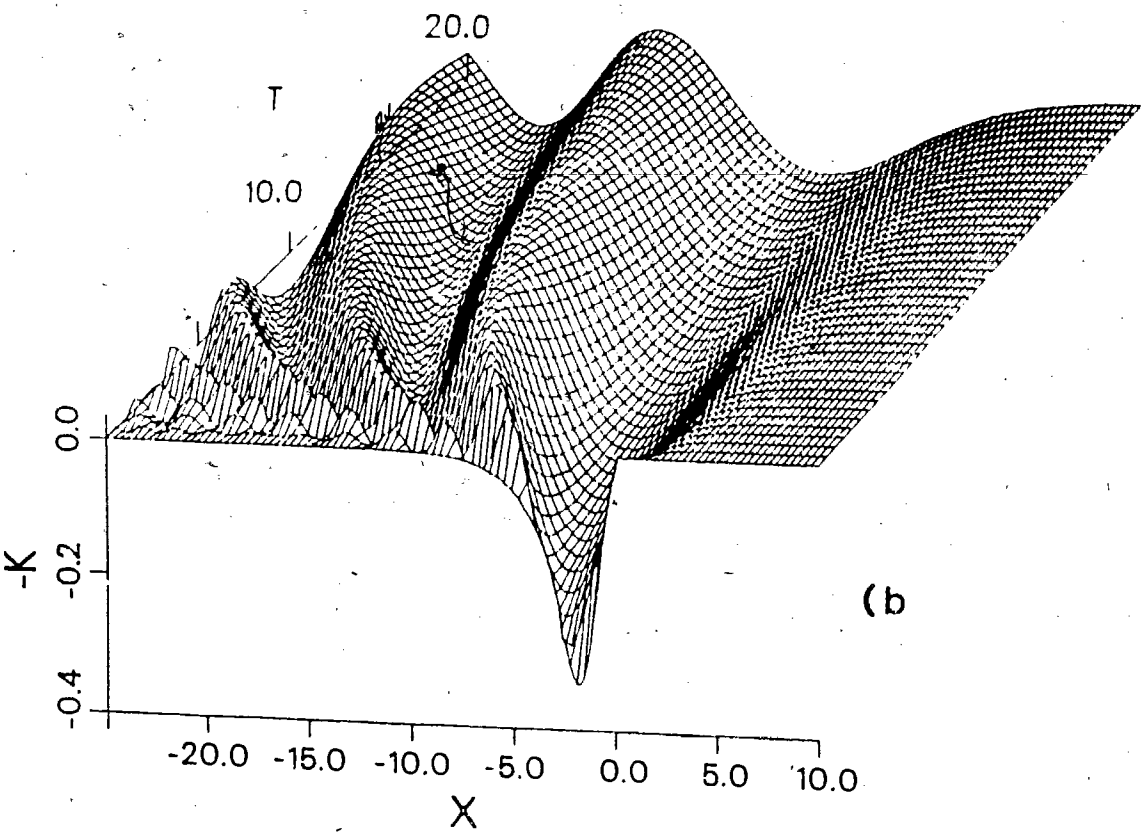
20.0
T
10.0
0.0
-K
-0.2
-0.4
-20.0 -15.0 -10.0 -5.0 0.0 5.0 10.0
X
(b

Figure 4.6 ; First term of Neumann series expansion, $-K_1(x,x;t)$, for w=10.0, a) Oscillator expansion, b) Numerical.

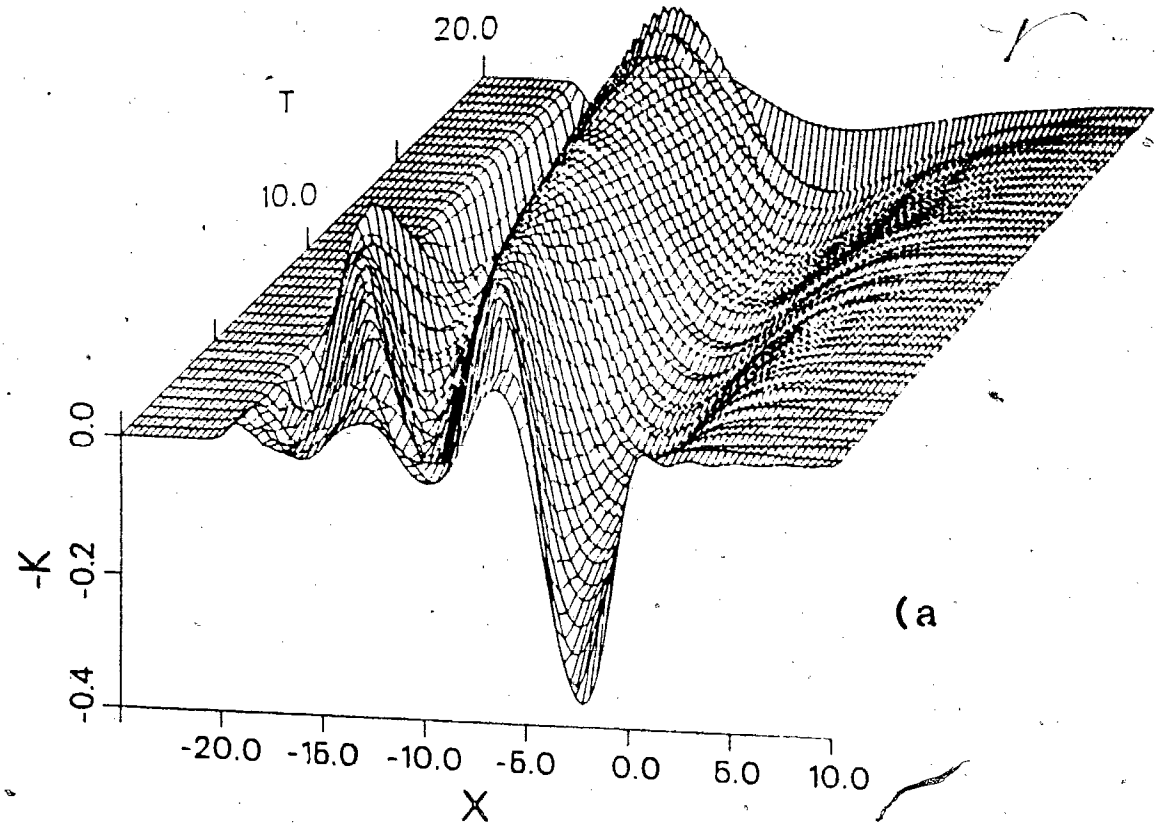
20.0
T
10.0
0.0
-0.2
-0.4
-K
-20.0 -15.0 -10.0 -5.0 0.0 5.0 10.0
X
(a

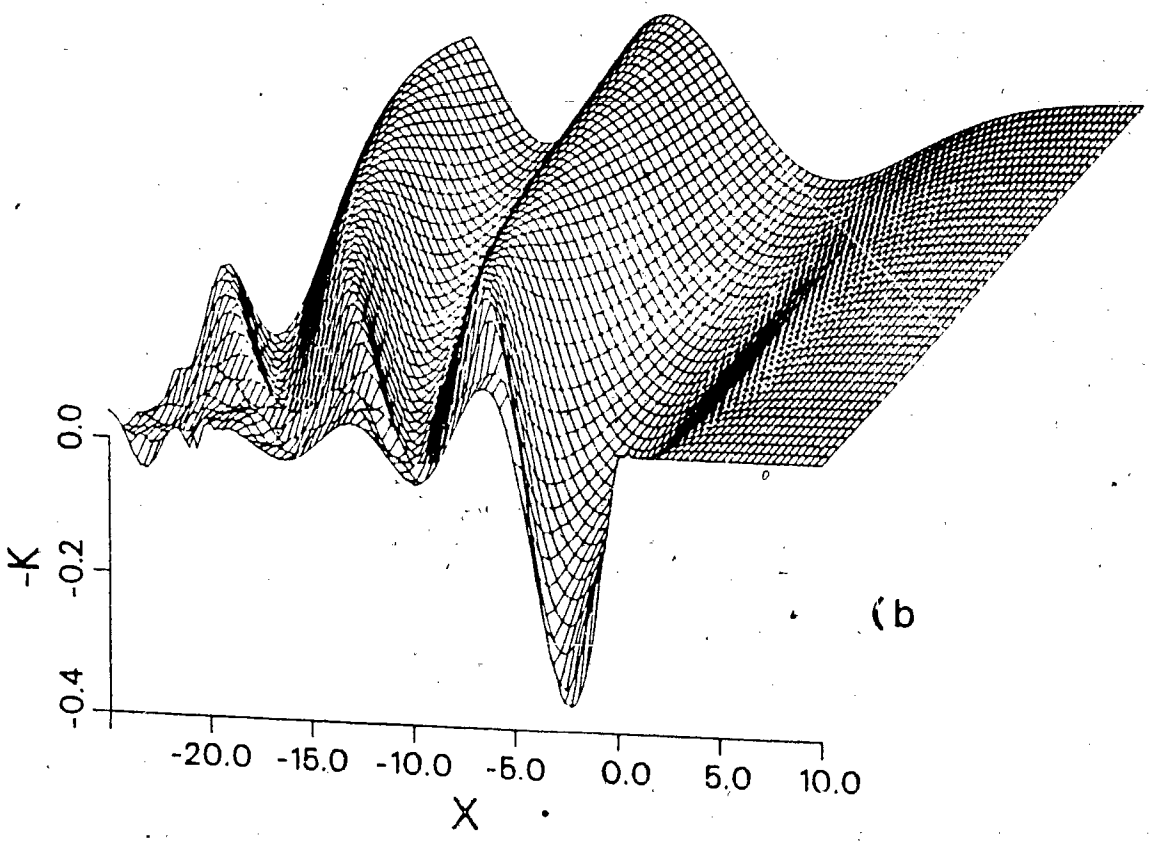
0.0
-0.2
-0.4
-K
-20.0 -15.0 -10.0 -5.0 0.0 5.0 10.0
X
(b

Visual comparison of the two plots in each figure shows that the Oscillator expansion procedure, taken to the high order of $m=\alpha=200$, does in fact capture the correct features of the function $K_1(x,x;t)$ over this portion of space-time, for each of the three widths. However the comparisons also bring to light some of the expansion method's failings. As is evident, the direct numerical plots are much smoother than the expansion plots. The major reason for this is the truncation of the expansion, both temporally and spatially at 200 terms. This truncation in effect acts as a filter to eliminate the high frequency components needed to smooth the surfaces. This lack of high frequency components, which leads to Gibb's phenomona, is best seen along the T=0 curves, of the surfaces shown, in the neighbourhood of X=0, where the expansion is trying to fit to a discontinuity.

In comparing the three Oscillator expansion plots in figures 4.4-4.6 it is interesting to note that out of the three cases it is the w=0.1 case that exhibits the most noise, where as the w=1.0 and w=10.0 cases are relatively smooth. This behaviour of the expansion procedure can be explained in terms of the effective range of the Oscillator functions in relation to the width of the function $K_1(x,x;t)$ at t=0. As can be seen by comparing the the T=0 curves for each of the surfaces, the one corresponding to w=0.1 (figure 4.4) has a comparatively long non-zero range, thus requiring a large number of terms from the Oscillator expansion, which have effective range $\sqrt{n}$, to cover

it. This is supported in chapter 5 where the 'spectra' of the expansions are discussed.

Another draw-back of the expansion procedure is evident in the the sharp cutoffs exhibited on the expansion plots in the regions $X<-20.0$ and $t>20.0$. This is again due to the truncation of the series at $m=\alpha=200$, and demonstrates the rapid fall-off in the Oscillator functions due to the Gaussian weight function.

Aside from the detracting features of the Oscillator expansion procedure the general aggreement between the results generated by it and and numerical integration indicates that the method works, albeit for limites spatial and temporal extent.

Putting the expansion procedure aside it is interesting to note some of the features evident in the lowest term of the Neumann series.

1. For each of the widths the initial profiles do not correspond to the actual initial conditions imposed, in that $u(x,0) \neq 2dK_1(x,x,0)/dx$. In fact, for the initial conditions chosen (the square well) it turns out that K_1 asymptotically ($|x| \longrightarrow \infty$) goes to zero, which is contrary with the fact that $2K(x,x,0) = \int_x^\infty u(x',0)dx'$, is not asymptotically zero.
2. The initial profile of $K(x,x,0)$ switches from simple truncated exponential behaviour, for small initial pulse width, to a long range oscillatory behaviour for large width as the pulse width is increased.
3. In a relatively short time the pulses, for all three initial

widths, demonstrate modulated Airy function-like behaviour with the crests and troughs moving off along curves, dictated by the scaling solution (see chapter 5) $t = cx^3$.

With the agreement between numerical and theoretical calculations to lowest order in the Neumann series the second term can be calculated with confidence. Recalling from chapter 3 that the second term of the Neumann series, for $K(x,x;t)$, has the form

$$K_2(x,x;t) = f_{m\alpha} f_{n\beta} I_{mnp} P_{\alpha\beta\gamma} \theta_p(x) \theta_\gamma(t) \quad . \qquad 8$$

Initially this was approached with the straight-forward idea of simply summing the terms of the multiple sums, however several attempts at getting 8 to produce uniformly convergent results, failed. This failure was found to be due to the dominance of the complimentary error function behaviour implicit in the matrix I_{mnp} (see Appendix 5 equation 26) and consequently in the second term of the Neumann series. This was in fact found to be the case when the second term of the Neumann series was evaluated numerically, at t=0, and was compared to the complimentary error that was scaled to have the same height (see figure 4.7).

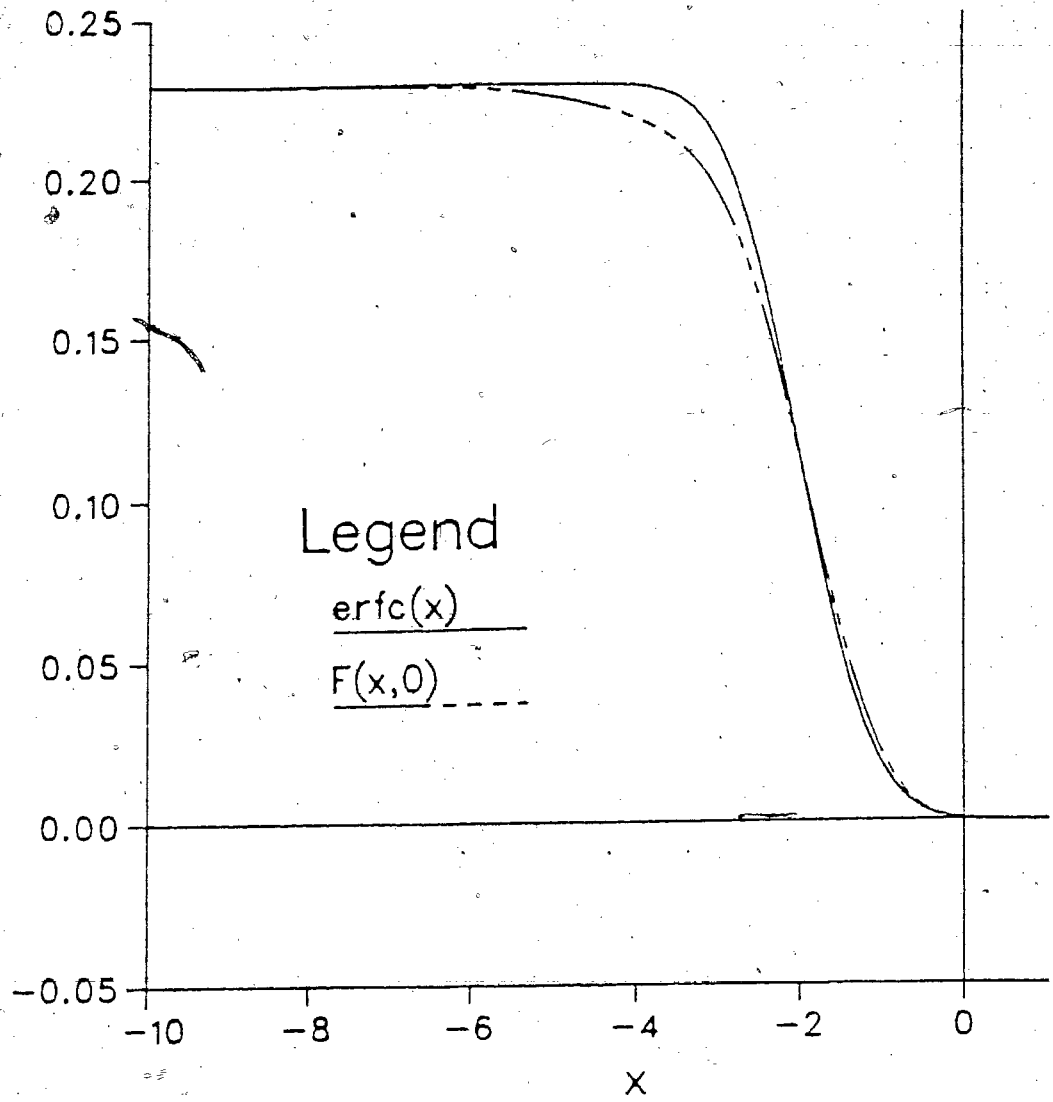

Figure 4.7 ; Comparision between second term of Neumann series expansion and a scaled complementary error function (erfc(x)) for t=0 and w=1.0.

With this in mind the matrix I_{mnp} was split into two parts,

$$I_{mnp} = I^{(1)}_{mnp} + I^{(2)}_{mnp}$$

along the lines that

$$\text{erfc}(x) = I^{(2)}_{mnp}\Theta_p(x) \quad . \qquad 9$$

This division leads to the natural form

$$K_2(x,x;t) = f_{m\alpha}f_{n\beta}\, I^{(1)}_{mnp}P_{\alpha\beta\gamma}\Theta_p(x)\,\Theta_\gamma(t) +$$

$$+ f_{m\alpha}f_{m\beta}\, P_{\alpha\beta\gamma}\Theta_\gamma(t)\,\text{erfc}(x). \qquad 10$$

for the second term of the Neumann expansion. These two terms were subsequently evaluated, for the three initial widths of $w=0.1$, 1.0, and 10.0 for $m=n=\alpha=\beta=60$, and $p=\gamma=90$. The particular choice for the maximal values of the sum indices m, n, α, β, p, and γ was dictated by the limits imposed by the computing facilities for both the available memory space and the execution time required to do the internal sums. The maximal value for p and γ were further constrained by convergence considerations. By

definition

$$\theta_m(x)\ \theta_n(x) = P_{mnp}\theta_p(x) \qquad 11$$

where the sum on p is infinite. However, to use a truncated version it was found that, as a crude rule of thumb, p should be at least 3/2 larger than either m or n in order to get reasonable convergence. The same criteria was extended to the sums on $I^{(1)}_{mnp}$.

The results of the calculation of K_2 for this set of parameters are shown in the following pair of figures. The first of these, figure 4.8, shows the behaviour of the complimentary error function contribution to the second term of the Neumann expansion, i.e. the

$$f_{m\alpha} f_{m\beta}\ P_{\alpha\beta\gamma}\theta_\gamma(t)\ \mathrm{erfc}(x).$$

part, for all three initial pulse widths, taken over the same portion of space-time as in the previous set of figures, $-25.0<X<10.0$ and $0<T<20.0$.

Figure 4.8 ; Complementary error function contribution to the second term of the Neumann series expansion of $K_2(x',x;t)$ for a) w=0.1, b) w=1.0, c) w=10.0.

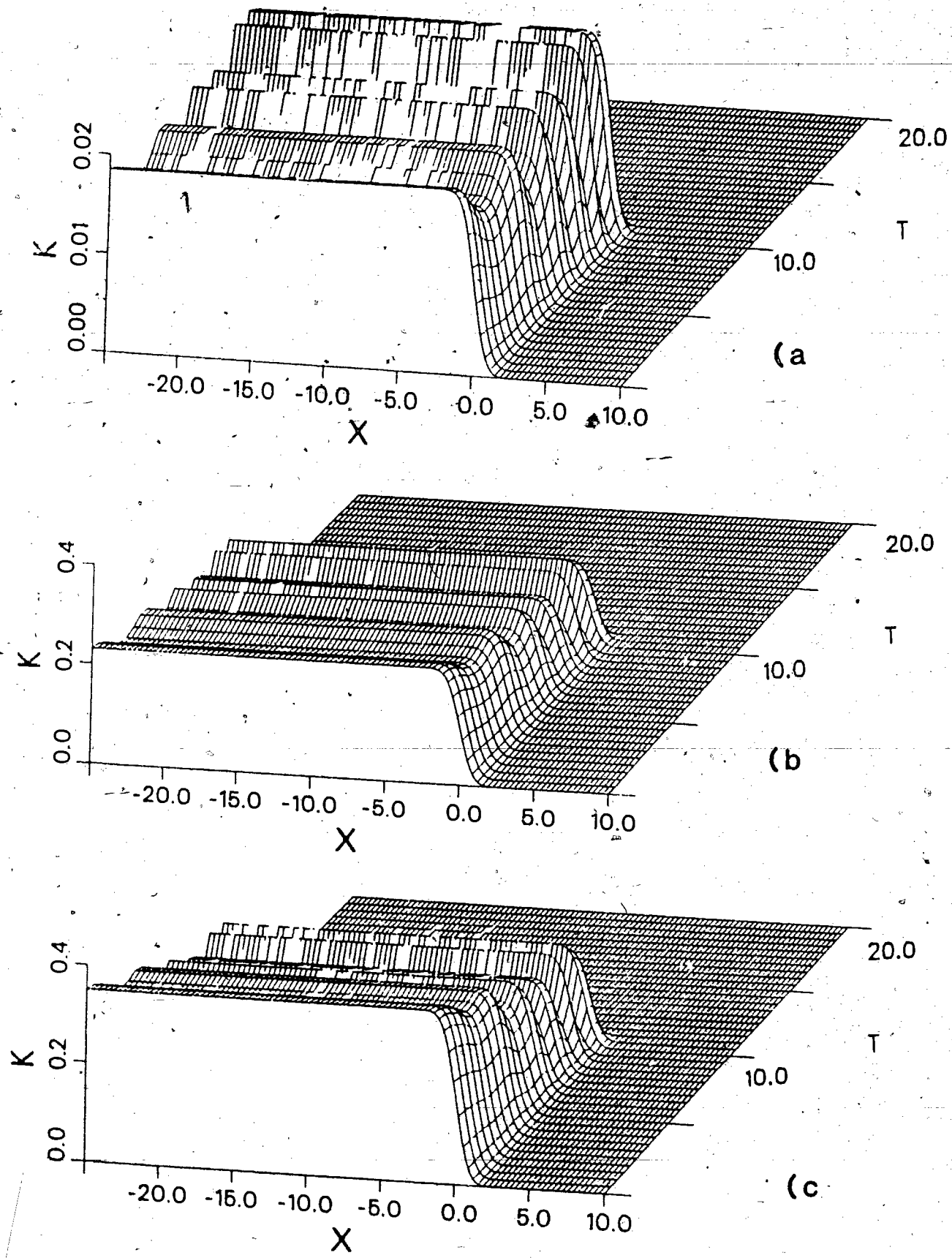
0.02
0.01
0.00
K
1
-20.0 -15.0 -10.0 -5.0 0.0 5.0 10.0
X
20.0
T
10.0
(a
0.4
0.2
0.0
K
-20.0 -15.0 -10.0 -5.0 0.0 5.0 10.0
X
20.0
T
10.0
(b
0.4
0.2
0.0
K
-20.0 -15.0 -10.0 -5.0 0.0 5.0 10.0
X
20.0
T
10.0
(c

Since the spatial dependence of this term is perfectly determined by the complimentary error function, the cross-sections taken spatially are exact in shape, but not necessarily in height since this is determined by the term's temporal expansion. However, by the convergence in lowest order (K_1) to the numerical results, it was thought that the temporal ripple exhibited on these surfaces for short time is real, and is due to some unidentifiable slowly diminishing long time behaviour.

Independent of the ripples it is interesting to note that the errror function contribution for the two large pulses start to diminish from their initial values at t=0, where as the same contribution for the smallest widths grows.

The steep cutoff in the neighbourhood of T=10. is due solely to the truncation of the sum at 90 terms.

With respect to the convergence of the Neumann series, it should be noted that this second order contribution is of the same order of magnitude as the first contribution, indicating that the convergence will be slow.

The second sequence of plots, figure 4.9, in this set show the behaviour of the remaining part of the second order term of the Neumann series.

Figure 4.9 ; Second localized contribution to second term of the Neumann series expansion of $K_2(x,x;t)$ for a) w=0.1, b) w=1.0, c) w=10.0.

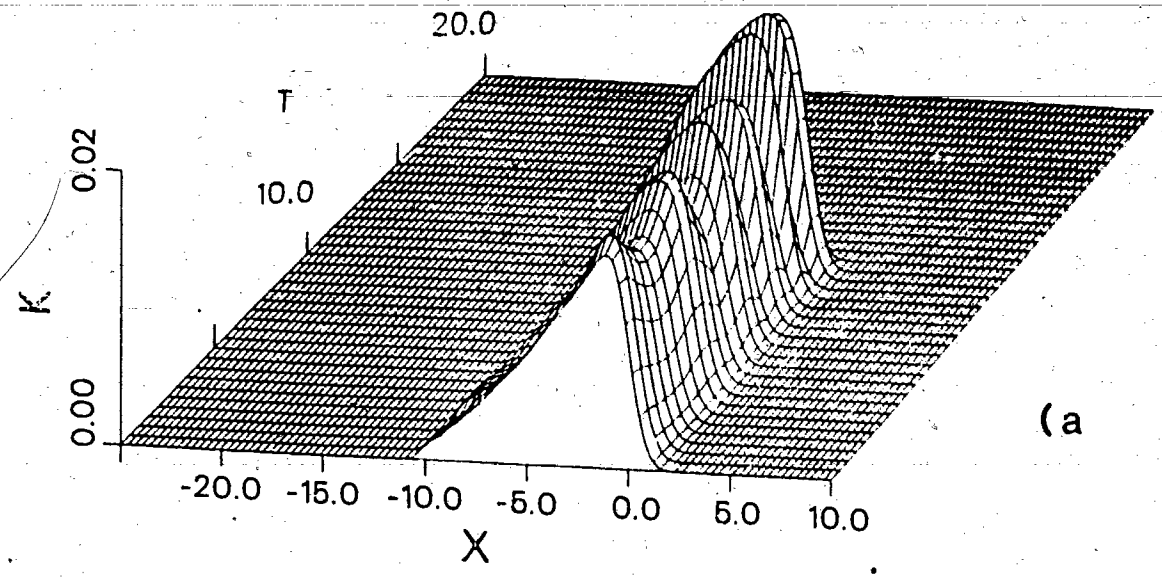
20.0
T
10.0
0.02
K
0.00
-20.0 -15.0 -10.0 -5.0 0.0 5.0 10.0
X
(a

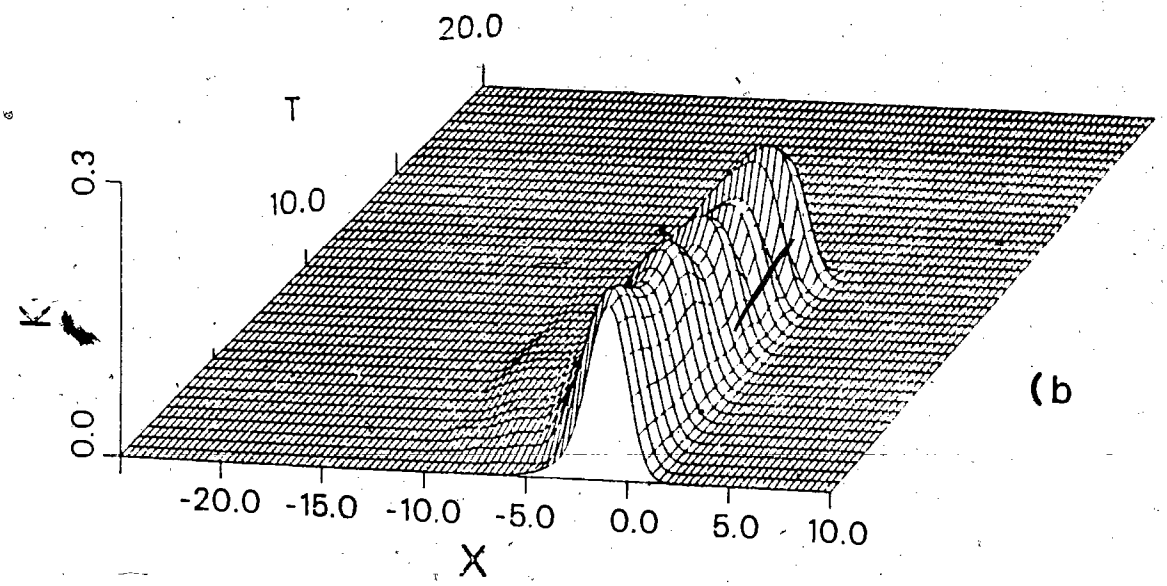
20.0
T
10.0
0.3
K
0.0
-20.0 -15.0 -10.0 -5.0 0.0 5.0 10.0
X
(b

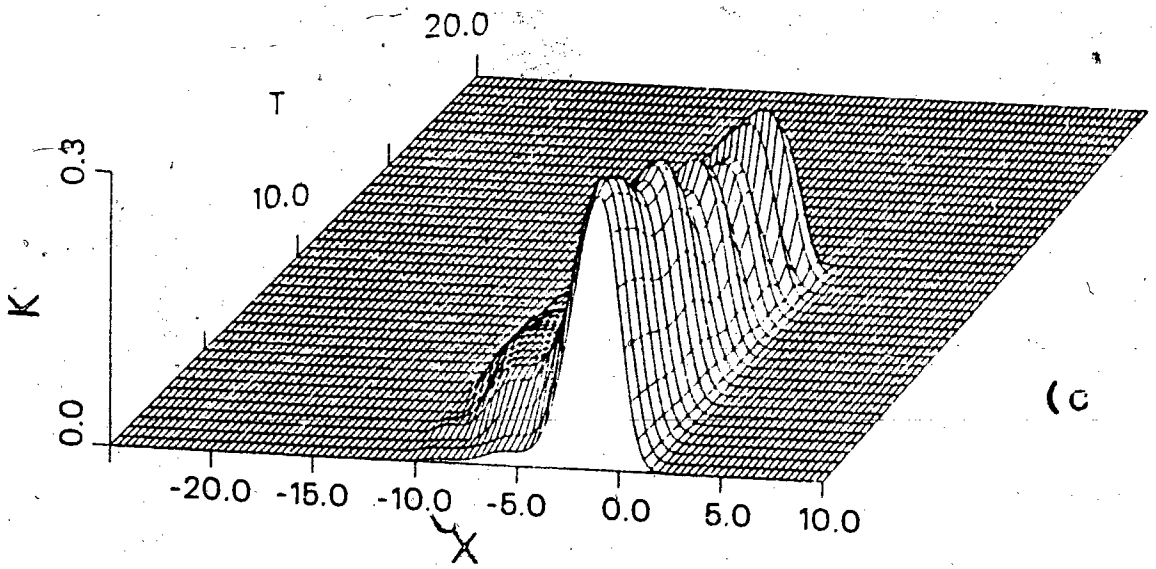
20.0
T
10.0
0.3
K
0.0
-20.0 -15.0 -10.0 -5.0 0.0 5.0 10.0
X
(c

As can be seen from these plots this term is a slowly spreading localized pulse, that is stationary in this reference frame. This term acts so as to diminish the edge of the error function contribution as time evolves, causing it to become less steep. This flattening of the curve manifests itself physically as a broadening of the pulse since the plots shown here are integrals of the solution of the kdV equation. Again, the ripple mentioned earlier is evident here, as is the growth of the small area pulse.

The next sequence of plots, figure 4.10-4.12 show the sum of the first and second (both parts) terms of the Neumann series calculated both through the Oscillator expansion and numerically for each of the three widths. The plots are again arranged in pairs according to pulse width, the top one showing the result from the Oscillator expansion and the lower the numerical result.

Figure 4.10 ; Sum of the first two terms of the Neumann series expansion (K_1+K_2) for w=0.1 a) Oscillator expansion b) Numerical.

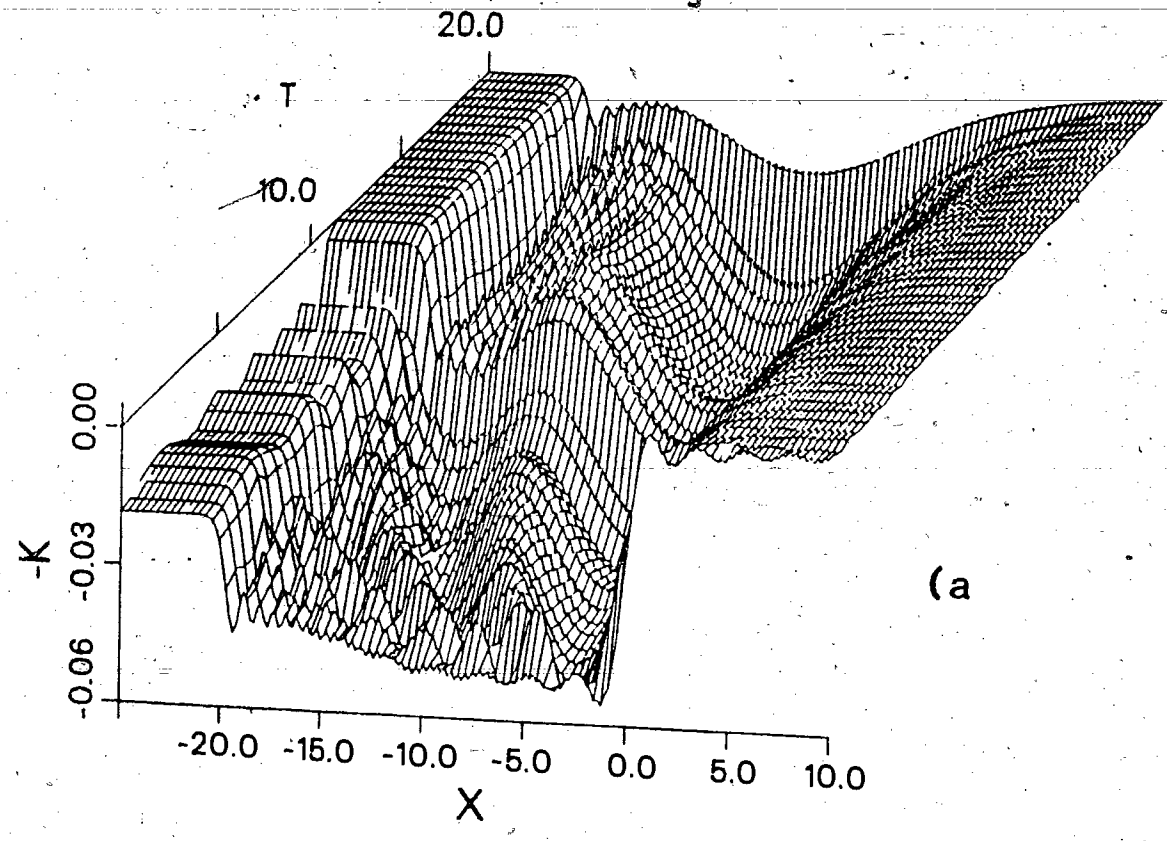
20.0
T
10.0
0.00
-0.03
-0.06
-K
-20.0 -15.0 -10.0 -5.0 0.0 5.0 10.0
X

(a

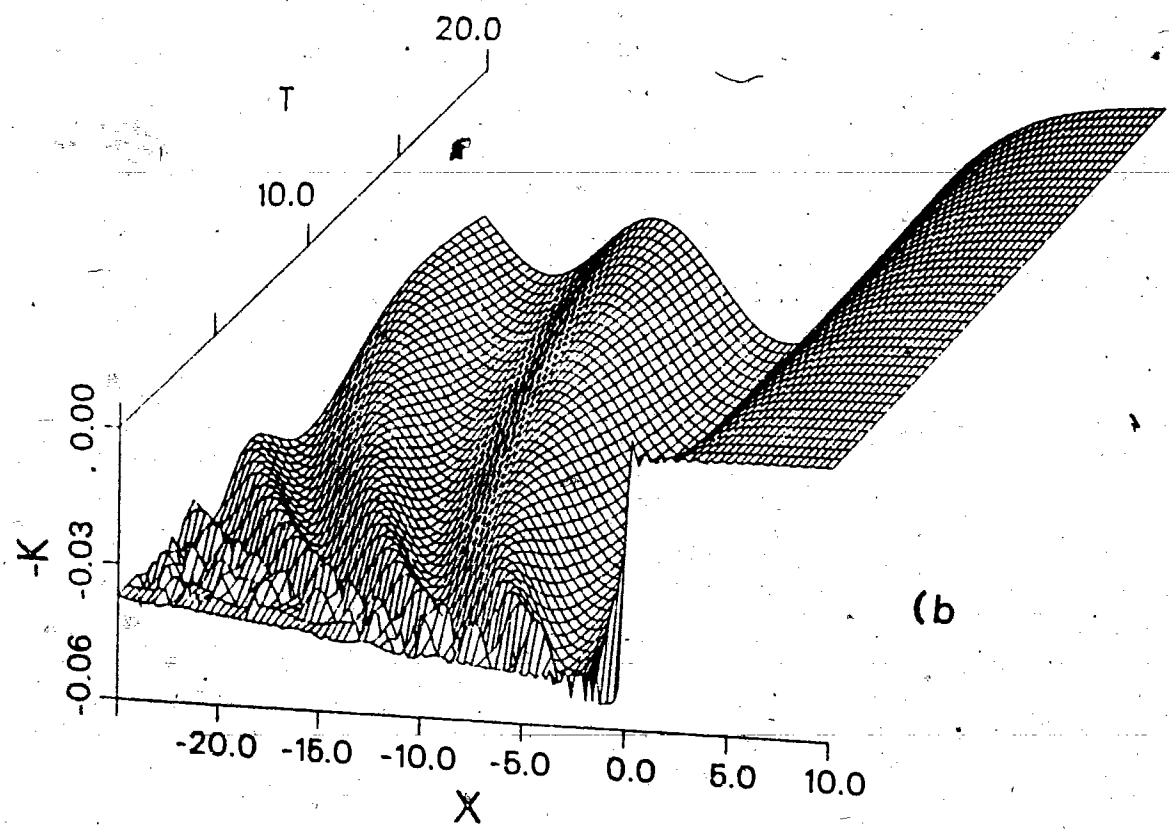
20.0
T
10.0
0.00
-0.03
-0.06
-K
-20.0 -15.0 -10.0 -5.0 0.0 5.0 10.0
X

(b

Figure 4.11 ; Sum of the first two terms of the Neumann series expansion (K_1+K_2) for w=1.0 a) Oscillator expansion b) Numerical.

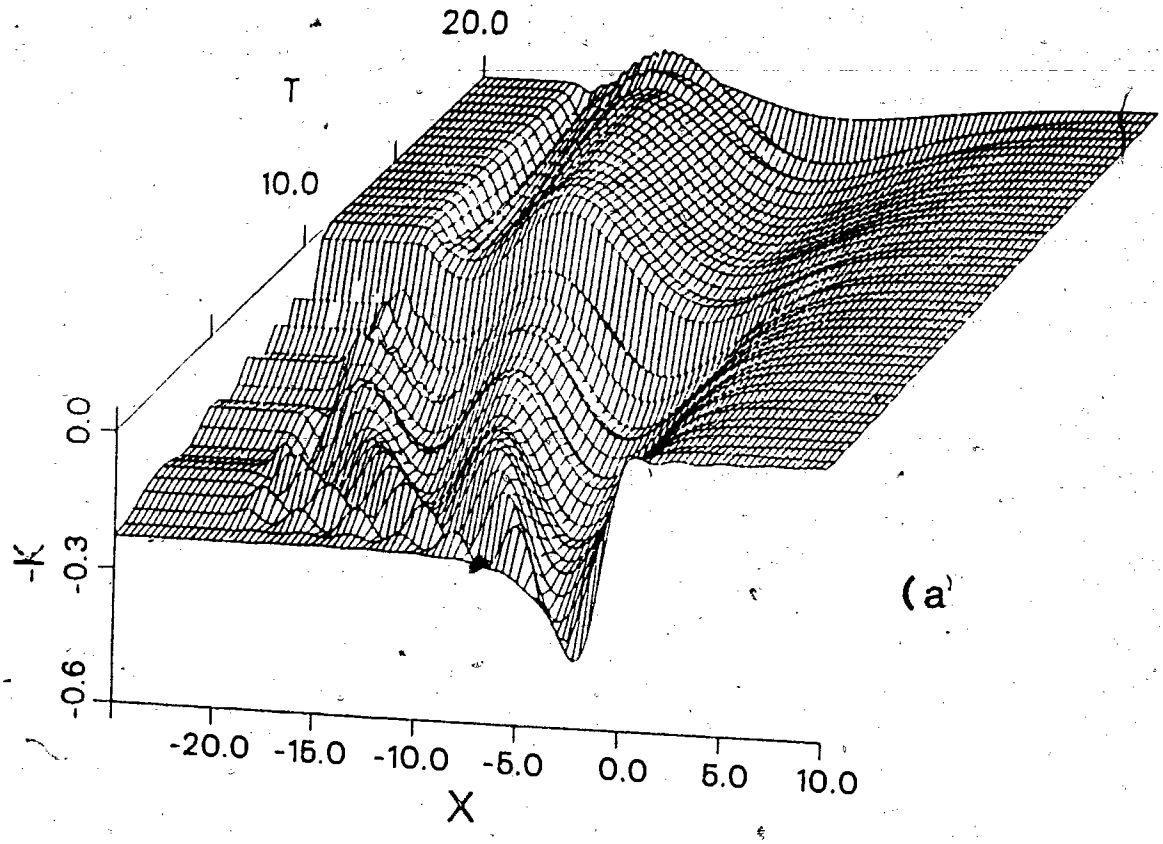
20.0
T
10.0
0.0
-K
-0.3
-0.6
-20.0 -15.0 -10.0 -5.0 0.0 5.0 10.0
X
(a)

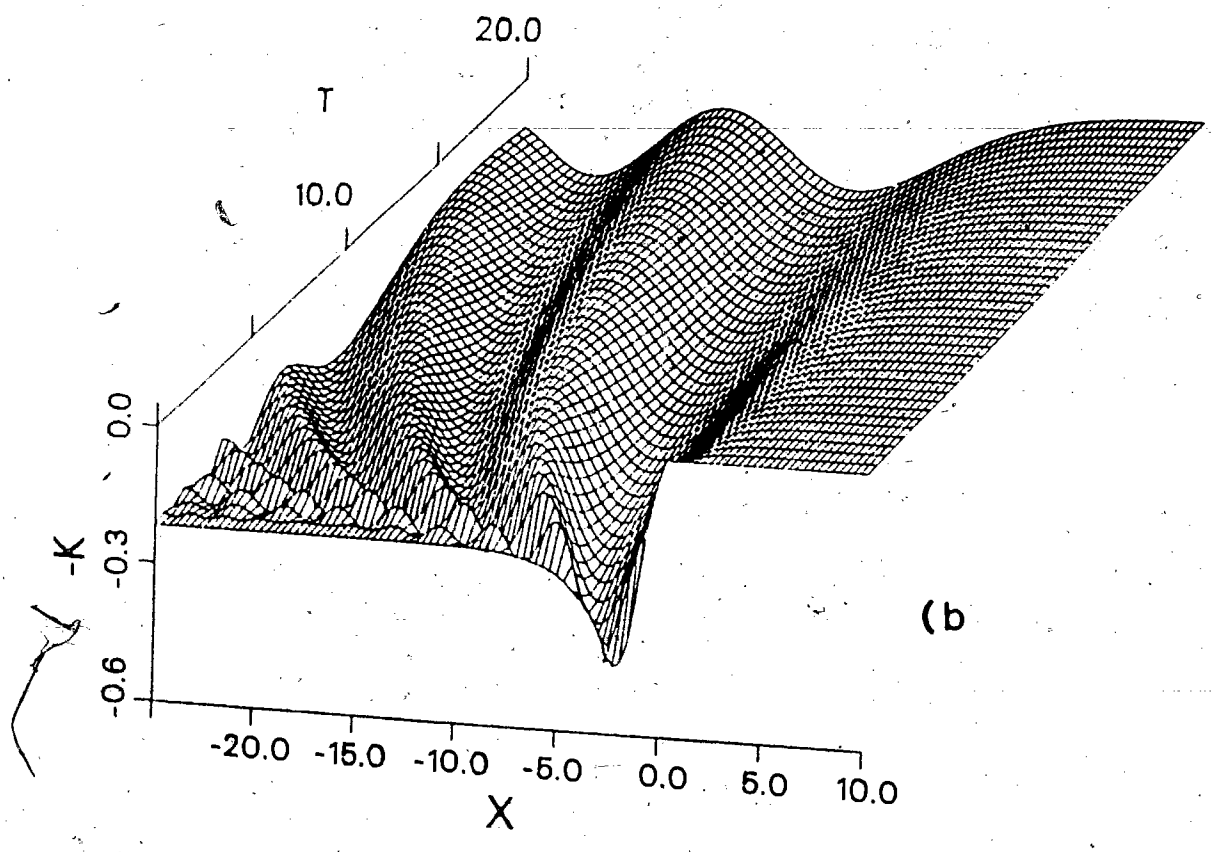
20.0
T
10.0
0.0
-K
-0.3
-0.6
-20.0 -15.0 -10.0 -5.0 0.0 5.0 10.0
X
(b

Figure 4.12 ; Sum of the first two terms of the Neumann series expansion (K_1+K_2) for w=10.0 a) Oscillator expansion b) Numerical.

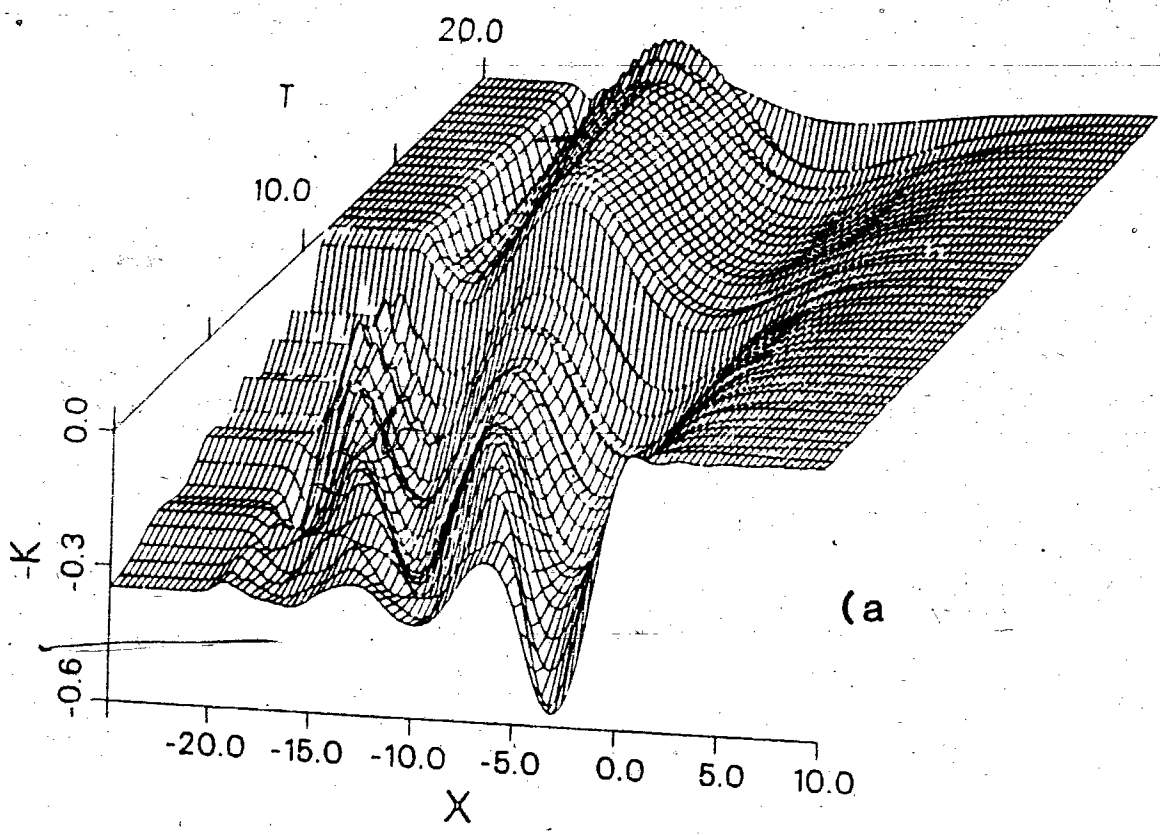
20.0
T
10.0
0.0
-0.3
-0.6
-K
-20.0 -15.0 -10.0 -5.0 0.0 5.0 10.0
X
(a

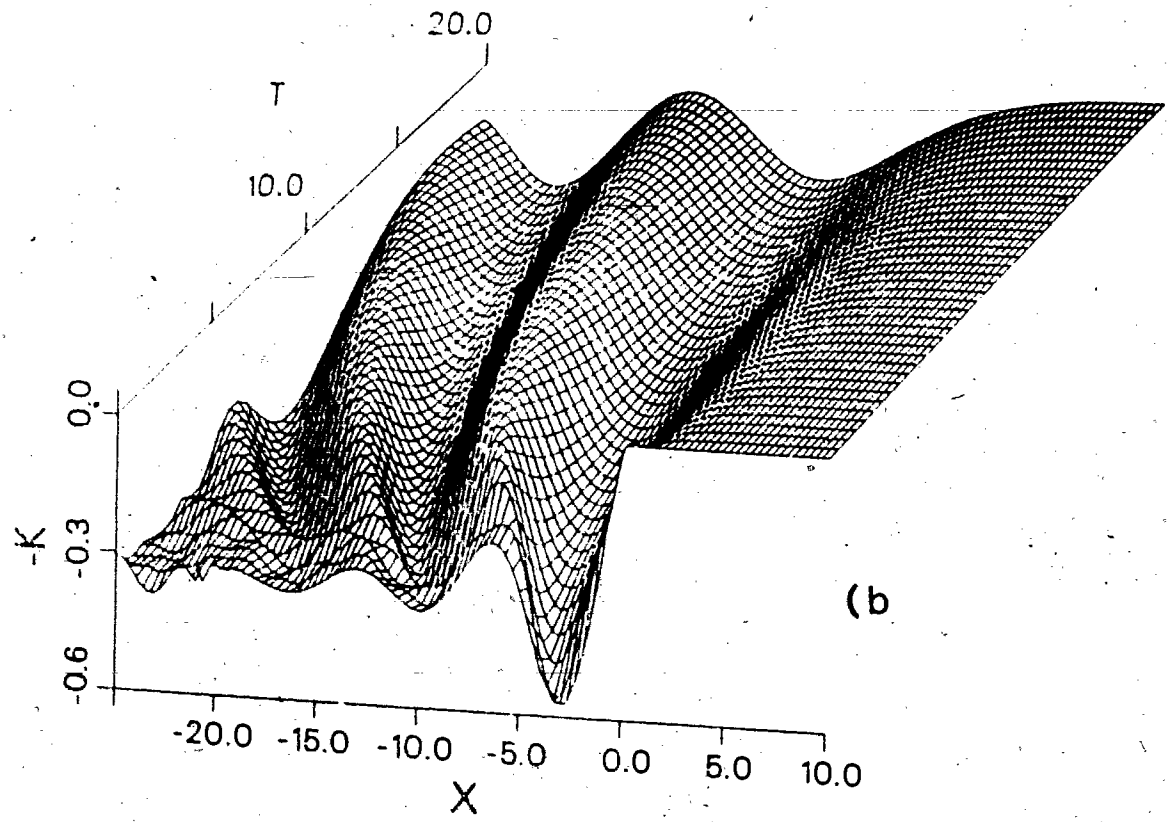
20.0
T
10.0
0.0
-0.3
-0.6
-K
-20.0 -15.0 -10.0 -5.0 0.0 5.0 10.0
X
(b

In this set of plots the failings of the Oscillator expansion are evidenced by the abrupt changes observed at T=10.0, and for X<-20.0. The change at T=10.0 is due to the cutoff of the second order contribution, and that for X<-20.0 is due to the cutoff of the lowest order contribution at X=-20.0. However in the region -20.0<X<10.0 and 0<T<10.0, we see that the Oscillator expansion procedure has captured the essential features shown by the numerical solutions. The w=0.1 result exhibiting the most noise, as previously mentioned. Physically the addition of the first order correction has essentially pulled that region of the surface to the left of X=0 down by the amount dictated by the error function contribution. The wavelike nature of the first order term is basically unaffected by the addition of the second term.

To get a better understanding of the effect of the addition of the second term, we isolated the T=0 curve for all three pulse widths from the numerical plots of the first order term and the combined first and second order terms. These curves are shown in figure 4.13 along with the expected result, for the square well initial pulse, derived from the relationship, equation 2.28, between u(x,0) and K(x,x;0). The exact result is in essence the integral of a square well.

Figure 4.13 ; The t=0 behaviour for the first and the sum of the first and second terms of F(x,t) for a) w=0.1, b) 1.0, and c) 10.0.

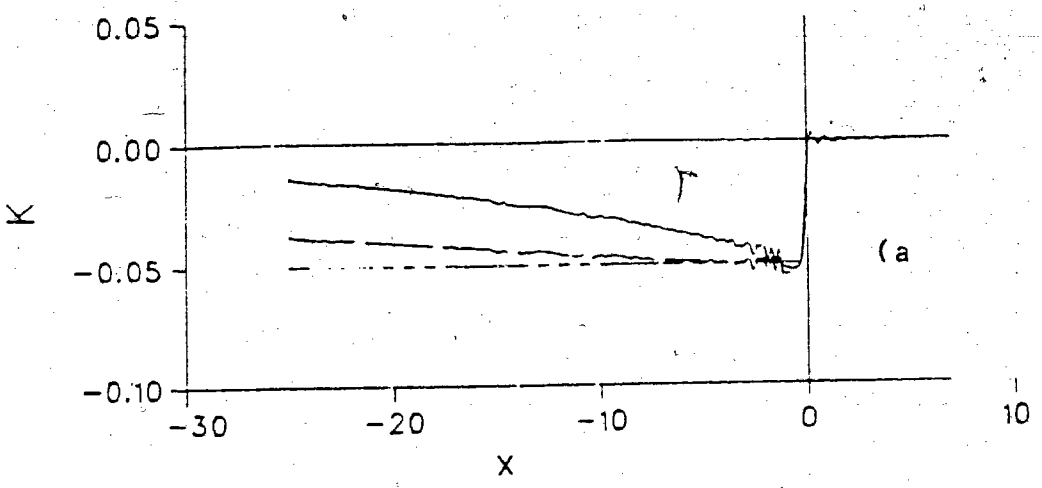
0.05
0.00
−0.05
−0.10
K
−30
−20
−10
0
10
X
(a

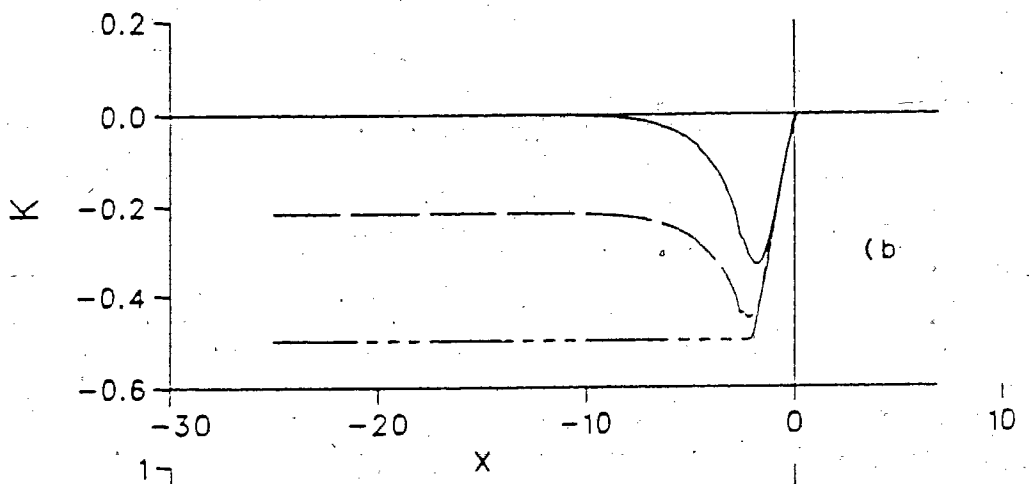
0.2
0.0
−0.2
−0.4
−0.6
K
−30
−20
−10
0
10
X
(b

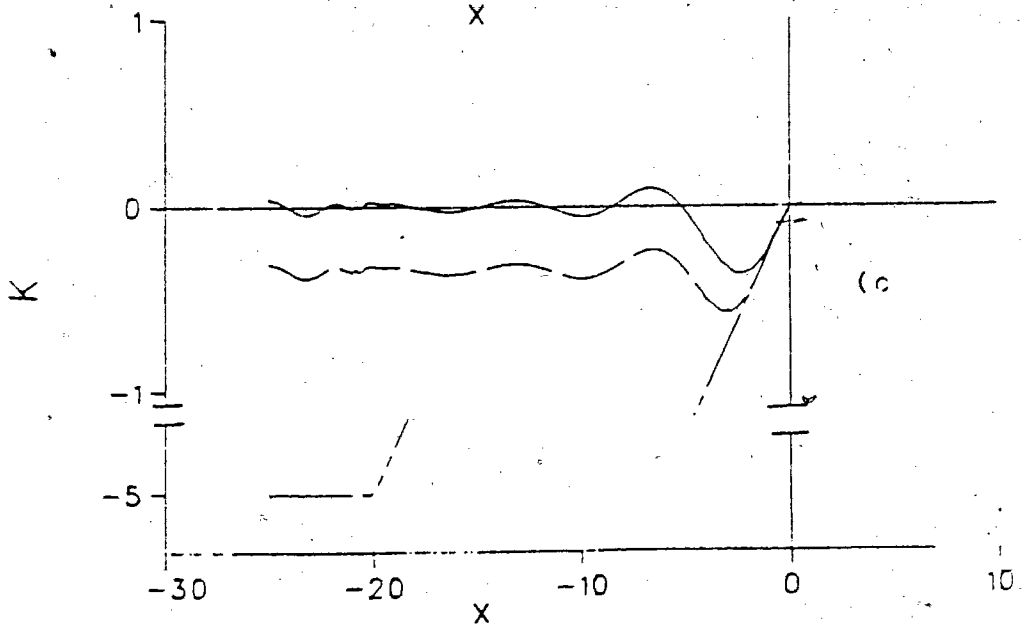
1
0
−1
−5
K
−30
−20
−10
0
10
X
(c

As can be seen from this set of plots the addition of the second term of the Neumann series does have the stated effect of pulling the $X<0$ portion of $K(x,x;0)$ down. In all three cases the two term approximation is a better representation of the actual behaviour than is the single term approximation. However, by comparing the convergence of the three cases it appears that the small area case is converging to the actual behaviour much more rapidly than do the larger area cases, as is evidenced by the disparity between the expected results and the two term results. Note the vast difference for the $w=10.0$ case, wherein many higher order terms of the Neumann series would be needed to fill in the gap, from $K=-1.0$ to $K=-5.0$, between the two term approximation and the exact results.

The trend of fast convergence for small width to slow convergence for large width, exhibited here, would lead to the conclusion that the convergence of the Neumann series is highly dependent upon the size of the initial disturbance, with the rate of convergence diminishing rapidly with size.

CHAPTER V

THE ASYMPTOTIC BEHAVIOUR

In chapter 4 the full biorthogonal expansion procedure was used in an attempt to obtain the complete behaviour of the radiation solutions of the KdV equation. However, it was found that by using a single expansion procedure some information about the asymptotic behaviour of the solution could be extracted.

From the Green's function solution to the linear part of the KdV equation,

$$U_t + U_{xxx} = 0,$$

$$U(x,t) = \frac{1}{(3t)^{1/3}} \int_{-\infty}^{\infty} U(y,0)\,Ai\left(\frac{y-x}{(3t)^{1/3}}\right)dy, \qquad 1$$

we see that a natural coordinate for the solutions of the KdV is the ratio $\epsilon = \frac{x}{(3t)^{1/3}}$. This can also be seen to hold for the full KdV equation if a solution of the form

$$U = \frac{1}{t^{\alpha}} f\left(\frac{x}{t^{\beta}}\right), \qquad 2$$

is sought. On substitution of equation 2 into the KdV equation we get the ordinary differential equation

$$-\frac{2f}{3} - \frac{\epsilon f'}{3} + 6f'f + f^{(3)} = 0 \qquad 3$$

in the variable $\epsilon = \frac{x}{t^{1/3}}$, where $\beta = 1/3$ and $\alpha = 2/3$. The choices for β and α being natural for the requirement that the ensuing equation be ordinary. This type of similarity solution was first suggested by A. Fokas[25] and was used by Ablowitz and Segur in their calculation of the asymptotic behaviour of the KdV equation mentioned previously. It is conjectured that the radiation solutions of the KdV equation approach this form of similarity solution asymptotically.

If this conjecture is true then the terms of the Neumann series expansion for the Marchenko equation must reflect this behaviour. To test this hypothesis we returned to the definition of the kernel of the Marchenko equation

$$F(x,t) = \frac{1}{2\pi} \int_{-\infty}^{\infty} r(k)\, e^{ikx + 8ik^3t} dk$$

and cast it in the form

$$F'(\epsilon,t) = \frac{1}{4\pi t^{1/3}} \int_{-\infty}^{\infty} r\left(\frac{k'}{2t^{1/3}}\right) e^{ik'\epsilon + ik'^3}\, dk'$$

by using the transformations $k=k'/2t^{1/3}$ and $\epsilon=x/2t^{1/3}$. Here we can apply a single variable expansion, in terms of the new variable ϵ, over the oscillator functions, with t being taken as a parameter, and write,

$$F'(\epsilon,t) = f_m(t)\Theta_m(\epsilon)$$

where all of the temporal dependence of the kernel $F'(\epsilon,t)$ is shifted to the expansion coefficients. This provides a method of examining the temporal behavior of the kernel through the temporal behaviour of the expansion coefficients.

The explicit form of the expansion coefficients is found through the orthogonality of the oscillator functions, i.e.

$$f_m(t) = \frac{i^m}{\sqrt{2\pi}2t^{1/3}} \int_{-\infty}^{\infty} r\left(\frac{k}{2t^{1/3}}\right) e^{ik^3}\Theta_m(k)\, dk. \qquad 4$$

Since the reflection coefficient of the square well can be written as

$$r(k) = R(k)e^{i\phi(k/2t^{1/3})} - 2ikw, \qquad 5$$

see chapter 4, a more convenient way to express the expansion is in terms of a new variable,

$$z = \frac{x-2w}{2t^{1/3}}, \qquad 6$$

and get that

$$F'(z,t) = f_m(t)\Theta_m(z) = f_m(t)\Theta_m\left(\frac{x-2w}{2t^{1/3}}\right),$$

and that

$$f_m(t) = \frac{i^m}{\sqrt{2\pi}2t^{1/3}} \int_{-\infty}^{\infty} R\left(\frac{k}{2t^{1/3}}\right) e^{i(\phi(k)+k^3)}\Theta_m(k)\, dk. \qquad 7$$

The translation of $\epsilon \longrightarrow z=\epsilon-2w/2t^{1/3}$ corresponds to expanding about the leading "edge" of the wave.

From the plots of R(k) given in chapter 4 (fig4.1) we see that R(k) is compact on the interval (-1,1), as such we expect the region of support of the function $R(k/2t^{1/3})$ to expand, as $t \longrightarrow \infty$. Thus the dominant behaviour of $R\left(\frac{k}{2t^{1/3}}\right)$ in this asymptotic limit is determined by the leading term in the Taylor

expansion of R(k) about k=0. In the case of the KdV equation the leading term is unity. Asymptotically we get that

$$\underset{t \longrightarrow \infty}{f_m(t)} = \frac{i^m}{\sqrt{2\pi} 2t^{1/3}} \int_{-\infty}^{\infty} e^{ik^3} \theta_m(k)\, dk + O\left(\frac{1}{t^{2/3}}\right) \qquad 8$$

thus all the expansion coefficients have the same temporal behaviour asymptotically.This representation of the expansion coefficients would return a functional form of

$$F(z,t) = \frac{const}{4\pi t^{1/3}} Ai(z)$$

for the asymptotic behaviour of the Kernel of the Marchenko equation, with Ai(x) being the Airy function.

By following the temporal behaviour of several of the expansion coefficients, we can estimate the time needed for the kernel of the Marchenko equation to relax to its $t^{1/3}$ behaviour, and thus get an estimate of the time needed for the radiation solution to relax to the self-similar solution of equation 3.

These calculations were done for the three initial pulse widths w = 0.1,1.0, and 10.0, for coefficients up to order 50, over a time range from $e^1 < t < e^{25}$. The results of the calculation are shown in figures 5.1 to 5.3, for the first six

expansion coefficients m=0,1,2,3,4, and 5, which were representative of the behaviour of the higher order coefficients with respect to the decay time. The first plot of each figure is a plot of $\ln(f_m)$ verses $\ln(t)$, the second is of $d\ln(f_m)/d\ln(t)$ verses $\ln(t)$, and the third is of $d^2\ln(f_m)/d(\ln(t))^2$ verses $\ln(t)$. The last two plots in each figure are included to show, in the case of the first derivative, that the expansion coefficients do in fact exhibit the requsite $t^{1/3}$ behaviour asymptotically, and in the last plot, the time taken for the second derivative to go to zero, thus giving an estimate of the relaxation time.

Figure 5.1 ; Behaviour of the first six expansion coefficients as functions of t, for w=0.1, a) log-log plot of $f_m(t)$, b) first derivative, c) second derivative.

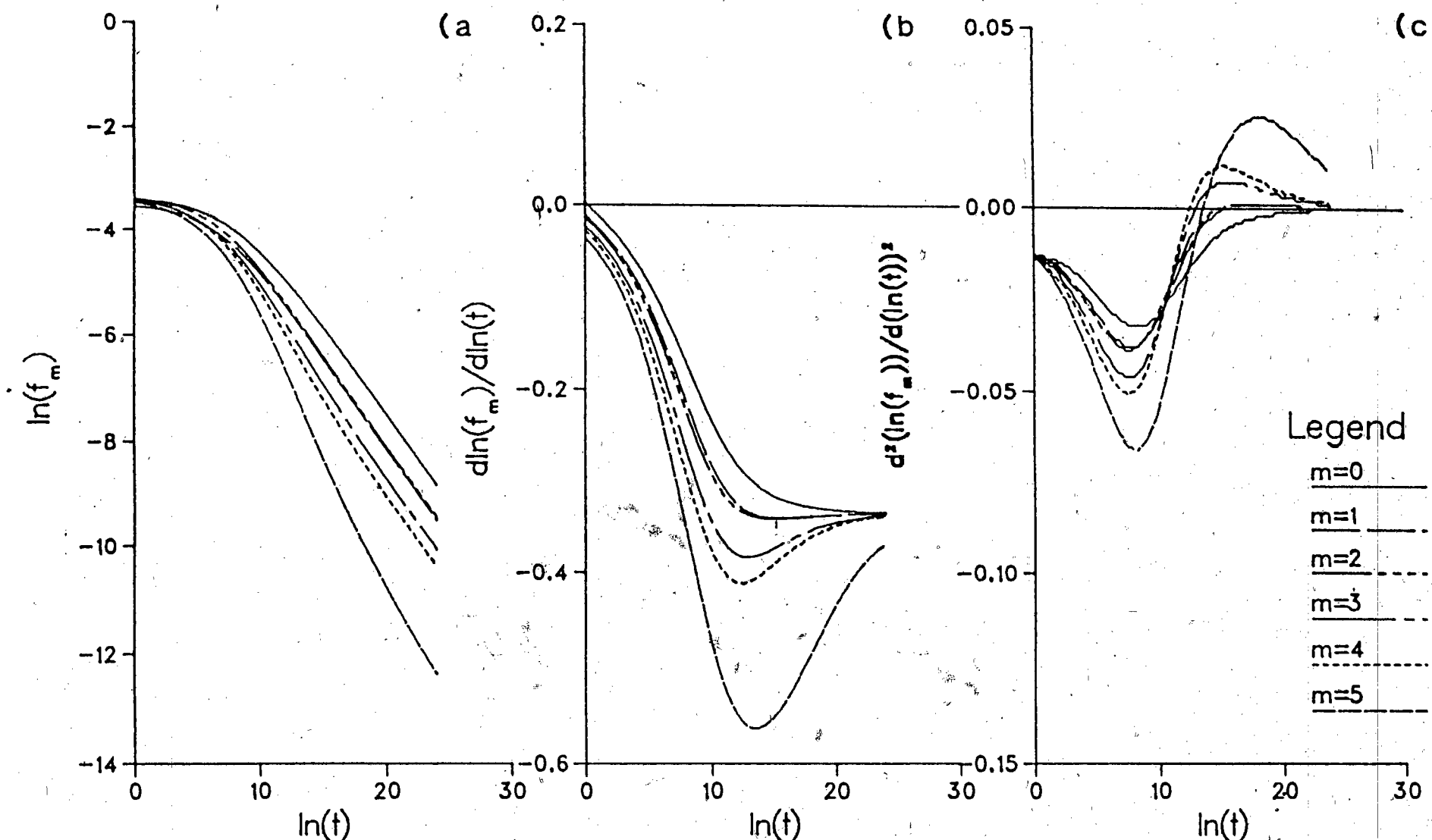
(a
(b
(c
ln(f_m)
dln(f_m)/dln(t)
d²(ln(f_m))/d(ln(t))²
ln(t)
ln(t)
ln(t)
Legend
m=0
m=1
m=2
m=3
m=4
m=5

1016

Figure 5.2 ; Behaviour of the first six expansion coefficients as functions of t, for w=1.0, a) log-log plot of $f_m(t)$, b) first derivative, c) second derivative.

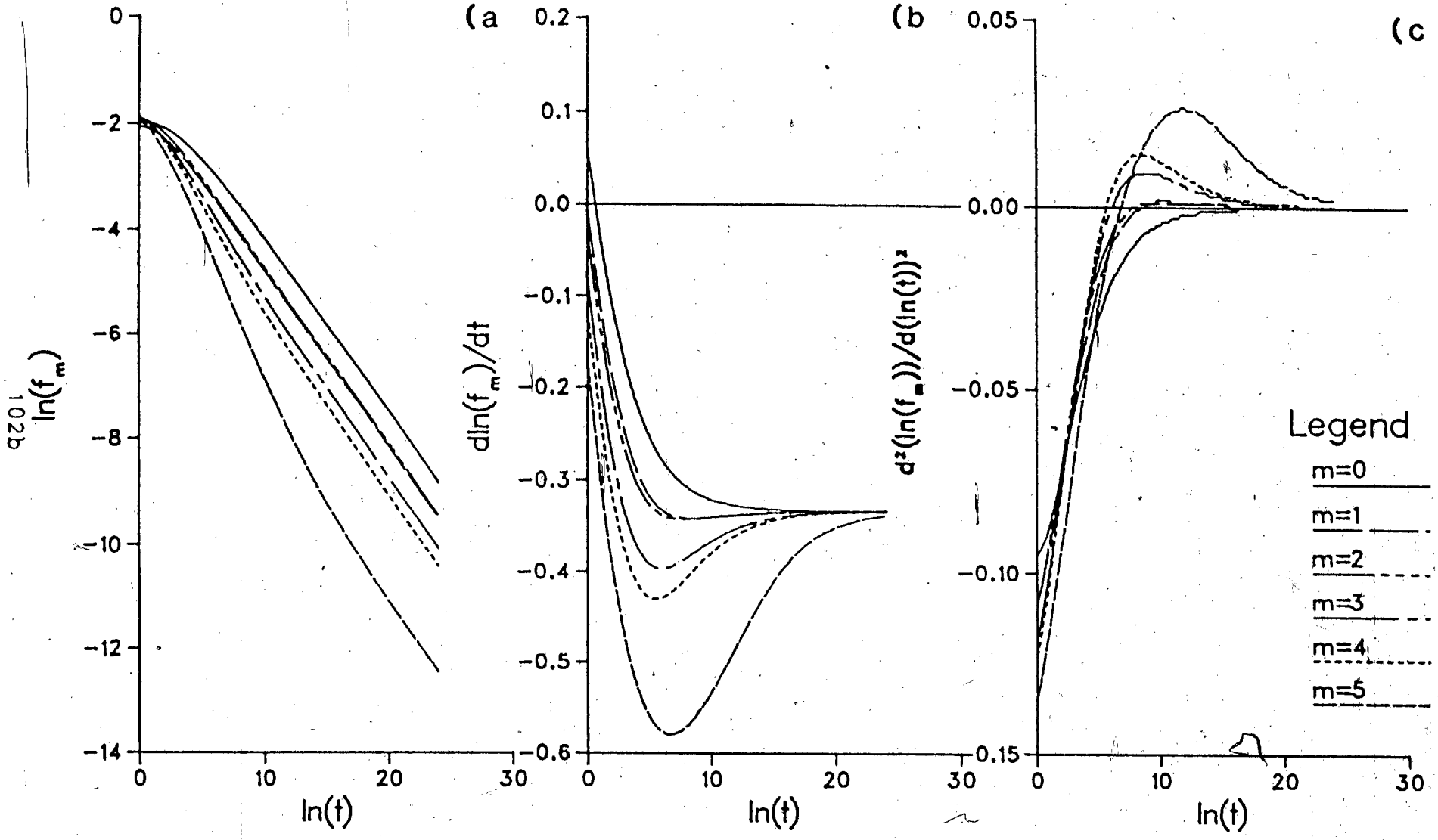
(a
(b
(c
ln(f_m)
dln(f_m)/dt
d²(ln(f_m))/d(ln(t))²
ln(t)
ln(t)
ln(t)
Legend
m=0
m=1
m=2
m=3
m=4
m=5

Figure 5.3 ; Behaviour of the first six expansion coefficients as functions of t, for w=10.0, a) log-log plot of $f_m(t)$, b) first derivative, c) second derivative.

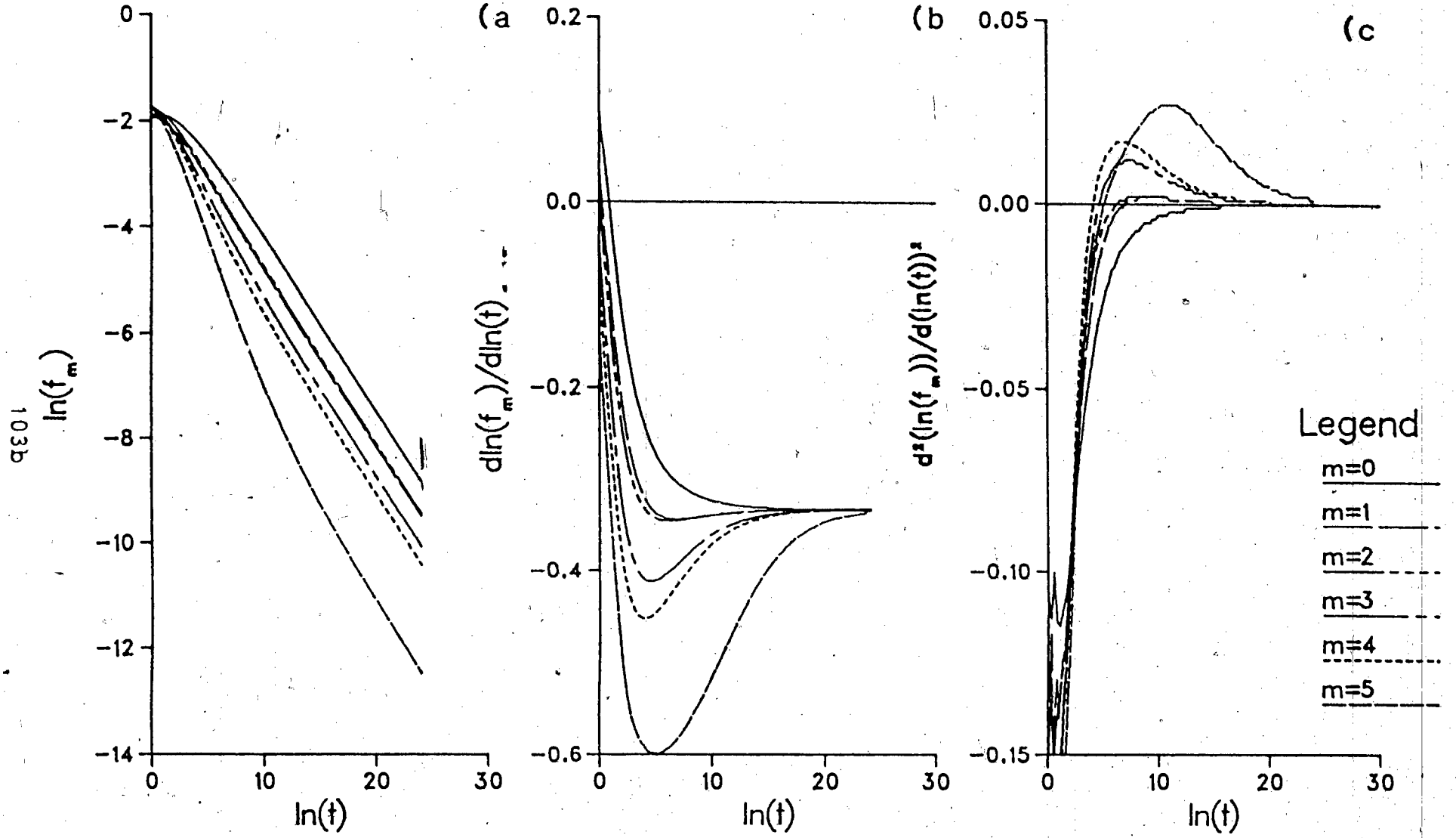
(a
(b
(c
ln(f_m)
dln(f_m)/dln(t)
d²(ln(f_m))/d(ln(t))²
ln(t)
ln(t)
ln(t)
Legend
m=0
m=1
m=2
m=3
m=4
m=5

From the sequences of plots shown in figures 5.1 to 5.3 we get an estimate of the relaxation time τ in terms of the expansion in oscillator functions of the order of e^{20}. In terms of real time, recalling that time has been scaled through $t_{real} = \sqrt{h/g}\tau$, the real relaxation time is also of order e^{20}. Due to the considerable length of this relaxation time we can conclude that it would be impossible to observe the asymptotic behaviour of the radiation solutions of the KdV equation experimentally. This conculsion is reinforced by the fact that in the derivation of the KdV equation viscous forces were neglected. However over the time calculated for the relaxation of the radiation solutions the viscous forces acting in a real fluid would have damped the motion to zero, which would then negate the experimental observation of the asymptotic behaviour of the radiation solutions.

A secondary result for the figures presented is that the small (w=0.1) pulse has a longer relaxation time than the larger ones w=1.0 and 10.0, which can be seen by comparing the three second derivative curves. It is conjectured that this behaviour is a manifestation of the fact that the linear KdV equation admits similarity solutions of all decay rates of the form $t^{-n/3}$, for n=1,2,3... where as the KdV equation admits only similarity solutions of decay rate $t^{-1/3}$. Thus for small initial pulses the non-linear aspects of the KdV equation play a weaker role in the evolution of the pulse than large initial pulses and as such the smaller disturbance pulse evolves according to the

linear KdV.

On a more direct level this behaviour is due solely to the comparitive width of the smaller width reflection coefficient to that of the larger, i.e. the width is narrower to begin with and thus takes longer to reach the asymptotic limit, see figure 4.1.

To get a fuller picture of how the expansion coefficients were evolving with time, we calculated them up to order 800 for the times $t= e^{-1}, e^{1}, e^{5}, e^{10}$, and e^{100}, for the three initial widths w=0.1,1.0,and 10.0. These sequences of spectra up to order 200 are shown in figures 5.4 through 5.6 The final two plots of each sequence exhibit numerical noise, as a consequence of the truncation of the sequence at 800 terms.

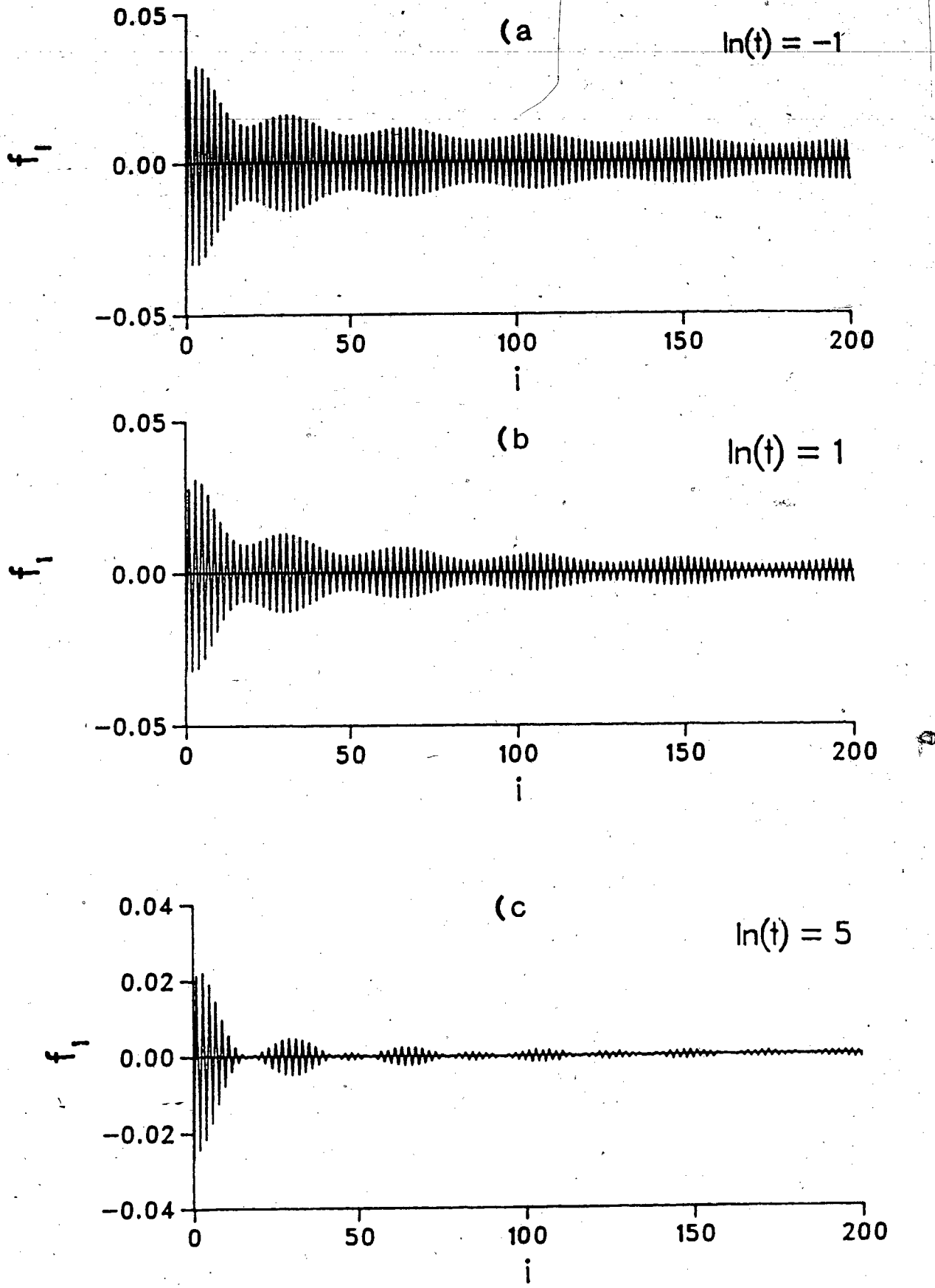
(a
ln(t) = −1
0.05
0.00
−0.05
0
50
100
150
200
i
(b
ln(t) = 1
0.05
0.00
−0.05
0
50
100
150
200
i
(c
ln(t) = 5
0.04
0.02
0.00
−0.02
−0.04
0
50
100
150
200
i

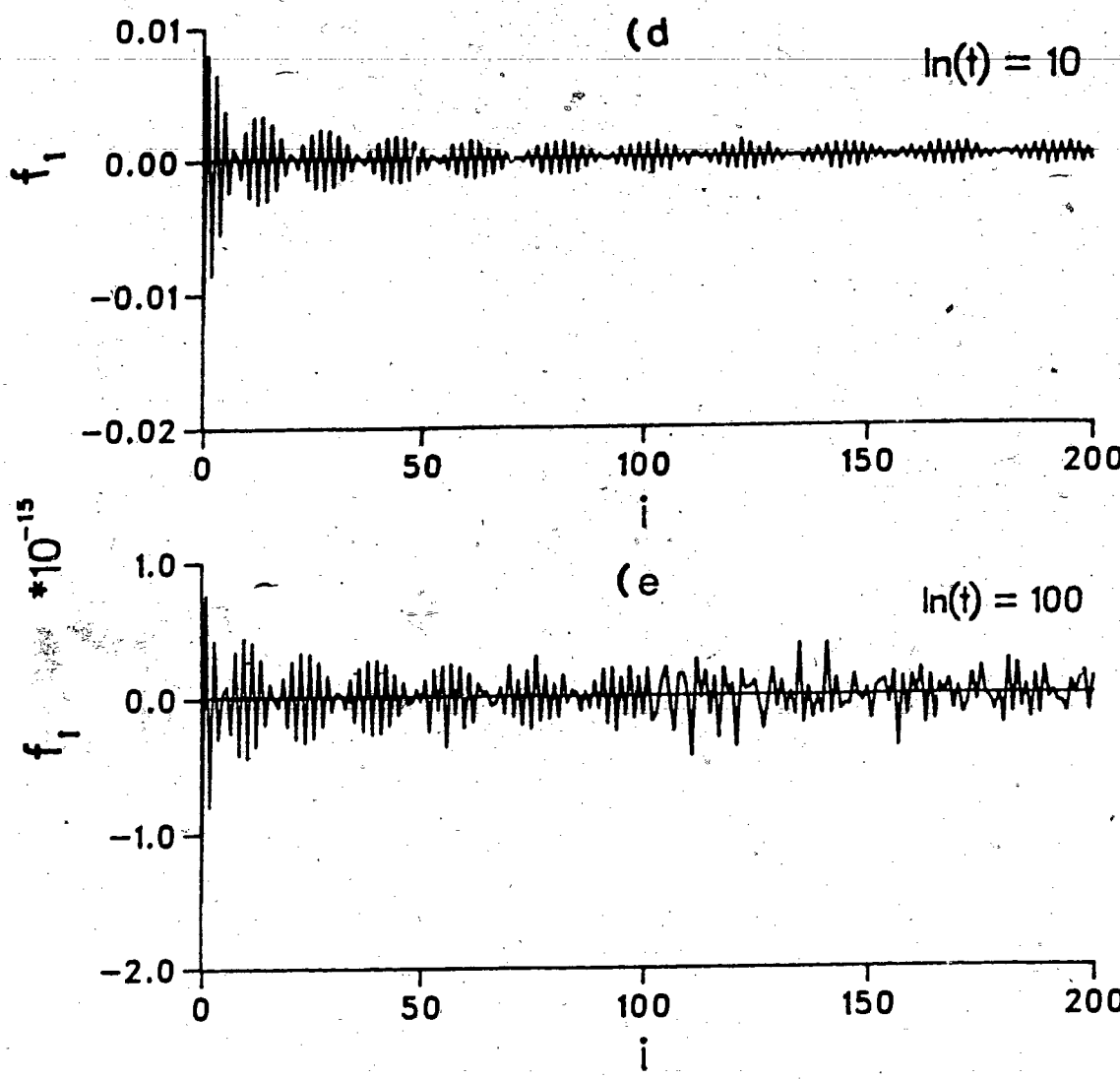

Figure 5.4 ; Oscillator expansion spectrum for w=0.1 for orders 0-200, at a) ln(t)=-1, b) 1, c) 5, d) 10, and e) 100.

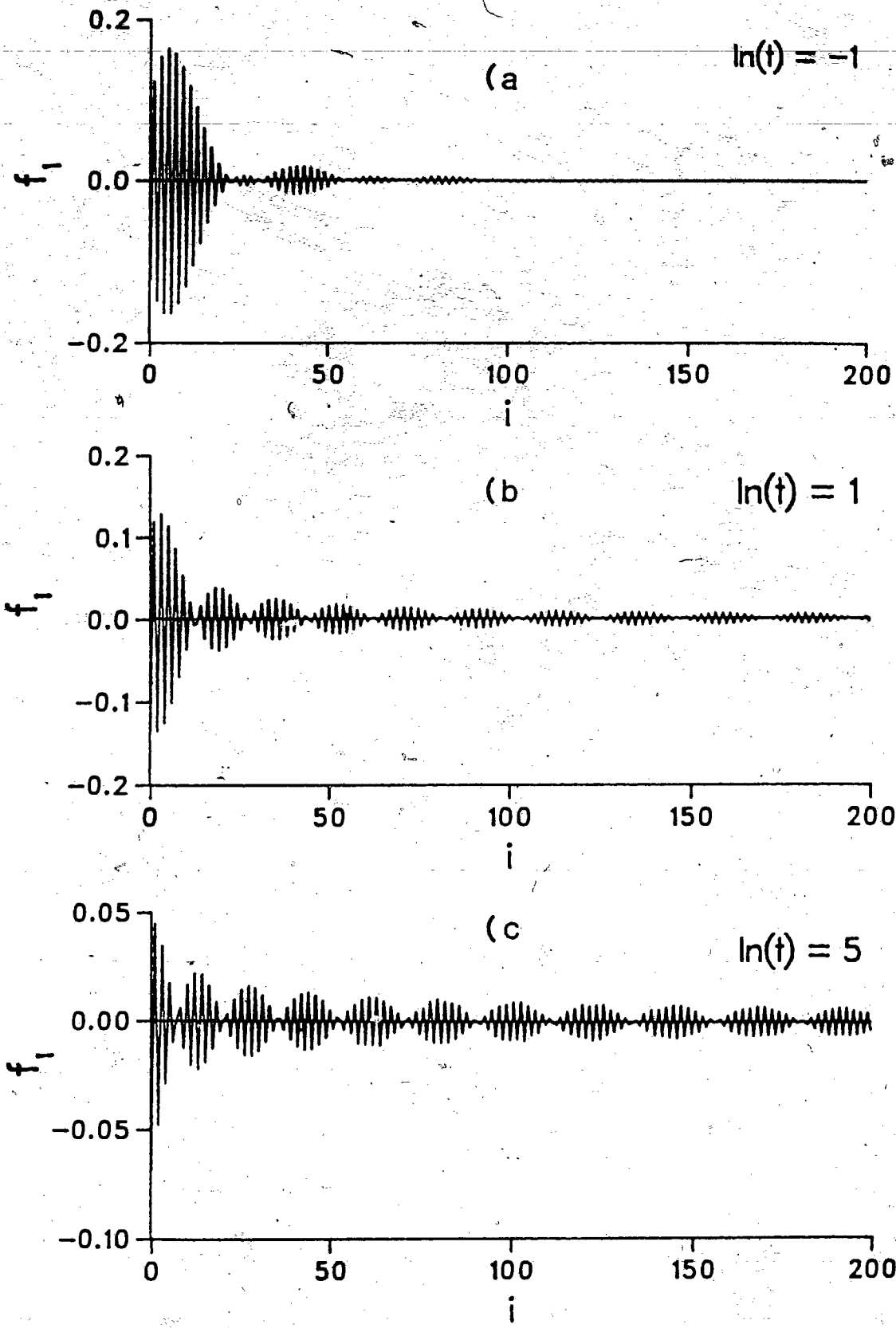
(a
ln(t) = −1
0.2
0.0
−0.2
0
50
100
150
200
i
(b
ln(t) = 1
0.2
0.1
0.0
−0.1
−0.2
0
50
100
150
200
i
(c
ln(t) = 5
0.05
0.00
−0.05
−0.10
0
50
100
150
200
i

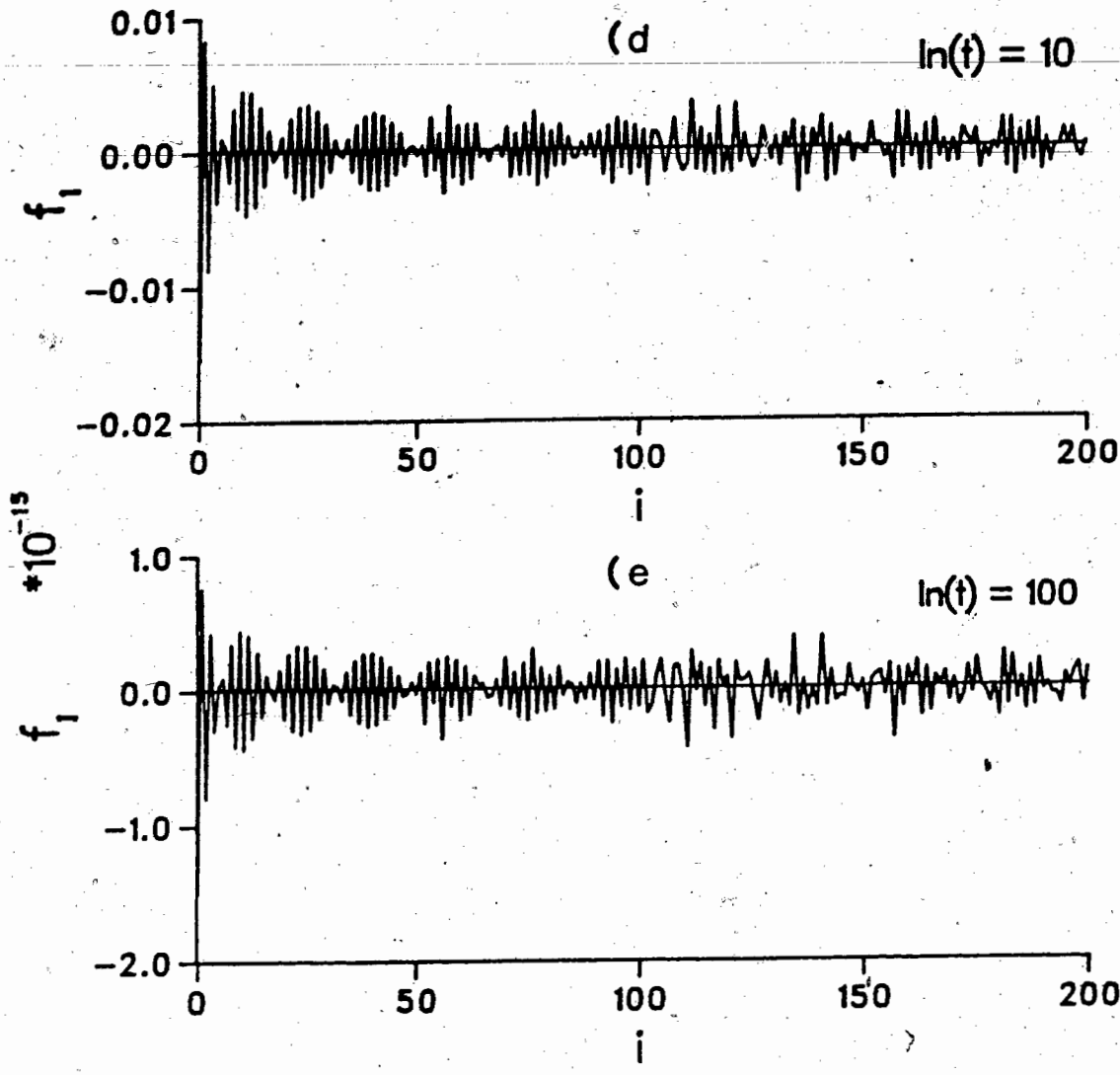

Figure 5.5 ; Oscillator expansion spectrum for w=1.0 for orders 0-200, at a) ln(t)=-1, b) 1, c) 5, d) 10, and e) 100.

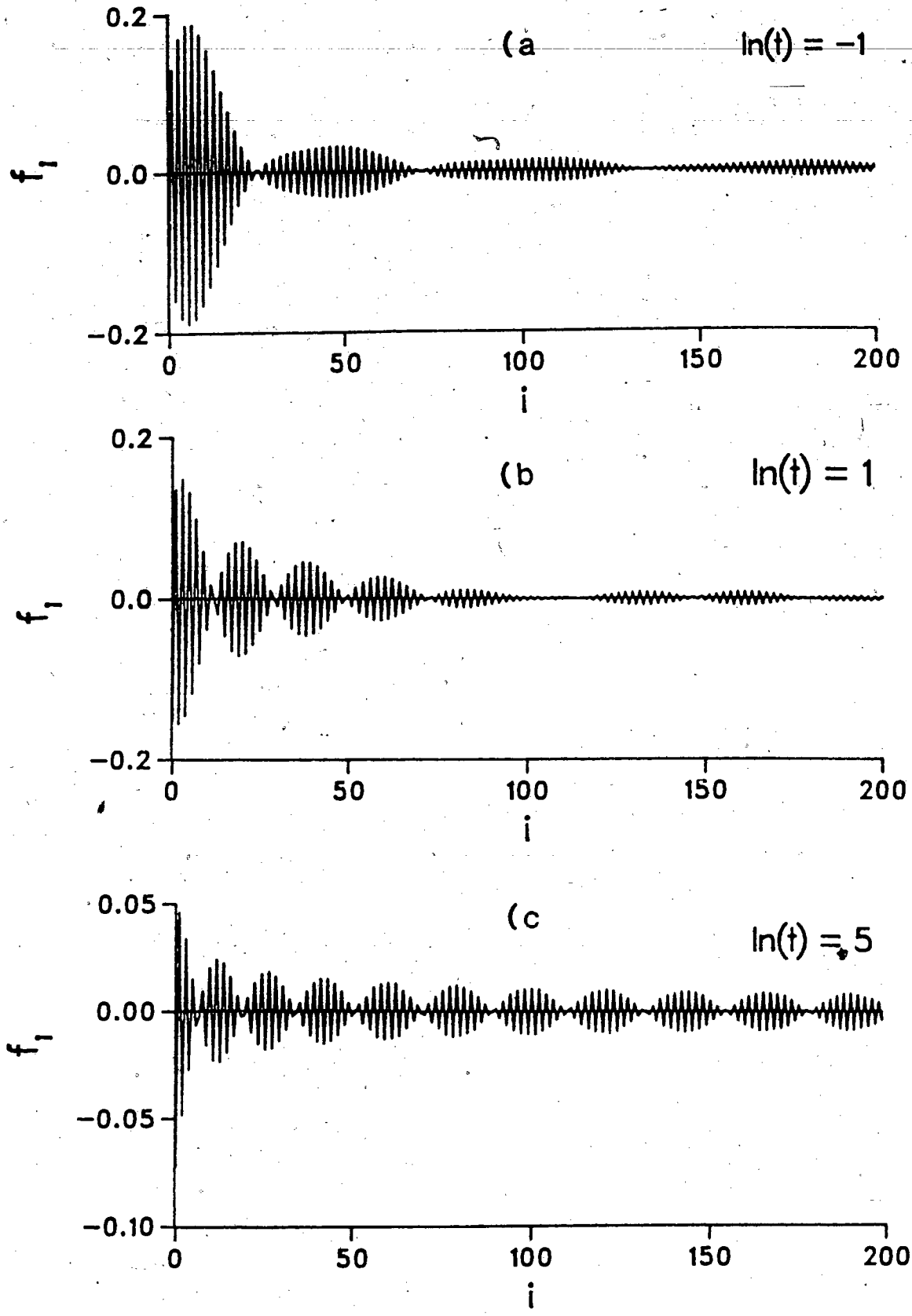
(a
ln(t) = −1
0.2
0.0
−0.2
0
50
100
150
200
i
(b
ln(t) = 1
0.2
0.0
−0.2
0
50
100
150
200
i
(c
ln(t) = 5
0.05
0.00
−0.05
−0.10
0
50
100
150
200
i

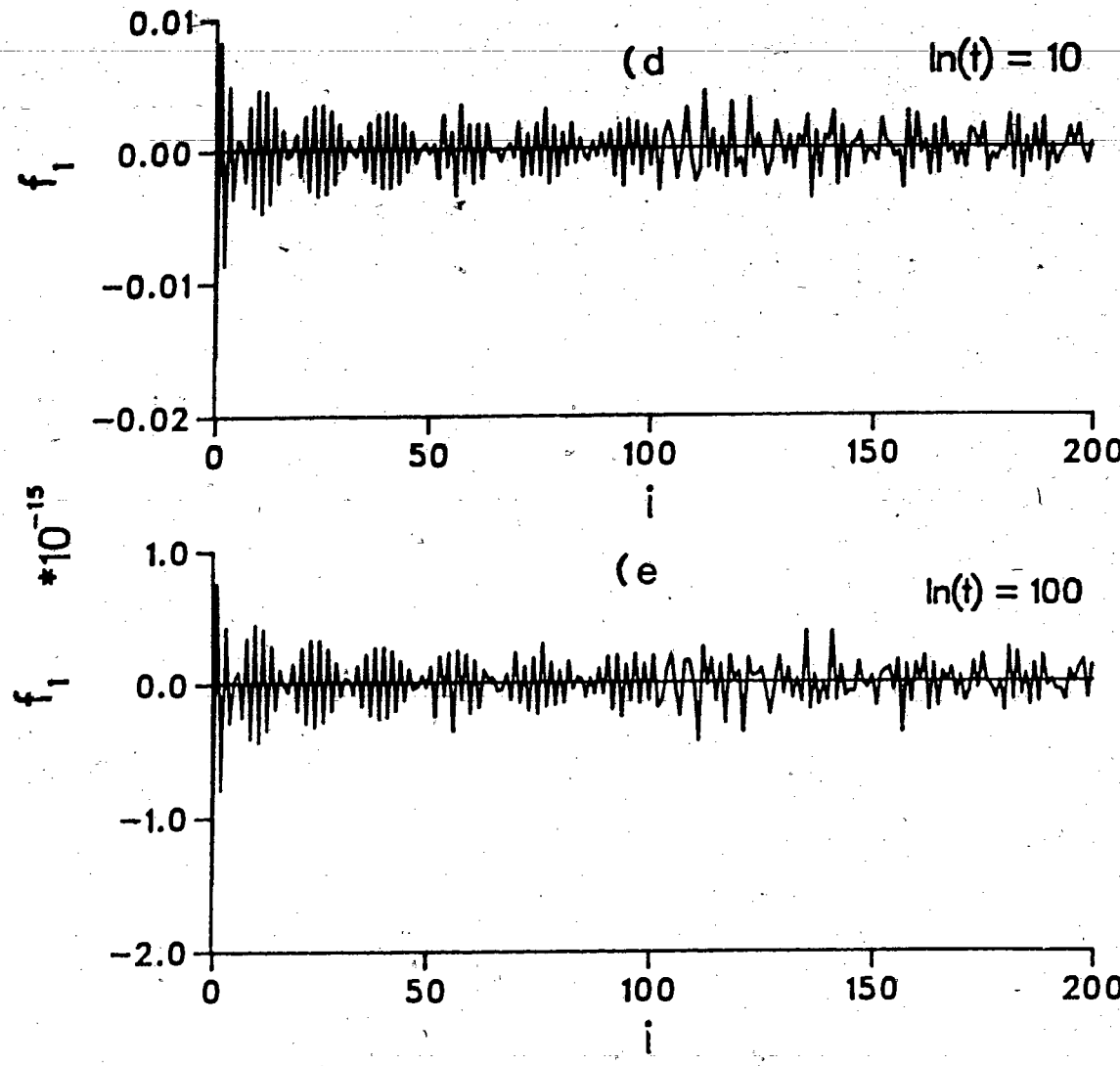

Figure 5.6 ; Oscillator expansion spectrum for w=10.0 for orders 0-200, at a) ln(t)=-1, b) 1, c) 5, d) 10, and e) 100.

By looking at the final plot of each of the sequences of spectra it was noted that the final spectra were identical. This observation would indicate that the asymptotic form of the radiation solutions was independent of the initial pulse width. This is born out by equation 7, which is independent of the parameters of the initial pulse, and thus the asymptotic form of the solution must be independent of the initial parameters. From these results it might be conjectured that all physically meaningful initial pulse profiles will exhibit the same asymptotic form.

The beats that appear in the spectra plotted are manifestations of the phase factor, $e^{i(\phi(k/t^{1/3}) + k^3)}$, of the reflection coefficient, beating against the "waves" of the Oscillator functions. The beating is weaker for the small width (w=0.1) pulse than for the other two, because of the narrowness of the modulus of the reflection coefficient limiting the effective range of integration over the wave number. By the same token the decay rate of the "spectral" coefficients is also slower for the small pulse.

With the expansion coefficients calculated for the times e^1 through e^{100} it was a small matter to invert them to regain the profile for the kernel in terms of the variable z at those times. These results are plotted in figures 5.7 through 5.9 for the three different pulse widths w= 0.1, 1.0, and 10.0 and for 800 terms of the Oscillator expansion.

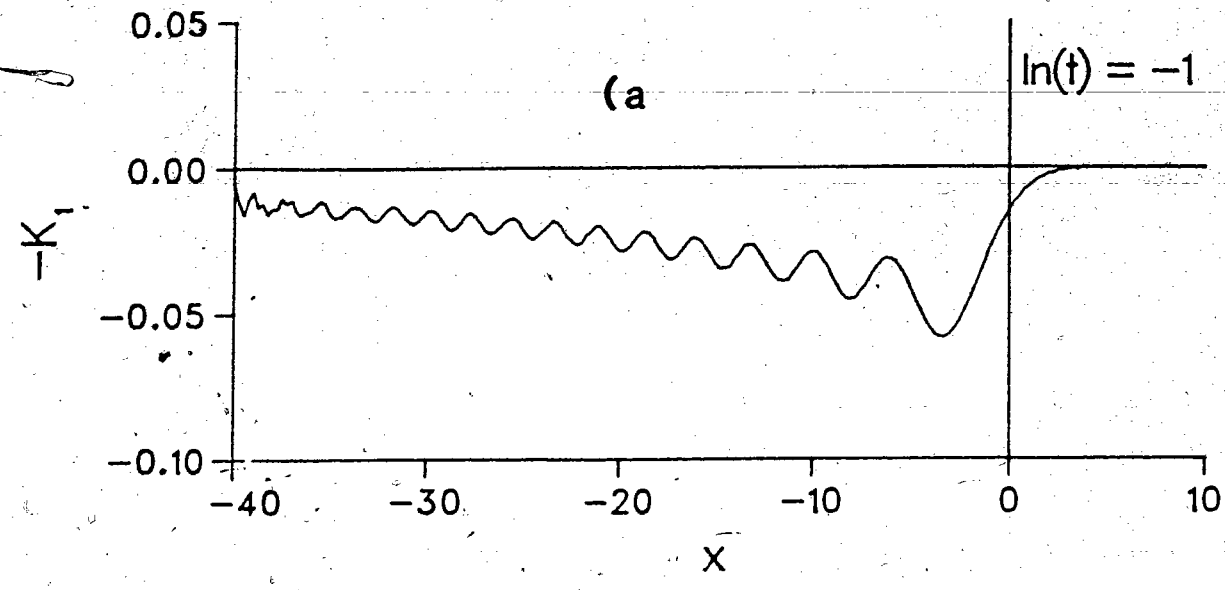
(a
ln(t) = −1
0.05
0.00
−0.05
−0.10
K
−40
−30
−20
−10
0
10
X

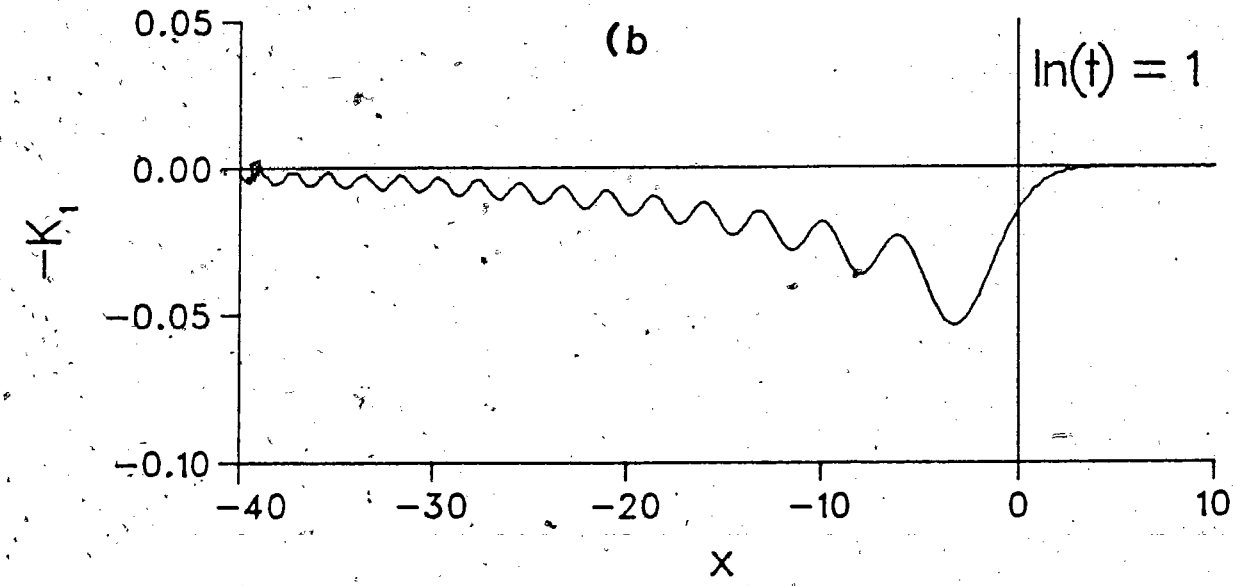
(b
ln(t) = 1
0.05
0.00
−0.05
−0.10
K
−40
−30
−20
−10
0
10
X

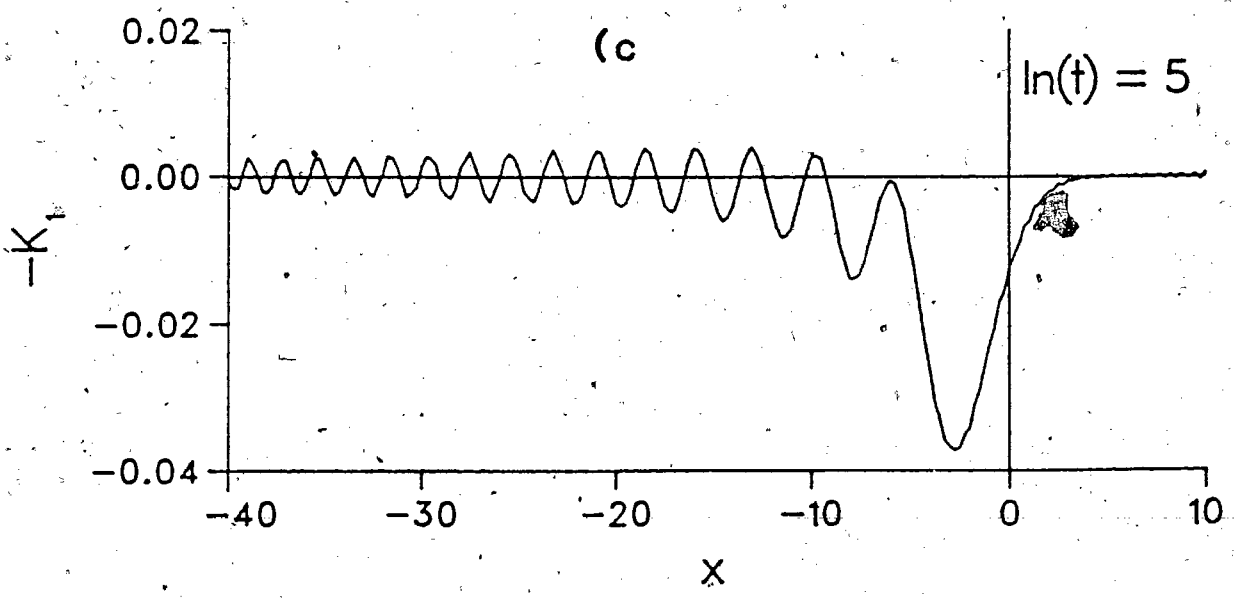
(c
ln(t) = 5
0.02
0.00
−0.02
−0.04
K
−40
−30
−20
−10
0
10
X

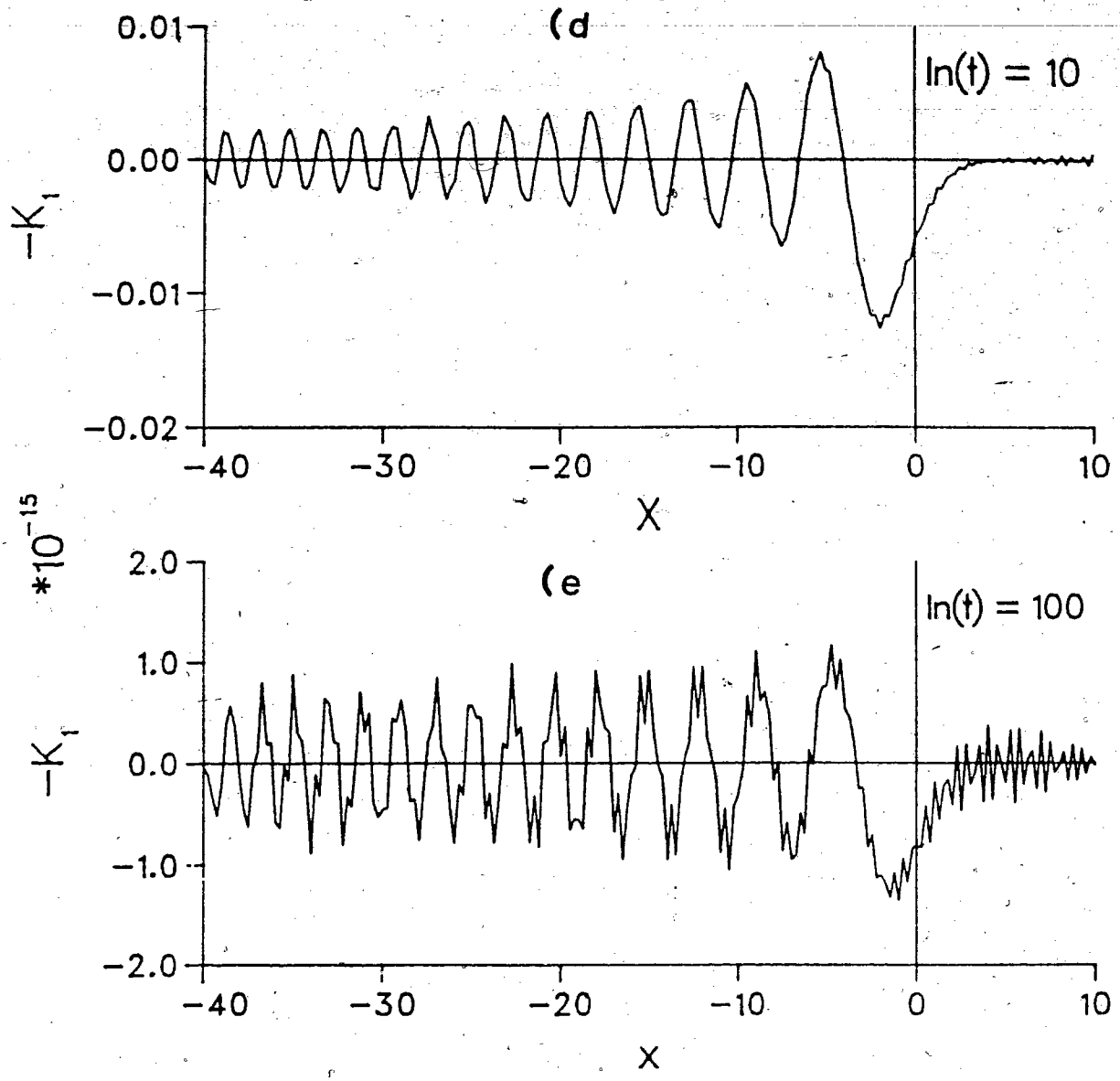

Figure 5.7 ; First term contribution to Neumman series expansion for w=0.1 at a) ln(t)=-1, b) 1, c) 5, d) 10, and e) 100.

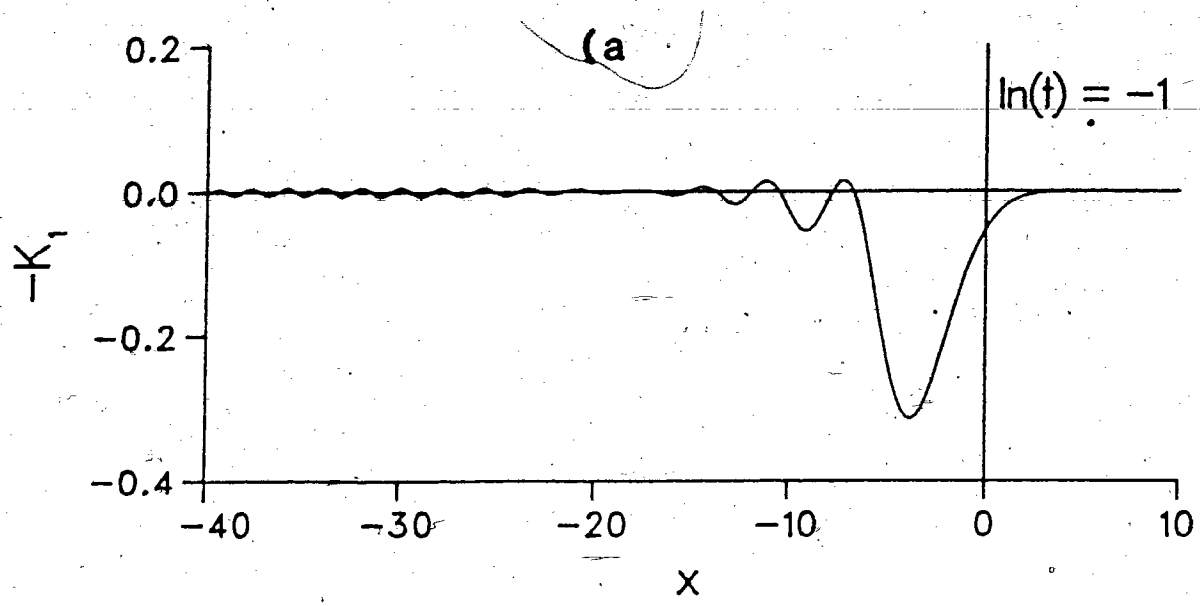
(a
ln(t) = −1
0.2
0.0
−0.2
−0.4
−40
−30
−20
−10
0
10
X

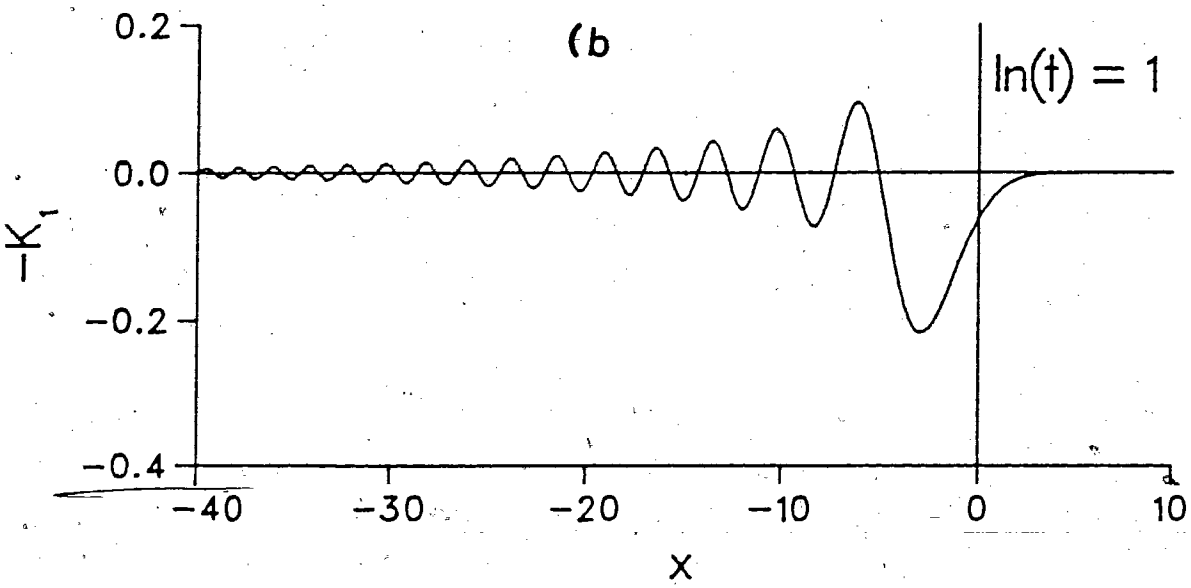
(b
ln(t) = 1
0.2
0.0
−0.2
−0.4
−40
−30
−20
−10
0
10
X

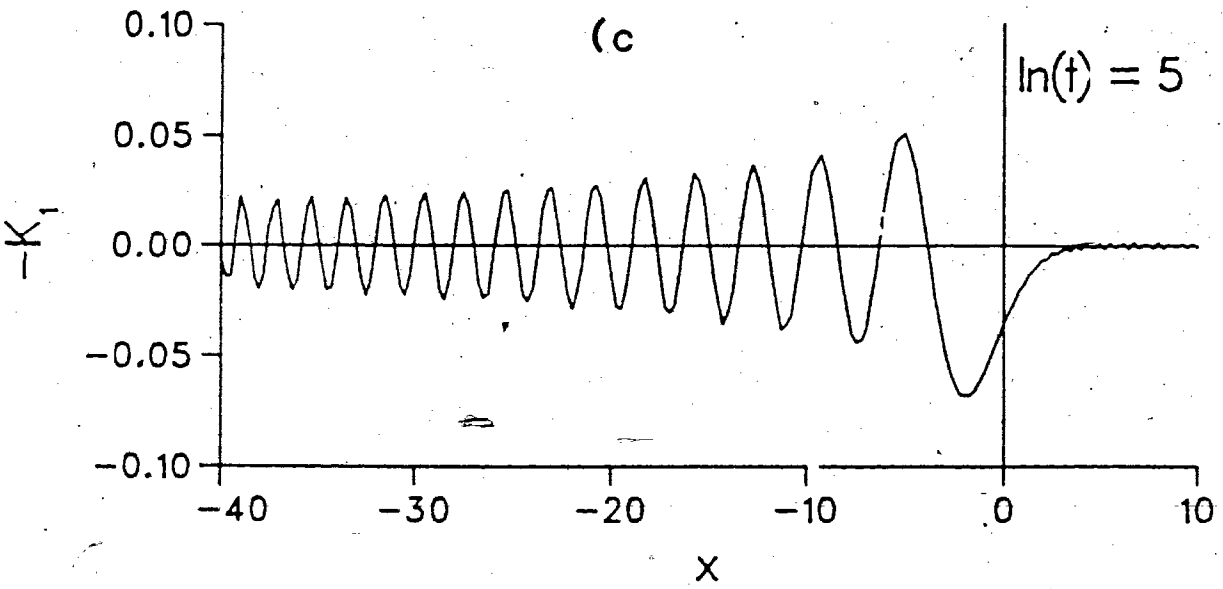
(c
ln(t) = 5
0.10
0.05
0.00
−0.05
−0.10
−40
−30
−20
−10
0
10
X

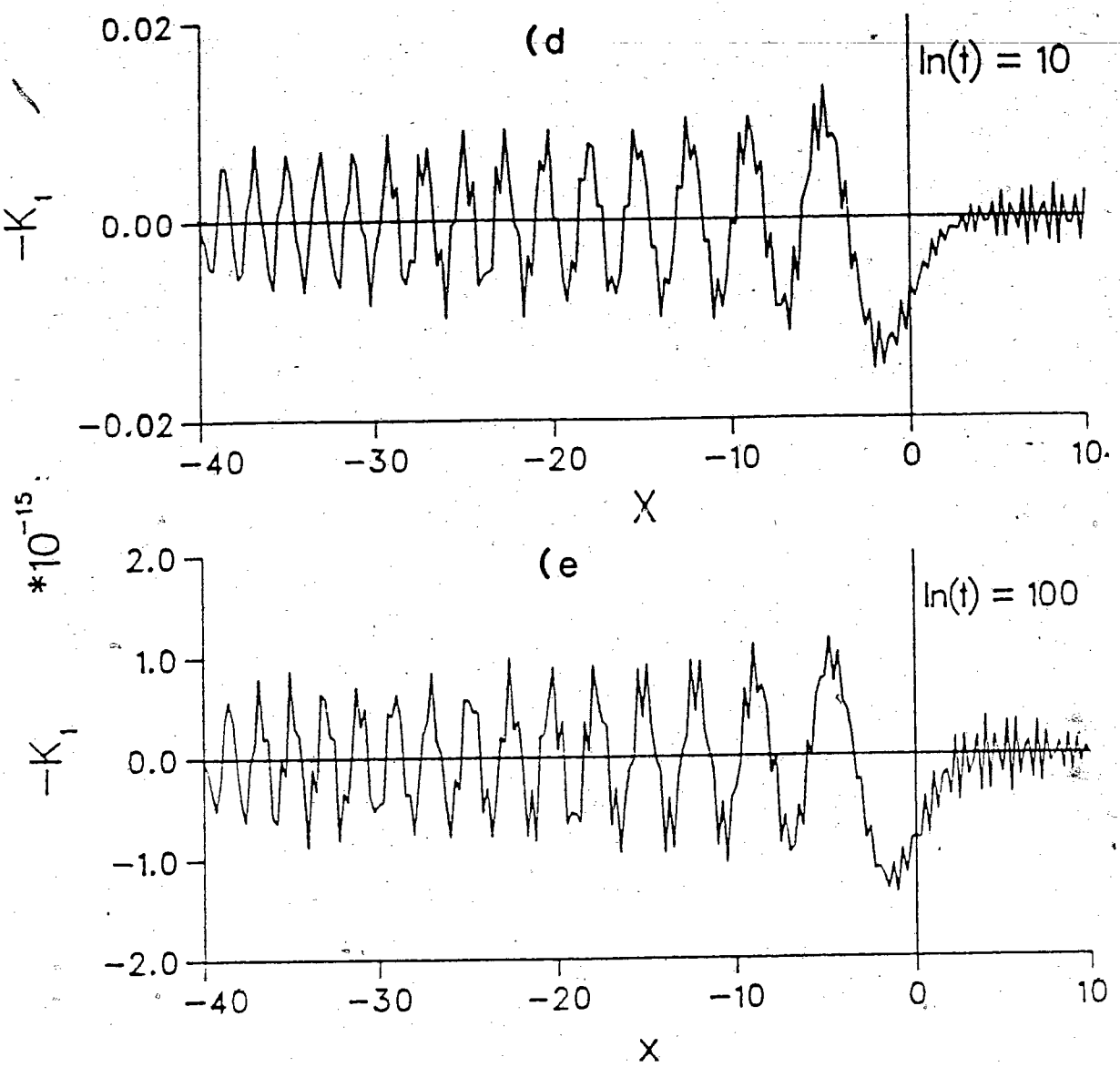

Figure 5.8 ; First term contribution to Neumann series expansion for w=1.0 at a) ln(t)=-1, b) 1, c) 5, d) 10, and e) 100.

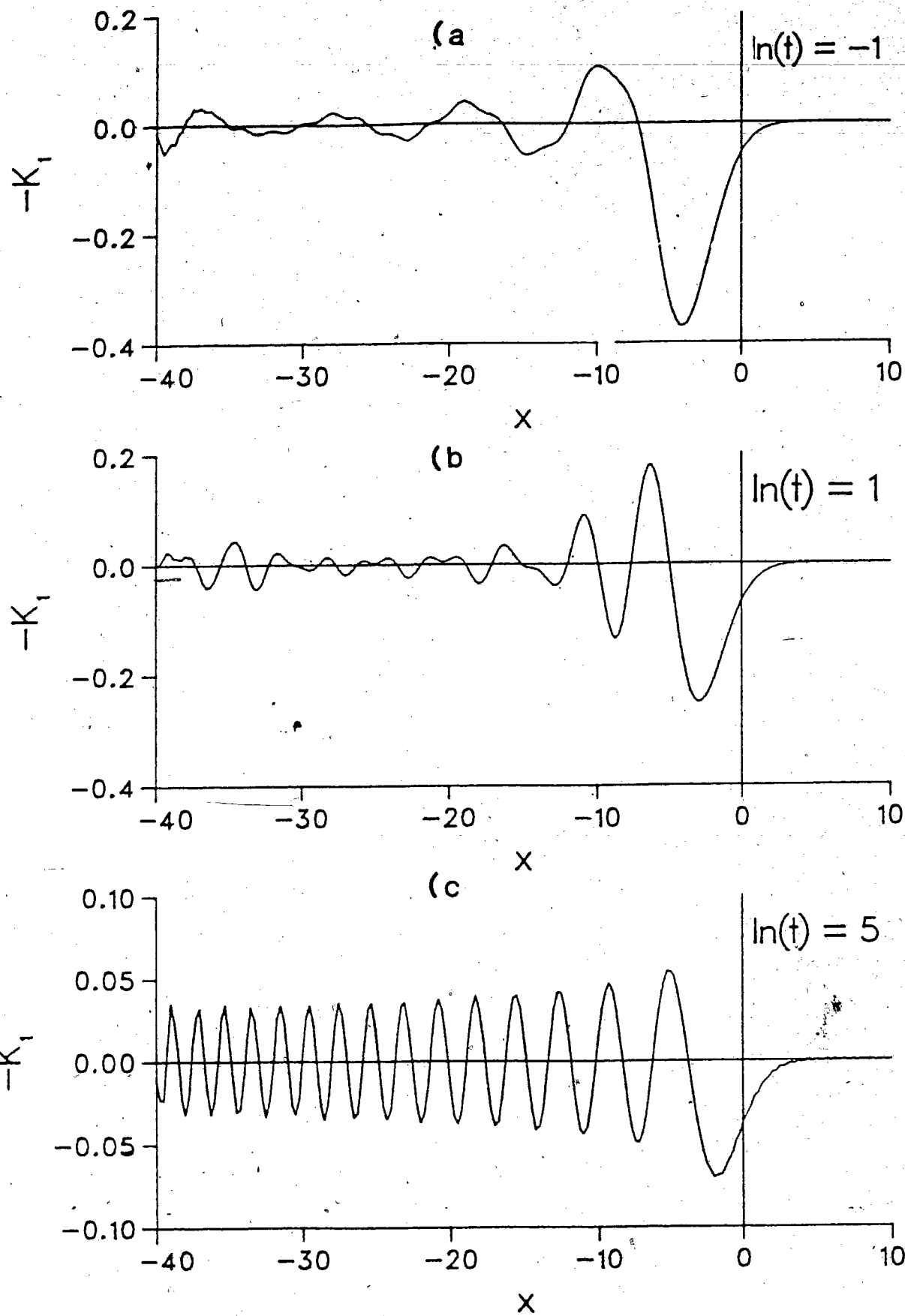
(a
ln(t) = −1
0.2
0.0
−0.2
−0.4
K
−40
−30
−20
−10
0
10
X
(b
ln(t) = 1
0.2
0.0
−0.2
−0.4
K
−40
−30
−20
−10
0
10
X
(c
ln(t) = 5
0.10
0.05
0.00
−0.05
−0.10
K
−40
−30
−20
−10
0
10
X

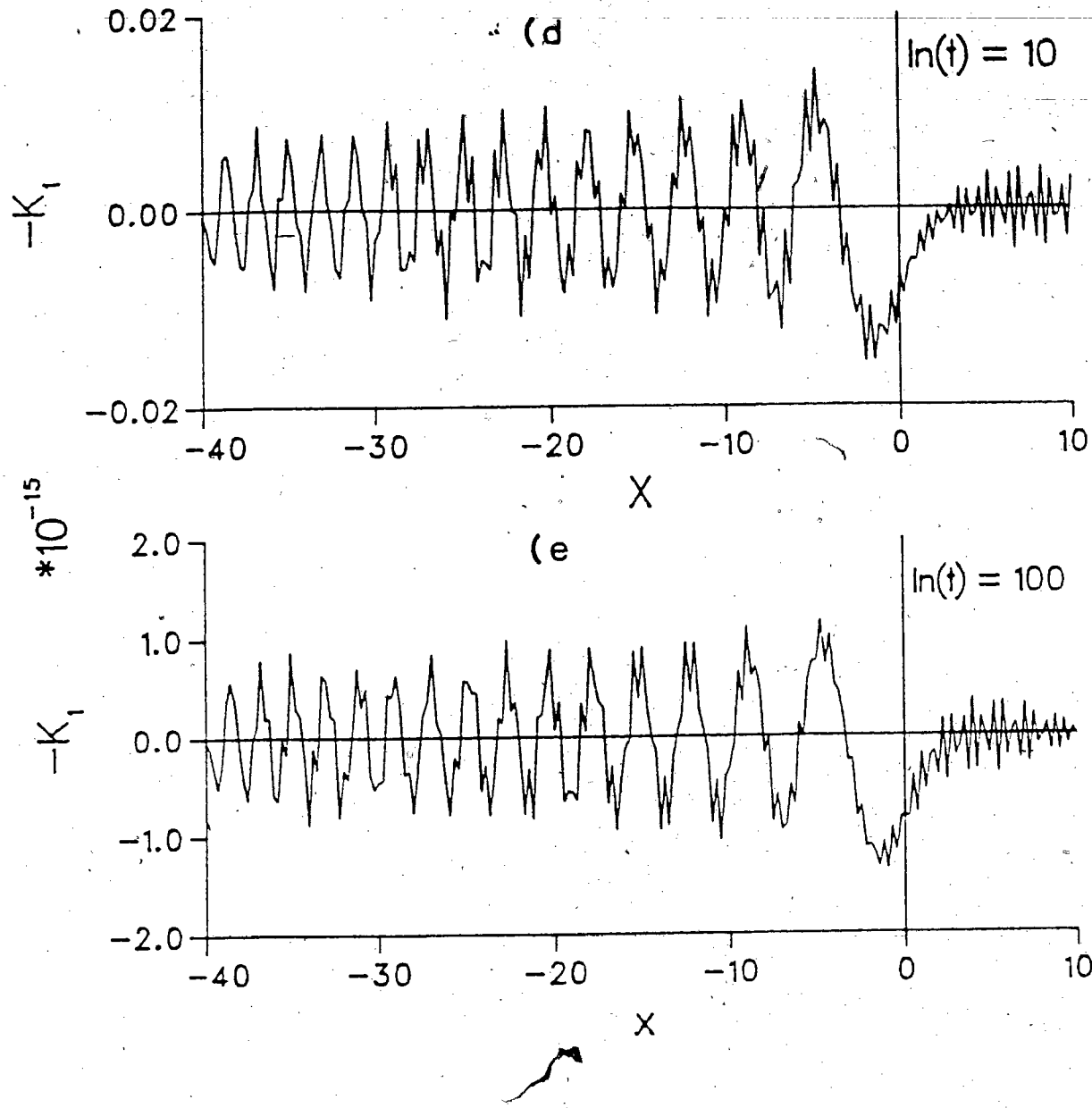

Figure 5.9 ; First term contribution to Neumann series expansion for w=10.0 at a) ln(t)=-1, b) 1, c) 5, d) 10, and e) 100.

The final plot of each figure shows explicitly that the asymptotic form of the radiation solutions are in fact identical to within the accuracy of this calculation. The ln(t) = 10 plots from the figures show clearly that large parameter profile settle down to the asymptotic behavior faster than the smaller parameter profile (w=0.1).It should be kept in mind that even though there is a considerable amount of noise present in the long time profiles the different cases all exhibit the same noise, and the same basic shape independent of the width parameter.

In a similar fashion it was possible to evaluate the first order correction term in the Neumann series expansion, i.e.

$$K(x,x,t) = -F(2x,t) + \int_x^\infty F(x+y)F(y+x)\,dy \qquad 9a$$

$$= -f_m(t)\Theta_m(z) + f_m(t)f_n(t)\,2t^{1/3}I_{mnp}\Theta_p(z)\,, \qquad 9b$$

where $z=(2x-2w)/2t^{1/3}$, and the first order correction is the second term on the right-hand side.

As was done in chapter 4 the matrix I can be split into two distinct parts

$$I_{mnp} = I^{(1)}_{mnp} + I^{(2)}_{mnp}\,,$$

where $$I^{(2)}_{mnp}\theta_p(z) = \frac{1}{2}\mathrm{erfc}(z)\delta_{mn}.$$

Thus the first order correction term becomes the sum

$$f_m(t)f_n(t)2t^{1/3}\, I^{(1)}_{mnp}\theta_p(z) + f_m(t)f_m(t)t^{1/3}\mathrm{erfc}(z). \qquad 10$$

Due to the limits of calculation time these terms were only calculated up to order 60 on the subscripts m and n, and order 90 on $\tilde{p}$ as discussed in chapter 4. Plots of these contributions for the set of times $t= e^{-1}, e^{1}, e^{5}, e^{10}$, and e^{100} are shown in figures 5.10 through 5.12, for the initial pulse width w= 1.0, which was representative of the behaviour of the other two. The first figure 5.10 shows the time evolution of the first term of the correction

$$f_m(t)f_n(t)2t^{1/3}\, I^{(1)}_{mnp}\theta_p(z) .$$

The second figure, 5.11 shows the second term of the correction

$$f_m(t)f_n(t)t^{1/3}\mathrm{erfc}(z).$$

The final figure 5.12 shows the sum of the two contributions that comprise the correction.

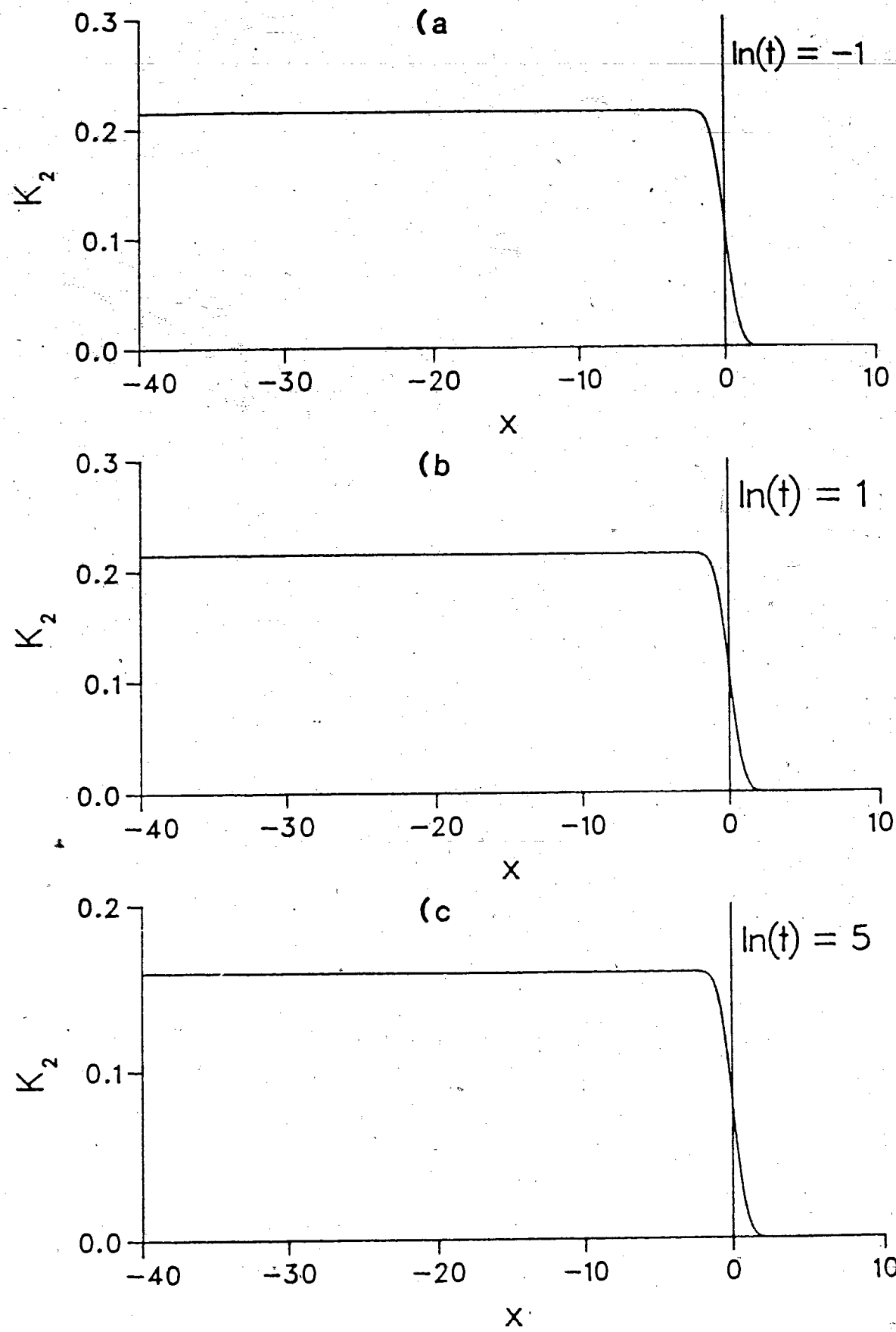
(a
ln(t) = −1
0.3
0.2
0.1
0.0
K2
−40
−30
−20
−10
0
10
X
(b
ln(t) = 1
0.3
0.2
0.1
0.0
K2
−40
−30
−20
−10
0
10
X
(c
ln(t) = 5
0.2
0.1
0.0
K2
−40
−30
−20
−10
0
10
X

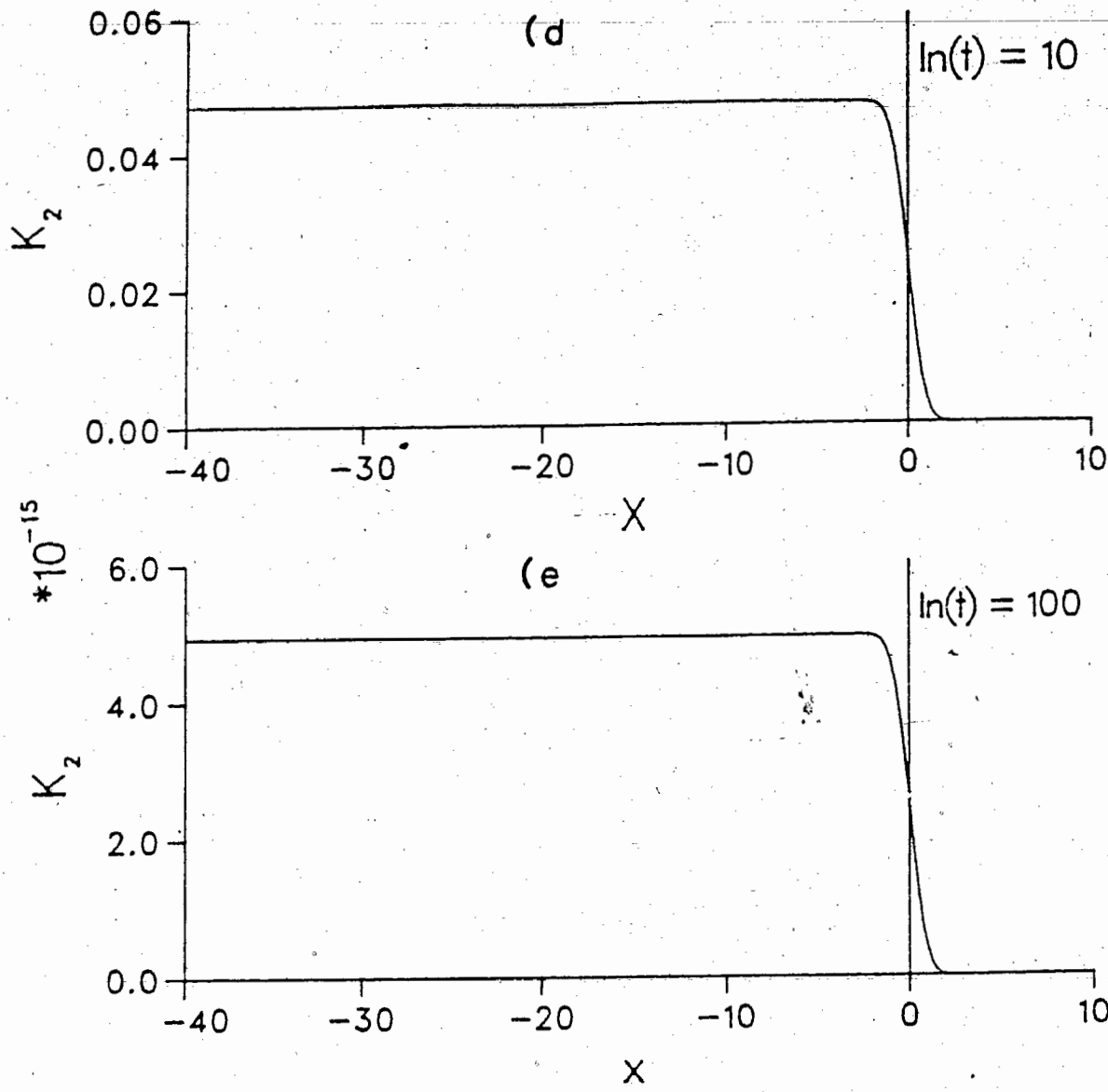

Figure 5.10 ; Complimentary error function contribution to second term of Neumann series expansion for w=1.0 at a) ln(t)=-1, b) 1, c) 5, d) 10, and e) 100.

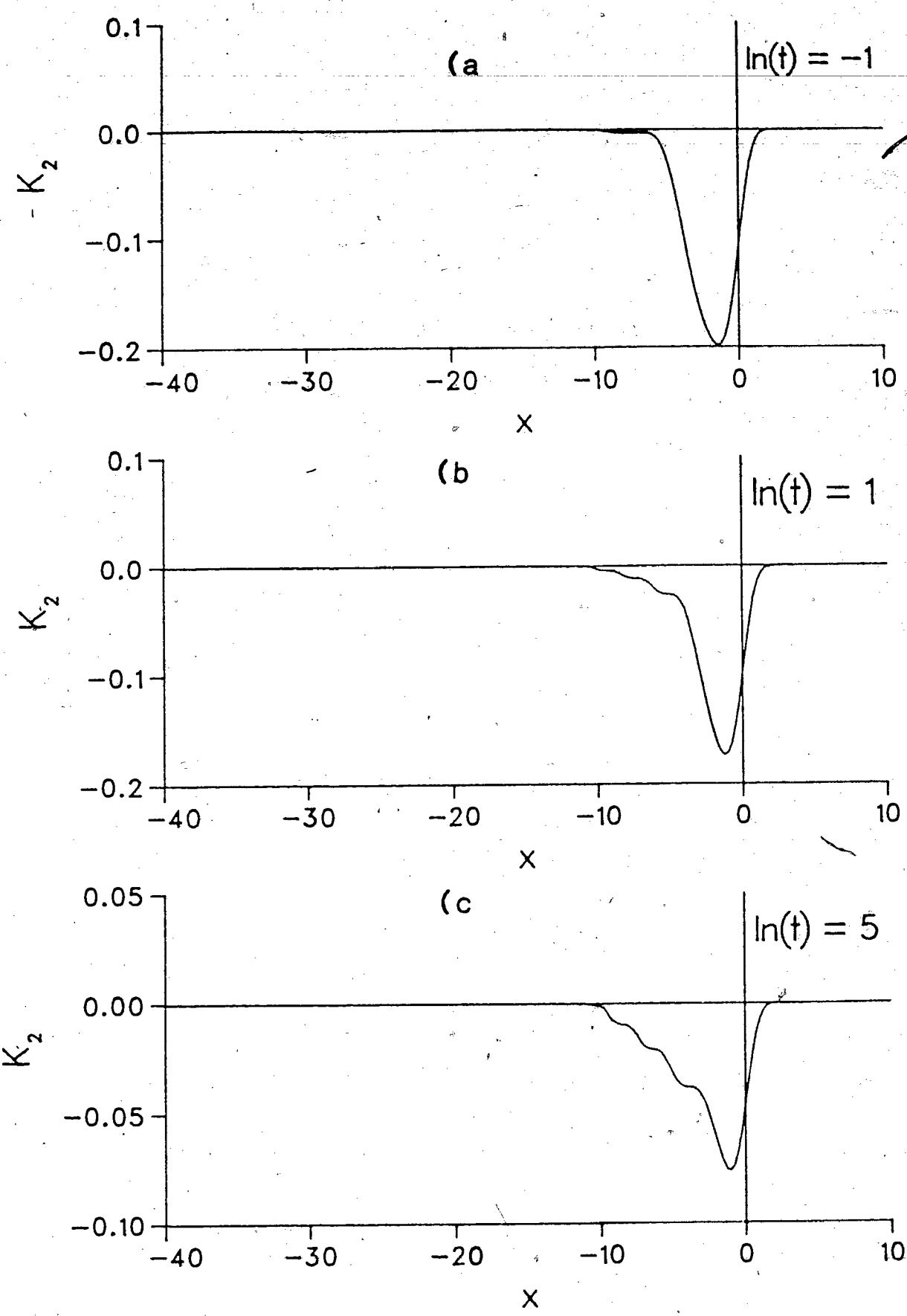
(a
ln(t) = −1
0.1
0.0
−0.1
−0.2
−K2
−40
−30
−20
−10
0
10
X
(b
ln(t) = 1
0.1
0.0
−0.1
−0.2
K2
−40
−30
−20
−10
0
10
X
(c
ln(t) = 5
0.05
0.00
−0.05
−0.10
K2
−40
−30
−20
−10
0
10
X

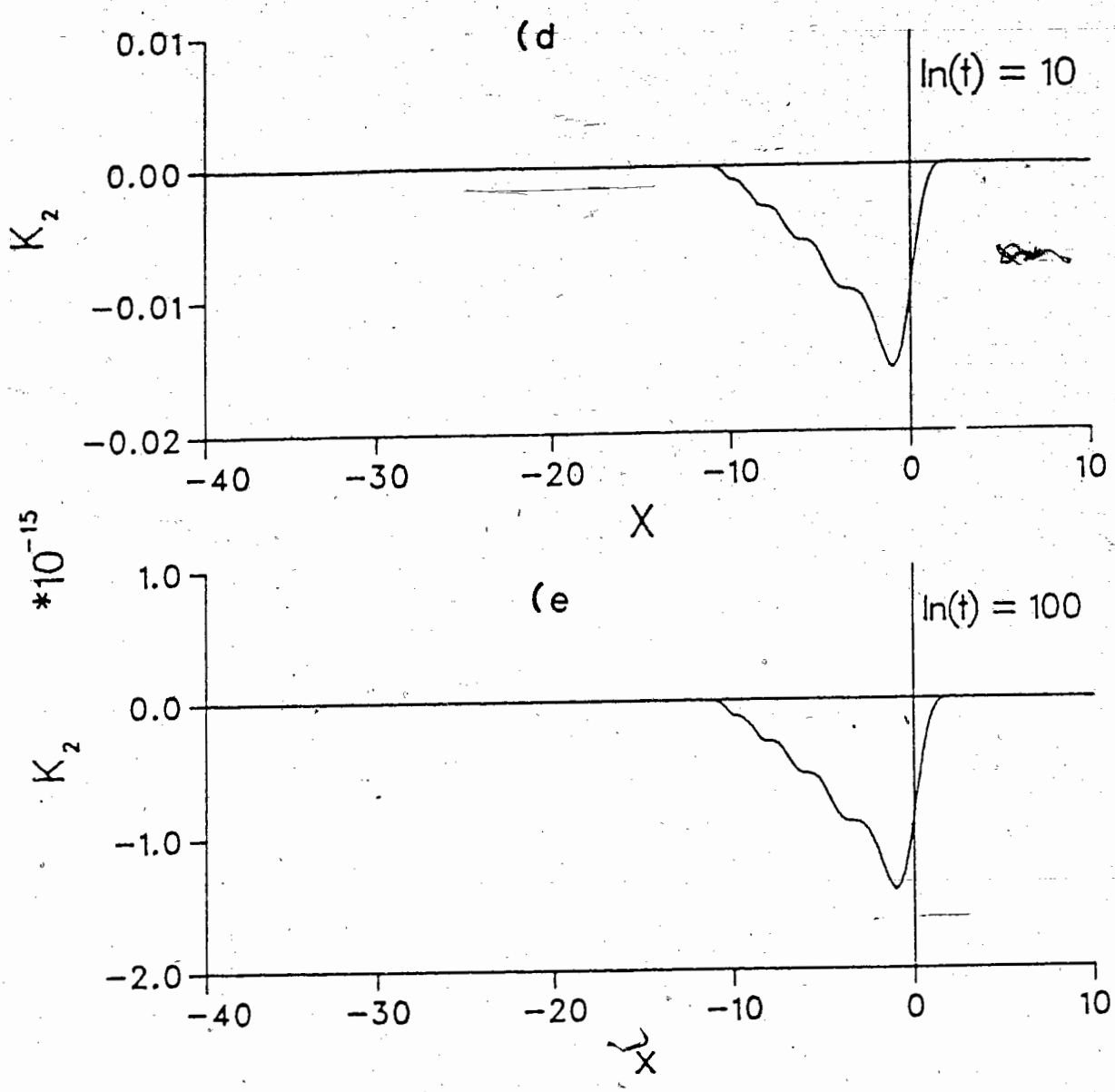

Figure 5.11 ; Second localized contribution to the second term of the Neumann series expansion for w=1.0 at a) ln(t)=-1, b) 1, c) 5, d) 10, and e) 100.

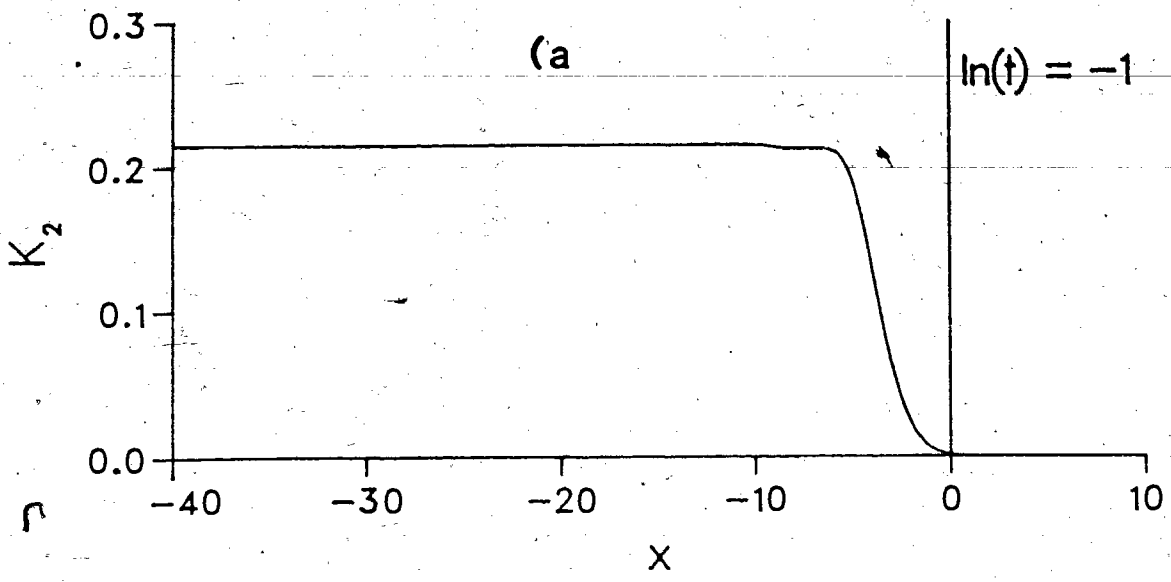
(a
ln(t) = −1
0.3
0.2
0.1
0.0
K2
−40
−30
−20
−10
0
10
X

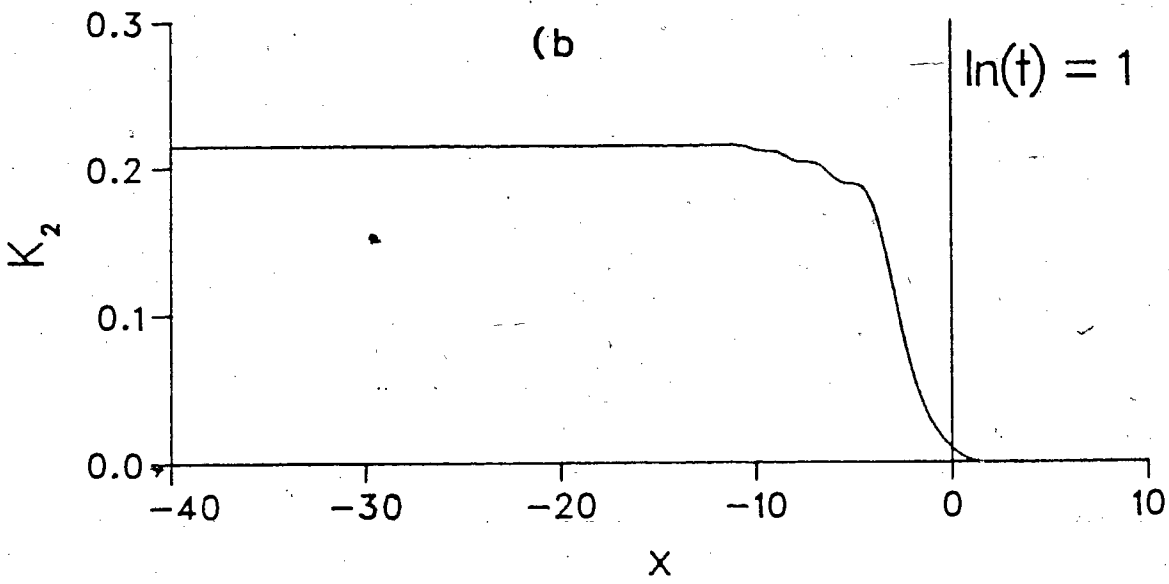
(b
ln(t) = 1
0.3
0.2
0.1
0.0
K2
−40
−30
−20
−10
0
10
X

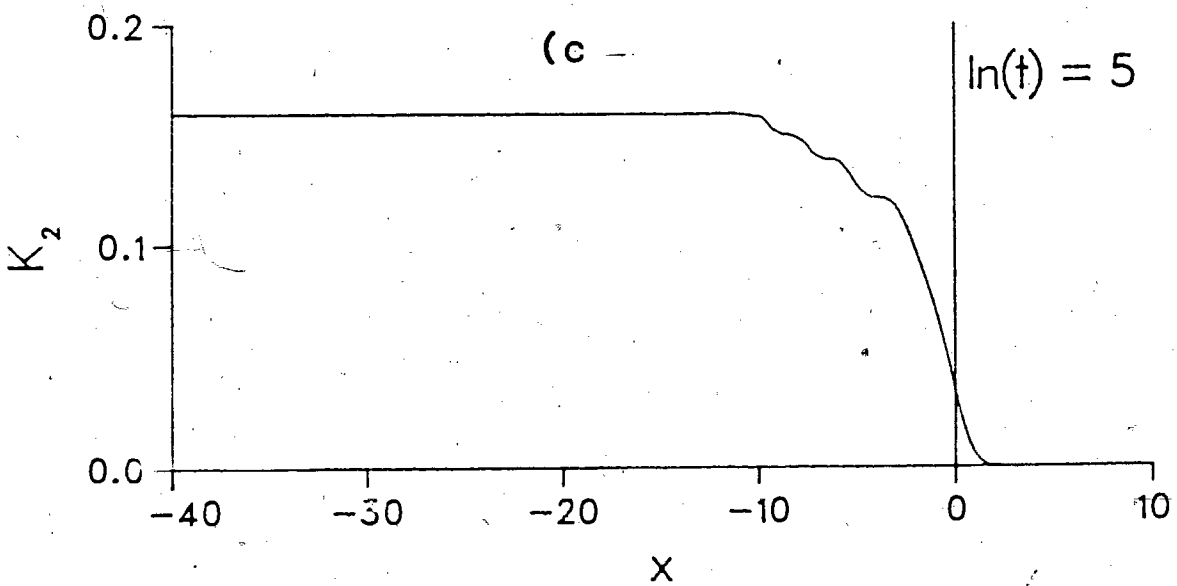
(c
ln(t) = 5
0.2
0.1
0.0
K2
−40
−30
−20
−10
0
10
X

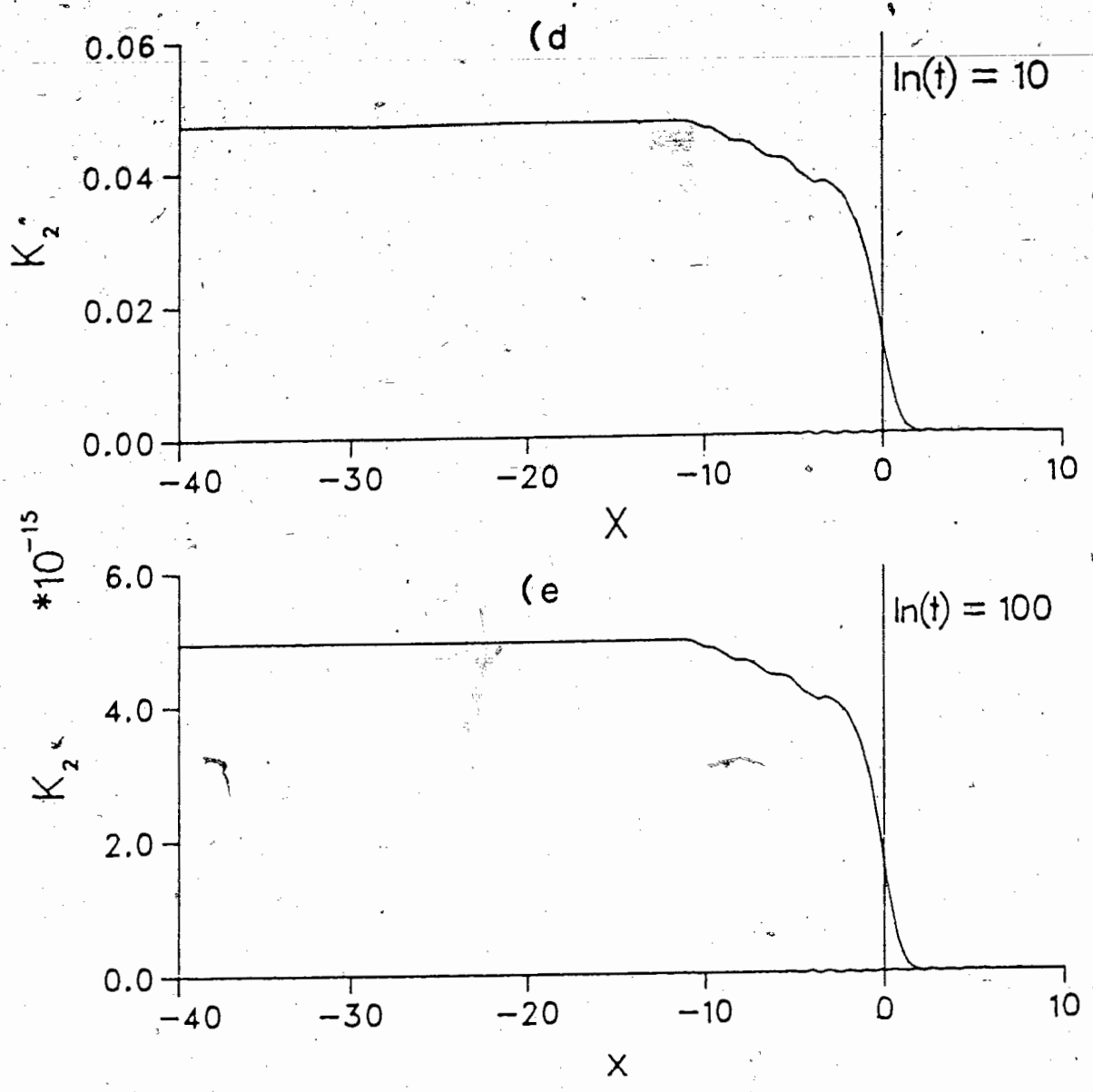

Figure 5.12 ; Complete Second order correction for the Neumann series expansion for w=1.0 at a) ln(t)=-1, b) 1, c) 5, d) 10, and e) 100.

As can be seem from the plots the first order correction to the Neumann series is of comparable order to the first term of the series, compare figure 5.8 with figures 5.10-5.12. This would suggest that the Neumann series converges slowly, and that it is not sufficient to truncate the expansion at the first order correction. This corroborates the findings for the last part of chapter 4. Nevertheless we persued this part of the calculation to its logical end by calculating the wave profile that would be obtained by retaining only the first two terms of the Neumann series through the relation

$$U(x,t) = 2\,\frac{dK(x,x,t)}{dx}, \qquad 11a$$

$$= \frac{2}{t^{1/3}}\,\frac{dK'(z,t)}{dz}, \qquad 11b$$

where $K'(z,t) = K(x,x,t)$ if $z=(2x-2w)/2t^{1/3}$. The results of this calculation, for all three pulse widths, are shown in figures 5.13-5.15.

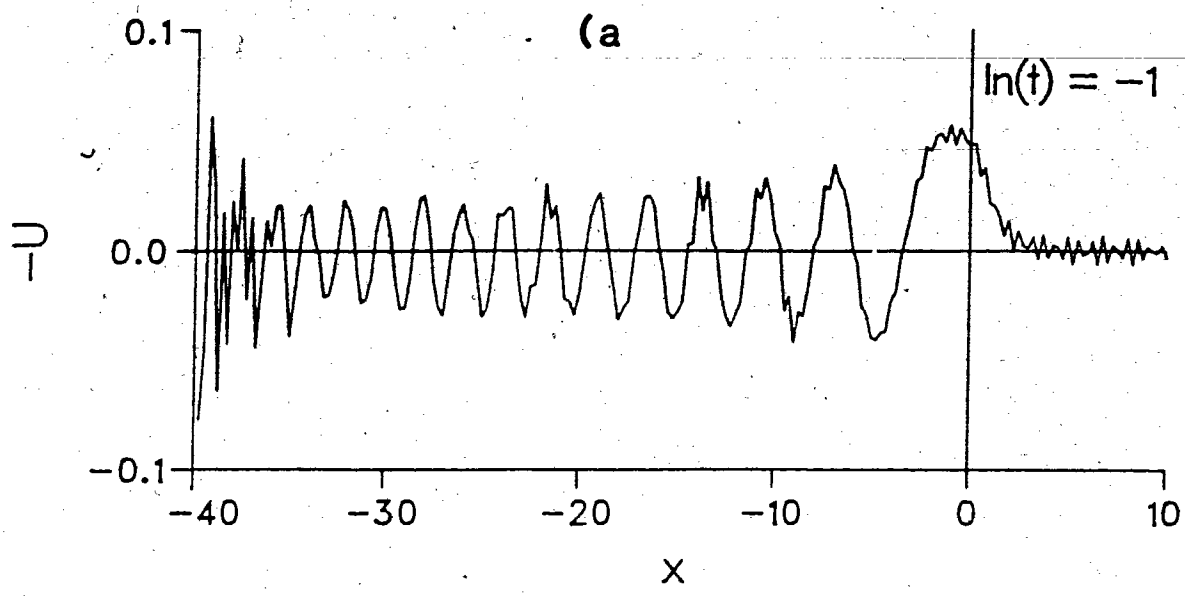
(a
ln(t) = −1
0.1
0.0
−0.1
−40
−30
−20
−10
0
10
X

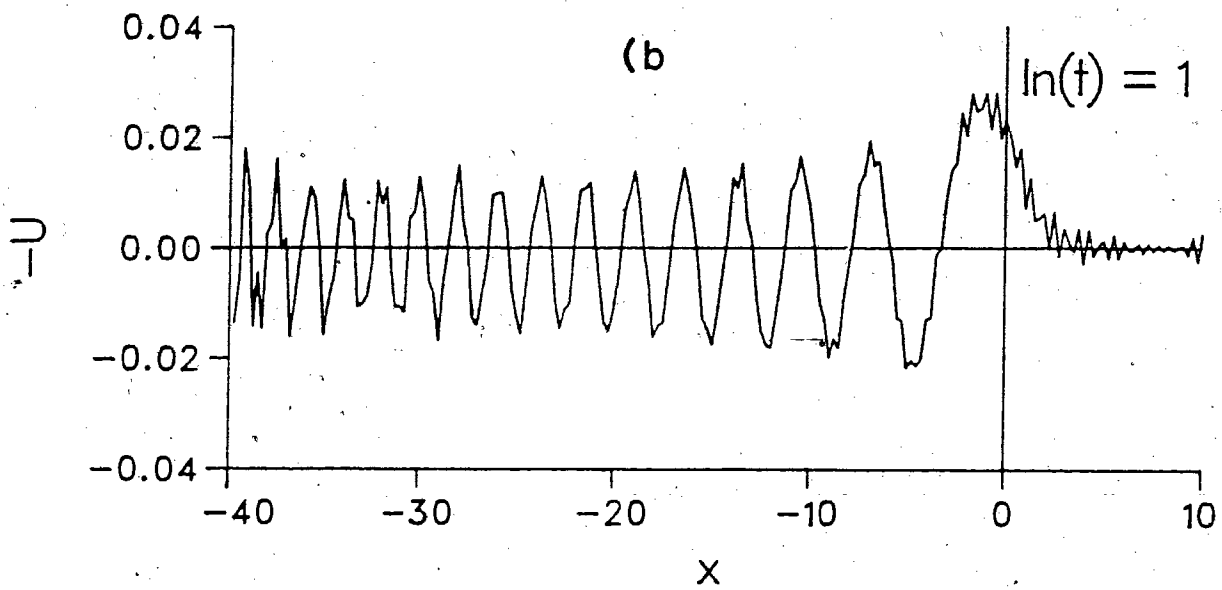
(b
ln(t) = 1
0.04
0.02
0.00
−0.02
−0.04
−40
−30
−20
−10
0
10
X

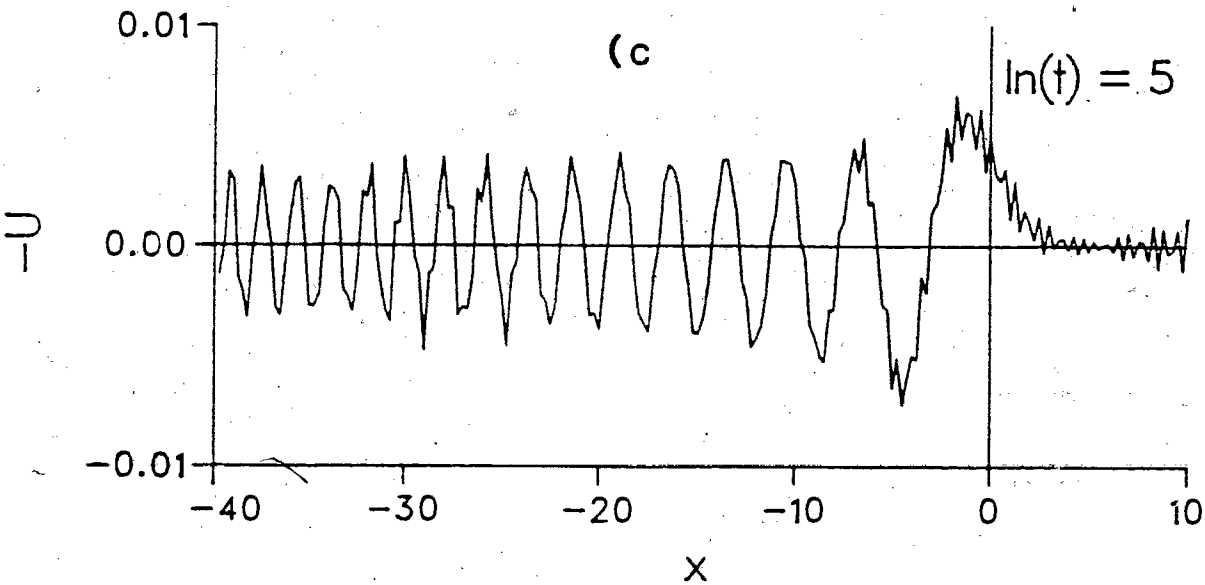
(c
ln(t) = 5
0.01
0.00
−0.01
−40
−30
−20
−10
0
10
X

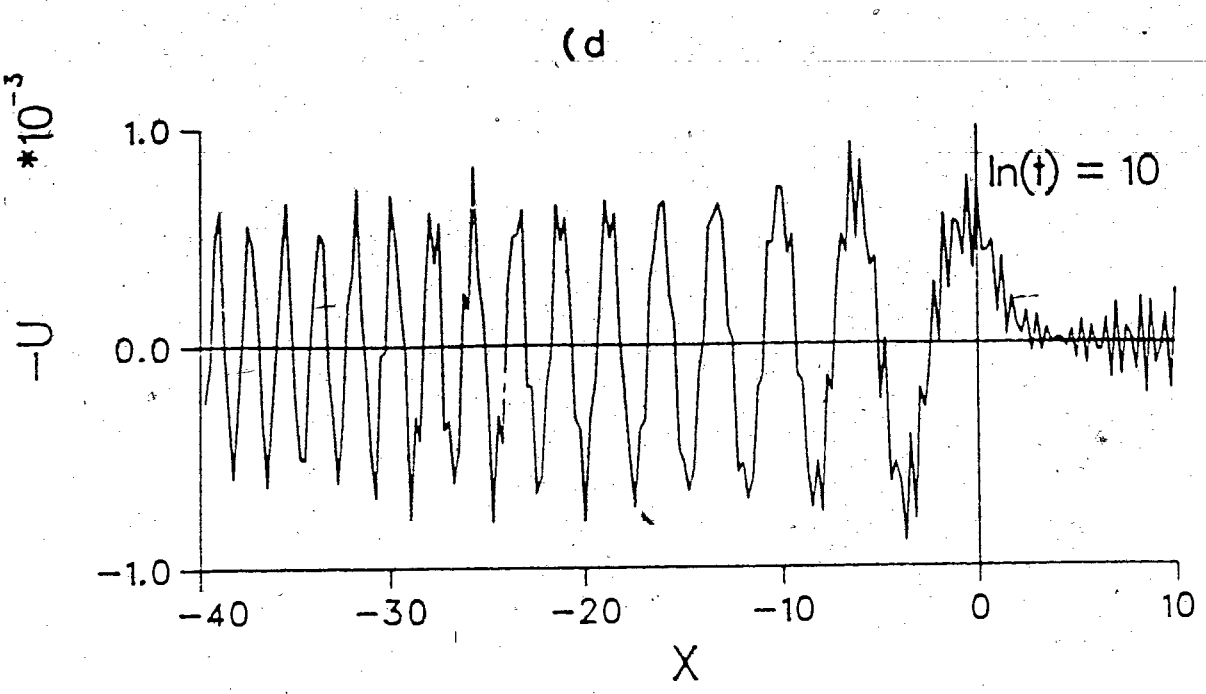

Figure 5.13 ; Profiles for u(x,t) calculated from first two terms of the Neumann series expansion for w=0.1 at a) ln(t)=-1, b) 1, c) 5, and d) 10.

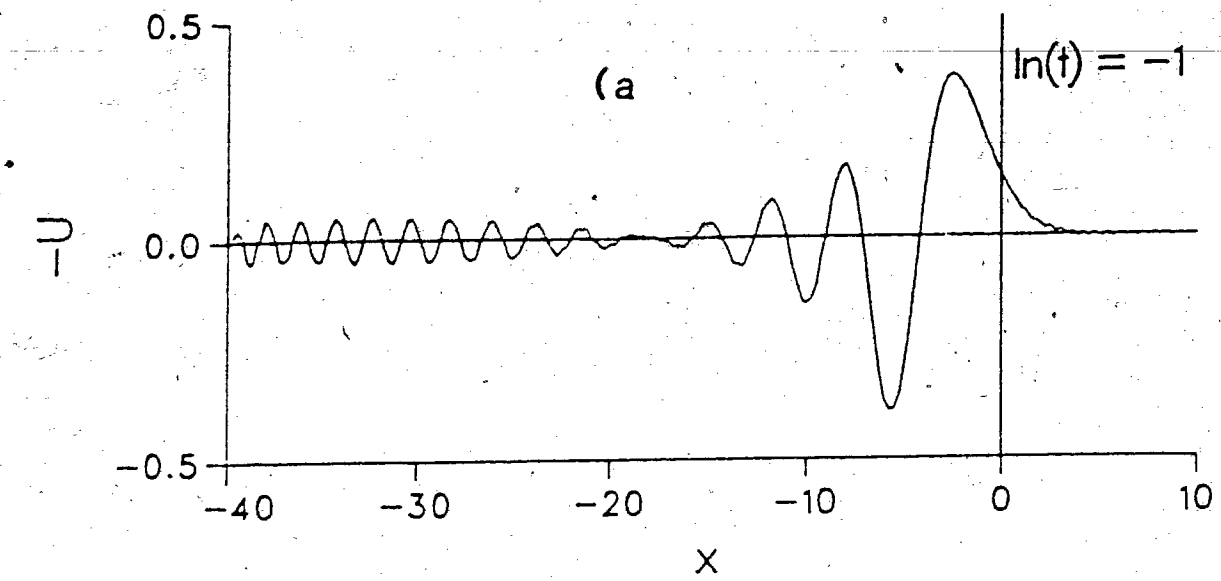
(a
ln(t) = −1
0.5
0.0
−0.5
−40
−30
−20
−10
0
10
X
Ψ

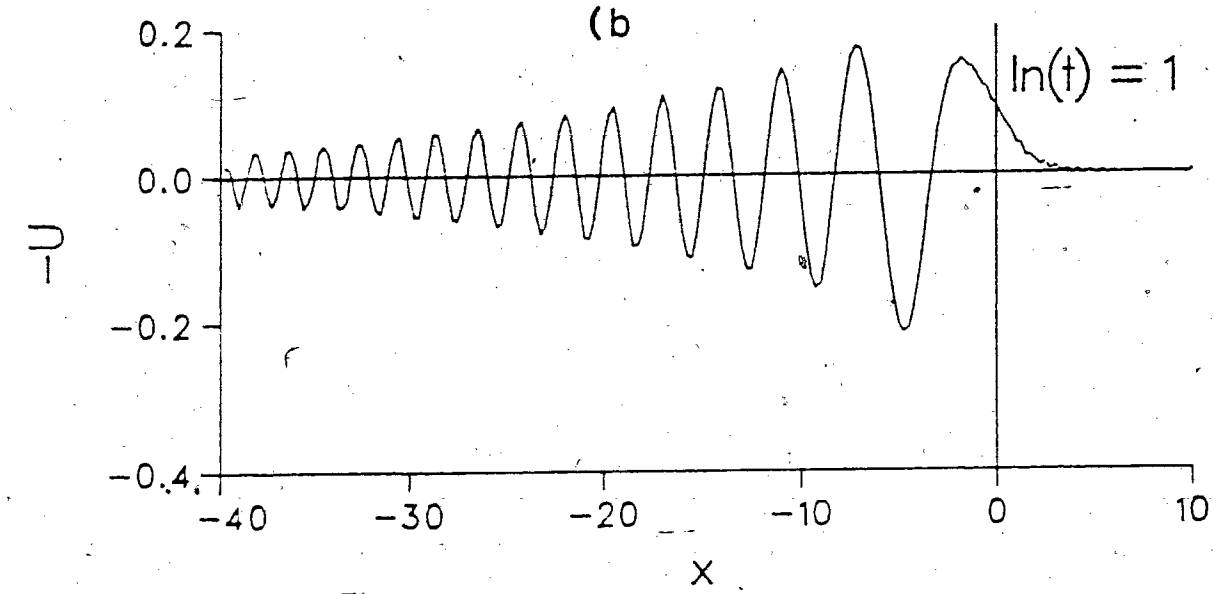
(b
ln(t) = 1
0.2
0.0
−0.2
−0.4
−40
−30
−20
−10
0
10
X
Ψ

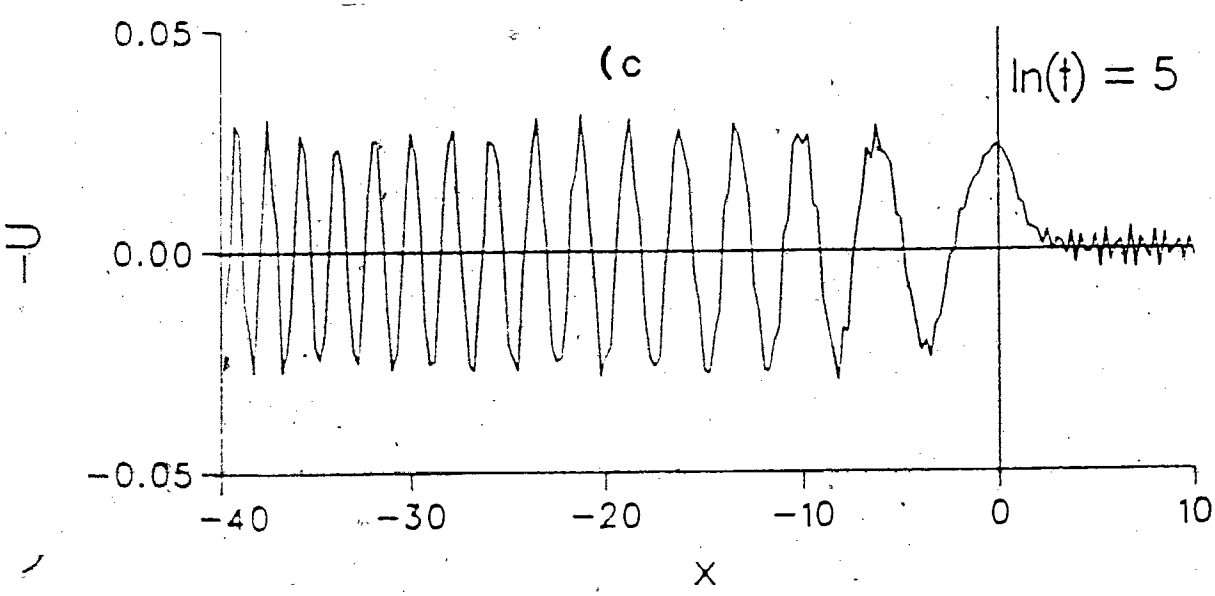
(c
ln(t) = 5
0.05
0.00
−0.05
−40
−30
−20
−10
0
10
X
Ψ

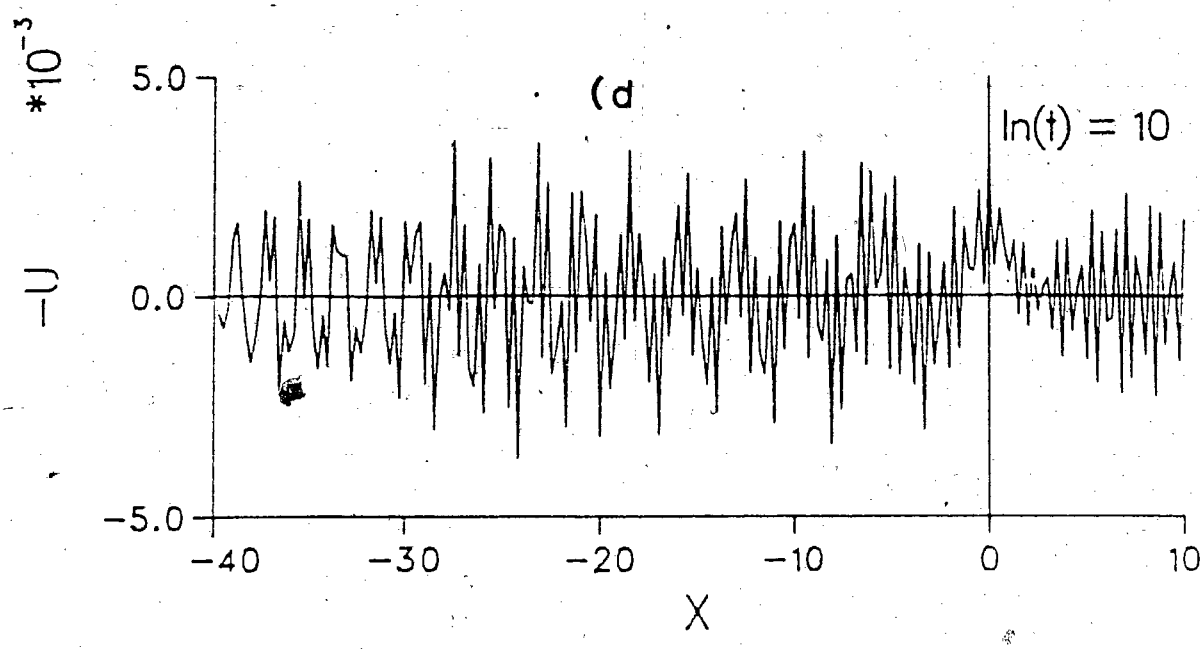

Figure 5.14 ; Profiles for u(x,t) calculated from first two terms of the Neumann series expansion for w=1.0 at a) ln(t)=-1, b) 1, c) 5, and d) 10.

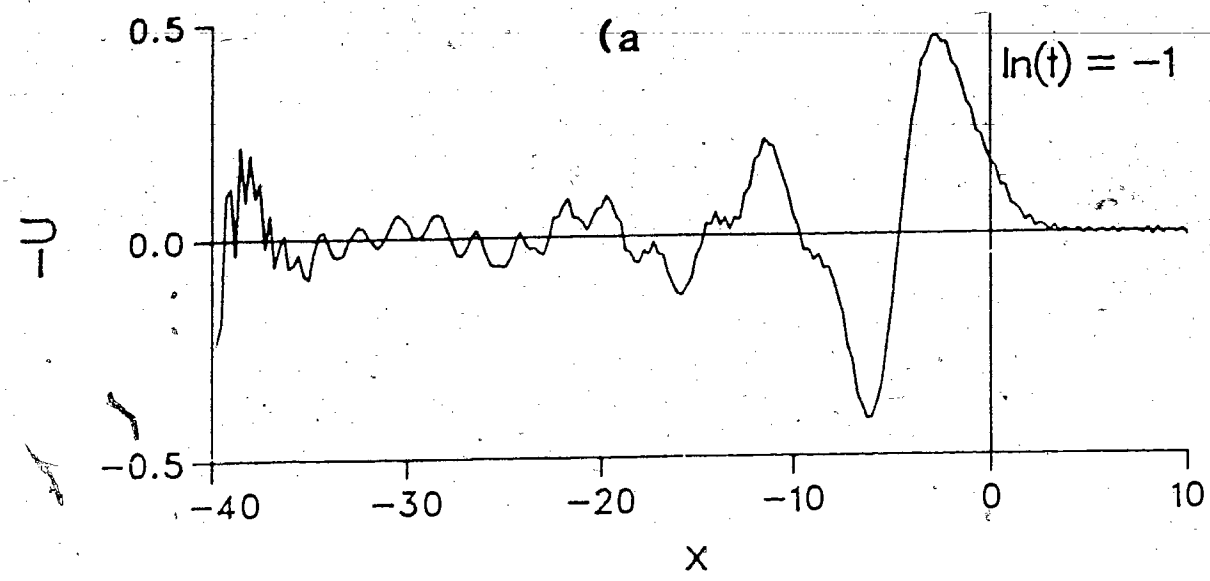
(a
ln(t) = −1
0.5
0.0
−0.5
−40
−30
−20
−10
0
10
X

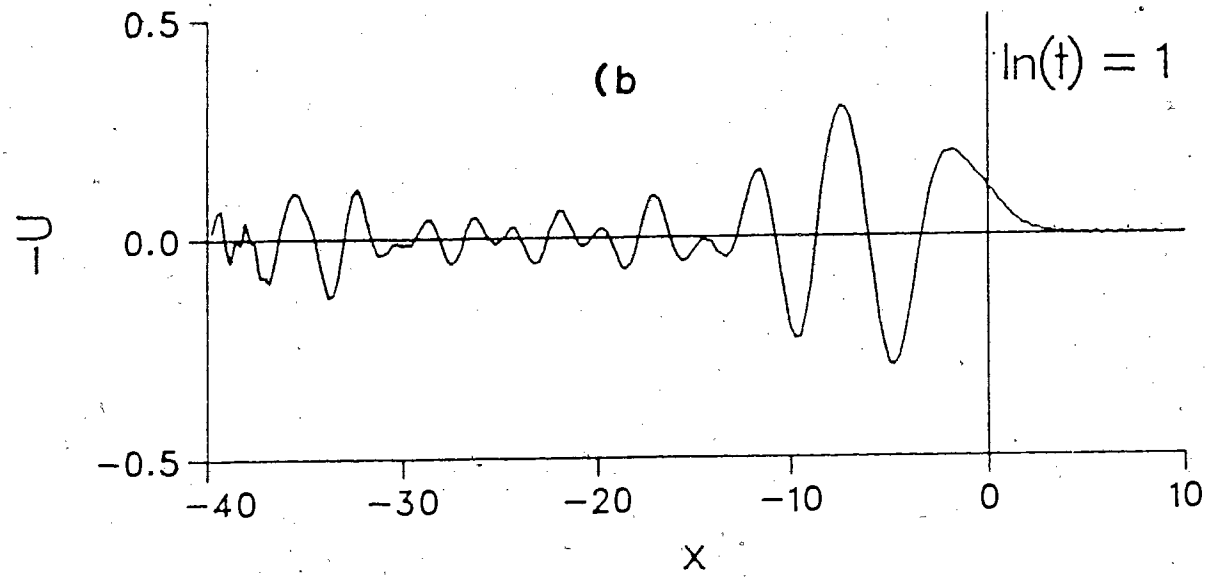
(b
ln(t) = 1
0.5
0.0
−0.5
−40
−30
−20
−10
0
10
X

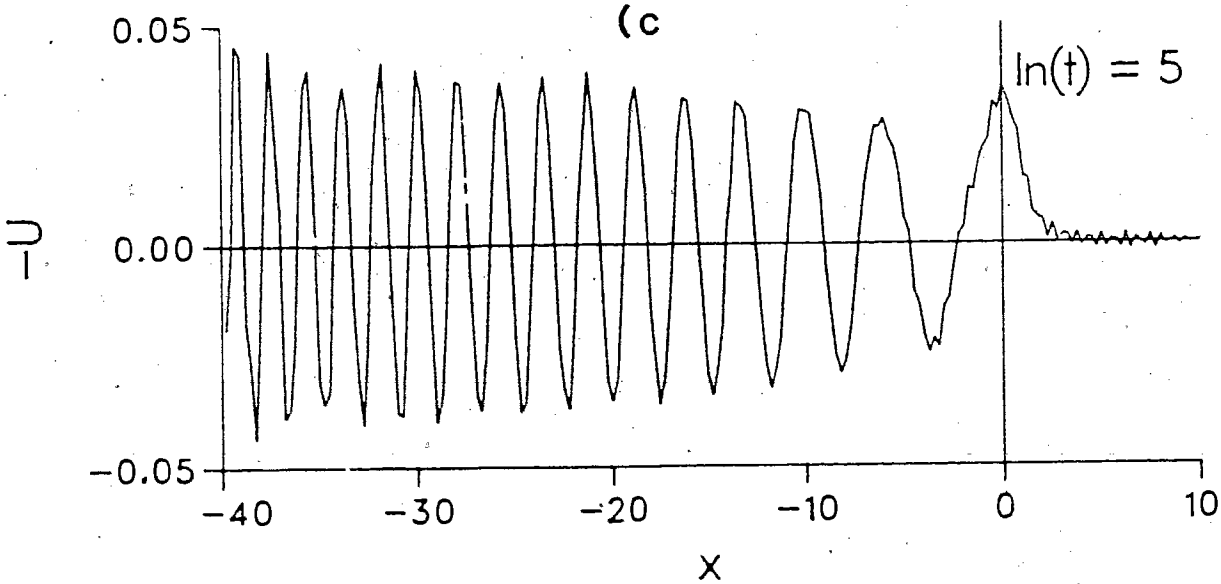
(c
ln(t) = 5
0.05
0.00
−0.05
−40
−30
−20
−10
0
10
X

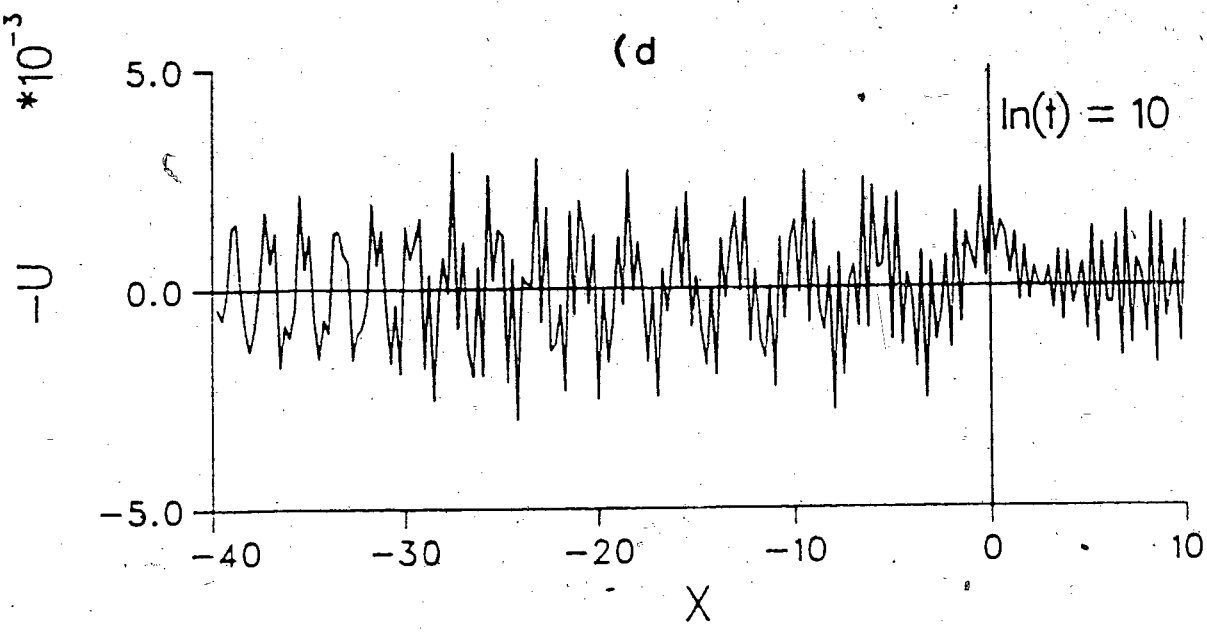

Figure 5.15 ; Profiles for u(x,t) calculated from first two terms of the Neumann series expansion for w=10.0 at a) ln(t)=-1, b) 1, c) 5, and d) 10.

By comparing the ln(t)=5 plots of each figure we again confirm that the large area pulses tend to settle down to the asymptotic regime faster than the small area pulse as is evidenced by the similarity between these profiles for both w=1.0 and w=10.0 but not w=0.1. However, it is interesting to note that the sequence of profiles for w=0.1 do not undergo as radical a change in shape with time, as do the other two. Where as for the w=1.0 and w=10.0 profiles at t=0 we see evidence of a short range envelope function, this is absent for the w=0.1 profile. On examining the profiles for w=1.0 more closely it can be seen that the wavelengthof the envelope function gets longer with the beat moving off to the left as time evolves. This is not so evident for the w=10.0 profiles, however, the transition between the ln(t)=1 and ln(t)=5 profile, for this width, would suggest a similar mechanism.

As a final note it appears that the two term approximations for all of the cases are displaying modulated Airy function-like behaviour (see AMS 55), which is pointed out in the literature. In the case of the w=10.0 pulse the ln(t)=5 profile is reminiscent of derivative Airy function-like behaviour.

CHAPTER VI

EXPERIMENTAL COMPARISON

In the previous chapters the mathematical and technical machinery for finding the solutions, or at least partial solutions, for the radiative nature of the KdV equation was developed and explored for a specific initial wave profile. However, no attempt was made to correlate these findings with actual experimental results. This chapter looks at this correlation.

A paper authored by the team of J.L.Hammack and H.Segur[26], provided several experimental results in the form of wave profiles, depicting the evolution of shallow water wave trains, for various initial conditions. For one set of these wave trains, the initial conditions used were of the same form as those discussed in this thesis; the square well. These experimental results could then provide a proving ground for the theory.

In the Hammack and Segur experiments, several probes were placed in a narrow wave tank at various distances downstream from the initial disturbance. The profile of the wave was recorded as it travelled past the probes. This type of measurement yields a temporal cross-section of the wave profile as opposed to a spatial cross-section, which is what one would see. In terms of the laboratory coordinates X and T, where X is measured along the wave tank from the trailing edge of the

initial pulse, the picture that we would get would be,

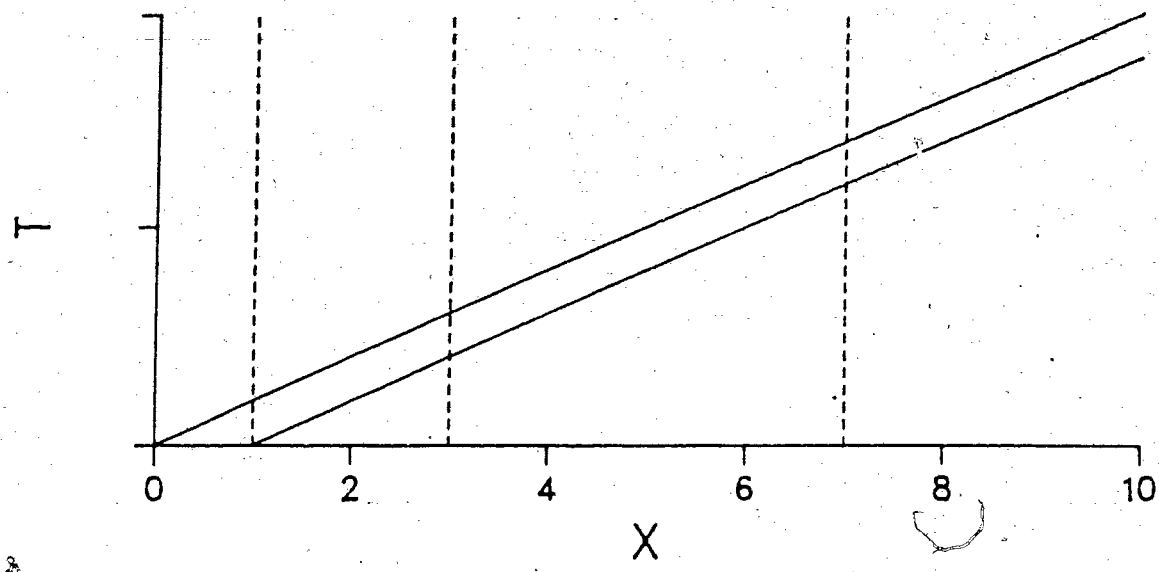

Figure 6.1

where the solid lines represent the leading and the trailing "edges" of the pulse as it propagates with speed $\sqrt{gh}$ and the dotted vertical lines represent the lines, in time, along which the experimental wave profiles were recorded.

In order to make the proper correspondence between the experimental results and the theoretical predictions, it must be kept in mind that the KdV equation in normal form has been transformed through scaling transformations and coordinate rotations. This correspondence can be established by starting with Hammack and Segur's form for the right running dimensional KdV equation,

$$H_T + \sqrt{gd}H_X + \frac{3}{2}\sqrt{g/d}HH_X + \frac{1}{6}d^2\sqrt{gd}H_{XXX} = 0, \qquad 1$$

where H represents the true height of the wave above the still surface, d the depth of the still water, g the acceleration of gravity near the surface of the earth, and X and T laboratory space and time. Introducing the coordinate and scale transformations,

$$V = \frac{H}{\eta}, \qquad 2a$$

$$x = \frac{1}{d}\sqrt{3\eta/2d}(X - \sqrt{gd}T), \qquad 2b$$

$$t = \frac{\eta}{4d^2}\sqrt{3g\eta/2}T, \qquad 2c$$

where $\eta = |H|_{max}$, at T=0, recovers the KdV equation in normal form, i.e.

$$V_t + 6VV_x + V_{xxx} = 0. \qquad 3$$

Through this transformation the correspondence between the

experimental and the theoretical quantities is established. It should be noted that this transformation is not unique and is in fact different from the one given in the paper by Hammack and Segur. The reason for this particular choice is that it normalizes the height of the pulse to unity, which is consistent with all previous calculations.

In terms of the new coordinates x and t the situation depicted in figure 6.1 becomes,

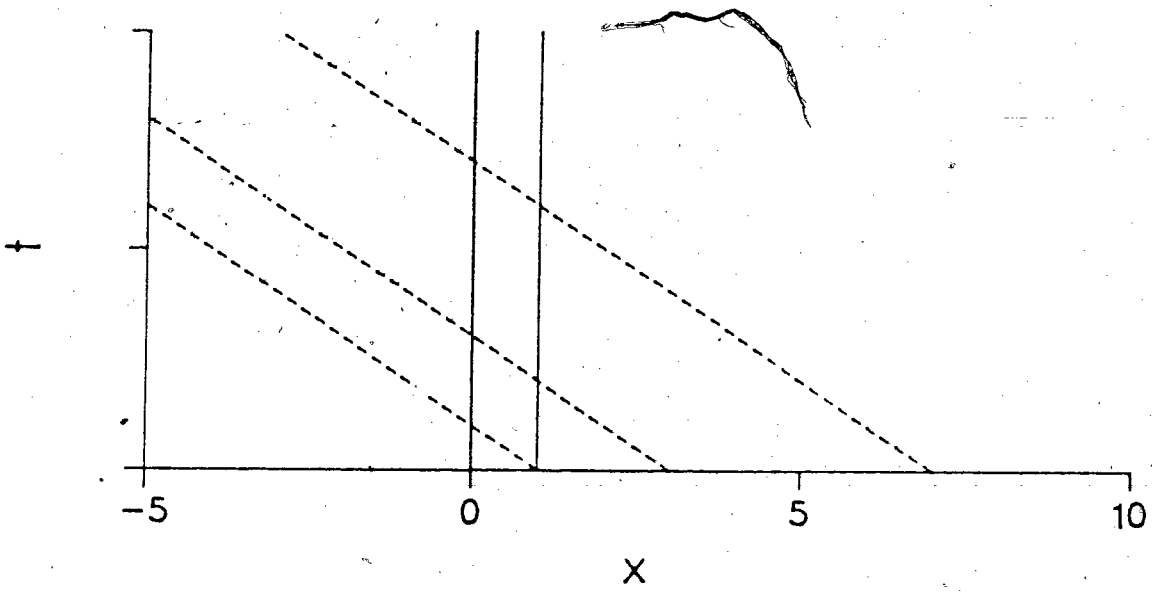

Figure 6.2

where again the solid lines represent the leading and the trailing "edges" of the pulse as it propagates, and the dashed lines the observation points, i.e. X=constant. In terms of x and t, the lines X=constant become

$$x = \frac{1}{d}\sqrt{3\eta/2d}X - \frac{4d}{\eta}t. \qquad 4$$

Noting that if X is written as $W+X_0$, with W being the initial width of the pulse, and X_0 the distance from the leading edge of the pulse to the probe at T=0, that the observation lines can be written as

$$x = w + x_0 - \frac{4d}{\eta}t, \qquad 5$$

where $w = \frac{1}{d}\sqrt{3\eta/2d}W$ and $x_0 = \frac{1}{d}\sqrt{3\eta/2d}X_0$.

From the Inverse Scattering formalism the theoretical results for the experimental setup of Hammack and Segur can be obtained by calculating the kernel for the Marchenko equation, i.e.

$$F(x,t) = \frac{1}{2\pi}\int_{-\infty}^{\infty} r(k)\, e^{ikx+8ik^3t}\, dk,$$

where r(k) is the reflection coefficient for the square well, and then using the Neumann series expansion to solve for the function K(x,x,t), which is related to the radiation solution of the KdV equation through

$$V(x,t) = 2\frac{dK(x,x,t)}{dx}, \qquad 6$$

as dicussed in chapter 2.

Since seeking solutions along the observation lines makes the differentiation of equation 6 difficult, the method of expanding in terms of Oscillator functions will not be employed here. The equations will be integrated numerically.

From the Neumann series solution of the Marchenko equation

$$K(x,x,t) = -F(2x,t) + \int_x^\infty F(x+y)F(y+x)dy + \ldots. \qquad 7$$

we get that

$$V(x,t) = -2\frac{\partial F(2x,t)}{\partial x} - 4F^2(2x,t) + \ldots . \qquad 8$$

The first two terms of equation 9 can easily be evaluated in terms of the explicit form of the kernel $F(x,t)$, i.e.

$$\frac{\partial F(2x,t)}{\partial x} = \frac{i}{\pi}\int_{-\infty}^{\infty} kr(k)\, e^{2ikx+8ik^3t}\, dk, \qquad 9a$$

and

$$F^2(2x,t) = \left(\frac{1}{2\pi}\int_{-\infty}^{\infty} r(k)\, e^{2ikx+8ik^3t}\, dk\right)^2, \qquad 9b$$

and thus $V(x,t)$ becomes

$$V_2(x,t) = -\frac{2i}{\pi}\int_{-\infty}^{\infty} kr(k)\, e^{2ikx+8ik^3t}\, dk$$

$$-\frac{1}{\pi^2}\left(\int_{-\infty}^{\infty} r(k)\, e^{2ikx+8ik^3t}\, dk\right)^2, \qquad 10$$

where the subscript 2 indicates the truncation of the series solution at the second term.

Recalling that the reflection coefficient has the form

$$r(k) = R(k)e^{i(\phi(k)-2kw)}, \qquad 11$$

and that $V_2(x,t)$ is to be evaluated along the lines given by equation 5 we get that

$$V_2(x,t) = -\frac{2i}{\pi}\int_{-\infty}^{\infty} kR(k)\, e^{i(\phi(k)+2kx_0+8(k^3-(d/\eta)k)t)}\, dk$$

$$-\frac{1}{\pi^2}\left(\int_{-\infty}^{\infty} R(k)\, e^{i(\phi(k)+2kx_0+8(k^3-(d/\eta)k)t)}\, dk\right)^2. \qquad 12$$

This final expression was evaluated numerically for the physical parameters d = 5cm, η = 0.5cm (down), and pulse width W = 122cm with probes at X = W, W+100cm, W+900cm, and W+2000cm. The results of these calculations are presented in figures 6.3 to 6.5. The first plot of each figure represents the first term of V_2 from equation 13, the second plot the negative of the second term of V_2, and the third plot represents V_2 (both terms). For comparison, the results of the Hammack and Segur experiment are shown in the fifth plot of each figure. The fourth plot of each figure shows the results of the work done by R. Enns and S.S. Rangnekar. To get these results they assumed that the reflection coefficient, see chapter 4, could be represented as an expansion in the system parameter $S = w\sqrt{\delta}$, with w being the width of the initial pulse and δ the height in dimensionless units, i.e.

$$r(k) = \frac{-i\delta\sin(\sqrt{k^2-\delta}w)\, e^{2ikw}}{2k\sqrt{k^2-\delta}\cos(\sqrt{k^2-\delta}w) - i(2k^2-\delta)\sin(\sqrt{k^2-\delta}w)}, \qquad 13a$$

$$= \frac{-i\sin(kw)e^{ikw}}{2k^2w^2}S^2 + O(S^4), \qquad 13b$$

and that the solution for the KdV equation could be similarly

expanded through

$$V = v_0 S^2 + v_1 S^4 + \ldots . \qquad 14$$

To lowest order in S (S^2), by equation 9, with $\delta=1$ we get

$$V_1 = v_0 S^2$$

$$= -\frac{1}{\pi}\int_{-\infty}^{\infty} \frac{\sin kw}{k} e^{ik(2x-w)+8ik^3t}\, dk$$

and along the observation lines,

$$V_1 = v_0 S^2$$

$$= -\frac{1}{\pi}\int_{-\infty}^{\infty} \frac{\sin kw}{k} e^{ik(2x_0+w)+8i(k^3-(\eta/d)k)t}\, dk. \qquad 15$$

The second term cannot be evaluated in terms of this simple approach because of the pole at k=0. However, Enns and Rangnekar were able to renormalize the calculation to extract the second order correction at t=0.

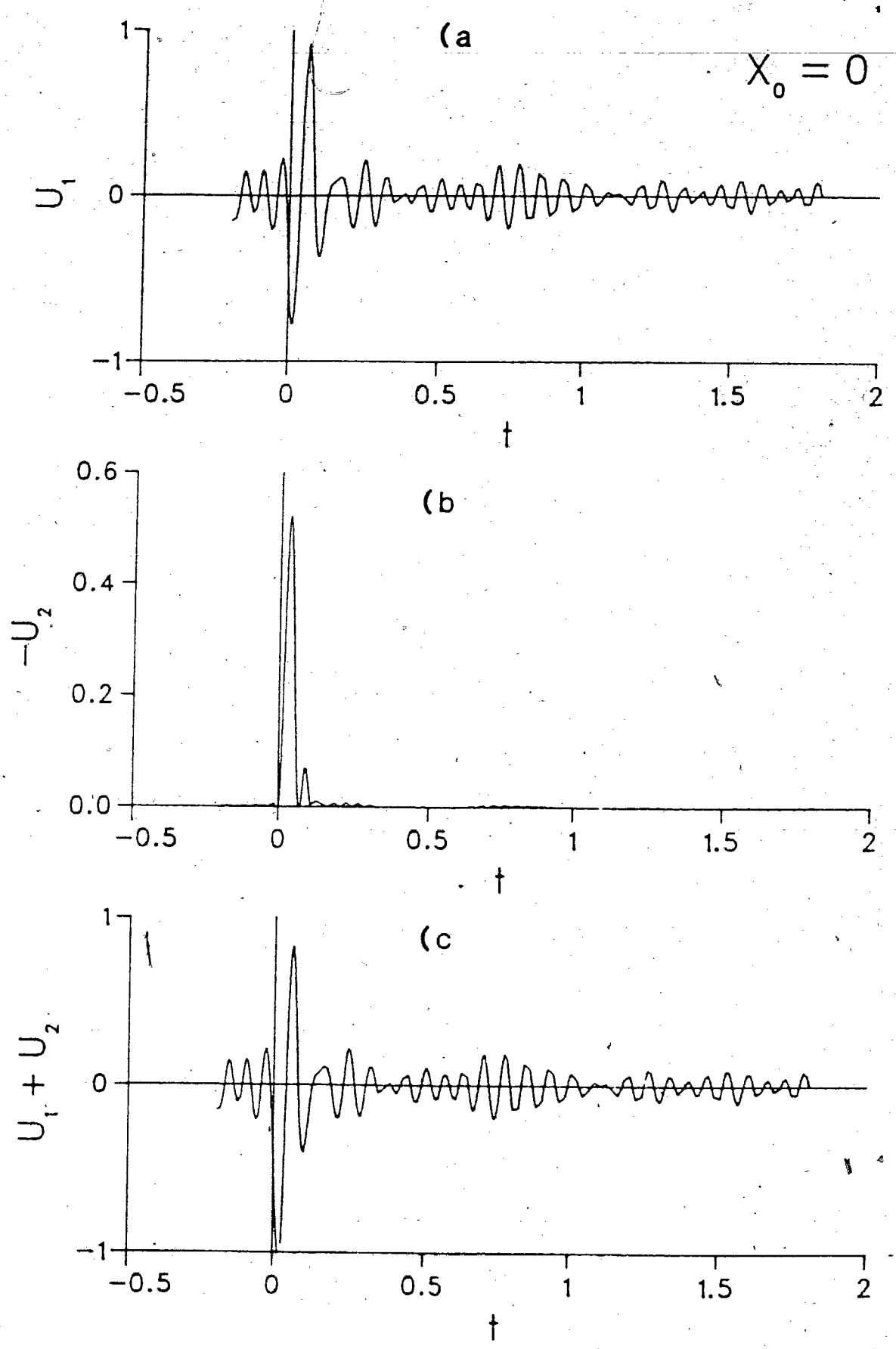
(a
$X_0 = 0$
U_1
1
0
−1
−0.5
0
0.5
1
1.5
2
t
(b
$-U_2$
0.6
0.4
0.2
0.0
−0.5
0
0.5
1
1.5
2
t
(c
$U_1 + U_2$
1
0
−1
−0.5
0
0.5
1
1.5
2
t

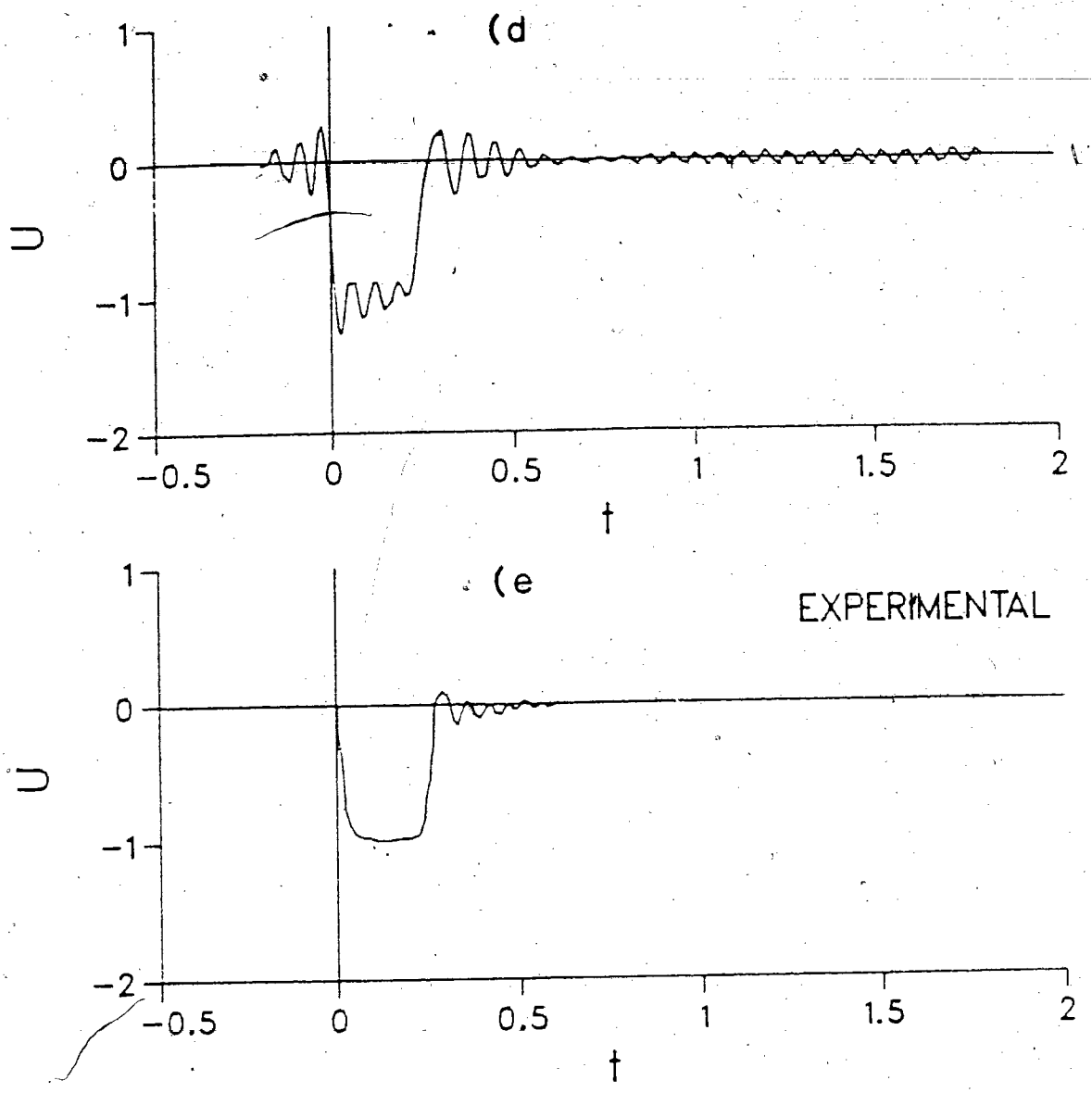

Figure 6.3 ; Comparision of the theoretical results of the exact Neumann series expansion for U(x,t) to two terms with a linearized calculation and experimental results a) first term of the Neumann series, b) second term of the Neumann series, c) sum of the first two terms, d) linearized result, and e) experimental results, all for $X_0 = 0$.

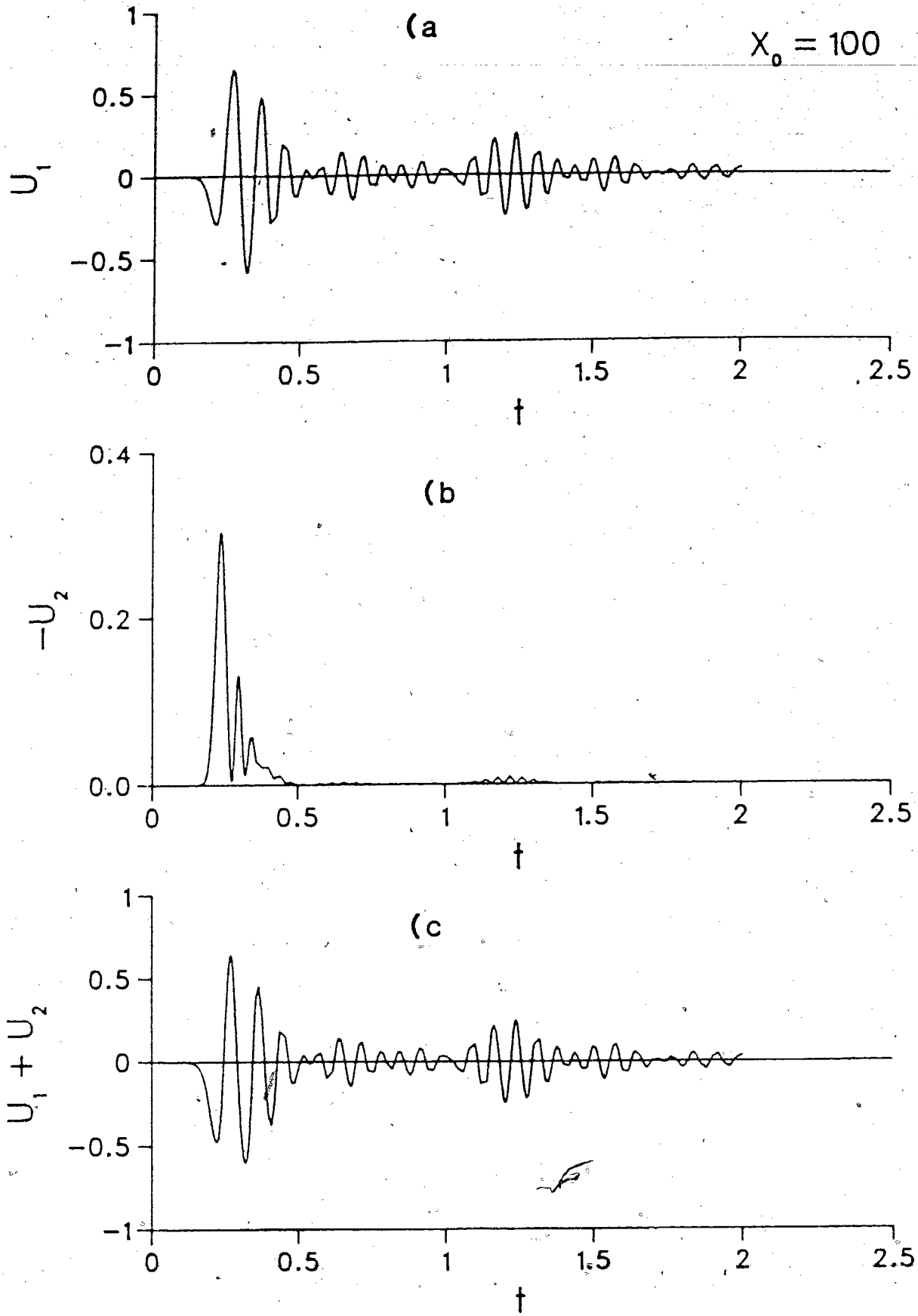
(a
$X_0 = 100$
U_1
1
0.5
0
−0.5
−1
0
0.5
1
1.5
2
2.5
t
(b
$-U_2$
0.4
0.2
0.0
0
0.5
1
1.5
2
2.5
t
(c
$U_1 + U_2$
1
0.5
0
−0.5
−1
0
0.5
1
1.5
2
2.5
t

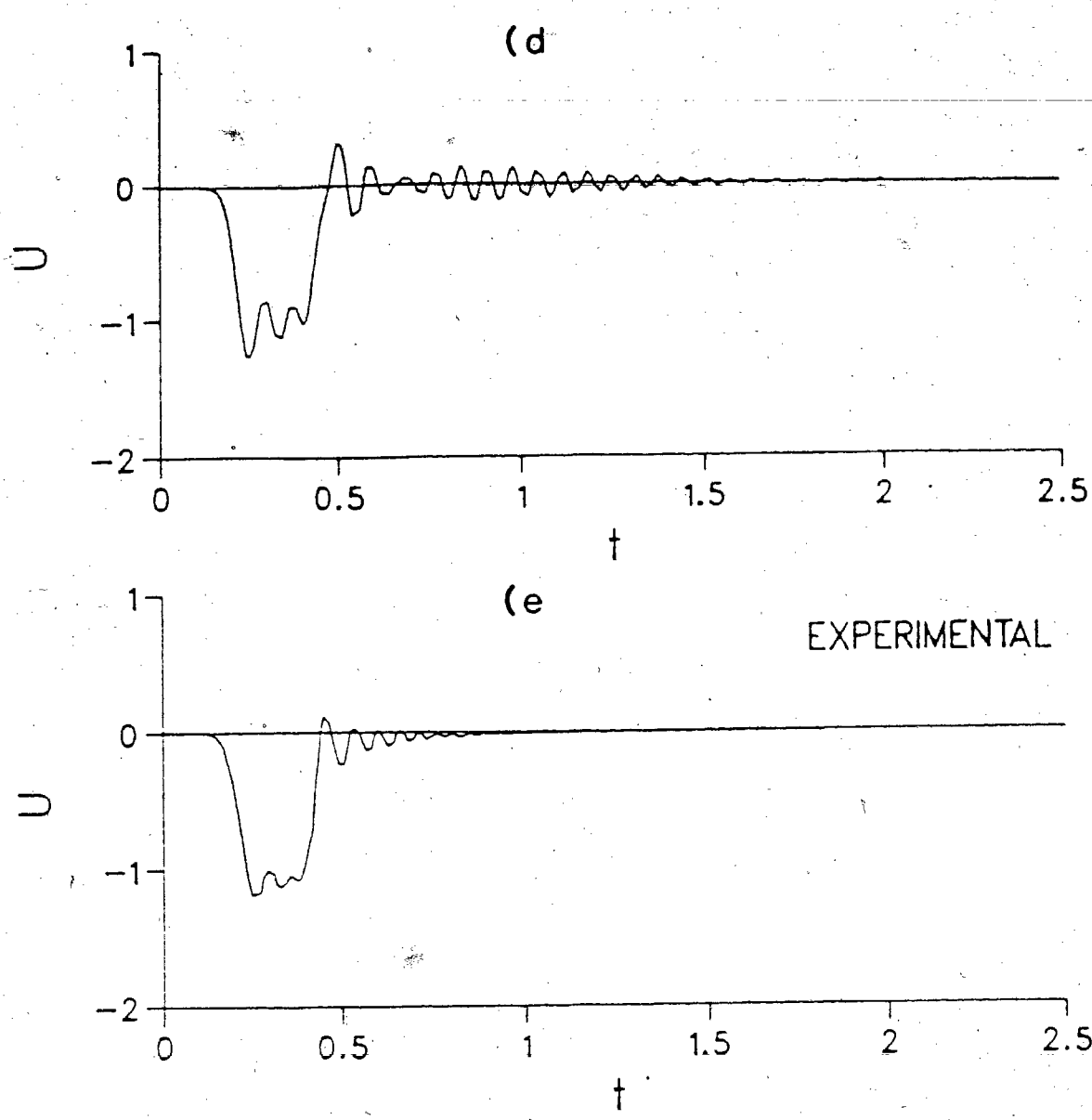

Figure 6.4 ; Comparision of the theoretical results of the exact Neumann series expansion for U(x,t) to two terms with a linearized calculation and experimental results a) first term of the Neumann series, b) second term of the Neumann series, c) sum of the first two terms, d) linearized result, and e) experimental results, all for $X_0 = 100$.

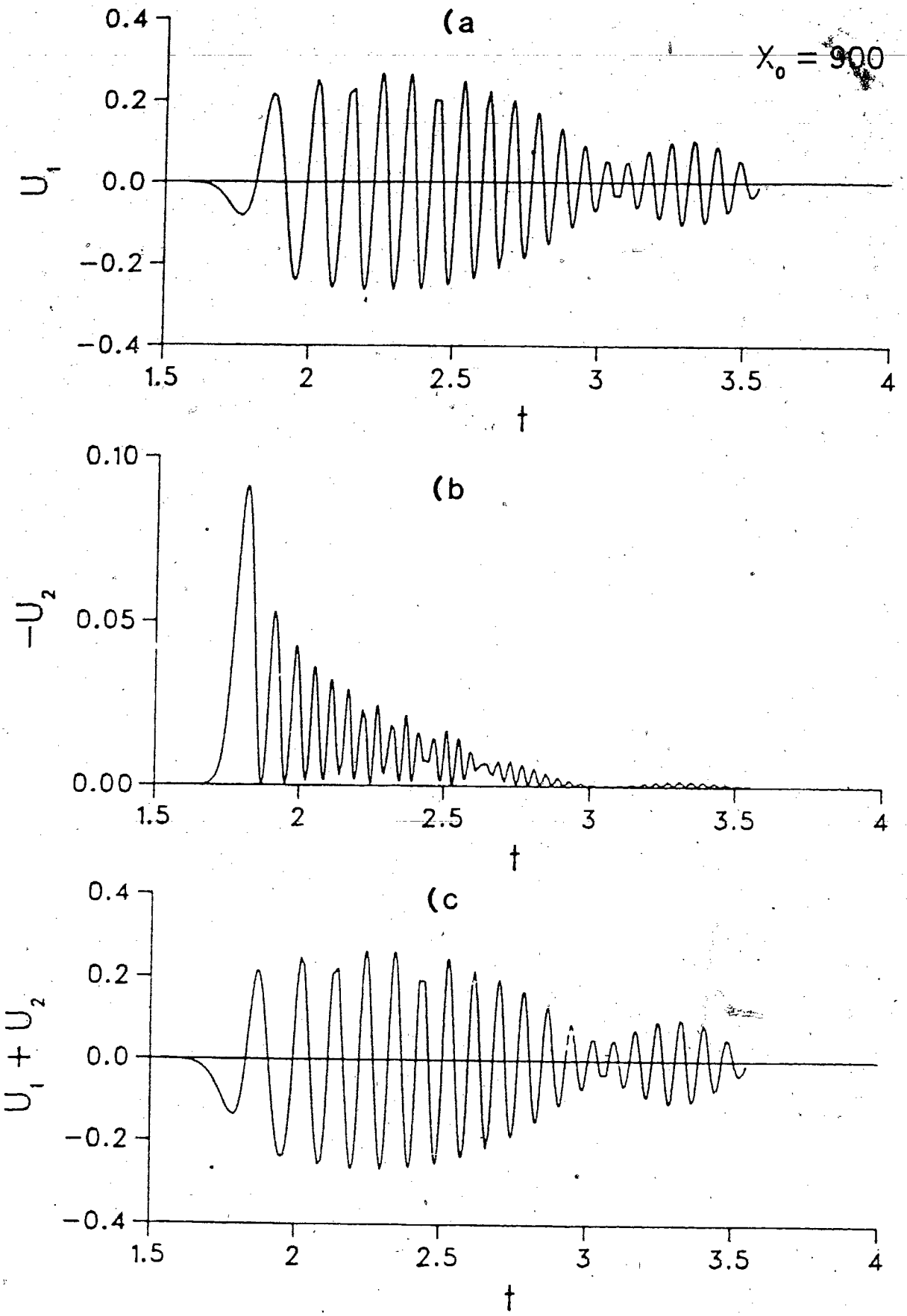
(a
$X_0 = 900$
U_1
0.4
0.2
0.0
−0.2
−0.4
1.5
2
2.5
3
3.5
4
t
(b
$-U_2$
0.10
0.05
0.00
1.5
2
2.5
3
3.5
4
t
(c
$U_1 + U_2$
0.4
0.2
0.0
−0.2
−0.4
1.5
2
2.5
3
3.5
4
t

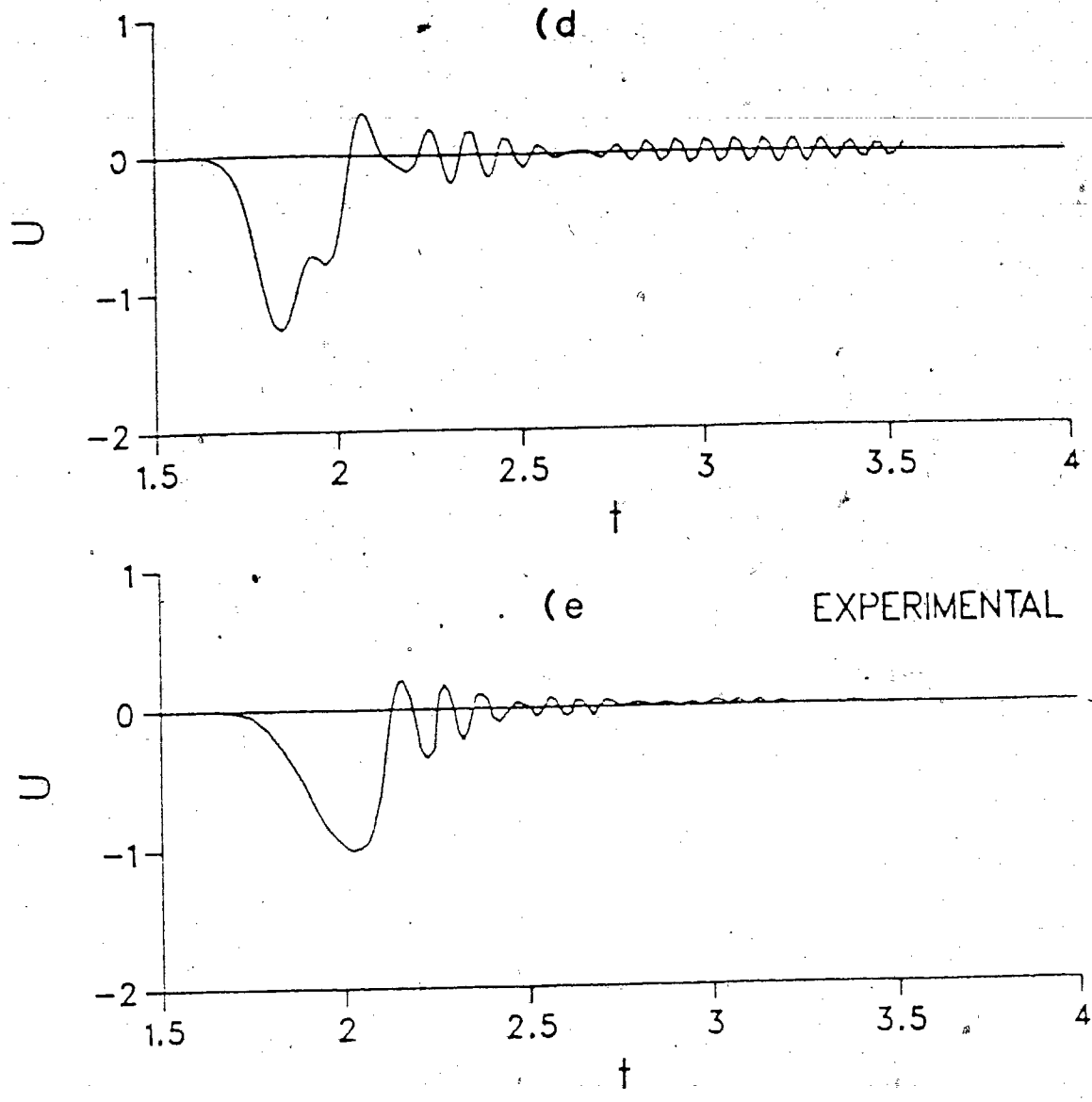

Figure 6.5 ; Comparision of the theoretical results of the exact Neumann series expansion for U(x,t) to two terms with a linearized calculation and experimental results a) first term of the Neumann series, b) second term of the Neumann series, c) sum of the first two terms, d) linearized result, and e) experimental results, all for X_0 = 900

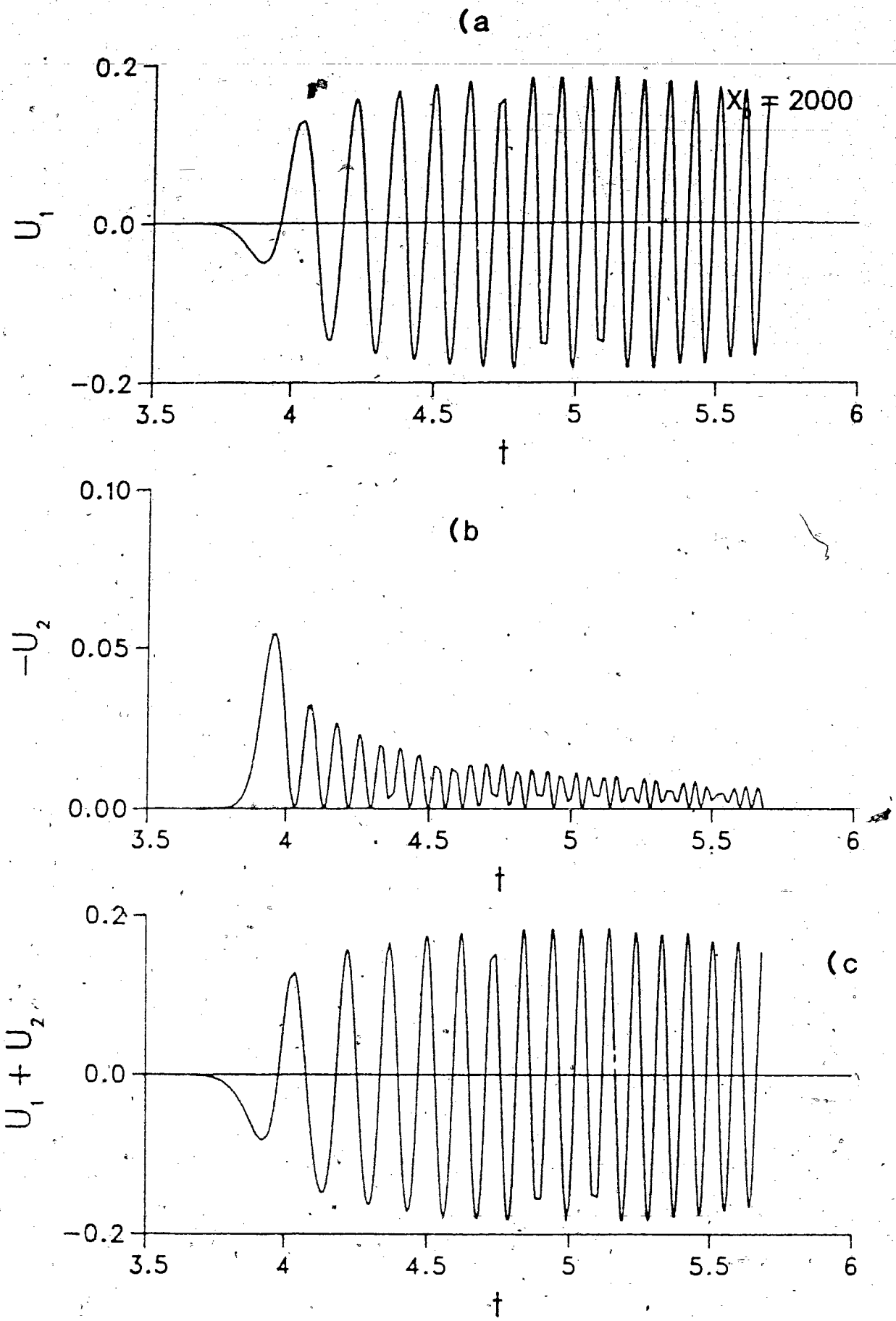
(a
0.2
0.0
−0.2
U_1
$X_0 = 2000$
3.5
4
4.5
5
5.5
6
t
0.10
0.05
0.00
(b
$-U_2$
3.5
4
4.5
5
5.5
6
t
0.2
0.0
−0.2
$U_1 + U_2$
(c
3.5
4
4.5
5
5.5
6
t

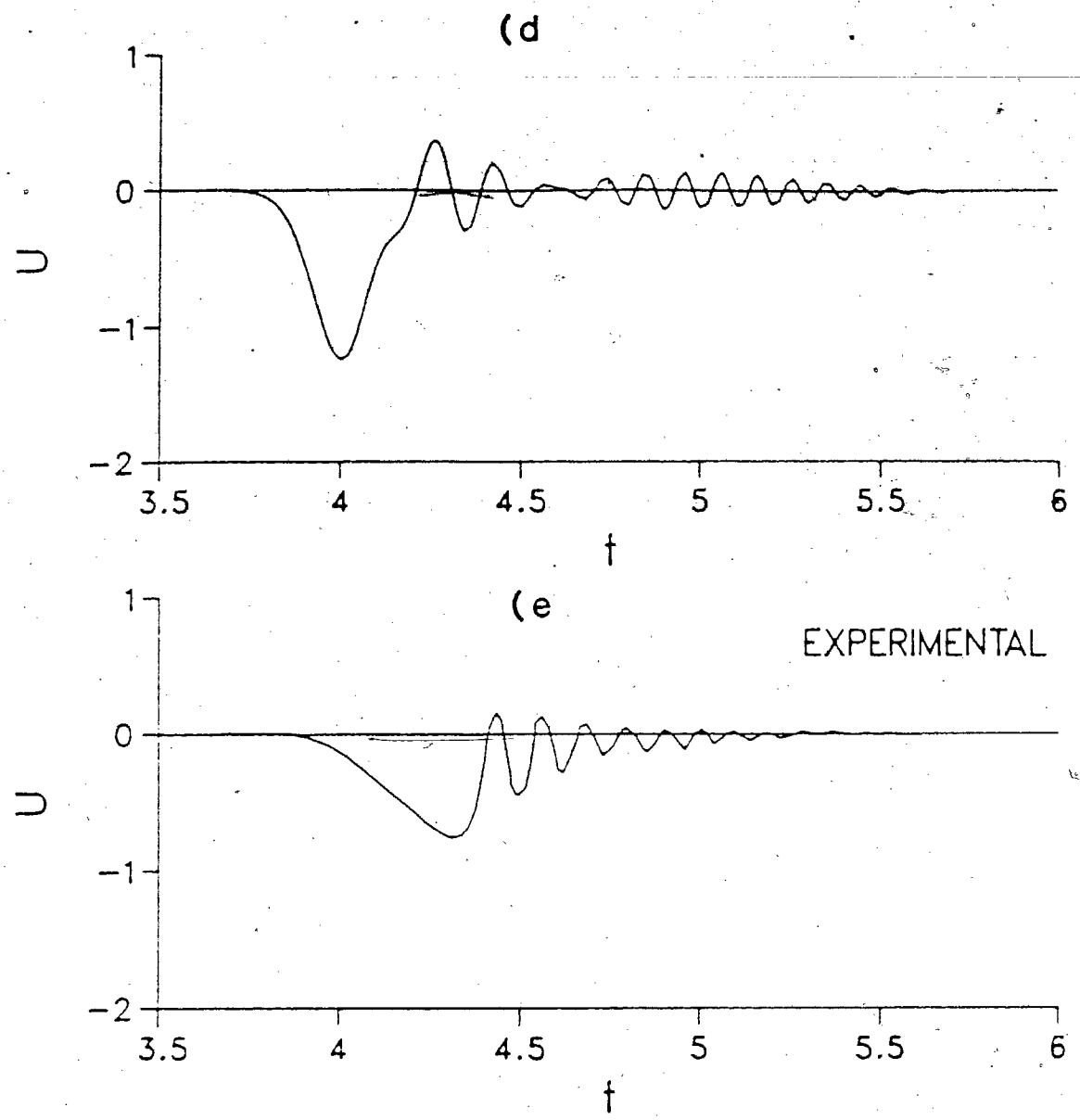

Figure 6.6 ; Comparision of the theoretical results of the exact Neumann series expansion for U(x,t) to two terms with a linearized calculation and experimental results a) first term of the Neumann series, b) second term of the Neumann series, c) sum of the first two terms, d) linearized result, and e) experimental results, all for X_0 = 2000

By comparing the third and fifth plots of each figure, i.e. theoretical calculation of the first two terms of the Neumann series expansion for the solution of the KdV equation and the experimental results, we note that there is no qualitative correlation between the two. Initially this lack of correlation was thought to be due to computational error, however, on thorough inspection of the algebra involved in the theoretical calculation this was not the case. As a test for the accuracy of the calculation we applied the alternate method of the single variable expansion in Oscillator functions to this problem, and found that the results were in agreement with the initial numerical integration method. This agreement ruled out the possibility of generating erroneous results from the methods chosen to evaluate the terms of V_2. This agreement between numerical and oscillator expansion calculations was demonstrated in chapter 4. The only remaining source of error was the routine developed to calculate the reflection coefficient r(k). To test this routine for accuracy an alternate routine was developed and the results of this and the previous routine were found to agree, thus eliminating this as an error source. As an additional test the linearized reflection coefficient of Enns and Rangnekar (equation 13b) was used in place of the full reflection coefficient in the algorithm used to calculate the first term of V_2. The ensueing results agreed with those generated by Enns and Rangnekar, again indicating that the method used to calculate V_2 was not erroneous. Finally, as a crude indication of accuracy, the velocity of the leading edge

of the theoretical waves is identical with those of the experimental waves.

Since the theoretical results depicted in plots (a through (c for figures 6.3 - 6.6 passed all of the tests applied, they were considered to be faithful representations of the theory. As such it was concluded, from comparing these results with those of the experiment that, to second order, the Neumann series expansion does not return an accurate, or for that matter a qualitative, representation of radiative shallow water waves, and, by virtue of the relative sizes of the first and second terms of the expansion, that if the Neumann series does converge to a faithful representation of shallow water waves, that it does so slowly. The slow convergence of the Neumann series indicates that it is not, in itself, a useful tool for calculating the evolution of shallow water waves, through the KdV equation, and that an alternate form for approximating the solutions of the Marchenko equation needs to be found.

As a starting point for this search, the qualitative success, for short time, of the Enns-Rangnekar expansion procedure, as seen by comparing the fourth and fifth plots of figures 6.3-6.6, should be noted. This expansion method acts as a 'filter' to deconvolute the reflection coefficient so that qualitatively correct results appear in lowest order. It can alternately be thought of as a perturbation expansion about the solution of the linearized KdV equation, using the correct initial conditions. Unfortunately this method breaks down as was

mentioned earlier in chapter 3.

CHAPTER VII

SUMMARY AND CONCLUSIONS

Radiation solutions of the KdV equation for square well initial input were explored for three well areas via the Inverse Scattering Method. In particular the first two terms of the Neumman series expansion of the Marchenko equation through an expansion procedure in terms of Oscillator functions.

By comparing the results of the Oscillator function expansion's solution for the terms of the Neumman series with those generated by direct numerical evalution of the same terms of the Neumman series it was found that the Oscillator Expansion procedure captured the correct behaviour of the terms of the series, within the effective range of the expansion. The expansion procedure was limited by the computing facilities available for both the order to which the Neumman series could be calculated and the order to which the Oscillator expansion could be calculated.

Examination of the T=0 behaviour of the successive contributions to the Neumman series, up to second order, lead to the conclusion that the convergence of the series gets progressively worse as the initial input area is increased.

Through a single variable expansion procedure it was found that, with the expansion in Oscillator functions, the small area pulse approaches its asymptotic limit slower than the large area

pulses. Similarly it was found that the typical relaxtion time, for those initial pulses examined, to their asymptotic limit was of the order of e^{20}, and that these asymptotic profiles displayed the much cited Airy function-like behaviour.

In a comparison of the two term Neumman series result for the radiative solutions of the KdV equation with the few specific experimental resultsavailable it was found that for the specific set of parameters used the agreement between theory and experiment was poor.

APPENDIX 1

The KdV equation is invariant under a certain scale transformation that involves both of the independent variables x and t and the dependent variable U.

As a reminder the KdV equation in standard form is

$$U_t + 6UU_x + U_{xxx} = 0.$$

If the scale transformations

$$U \longrightarrow V(\xi,\tau) = \frac{1}{\epsilon}U(x,t) \qquad 1a$$

$$x \longrightarrow \xi = \frac{x}{\lambda} \qquad 1b$$

$$t \longrightarrow \tau = \frac{t}{\nu}. \qquad 1c$$

are introduced then we get that the respective partial derivatives in terms of the new variables become

$$\frac{\partial U}{\partial x} = \frac{\epsilon}{\lambda}\frac{\partial V}{\partial \xi} \qquad 2a$$

and $$\frac{\partial U}{\partial t} = \frac{\epsilon}{\nu}\frac{\partial V}{\partial \tau}. \qquad 2b$$

Substitution of these transformed variables in the KdV equation yields

$$\frac{\epsilon}{\nu}V_\tau + 6\frac{\epsilon^2}{\lambda}VV_\xi + \frac{\epsilon}{\lambda^3}V_{\xi\xi\xi} = 0.$$

Choosing

$$\nu = \lambda^3 \qquad \epsilon = \frac{1}{\lambda^2} \qquad 3$$

recaptures the original form of the KdV equation,

$$V_\tau + 6VV_\xi + V_{\xi\xi\xi} = 0, \qquad 4$$

in terms of the new variables,

$$\xi = \frac{x}{\lambda} \qquad \tau = \frac{t}{\lambda^3}.$$

If $\lambda > 1$ then the new time τ and new space ξ are compressed, conversely if $\lambda < 1$ then the time and space are expanded.

For standardization it was chosen that the maximum (minimum) height of the initial conditions would be normalized to unity through the use of this transformation. If the real height of the pulse was h then in terms of the new coordinates this would be scaled to unity by letting $\lambda = 1/\sqrt{h}$. This in turn defined the transformation for the coordinates x and t by

$$\xi = \sqrt{h}\, x \qquad \text{and} \qquad \tau = \sqrt{h^3}\, t. \qquad 5$$

If this is applied to the square well initial profile of height h and width w we would get that the transformed initial conditions would be

$$V = \{\ 0:\ \xi < 0,\ 1:\ 0 < \xi < \sqrt{h}w,\ 0:\ \sqrt{h}w < \xi\ \}.$$

As an aside it should be mentioned that it was this factor of $\sqrt{h}w$ that played the role of the natural expansion parameter

in the expansion procedure of Enns and Rangnekar in their analysis of the KdV equation.

APPENDIX 2

The existence of the imaginary eigenvalues (k^2) for the Schroedinger operator determines whether or not any solitons will arise in the solution of the particular initial value problem at hand. Here we will show, in particular, that it is possible to find initial conditions for which no imaginary eigenvalues exist, and thus that the solution contains no solitons.

In order to begin this discussion we will start with some of the results derived in chpt 4 for the scattering data. From equation 4.1 we see that if Ψ_1 is to be a bounded solution for $x > 0$, with the eigenvalue $k=i\kappa$, then the coefficient A must be 0, since $e^{-i(i\kappa)x} = e^{\kappa x}$ is divergent. Implicit in this is the fact that we are restricted to deal exclusively in the regime that $Im(k) > 0$, as required by the contours chosen in deriving the Marchenko equation in chapter 2. Thus all that we really need to find are the zeros of the coefficient A for imaginary k in order to determine the discrete spectrum of the problem. If no zeros exist then there are no solitons. It can be shown with a little algebra that the condition A=0 for the square well initial data implies the transcendental condition,

$$i\tan(\sqrt{k^2 + 1}w) = \frac{2k\sqrt{k^2 + 1}}{2k^2 + 1} \qquad 1$$

where we have made use of the fact that we can normalize the height of the pulse to unity. If k is real then this equation has no solution, however if we let k be purely imaginary by $k=i\kappa$ we get for $\kappa \leq 1$ the condition

$$\tan(\sqrt{1-\kappa^2}w) = \frac{2\kappa\sqrt{1-\kappa^2}}{1-2\kappa^2}, \qquad 2a$$

and for $\kappa > 1$ the condition

$$\tanh(\sqrt{\kappa^2-1}w) = \frac{2\kappa\sqrt{\kappa^2-1}}{1-2\kappa^2}. \qquad 2b$$

To get a feel for these conditions a plot for w=1 is shown in figure A3.1.

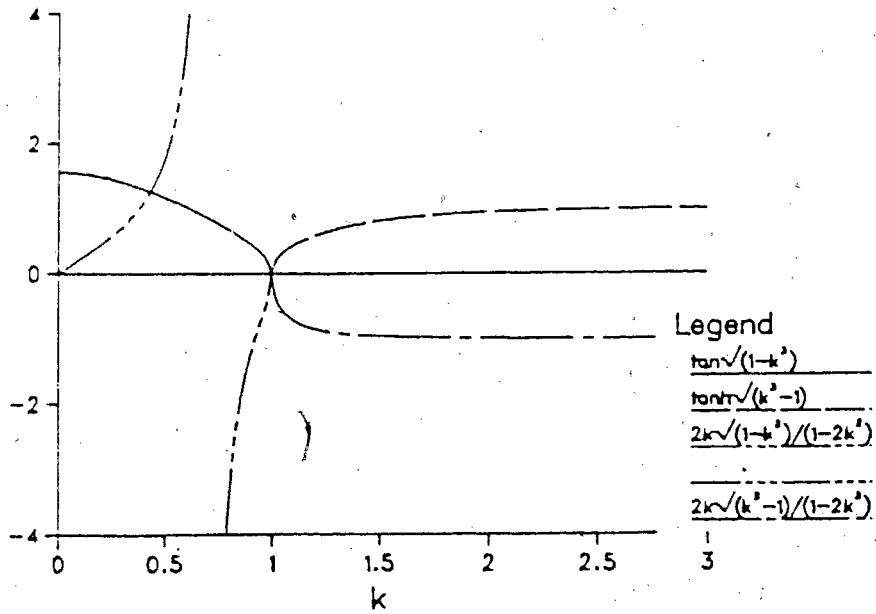

From figure A2.1 we see that we will get one soliton corresponding to the curves intersection at $\kappa \simeq 1/2$. If w is increased more solitons will occur, the number of them depending on the number of branches of the tangent function that reside in the interval $0 \leq \kappa \leq 1$. Physically this situation corresponds to having the water elevated initially. If on the other hand we consider the case for which we push the water down, h=-1 we get the condition

$$\tanh(\sqrt{\kappa^2 + 1}w) = \frac{-2\kappa\sqrt{\kappa^2 + 1}}{2\kappa^2 + 1} . \qquad 3$$

To get an understanding for what the condition implies this was also plotted for w=1 and is shown in figure A2.2.

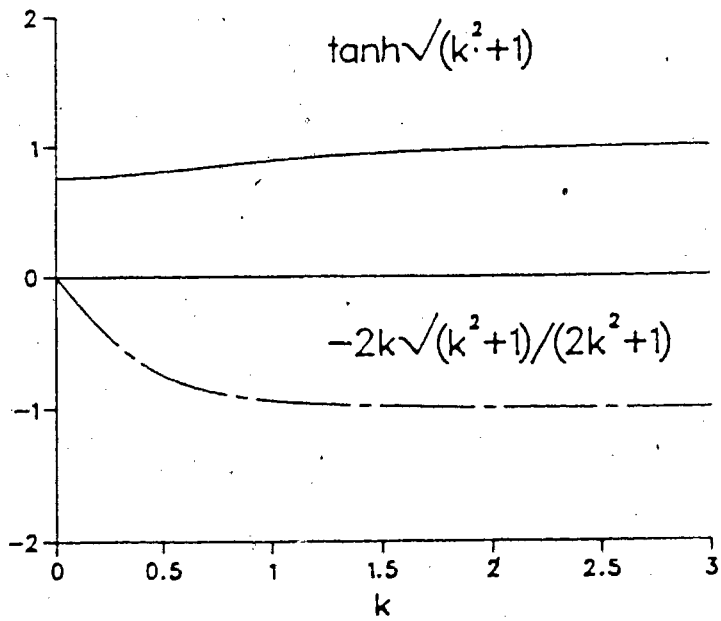

From this figure we see that the two curves do not intersect and consequently there are no imaginary eigenvalues. Thus if the fluid is initially pushed down no solitons arise, and the solution of the KdV equation will be purely radiative in nature.

APPENDIX 3

The numerical calculation of the expansion coefficients required the calculation of the normalized oscillator functions

$$\Theta_m(x) = \frac{1}{\sqrt{2^m m!\sqrt{\pi}}} e^{-x^2/2} H_m(x) , \qquad 1$$

with $H_m(x)$ being the Hermite polynomials. This can be accomplished in a relatively simple fashion by resorting to the explicit form of the Hermite polynomials. From AMS-55 sec.22.3

$$H_m(x) = m! \sum_{k=0}^{[m/2]} (-1)^k \frac{1}{k!(m-2k)!} (2x)^{m-2k}. \qquad 2$$

where [m/2] denotes the largest whole number less than or equal to m/2. This explicit form can then be directly evaluated and then multiplied by the damping factor $e^{-x^2/2}$. However, this method breaks down for large order when using finite arithmetic. In any finite arithmetic system there is a limited dynamic range of the numbers. For Fortran 77 that range is between 10^{-77} and 10^{77}. With these limits the maximum possible factorial that can be generated is 56! and the minimum number is the reciprocal of 56!. If the lower limit is exceeded a 0 is returned and all information is lost and if the upper limit is exceeded an error

occurs and all processing stops.

In light of these technical problems a more sophisticated method was used to generate the oscillator functions. It is well known that the Hermite polynomials obey a three term recurrence relation with respect to order,

$$H_{m+1}(x) = 2x\, H_m(x) - 2m\, H_{m-1}(x) \quad . \qquad 3$$

By iterating this equation, starting from $H_0(x) = 1$ and $H_1(x) = 2x$ successive orders of the Hermite polynomials can be generated.

This type of procedure is not without pitfalls. Depending on the direction of iteration (increasing or decreasing order) the recurrence relation may be either stable or unstable. The question of stablity arises from the fact that these three term recurrence relations are manifestations of second order differential equations and as such admit two independent solutions. In finite arithmetic the error generated by truncation manifests itself in the recurrence relation as part of the second solution branch. If the second solution increases quicker than the first, on iteration, then the first will get lost in the second.

In lieu of any standard theoretical test that can be applied to determine which direction of iteration is stable we simply applied the recurrence relation and compared the results with our expectations, guided by previous knowledge of the oscillator functions behaviour. As a test for the accuracy of the numerical routine we calculated the integral

$$\int_{-\infty}^{\infty} \Theta_m(x)\ \Theta_m(x)\ dx$$

numerically and compared the result with the expected result of unity. Other tests for accuracy were to compare the numerical value of the oscillator functions at the origin with the theoretical value of

$$\Theta_m(0) = \{\ 0 \text{ if } m \text{ odd};\ (-1/2)^{m/2}/(m/2)!\ \sqrt{m!}/\sqrt{\pi} \text{ if } m \text{ even }\},$$

and to count the number of zeros of the generated functions with the number of expected zeros (the order of the function).

Some selected Oscillator functions (m=0,10,25,,50,100), as calculated from the iterative algorithm developed, are shown in figure A4.1. Those readers who have had occassion to work with these functions can verify for themselves that the functions

generated have the expected behaviour of the Oscillator functions.

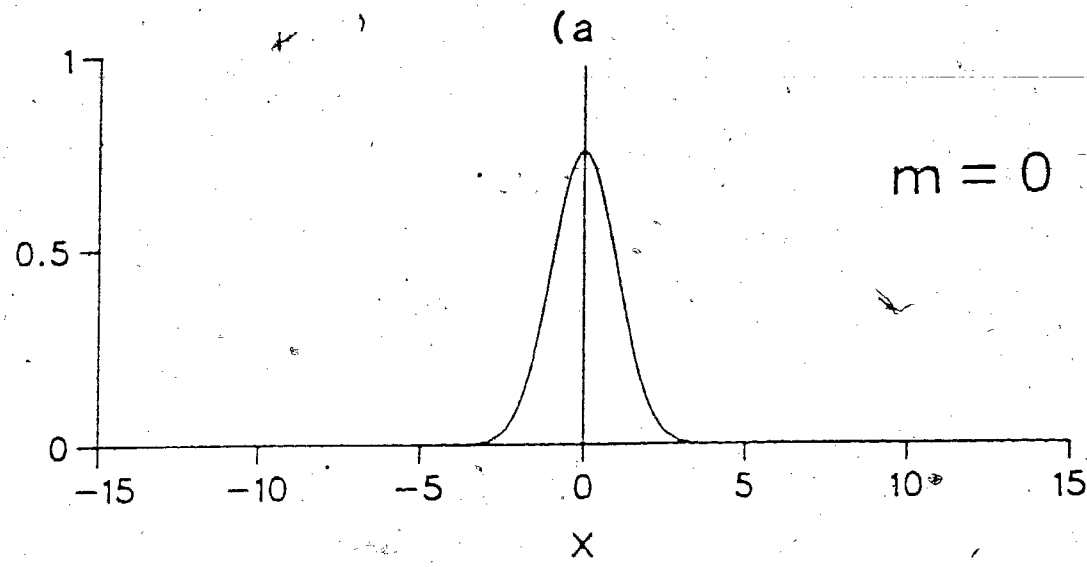
(a
m = 0
1
0.5
0
−15
−10
−5
0
5
10
15
X

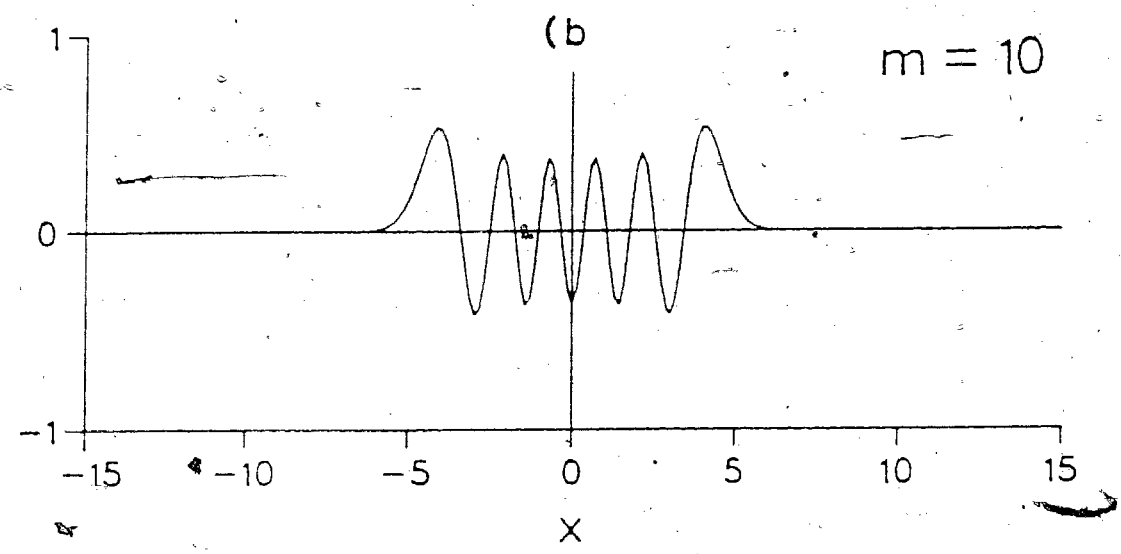
(b
m = 10
1
0
−1
−15
−10
−5
0
5
10
15
X

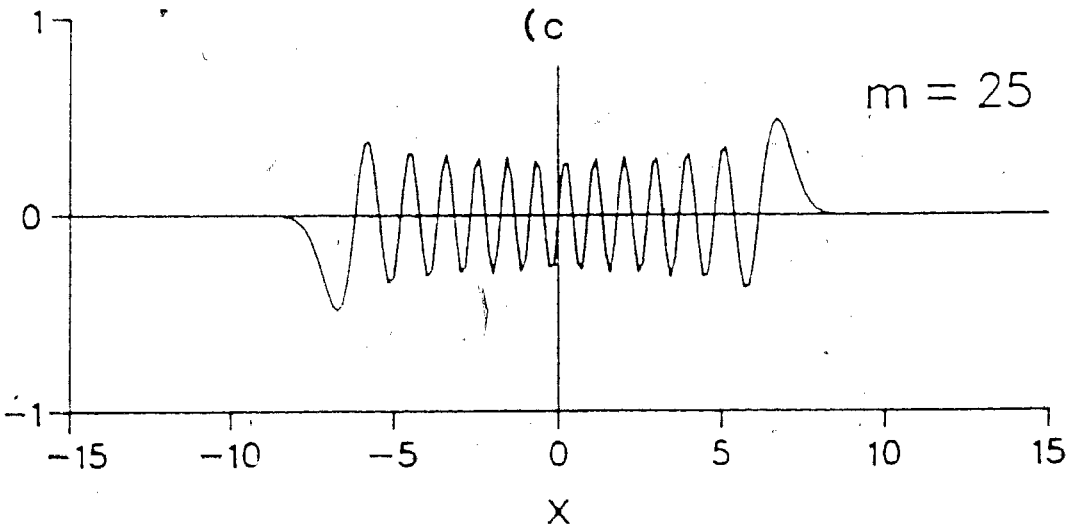
(c
m = 25
1
0
−1
−15
−10
−5
0
5
10
15
X

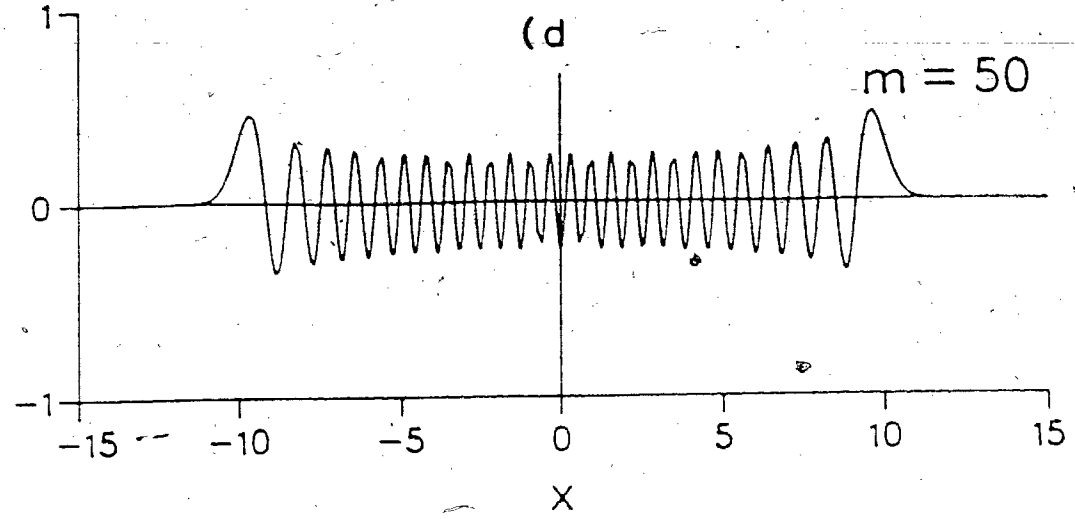

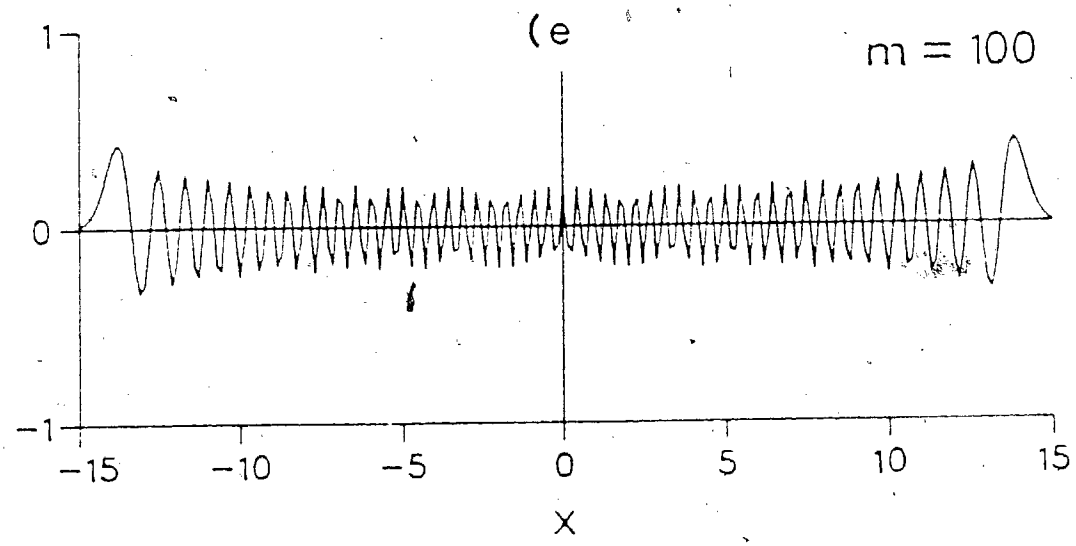

Figure A3.1 ; Sellected Oscillator function for a) m=0, b) m=10, c) m=25, d) m=50, and e)m=100 .

For reasons of posterity a copy of the Fortran 77 program that was used to generate the Oscillator functions is included here. The basic principal motivating the form of the program resides in the fact that at each point all of the Oscilator functions up to some order were needed. The subroutine OSCR, listed below returns an array OS of lenght LO, with I entries calculated, where the entries of OS are the values of the Oscillator function of the order of the entry's subscript, calculated at Z (a real number). Thus, for example, OS(10) corresponds to $\theta_{10}(z)$. Note that I must be smaller than or equal to LO the global order parameter.

```
      SUBROUTINE OSCR(I,OS,Z,LO)
      REAL*8 OS(0:LO)
      REAL*8 Z,X,Y,OS0,OS1,OS2,PI,AJ,A,B,OSCL
      INTEGER I,J,K,L,N,M,FLAG,FLAG1
      PI=3.14159265358979320
      FLAG1=0
      FLAG=0
      IF (DABS(Z).LT.17.D0) THEN
      OS0=DEXP(-Z*Z/2.D0)/DSQRT(DSQRT(PI))
      OS1=DSQRT(2.D0/DSQRT(PI))*Z*DEXP(-Z*Z/2.D0)
      OS(0)=OS0
      OS(1)=OS1
      ELSE
      OS0=1.D0/DSQRT(DSQRT(PI))
      OS1=DSQRT(2.D0/DSQRT(PI))*Z
      OS(0)=OS0*DEXP(-Z*Z/2.D0)
      OS(1)=OS1*DEXP(-Z*Z/2.D0)
      FLAG=1
      ENDIF
      IF (I.EQ.0) THEN
      OSCL=OS0
      ELSE IF (I.EQ.1) THEN
      OSCL=OS1
      ELSE
      DO 1 J=1,I-1
      K=J+1
      AJ=DFLOAT(J)
```

```
      OS2=DSQRT(AJ/(AJ+1.D0))*(OS1*Z*DSQRT(2.D0/AJ)-OS0)
      IF (OS2.EQ.0.D0) THEN
      OS(K)=0.0
      ELSE
      OS(K)=DSIGN(1.D0,OS2)*DEXP(DLOG(DABS(OS2))-
     & DFLOAT(FLAG)*Z*Z/2.D0+DFLOAT(FLAG1)*71.D0*DLOG(10.D0))
      ENDIF
      IF (DABS(OS2).GT.10.D70) THEN
      OS0=OS1/10.D70
      OS1=OS2/10.D70
      FLAG1=FLAG1+1
      ELSE
      OS0=OS1
      OS1=OS2
      ENDIF
1 CONTINUE
      ENDIF
      RETURN
      END
```

APPENDIX 4

Having adopted the Oscillator functions, which are defined by

$$\Theta_m(x) = N_m e^{-x^2/2} H_m(x) , \qquad 1$$

as basis functions, where the N_m's are the normalization factors, $N_m = \frac{1}{\sqrt{2^m m! \sqrt{\pi}}}$, and the $H_m(x)$'s are the Hermite polynomials, we can explicitly calculate the components of the matrices P_{ijk} and I_{ijk}.

These matrices are defined by the relationships

$$\Theta_i(x)\ \Theta_j(x) = P_{ijk}\Theta_k(x) , \qquad 2a$$

$$\int_x^\infty \Theta_i(z)\ \Theta_j(z)\ dz = I_{ijk}\Theta_k(x) . \qquad 2b$$

By virtue of the orthogonality of the Oscillator functions we get that

$$P_{ijk} = \int_{-\infty}^{\infty} \Theta_i(x)\ \Theta_j(x)\ \Theta_k(x)\ dx, \qquad 3a$$

and $$I_{ijk} = \int_{-\infty}^{\infty} \theta_k(x) \int_{x}^{\infty} \theta_i(z)\, \theta_j(z)\, dz dx. \qquad 3b$$

In order to evaluate these matrices we need to return to the explicit definition of the $\theta_m(x)$'s, consequently

$$P_{ijk} = N_i N_j N_k \int_{-\infty}^{\infty} e^{-3x^2/2} H_i(x)\, H_j(x)\, H_k(x)\, dx. \qquad 4$$

From Appendix 6 we note that the product of two Hermite polynomials can be written as a finite sum of Hermite polynomials, i.e.

$$H_i(x)\, H_j(x) = \sum_{m=0}^{\min(i,j)} \frac{2^m i!\, j!}{m!\,(i-m)!\,(j-m)!} H_{i+j-2m}(x) .$$

With this identity equation 4 becomes

$$P_{ijk} = N_i N_j N_k \bullet$$

$$\bullet \sum_{m=0}^{\min(i,j)} \frac{2^m i!\, j!}{m!\,(i-m)!\,(j-m)!} \int_{-\infty}^{\infty} e^{-3x^2/2} H_{i+j-2m}(x)\, H_k(x)\, dx.$$

By G-R sec. 7.374

$$\int_{-\infty}^{\infty} e^{-2a^2x^2} H_m(x) H_n(x) =$$

$$= (\pi/2a^2)^{1/2} \left(\frac{1-2a^2}{2a^2}\right)^{(m+n)/2} \frac{(m+n)!}{((m+n)/2)!} \bullet$$

$$\bullet \ {}_2F_1(-m,-n;(1-m-n)/2;a^2/(2a^2-1)), \qquad \text{if } m+n \text{ even} \qquad 5a$$

$$\text{else} \qquad = 0 \qquad \text{if } m+n \text{ odd}, \qquad 5b$$

where ${}_2F_1$ is a hypergeometric function. By identifying $m \longrightarrow i+j-2m$, $n \longrightarrow k$, and $2a^2 = 3/2$, the integral in the definition of P_{ijk} becomes

$$(2\pi/3)^{1/2} \left(-\frac{1}{3}\right)^{((i+j+k)/2)-m} \frac{(i+j+k-2m)!}{(((i+j+k)/2)-m)!} \bullet$$

$$\bullet \ {}_2F_1(2m-i-j,-k;((1-i-j-k)/2)+m;3/2),$$

and thus

$$P_{ijk} = N_i N_j N_k \; (2\pi/3)^{1/2} \; (-\tfrac{1}{3})^{(i+j+k)/2} \cdot$$

$$\cdot \sum_{m=0}^{\min(i,j)} \frac{2^m i!\,j!}{m!(i-m)!(j-m)!}(-3)^m \; \frac{(i+j+k-2m)!}{(((i+j+k)/2)-m)!} \cdot$$

$$\cdot \; {}_2F_1(2m-i-j,-k;((1-i-j-k)/2)+m;3/2). \qquad 6$$

This can be written in more elegant form by introducing the Pochammer symbol,

$$(a)_0 = 1 \;, \quad (a)_n = a(a+1)(a+2)\ldots(a+n-1) \quad n=1,2\ldots \;.$$

In terms of this symbol

$$(i-m)! = \frac{i!}{(-1)^m(-i)_m} \qquad 7a$$

and

$$(i-2m)! = \frac{i!}{2^{2m}(-i/2)_m((1-i)/2)_m}. \qquad 7b$$

With this notation equation 6 becomes

$$P_{ijk} = N_i N_j N_k \; (2\pi/3)^{1/2} \; (-\tfrac{1}{3})^{(i+j+k)/2} \; \frac{(i+j+k)!}{((i+j+k)/2)!} \cdot$$

$$\cdot \sum_{m=0}^{\min(i,j)} \frac{(-i)_m(-j)_m}{((1-(i+j+k))/2)_m} \frac{(3/2)^m}{m!} \cdot$$

$$\bullet \; {}_2F_1(2l-i-j,-k;((1-i-j-k)/2)+m;3/2). \qquad 8$$

If we explicitly introduce the forms for N_i, N_j, and N_k the prefactor to the sum becomes

$$(2/(3\sqrt{\pi}))^{1/2} \; (-\tfrac{1}{6})^{(i+j+k)/2} \; \frac{1}{\sqrt{i!j!k!}} \; \frac{(i+j+k)!}{((i+j+k)/2)!}, \qquad 9$$

and thus

$$P_{ijk} = (2/(3\sqrt{\pi}))^{1/2} \; (-\tfrac{1}{6})^{(i+j+k)/2} \bullet$$

$$\bullet \; \frac{1}{\sqrt{i!j!k!}} \; \frac{(i+j+k)!}{((i+j+k)/2)!} \sum_{m=0}^{\min(i,j)} \frac{(-i)_m(-j)_m}{((1-(i+j+k))/2)_m} \; \frac{(3/2)^m}{m!} \bullet$$

$$\bullet \; {}_2F_1(2l-i-j,-k;((1-i-j-k)/2)+m;3/2). \qquad 10$$

if i+j+k is even,

$$= 0$$

if i+j+k is odd. This result can be written in an even more compact form in terms of generalized hypergeometric functions of two variables. By using one of the quadratic transforms that the

type of hypergeometric function that occurs in equation 10 admits i.e.

$$ {}_2F_1(2l-i-j,-k;(1-i-j-k)/2+m;3/2) = $$

$$ = (-2)^k {}_2F_1(-k/2,(1-k)/2;((1-i-j-k)/2)+m;3/4), \qquad 11 $$

see AMS-55 sec. 15.3.29, and note the symmetry of the hypergeometric functions under interchange of the first two parameters. The non-zero components of P become

$$ P_{ijk} = (2/(3\sqrt{\pi}))^{1/2} \left(-\frac{1}{6}\right)^{(i+j+k)/2} \frac{(-2)^k}{\sqrt{i!j!k!}} \frac{(i+j+k)!}{((i+j+k)/2)!} \cdot $$

$$ \cdot \sum_{m=0}^{\min(i,j)} \frac{(-i)_m(-j)_m}{((1-(i+j+k))/2)_m} \frac{(3/2)^m}{m!} \cdot $$

$$ \cdot {}_2F_1(-k/2,(1-k)/2;((1-i-j-k)/2)+m;3/4). \qquad 12 $$

The sum in this equation can be identified with the third Appell series F_3, see Erdelyi vol. 2, and thus the components of P are

$$ P_{ijk} = (2/(3\sqrt{\pi}))^{1/2} \left(-\frac{1}{6}\right)^{(i+j+k)/2} \frac{(-2)^k}{\sqrt{i!j!k!}} \frac{(i+j+k)!}{((i+j+k)/2)!} \cdot $$

$$\bullet \; F_3(-i,-k/2;-j,(1-k)/2;(1-i-j-k)/2;3/2;3/4) \qquad 13a$$

with the condition that i+j+k is even, if i+j+k odd then

$$P_{ijk} = 0. \qquad 13b$$

With the components of the matrix P calculated we can now turn our attention to the components of the matrix I. These components, as defined by equation 3b, can be written explicitly in terms of Hermite polynomials by

$$I_{ijk} = N_i N_j N_k \int_{-\infty}^{\infty} e^{-x^2/2} H_k(x) \int_{x}^{\infty} e^{-y^2} H_i(y) H_j(y) \, dydx. \qquad 14$$

Using result 1 from Appendix 6 for the product of two Hermite polynomials again the components of I can be written as

$$I_{ijk} = N_i N_j N_k \sum_{m=0}^{\min(i,j)} \frac{2^m}{m!}(-i)_m(-j)_m \bullet$$

$$\bullet \int_{-\infty}^{\infty} e^{-x^2/2} H_k(x) \int_{x}^{\infty} e^{-y^2} H_{i+j-2m}(y) \, dydx. \qquad 15$$

The integral over y has been evaluated in general in Appendix 6, see result 6, and yields

$$\int_x^\infty e^{-y^2} H_{i+j-2m}(y)\, dy = e^{-x^2} H_{i+j-2m-1}(x) \qquad \text{if } i+j-2m \neq 0$$

$$= \frac{\sqrt{\pi}}{2}\text{erfc}(x) \qquad \text{if } i+j-2m = 0.$$

The complement of the error function will occur only if $i+j-2m = 0$, and this can only occur if $i=j$ due to the restriction on m having a maximum value of $\min(i,j)$.

Because of the various possible outcomes of these integrals depending on the values of the indices of the matrix component we must evaluate them case by case. The partitions are,

1. $i \neq j$
   a. $i+j+k$ even
   b. $i+j+k$ odd
2. $i = j$
   a. $i+j+k$ even
   b. $i+j+k$ odd

where the division into odd and even cases is due to symmetry considerations of the integrand in the integral over x.

Taking the first case for $i \neq j$,we get

$$I_{ijk} = N_i N_j N_k \sum_{m=0}^{\min(i,j)} \frac{2^m}{m!}(-i)_m(-j)_m \bullet$$

$$\bullet \int_{-\infty}^{\infty} e^{-3x^2/2} H_k(x)\, H_{i+j-2m-1}(x)\, dx. \qquad 16$$

From the symmetry of the constituents of the integrand we see that

$$I_{ijk} = 0 \qquad 17$$

if i+j+k is even, thus solving case 1a. If, however, i+j+k is odd we can again appeal to the result from G-R, equations 5a and 5b; that were cited in the derivation of the P_{ijk}'s to do the remaining integral by letting m —> m + 1/2, i.e.

$$\int_{-\infty}^{\infty} e^{-3x^2/2} H_k(x)\, H_{i+j-2m-1}(x)\, dx =$$

$$= (2\pi/3)^{1/2} \left(-\frac{1}{3}\right)^{(i+j+k-1)/2} \frac{(i+j+k-1)!}{((i+j+k-1)/2)!}\left(\frac{3}{4}\right)^m \bullet$$

$$\bullet \frac{1}{((2-(i+j+k))/2)_m} {}_2F_1(2m+1-i-j,-k;(2-i-j-k)/2+m;3/2). \qquad 18$$

With this result

$$I_{ijk} = N_i N_j N_k \; (2\pi/3)^{-1/2} \; (-\tfrac{1}{3})^{(i+j+k-1)/2} \cdot$$

$$\cdot \; \frac{(i+j+k-1)!}{((i+j+k-1)/2)!} \sum_{m=0}^{\min(i,j)} \frac{(-i)_m (-j)_m}{((2-(i+j+k))/2)_m} \frac{(3/2)^m}{m!} \cdot$$

$$\cdot \; {}_2F_1(2m+1-i-j,-k;(2-i-j-k)/2+m;3/2). \qquad 19$$

By using the same quadratic transformation as in equation 11,

$${}_2F_1(2m+1-i-j,-k;(2-i-j-k)/2+m;3/2) =$$

$$= (-2)^k \, {}_2F_1(-k/2,(1-k)/2;(2-i-j-k)/2+m;3/4), \qquad 20$$

on the hypergeometric function we get for equation 18,

$$I_{ijk} = N_i N_j N_k \; (2\pi/3)^{1/2} \; (-\tfrac{1}{3})^{(i+j+k-1)/2} (-2)^k \cdot$$

$$\cdot \; \frac{(i+j+k-1)!}{((i+j+k-1)/2)!} \sum_{m=0}^{\min(i,j)} \frac{(-i)_m (-j)_m}{((2-(i+j+k))/2)_m} \frac{(3/2)^m}{m!} \cdot$$

$$\cdot \; {}_2F_1(-k/2,(1-k)/2;(2-i-j-k)/2+m;3/4). \qquad 21$$

Again the sum can be identified as the third Appell series and

as such the components of I can be written

$$I_{ijk} = N_i N_j N_k \sqrt{2\pi/3} \left(-\frac{1}{3}\right)^{(i+j+k-1)/2} (-2)^k \bullet$$

$$\bullet \frac{(i+j+k-1)!}{((i+j+k-1)/2)!} F_3(-i,-k/2;-j,(1-k)/2;1-(i+j+k)/2;3/2;3/4) \qquad 22$$

On introducing the explicit form of the normalization constants we get

$$I_{ijk} = (1/3\sqrt{\pi})^{1/2} \left(-\frac{1}{6}\right)^{(i+j+k-1)/2} \frac{(-2)^k}{\sqrt{i!j!k!}} \frac{(i+j+k-1)!}{((i+j+k-1)/2)!} \bullet$$

$$\bullet F_3(-i,-k/2;-j,(1-k)/2;1-(i+j+k)/2;3/2;3/4). \qquad 23$$

Thus for the cases for which $i \neq j$ we have the results that

$$I_{ijk} = 0 \qquad \text{if } i+j+k \text{ even} \qquad 24a$$

and that $$I_{ijk} = (1/3\pi)^{1/2} \left(-\frac{1}{6}\right)^{(i+j+k-1)/2} \frac{(-2)^k}{\sqrt{i!j!k!}} \bullet$$

$$\bullet \frac{(i+j+k-1)!}{((i+j+k-1)/2)!} F_3(-i,-k/2;-j,(1-k)/2;1-(i+j+k)/2;3/2;3/4),$$

$$\text{if } i+j+k \text{ odd.} \qquad 24b$$

For the cases for which i=j we have from equation 14 and result 6 from Appendix 6 that in general

$$I_{iik} = N_i^2 N_k \bullet$$

$$\bullet \sum_{m=0}^{i} ((-i)_m)^2 \frac{2^m}{m!} \int_{-\infty}^{\infty} e^{-x^2/2} H_k(x) \begin{cases} e^{-x^2} H_{2i-2m-1}(x)\, dx; & m \neq i \\ \frac{\sqrt{\pi}}{2} \operatorname{ercf}(x)\, dx; & m = i. \end{cases} \quad 25$$

If k is even equation 25 becomes

$$I_{iik} = N_i^2 N_k i!\, 2^i \frac{\sqrt{\pi}}{2} \int_{-\infty}^{\infty} \operatorname{erfc}(x)\, H_k(x)\, e^{-x^2/2} dx \quad 26$$

since all of the other terms in the sum contain integrals whose integrands are anti-symmetric. Noting that the complementary error function can be written in terms of symmetric and anti-symmetric parts by definition

$$\operatorname{erfc}(x) = 1 - \operatorname{erf}(x)$$

where $$\operatorname{erf}(x) = -\operatorname{erf}(-x),$$

the integral in equation 26 becomes

$$I_{iik} = N_i^2 N_k i! 2^i \frac{\sqrt{\pi}}{2} \int_{-\infty}^{\infty} H_k(x)\, e^{-x^2/2} dx. \qquad 27$$

By G-R sec. 7.373 we get that

$$\int_{-\infty}^{\infty} H_k(\alpha x)\, e^{-x^2} dx = \sqrt{\pi}\, \frac{k!}{(k/2)!} (\alpha^2 - 1)^{k/2}$$

and thus

$$I_{iik} = N_i^2 N_k i! 2^i \frac{\pi}{\sqrt{2}} \frac{k!}{(k/2)!}, \qquad 28$$

or by introducing the explicit forms of normalization constants we get

$$I_{iik} = \left(\frac{\sqrt{\pi}}{2^{k+1}} \right)^{1/2} \frac{\sqrt{k!}}{(k/2)!}. \qquad 29$$

If, on the other hand, k is odd the generic form of I_{iik} (equation 25) becomes

$$I_{iik} = N_i^2 N_k \{ \left(\frac{2\sqrt{\pi}}{3}\right)^{-1/2} \sum_{m=0}^{i-1} ((-i)^m)^2 \frac{2^m}{m!} \left(-\frac{1}{3}\right)^{(k-1)/2+i-m} \cdot$$

$$\cdot \frac{(2i+k-2m-1)!}{((k-1)/2+i-m)!} {}_2F_1(2m+1-2i, -k; m+1-i-k/2; 3/2) -$$

$$- i! 2^i \frac{\sqrt{\pi}}{2} \int_{-\infty}^{\infty} \operatorname{erf}(x)\, e^{-x^2/2}\, H_k(x)\, dx \}, \qquad 30$$

where we have used previous results of this appendix to evaluate the integral in the summed term and the symmetry properties of the complementary error function to simplify the last term. This now leaves the integral

$$\int_{-\infty}^{\infty} \operatorname{erf}(x) e^{-x^2/2}\, H_k(x)\, dx \qquad 31$$

to be done.

The evaluation of this integral can be approached by resorting to the integral representation of the error function.

$$\operatorname{erf}(x) = \frac{2}{\sqrt{\pi}} \int_0^x e^{-y^2}\, dy. \qquad 32$$

With this 31 yields

$$\frac{\sqrt{\pi}}{2}\int_{-\infty}^{\infty} \operatorname{erf}(x)e^{-x^2/2}\,H_k(x)\,dx = \int_{-\infty}^{\infty}\int_{0}^{x} e^{-y^2}dy\; e^{-x^2/2}\,H_k(x)\,dx. \qquad 33$$

Interchanging the order of the integration and using the symmetry of the integrand the right hand side of equation 33 becomes

$$2\int_{0}^{\infty} e^{-y^2}\int_{y}^{\infty} e^{-x^2/2}\,H_k(x)\,dxdy. \qquad 34$$

To evaluate the inner integral we use the result 5 from appendix 7 that

$$H_k(x) = \sum_{m=0}^{[k/2]} \frac{k!}{m!(k-2m)!}2^{k/2-m}\,H_{k-2m}(x/\sqrt{2}),$$

and let $z=x/\sqrt{2}$, which then allows us to express 34 as

$$2\sqrt{2} \sum_{m=0}^{[k/2]} \frac{k!}{m!(k-2m)!} 2^{k/2-m} \int_0^{\infty} e^{-y^2} \int_{y/\sqrt{2}}^{\infty} e^{-z^2} H_{k-2m}(z)\, dzdy. \quad 35$$

Using the result 6 from appendix 7 the integral over z yields

$$e^{-y^2/2} H_{k-2m-1}(y/\sqrt{2}) ,$$

where the complementary error function is excluded by k being odd. With this result 35 becomes

$$\sqrt{2} \sum_{m=0}^{[k/2]} \frac{k!}{m!(k-2m)!} 2^{k/2-m} \int_{-\infty}^{\infty} e^{-3y^2/2} H_{k-2m-1}(y/\sqrt{2})\, dy, \quad 36$$

where the integral over y has been taken over to range $-\infty$ to ∞.

If we now let $z=y\sqrt{(3/2)}$ the final integral can be done by appealing to the previously cited result from G-R sec. 7.373, and yields for 36

$$2(2\pi/3)^{1/2} \sum_{m=0}^{[k/2]} \frac{k!}{m!(k-2m)!} \left(-\frac{4}{3}\right)^{(k-1)/2-m} \frac{(k-1-2m)!}{((k-1)/2-m)!}, \quad 37$$

which as usual can be rewritten using Pochammer symbols as

$$2(2\pi/3)^{1/2}\ (-\frac{4}{3})^{(k-1)/2-m}\ \frac{(k-1)!}{((k-1)/2)!}\ \bullet$$

$$\bullet\ \sum_{m=0}^{[k/2]}\ \frac{(-k/2)_m((1-k)/2)_m}{((2-k)/2)_m}\ \frac{(3/4)^m}{m!}. \qquad 38$$

The sum term can be identified as a hypergeometric function leaving the result that

$$\frac{\sqrt{\pi}}{2}\int_{-\infty}^{\infty} \mathrm{erf}(x)e^{-x^2/2}\ H_k(x)\ dx =$$

$$= 2(2\pi/3)^{1/2}\ (-\frac{4}{3})^{(k-1)/2}\ \frac{(k-1)!}{((k-1)/2)!}\ \bullet$$

$$\bullet\ {}_2F_1(-k/2,(1-k)/2;1-k/2;3/4) \qquad 39$$

and that

$$I_{iik} = (\frac{2\pi}{3})^{1/2}\ N_i^2 N_k\ \bullet$$

$$\bullet\ \{\ \sum_{m=0}^{i-1}((-i)_m)^2\ \frac{2^m}{m!}(-\frac{1}{3})^{(k-1)/2+i-m}\ \frac{(2i+k-2m-1)!}{((k-1)/2+i-m)!}\ \bullet$$

$$\bullet\ {}_2F_1(2m+1-2i,-k;m+1-i-k/2;3/2)\ -$$

$$- \; 2i!2^i \; (-\frac{4}{3})^{(k-1)/2} \; \frac{(k-1)!}{((k-1)/2)!} \; \bullet$$

$$\bullet \; {}_2F_1(-k/2,(1-k)/2;1-k/2;3/4) \; \}. \qquad 40$$

However, as was done previously, the hypergeometric function ${}_2F_1(2m+1-2i,-k;m+1-i-k/2;3/2)$ can be transformed to $(-2)^k {}_2F_1(-k/2,(1-k)/2;1-k/2;3/4)$ by a quadratic transform. In this case

$$I_{iik} = (\frac{2\pi}{3})^{1/2} \; N_i^2 N_k \; \bullet$$

$$\bullet \; \{ \; \sum_{m=0}^{i-1} ((-i)_m)^2 \; \frac{2^m}{m!} (-\frac{1}{3})^{(k+1)/2+i-m} (-2)^k \; \frac{(2i+k-2m-1)!}{((k-1)/2+i-m)!} \; \bullet$$

$$\bullet \; {}_2F_1(-k/2,(1-k)/2;m+1-i-k/2;3/4) \; -$$

$$- \; 2i!2^i \; (-\frac{4}{3})^{(k-1)/2-1} \; \frac{(k-1)!}{((k-1)/2)!} \; \bullet$$

$$\bullet \; {}_2F_1(-k/2,(1-k)/2;1-k/2;3/4) \; \}. \qquad 41$$

Noting that the term that is not under the summation sign in equation 41 in fact corresponds to the m=i term of the sum had the sum been extended to include this possibility, we get

$$I_{iik} = \left(\frac{2\pi}{3}\right)^{1/2} N_i^2 N_k \bullet$$

$$\bullet \sum_{m=0}^{i} ((-i)_m)^2 \frac{2^m}{m!}\left(-\frac{1}{3}\right)^{(k-1)/2+i-m}(-2)^k \frac{(2i+k-2m-1)!}{((k-1)/2+i-m)!} \bullet$$

$$\bullet \ {}^2F^1(-k/2,(1-k)/2;m+1-i-k/2;3/4). \qquad 42$$

On rearranging terms and introducing the explicit forms for the normalizing factors we get

$$I_{iik} = (1/(3\sqrt{\pi})^{1/2} \left(-\frac{1}{6}\right)^{i+(k-1)/2} \frac{(-2)^k}{i!\sqrt{k!}} \frac{(2i+k-1)!}{(i+(k-1)/2)!} \bullet$$

$$\bullet \sum_{m=0}^{i} \frac{((-i)_m)^2}{(1-i-k/2)_m} \frac{(3/2)^m}{m!} {}_2F_1(-k/2,(1-k)/2;m+1-i-k/2;3/4). \qquad 43$$

The sum can again be identified with the third Appell series and yields

$$I_{iik} = (1/(3\sqrt{\pi})^{1/2} \left(-\frac{1}{6}\right)^{i+(k-1)/2} \frac{(-2)^k}{i!\sqrt{k!}} \frac{(2i+k-1)!}{(i+(k-1)/2)!} \bullet$$

$$\bullet \ F_3(-i,-k/2;-i,(1-k)/2;1-i-k/2;3/2,3/4), \qquad 44$$

which matches the form obtained for the case that $i \neq j$ and $i+j+k$ odd, if i is taken to be equal to j.

In summary we have

$$P_{ijk} = (2/(3\sqrt{\pi}))^{1/2} \left(-\frac{1}{6}\right)^{(i+j+k)/2} \frac{(-2)^k}{\sqrt{i!j!k!}} \frac{(i+j+k)!}{((i+j+k)/2)!} \cdot$$

$$\cdot F_3(-i,-k/2;-j,(1-k)/2;(1-i-j-k)/2;3/2;3/4) \qquad 45a$$

if i+j+k even

$$P_{ijk} = 0 \qquad 45b$$

if i+j+k odd

and

$$I_{ijk} = (1/(3\sqrt{\pi}))^{1/2} \left(-\frac{1}{6}\right)^{(i+j+k-1)/2} \frac{(-2)^k}{\sqrt{i!j!k!}} \frac{(i+j+k-1)!}{((i+j+k-1)/2)!} \cdot$$

$$\cdot F_3(-i,-k/2;-j,(1-k)/2;1-(i+j+k)/2;3/2,3/4), \qquad 46a$$

if i+j+k odd

$$I_{ijk} = 0 \qquad \text{if } i+j+k \text{ even } (i \neq j), \qquad 46b$$

$$I_{ijk} = (\sqrt{\pi}/2^{k+1})^{1/2} \frac{\sqrt{k!}}{(k/2)!} \qquad \text{if } i=j \text{ and } k \text{ even.} \qquad 46c$$

APPENDIX 5

By definition the third Appell series, see Erdelyi sec. 5.7 vol.2, has the form

$$F_3(a,A;b,B;c;x,y) =$$

$$= \sum_{m,n=0}^{\infty} \frac{(a)_m(A)_n(b)_m(B)_n}{(c)_{m+n}} \frac{x^m}{m!} \frac{y^n}{n!}, \qquad 1a$$

or

$$= \sum_{m=0}^{\infty} \frac{(a)_m(b)_m}{(c)_m} \frac{x^m}{m!} {}_2F_1(A,B;c+m;y). \qquad 1b$$

If both of the pairs (a,b) and (A,B) contain a negative constant, as is the case for the components of the matrices I and P, calculated in Appendix 4, then the sums in the definition of the Appell series are finite stopping when $(a)_m$ and $(A)_m$ are zero, assuming that a and A are the negative integers in question.

From the initial derivation of the components of the matrices I and P, and from the definition of the Appell series it is apparent that the calculation of the matrices' components hinged on the ability to calculate hypergeometric functions of the form

$${}_2F_1(-i,-j;(1-(i+j))/2;z) =$$

$$= \sum_{m=0}^{\infty} \frac{(-1/2)_m((1-i)/2)_m}{((1-(i+j))/2)_m} \frac{z^m}{m!}. \qquad 2$$

As a first attempt to calculate these functions we approached the problem with the simpleminded idea of adding up the terms of the sum that defines the hypergeometric function. This approach lead to difficulties in that the dynamic range of the individual terms of the sum is large, and that the sum alternates with negative and positive parts being approximately equal. For large orders of the parameters i or j the difference between the negative and the postive contributions vanished for the accuracy of the numerical calculation. In a particular test case, the individual sums (positive and negative) were equal, to machine accuracy, and of the order of 10^{60} taking the difference of these two numbers returned a number of the order of 10^{44} in the 16 decimal, double precision finite arithmetic that was being used. The possible error associated with this calculation is then of the order of $\pm 10^{44}$.

Figure A5.1 illustrates the behaviour of the sum as successive terms are added, and figure A5.2 demonstrates the behaviour of the positive and negative sums as successive terms are added to each of them, for the particular case ${}_2F_1(-50,-50;-49.5;3/2)$.

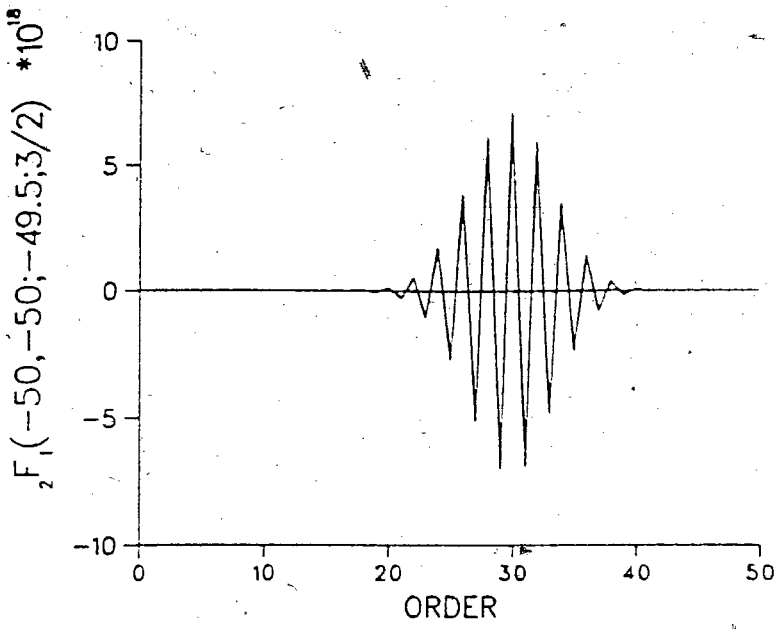

Figure A6.1 ; Sum of successive terms in the numerical summatior of the series representation of $_2F_1(-50,-50;-49.5;3/2)$.

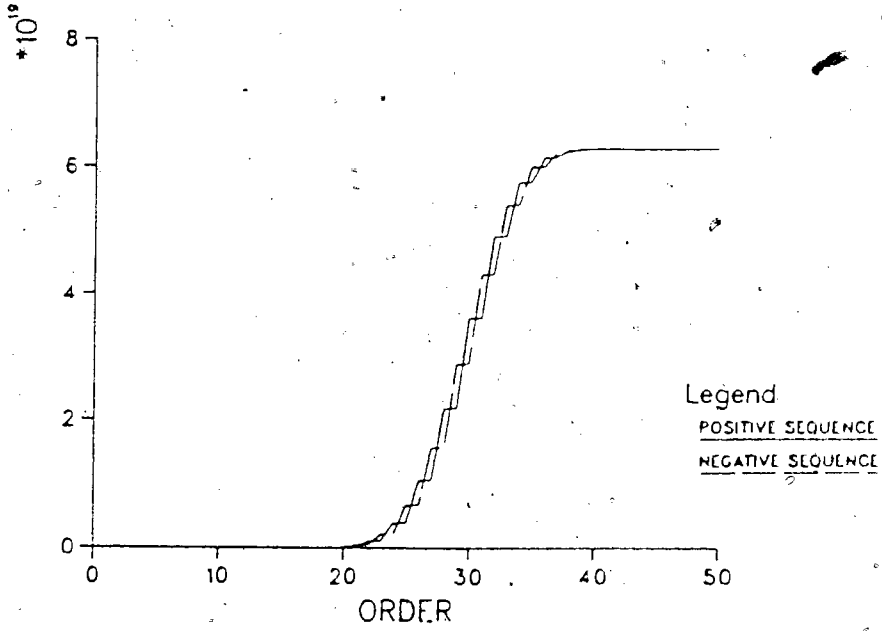

Figure A6.2 ; Behaviour of odd and even sums in the series representation of $_2F_1(-50,-50;-49.5;3/2)$.

In order to resolve this problem we turned to Gauss's relations for contiguous hypergeometric functions, a complete list of these being given in AMS-55 sec. 15.2. These relations are in essence three term recurrence relations, but slightly more generalized in that they act on any pair combination of the three parameters a,b,c of the hypergeometric function

$$ {}_2F_1(a,b;c;z). $$

Noting that $$ {}_2F_1(0,b;c;z) = 1 \qquad 3a $$

and that $$ {}_2F_1(-1,b;c;z) = 1 - \frac{b}{c}z \qquad 3b $$

we can, if it is stable, use the recurrence relation

$$ (c-a){}_2F_1(a-1,b;c;z) + (2a-c-az+bz){}_2F_1(a,b;c;z) + $$

$$ + a(z-1){}_2F_1(a+1,b;c;z) = 0 \qquad 4 $$

to generate successively lower orders of the hypergeometric function, by starting at the ground states given by equations 3a and 3b.

To apply this method to the specific form of hypergeometric function that arises in the calculation of the matrix components of I and P, given in 2, we need to start the recurrence relation 4 at

$$ {}_2F_1(0,(1-i)/2;(1-(i+j))/2;3/4) = 1 \qquad 5a$$

and $$ {}_2F_1(-1,(1-i)/2;(1-(i+j))/2;3/4) = 1 - \frac{(1-i)}{(1-(i+j))}\frac{3}{4}, \qquad 5b$$

and successively lower the leading parameter to obtain

$$ {}_2F_1(-i/2,(1-i)/2;(1-(i+j))/2;3/4),$$

where we have assumed that i is an even integer. If i is not an even integer we can make use of the symmetry property of the hypergeometric function,

$$ {}_2F_1(a,b;c;z) = {}_2F_1(b,a;c;z), \qquad 6$$

and then apply the recurrence relation 4 to get

$$ {}_2F_1((1-i)/2,-i/2;(1-(i+j))/2;3/4).$$

With the ideas outlined above a numerical algorithm can be written and executed, to generate a sequence of numbers, the final one being the value of the hypergeometric function desired. However, due to a lack of readily available published tables for this particular type of hypergeometric function, it was not known whether the recurrence relation was stable or not, and consequently whether or not the numbers calculated, represented the hypergeometric function.

To test the validity of the recurrence calculation the quadratic transformation

$$ {}_2F_1(a,b,(a+b+1)/2,z) = $$

$$ = (1-2z)^{-a}\,{}_2F_1\left(a/2,(1+a)/2;(1+a+b)/2;\ \frac{4z^2-4z}{(1-2z)^2}\right), \qquad 7 $$

was employed to generate two other representations of the desired hypergeometric function, see AMS-55 sec.15.3, i.e.

$$ {}_2F_1(-i/2,(1-i)/2;(1-i-j)/2;3/4) = $$

$$ = 2^{-i}\,{}_2F_1(-i,-j;(1-i-j)/2;3/2), \qquad 8a $$

and

$$ = 2^{j-i}\,{}_2F_1(-j/2,(1-j)/2;(1-i-j)/2;3/4). \qquad 8b $$

Since the number of iterations of the recurrence relations needed to generate the new forms is different from the number needed to generate the original one it was surmised that a comparison of the 3 values obtained would either corroborate each other or point to regions in parameter space for which the various recurrence relations were unstable, assuming that 2 out of 3 would agree for any given set of parameters. Figure A6.3 shows the results of this comparative test for the specific set of parameters; j=100 and i ranging from 1 to 200. In order to compress the information into a manageable scale the log of the absolute value is plotted as a function of the independent parameter i.

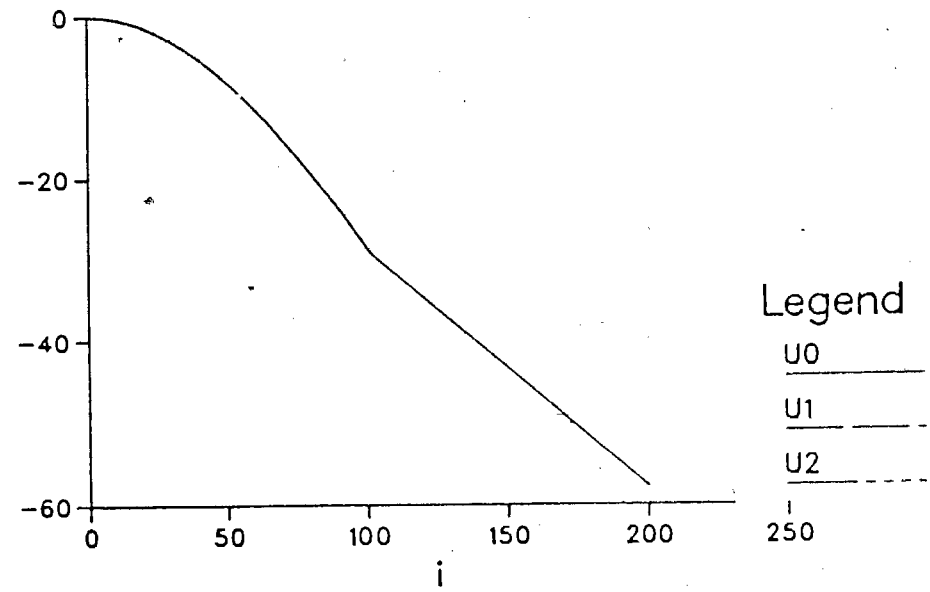

Figure A6.3 ; Results of comparision test for the three different iterative schemes used in calculating ${}_2F_1(i,-200;(i-i-100)/2;3/2)$, NOTE that the results of each of the schemes lie on the same curve indicating agreement over this range of parameters.

From these tests it was felt that we had reasonable assurance that the values calculated were in fact the values of the function

$$ {}_2F_1(-i/2,(1-i)/2;(1-i-j)/2;3/4) $$

for the ranges of parameter space that were of interest.

From the above analysis a stable algorithm for calculating the hypergeometric functions was written in Fortran 77. In calculating the hypergeometric functions the routine uses one of the two representations 2 or 8b depending on which of the two parameters i and j is the larger. If i is greater than j then 8b is used and if i is less than j then 2 is used. This was done to both save time and to minimize the accumulated error inherent in iterative schemes, since in this way the program iterated the minimum possible number of times.

As for the oscillator functions the routine used to calculate the hypergeometric functions is listed below, and figure A6.3 shows the cpu time required for a set of typical calls to the routine F21, for j=100, with i ranging from 0 to 200.

```
FUNCTION F21(I,J;Z)
REAL*16 Z,F0,F1,F2,F21,AI,AJ,AK,A,B,C
INTEGER I,J,K,KMAX,FLAG,L,M
IF (MOD(I+J,2) .NE. 0) THEN
WRITE(5,*) 'HYPERGEOMETRIC FUN HAS SINGULARITY F21'
F21=0.Q0
RETURN
ENDIF
IF ((I.GT.J).AND.(J.GE.0)) THEN
L=J
M=I
FLAG=1
ELSE
L=I
M=J
FLAG=0
ENDIF
IF (MOD(L,2) .EQ. 0) THEN
KMAX=L/2
A=-QFLOAT(KMAX)
B=5.Q-1+A
ELSE
KMAX=(L-1)/2
A=-QFLOAT(KMAX)
B=A-5.Q-1
ENDIF
C=QFLOAT(1-L-M)/2.Q0
```

```
      F0=1.Q0
      IF (A .EQ. 0.Q0) THEN
      F21=F0*(-QSQRT(1.Q0-Z))**(FLAG*(M-L))
      RETURN
      ELSE IF (A .EQ. -1.Q0) THEN
      F21=(1.Q0-B*Z/C)*(-QSQRT(1.Q0-Z))**(FLAG*(M-L))
      RETURN
      ELSE
      F1=1.Q0-B*Z/C
      DO 1 K=1,KMAX-1
      AK=-QFLOAT(K)
      F2=((C-B*Z-AK)*F1-AK*(Z-1.Q0)*(F0-F1))/(C-AK)
      F0=F1
      F1=F2
1 CONTINUE
      F21=F2*(-QSQRT(1.Q0-Z))**(FLAG*(M-L))
      RETURN
      ENDIF
      RETURN
      END
```

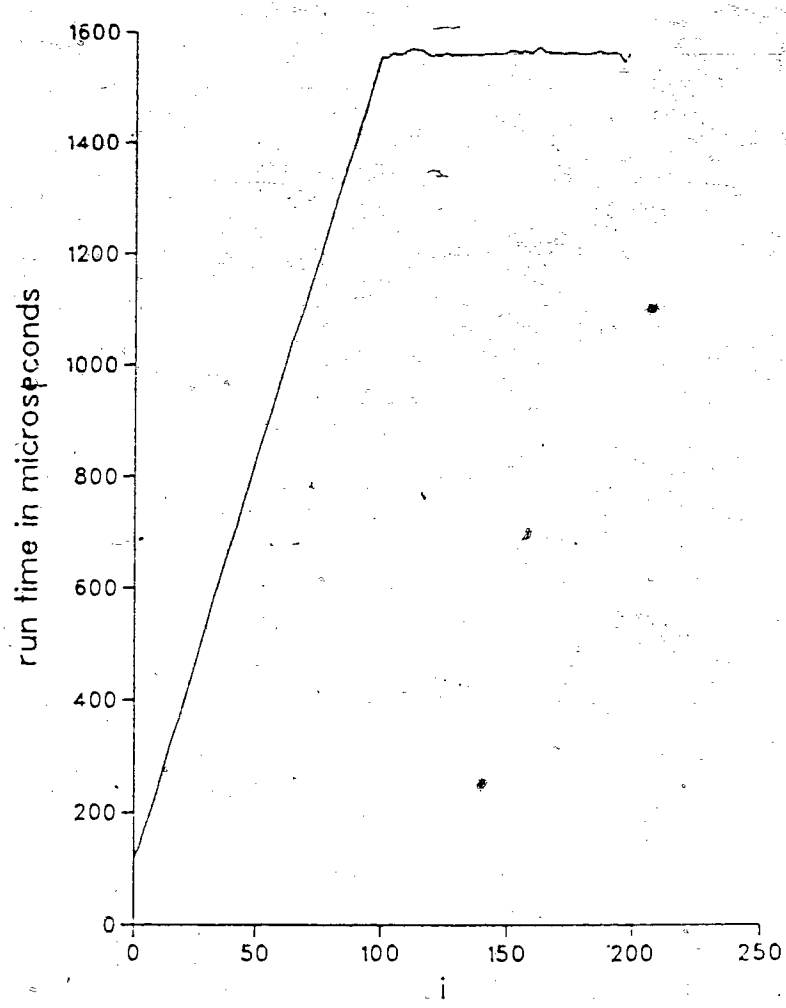

Figure A5.4 ; Indicative run time for the calculation of ${}_2F_1$ in milliseconds.

APPENDIX 6

EXPANSIONS AND OTHER TECHNICAL RESULTS

Altough some of these results are quoted in diverse literature we present the derivations here because of their importance to this thesis.

1. $$H_m(x)H_n(x) = \sum_{p=0}^{\min(m,n)} \frac{2^p m!n!}{p!(m-p)!(n-p)!} H_{m+n-2p}(x)$$

2. $$x^m = \sum_{n=0}^{[m/2]} \frac{1}{2^m} \frac{m!}{n!(m-2n)!} H_{m-2n}(x)$$

3. $$x^m H_n(x) =$$

$$\frac{m!n!}{2^m} \sum_{k=0}^{[m/2]} \sum_{j=0}^{\min(m-2k,n)} \frac{2^j}{k!j!(m-2k-j)!(n-j)!} H_{m+n-2(k+j)}(x)$$

4. $$H_m(x+y) = \sum_{n=0}^{m} \frac{m!}{n!(m-n)!} (2x)^n H_{m-n}(y)$$

5. $$H_m(\beta x) = \sum_{n=0}^{[m/2]} 2^n \frac{m!}{(2n)!!(m-2n)!} (\beta^2-1)^n \beta^{m-2n} H_{m-2n}(x)$$

6. $$\int_{\alpha x}^{\infty} e^{-u^2} H_m(u)\, du = e^{-(\alpha x)^2} H_{m-1}(\alpha x) \qquad \text{if } m \neq 0$$

$$= \frac{\sqrt{\pi}}{2} \operatorname{erfc}(\alpha x) \qquad \text{if } m = 0$$

Results 1 and 6 can be found in Erdelyi Vol. 2 along with a variation of result 5. Result 2 can be constructed by inverting the explicit form of the Hermite polynomials given in AMS-55 chpt. 15.

PROOFS

PROOF 1

$$H_m(x)H_n(x) = \sum_{p=0}^{\min(m,n)} \frac{2^p m!n!}{p!(m-p)!(n-p)!} H_{m+n-2p}(x)$$

Assume $$H_m^*(x)H_n(x) = \sum_p c_p H_p(x)$$

then $$c_p = \frac{1}{2^p p!\sqrt{\pi}} \int_{-\infty}^{\infty} e^{-x^2} H_p(x) H_m(x) H_n(x)\, dx$$

by G-R sec. 7.375

$$= \frac{2^{(m+n-p)/2} m!n!}{(s-p)!(s-m)!(s-n)!}$$

with the condition that $2s = p+m+n$.

This result is valid in the region of parameter space defined by

1. $s-p \geq 0 \longrightarrow$ $m+n \geq p$
2. $s-m \geq 0 \longrightarrow$ $p+n \geq m$
3. $s-n \geq 0 \longrightarrow$ $p+m \geq n$.

2 and 3 imply $p \geq m-n$ and $p \geq n-m$

giving $p \geq \max(m-n, n-m)$

thus $\max(m-n, n-m) \leq p \leq m+n.$

If now we let $p=m+n-2q$ then

$$\min(m,n) \geq q \geq 0$$

and,

$$s-p = q$$

$$s-m = n-q$$

$$s-n = m-q.$$

Thus the sum can be written as

$$H_m(x)H_n(x) = \sum_{q=0}^{\min(m,n)} \frac{2^q m!n!}{q!(m-q)!(n-q)!} H_{m+n-2q}(x).$$

PROOF 2

$$x^m = \sum_{n=0}^{[m/2]} \frac{1}{2^m} \frac{m!}{n!(m-2n)!} H_{m-2n}(x)$$

Assume that

$$x^m = \sum_n f_n H_n(x)$$

then $$f_n = \frac{1}{2^n n! \sqrt{\pi}} \int_{-\infty}^{\infty} e^{-x^2} x^m H_n(x)\, dx.$$

Since $$H_n(x) = (-1)^n e^{x^2} \frac{d^n e^{-x^2}}{dx^n}$$

then $$f_n = \frac{(-1)^n}{2^n n! \sqrt{\pi}} \int_{-\infty}^{\infty} x^m D^n(e^{-x^2})\, dx.$$

By integration by part the evaluation of this gives

1. if $n > m$ then $f_n = 0$
2. if $n = m$ then $f_n = \frac{1}{2^m}$
3. if $n < m$ and $n+m$ even then

$$f_n = \frac{(-1)^n}{2^n n! \sqrt{\pi}} \{x^m D^{n-1}(e^{-x^2}) \Big|_{\infty}^{\infty} - m \int_{-\infty}^{\infty} x^{m-1} D^{n-1} e^{-x^2}\, dx\}$$

$$= \frac{(-1)^n}{2^n n! \sqrt{\pi}} \{0+0+\ldots+(-1)^n \frac{m!}{(m-n)!} \int_{-\infty}^{\infty} x^{m-n} e^{-x^2}\, dx\},$$

by G-R sec. 3.461, evaluation of the remaining integral yields

$$f_n = \frac{1}{2^n n!} \frac{m!}{(m-n)!} \frac{(m-n-1)!!}{2^{(m-n)/2}}.$$

Therefore

$$x^m = \sum_{n=0}^{m} \frac{1}{2^n n!} \frac{m!}{(m-n)!} \frac{(m-n-1)!!}{2^{(m-n)/2}} H_n(x),$$

where the sum is taken over even m+n.

By changing the sum variable such that

$$n = m-2k$$

then by $$0 \le n \le m$$

we get $$m \ge 2k \ge 0.$$

If we define the symbol [m/2] to mean the largest whole number smaller than m/2, which is standard in most literature, then

$$[m/2] \ge k \ge 0.$$

Then the sum becomes

$$x^m = \sum_{k=0}^{[m/2]} \frac{1}{2^{m-k}} \frac{m!}{(m-2k)!(2k)!}(2k-1)!!\ H_{m-2k}(x).$$

This can be simplified even more by noting that the double factorial can be rewritten as

$$(2k-1)!! = \frac{(2k-1)!}{(2k)!!} 2k$$

$$= \frac{(2k)!}{2^k k!}.$$

Thus we get the final result that

$$x^m = \sum_{k=0}^{[m/2]} \frac{1}{2^m} \frac{m!}{k!(m-2k)!} H_{m-2k}(x).$$

PROOF 3

$$x^m H_n(x) =$$

$$\frac{m!n!}{2^m} \sum_{k=0}^{[m/2]} \sum_{j=0}^{\min(m-2k,n)} \frac{2^j}{k!j!(m-2k-j)!(n-j)!} H_{m+n-2(k+j)}(x)$$

By result 2 we get that

$$x^m = \sum_{k=0}^{[m/2]} \frac{1}{2^m} \frac{m!}{k!(m-2k)!} H_{m-2k}(x)$$

and by result 1 we get

$$H_n(x)H_{m-2k}(x) = \sum_{q=0}^{\min(m-2k,n)} \frac{2^q(m-2k)!n!}{q!(m-2k-q)!(n-k)!} H_{m+n-2(k+q)}(x).$$

Thus

$$x^m H_n(x) =$$

$$\frac{m!n!}{2^m} \sum_{k=0}^{[m/2]} \sum_{j=0}^{\min(m-2k,n)} \frac{2^j}{k!j!(m-2k-j)!(n-j)!} H_{m+n-2(k+1)}(x).$$

PROOF 4

$$H_m(x+y) = \sum_{k=0}^{m} \frac{m!}{k!(m-k)!}(2x)^k H_{m-k}(y)$$

By Taylor expanding $H(x+y)$ about $x=0$, we get

$$H_m(x+y) = H_m(y) + H_m'(y)\, x + H_m''(y)\, \frac{x^2}{2!} + \dots .$$

By G-R sec. 8.952

$$\frac{dH_m(x)}{dx} = 2m\, H_{m-1}(x).$$

Then

$$\frac{d^n H_m(x)}{dx^n} = 2^n m(m-1)(m-2)\dots(m-n+1)\, H_{m-n}(x).$$

With this a typical term in the Taylor series becomes

$$(2x)^n \frac{m!}{n!(m-n)!} H_{m-n}(y).$$

Since the order of the Hermite polynomials is diminishing the sum terminates when $m=n$ or $m-n=0$, thus we get

$$H_m(x+y) = \sum_{k=0}^{m} \frac{m!}{k!(m-k)!}(2x)^k H_{m-k}(y).$$

PROOF 5

$$H_m(\beta x) = \sum_{n=0}^{[m/2]} 2^n \frac{m!}{(2n)!!(m-2n)!}(\beta^2-1)^n \beta^{m-2n} H_{m-2n}(x)$$

Assume $$H_m(\beta x) = \sum_k c_{mk} H_k(x)$$

then $$c_{mk} = \frac{1}{2^k k! \sqrt{\pi}} \int_{-\infty}^{\infty} e^{-x^2} H_k(x) H_m(\beta x)\, dx.$$

By G-R sec. 7.374

$$= 0 \qquad \text{if } k>m$$

$$= 0 \qquad \text{if } k+m \text{ odd}$$

$$= 2^{(m-k)/2} \frac{m!}{k!(m-k)!!}(\beta^2-1)^{(m-k)/2} \beta^k \qquad m+k \text{ even.}$$

Therefore we get

$$H_m(\beta x) = \sum_{k=0}^{m} 2^{(m-k)/2} \frac{m!}{k!(m-k)!!} (\beta^2-1)^{(m-k)/2} \beta^k H_k(x).$$

Where the sum is taken over even m+k.

By letting $k = m-2n$

then by $m \geq k \geq 0$

we get $m \geq 2n \geq 0$

or $[m/2] \geq n \geq 0.$

With this change of sum variable we then get

$$H_m(\beta x) = \sum_{n=0}^{[m/2]} 2^n \frac{m!}{(2n)!!(m-2n)!}(\beta^2-1)^n \beta^{m-2n} H_{m-2n}(x).$$

PROOF 6

$$\int_{\alpha x}^{\infty} e^{-u^2} H_m(u)\, du = e^{-(\alpha x)^2} H_{m-1}(\alpha x) \qquad \text{if } m \neq 0$$

$$= \frac{\sqrt{\pi}}{2} \operatorname{erfc}(\alpha x) \qquad \text{if } m = 0$$

By G-R sec. 8.950 $\qquad H_m(x) = (-1)^m e^{x^2} \frac{d^m e^{-x^2}}{dx^m}$

then $\int_{\alpha x}^{\infty} e^{-u^2} H_m(u)\, du = \int_{\alpha x}^{\infty} e^{-u^2} (-1)^m e^{u^2} \frac{d^m e^{-u^2}}{du^m}\, du$

$$= \int_{\alpha x}^{\infty} (-1)^m \frac{d^m e^{-u^2}}{du^m}\, du = (-1)^m \frac{d^{m-1} e^{-u^2}}{du^{m-1}} \Big|_{\alpha x}^{\infty}$$

Since $\qquad \frac{d^{m-1} e^{-u^2}}{du^{m-1}} = H_{m-1}(u) (-1)^{m-1} e^{-u^2}$

the integral becomes

$$= -e^{-u^2} H_{m-1}(u) \Big|_{\alpha x}^{\infty}.$$

Since $\qquad \lim_{u \to \infty} e^{-u^2} H_m(u) \longrightarrow 0$

the integral becomes.

$$= e^{-(\alpha x)^2} H_{m-1}(\alpha x)$$

if $m \neq 0$.

If m=0 then the integral reduces to

$$\int_{\alpha x}^{\infty} e^{-u^2}\, du = \frac{\sqrt{\pi}}{2}\ \mathrm{erfc}(\alpha x).$$

APPENDIX 7

A short table of some of the representative spectral values for the biorthogonal Oscillator expansion, w=1.0, with

m\α	1	2	3	4
1 real	0.172E+00	-0.324E+00	0.113E+00	-0.249E+00
imag	0.183E-15	-0.357E-15	-0.531E-16	-0.271E-15
2	-0.604E-01	0.951E-01	0.393E-01	0.965E-01
	0.130E-14	-0.496E-15	0.126E-15	-0.648E-16
3	-0.538E-01	-0.129E+00	0.303E-01	-0.174E+00
	-0.160E-15	-0.491E-15	0.747E-16	-0.110E-15
4	-0.867E-02	0.156E+00	-0.431E-02	0.981E-01
	0.612E-15	-0.703E-16	0.110E-15	-0.168E-15
5	-0.106E+00	-0.885E-01	-0.282E-01	-0.114E+00
	-0.181E-15	-0.194E-15	0.527E-16	-0.198E-15
6	0.258E-01	0.176E+00	-0.198E-01	0.103E+00
	-0.217E-16	0.465E-16	0.805E-16	-0.217E-15
7	-0.103E+00	-0.829E-01	-0.661E-01	-0.686E-01
	-0.159E-15	-0.109E-15	-0.726E-16	-0.187E-15
8	0.414E-01	0.168E+00	-0.153E-01	0.108E+00
	-0.196E-15	0.751E-16	0.497E-16	-0.603E-16
9	-0.792E-01	-0.846E-01	-0.838E-01	-0.420E-01
	-0.105E-15	0.170E-16	-0.119E-15	-0.134E-15

m\α	1	2	3	4
10	0.431E-01	0.143E+00	-0.153E-02	0.110E+00
	-0.236E-15	0.725E-16	0.125E-17	0.137E-16
11	-0.499E-01	-0.837E-01	-0.847E-01	-0.304E-01
	0.597E-16	0.771E-16	-0.102E-15	-0.326E-16
12	0.364E-01	0.110E+00	0.135E-01	0.106E+00
	-0.234E-15	0.658E-16	-0.116E-15	0.837E-16
13	-0.229E-01	-0.778E-01	-0.736E-01	-0.289E-01
	0.105E-15	0.113E-15	-0.893E-16	0.452E-16
14	0.255E-01	0.763E-01	0.252E-01	0.956E-01
	-0.201E-15	0.393E-17	-0.128E-15	0.107E-15
15	-0.132E-02	-0.672E-01	-0.554E-01	-0.325E-01
	0.134E-15	0.261E-15	-0.689E-16	0.120E-15
16	0.137E-01	0.453E-01	0.316E-01	0.805E-01
	-0.155E-15	-0.656E-16	-0.124E-15	0.967E-16
17	0.140E-01	-0.536E-01	-0.342E-01	-0.373E-01
	0.139E-15	0.157E-15	-0.462E-17	0.169E-15
18	0.276E-02	0.196E-01	0.324E-01	0.620E-01
	-0.966E-16	-0.754E-16	-0.108E-15	0.855E-16
19	0.234E-01	-0.388E-01	-0.132E-01	-0.407E-01
	0.144E-15	0.155E-15	0.696E-16	0.182E-15
20	0.616E-02	-0.689E-04	0.286E-01	0.421E-01
	-0.352E-16	-0.835E-16	-0.857E-16	0.538E-16
21	0.279E-01	-0.244E-01	0.543E-02	-0.413E-01
	0.137E-15	0.139E-15	0.124E-15	0.190E-15

BIBLIOGRAPHY

1. D.J. Korteweg and G. de Vries, Philos, Mag. **39**(1895),422.

2. J.S. Russell, 14th Meeting of the British Assoc. Adc. Sci., John Murray, London, 1844, p. 311.

3. C.S. Gardner and G.K. Morikawa, Science Report #NYO-9082, 1960 (unpublished).

4. N.J. Zabusky, Proc. Sympos. on Nonlinear Partial Differential equations (Univ. of Delaware, Newark, Del, 1965), Academic Press, New York, 1967, p. 223.

5. M.D. Kruskal, Proc. Conf. on Math. Models in the Physical Sciences (Univ. of Notre Dame, South Bend, Ind., 1962), Prentice-Hall, Englewood Cliffs, N.J., 1963, p. 17.

6. H. Washimi and T.Taniuti, Phys. Rev. Lett. **17** (1966), 996.

7. L. van Wijngarten, J. Fluid Mech. **33** (1968), 465.

8. S. Leibovich, J. Fluid Mech. **42** (1970), 803.

9. G.A. Nariboli, 1969 (unpublished).

10. C.S. Gradner, J.M. Greene, M.D. Kruskal and R. Miura, Phys. Rev. Lett. **19** (1967), 1095.

11. S. Leibovich and A.R. Seebass (eds), Nonlinear Waves, Cornell University Press, Ithaca, N.Y. 1974, p. 103.

12. V.E. Zakharov, Lectures on the Inverse Scattering Method, Hungarian Acad. Sci.,Budapest, KFKI-1983-71, ISBN 963 372 111 3, 1983.

13. P.D. Lax, Comm. Pure Appl. Math. **21** (1968), 467.

14. M.H. Stone, Linear Transforms in Hilbert Space (American Math. Soc., New York, 1932).

15. I.M. Gel'fand and B.M. Levitan, Izvest. Akad. Nauk, **15** (1951), 309.

16. V.A. Marchenko, Dakl. Akad. Nauk. SSSR, **104** (1955), 695.

17. L.D. Faddeev, Uspekki Mat. Nauk. **14** (1959), 57.

18. F. Calogero and A. Degasperis, Spectral Transforms and Solitons 1, North-Holland, Amesterdam, Netherlands, 1982.

19. G.L. Lamb, Jr. Elements of Soliton Theory, John Wilson & Sons, New York, N.Y. 1980.

20. R.K. Dodd, J.C. Eilbeck, J.D. Gibbon and H.C. Morris, Solitons and Nonlinear Waves, Academic Press, New York, 1982.

21. M.J. Ablowitz and H. Segur, Studies Appl. Math. 57 (1977), 13.

22. R.H. Enns and S.S. Rangnekar, Can. J. Phys.,64 (1986), 53.

23. H. Segur, J. Fluid Mech.,59 (1973) 721.

24. I.S. Gradshteyn and I.M. Ryzhik, Tables of Integrals, Series, and Products, Academic Press, New York, N.Y. 1980.

25. A.S. Fokas and M.J. Ablowitz, J. Math. Phys. 23 (1982), 178.

26. M. Abramowitz and I. Stegun (eds), Handbook of Mathematical Functions, Dover, New York, 1965.

27. J.L. Hammack and H. Segur, J. Fluid Mech. 65 (1974), 289.